CRANFIELD UNIVERSITY

SCHOOL OF INDUSTRIAL AND MANUFACTURING SCIENCE

PhD THESIS

Academic Year 1996

K. GRIGOROUDIS

A study of the wear process related to twin-screw extruders

Supervisor : D.J. Stephenson

July 1996

This thesis is submitted for the degree of PhD

"To my father I owe my being,
to my teacher my well being"

Alexander the Great

Dedication

I dedicate this work to my parents whose heartfelt blessing and encouragement have always been a source of great strength and immense inspiration throughout this work.

I also dedicate this work to my supervisor, D.J. Stephenson with sincere appreciation and thanks for his invaluable advice and assistance given to me throughout the course of this study.

Acknowledgements

I am greatly thankful to Almighty God, for giving me the opportunity to undertake this work and ability to make life worth living.

Apart from my deep gratitude to my supervisor D.J.Stephenson for his enthusiastic help and Dr Darlington for monitoring the project, the assistance of the technical staff, particularly Messrs J.Hedge, T. Prayor, A. Baldwin, A. Nelson, C. Matthews and A.Dyer in preparing the specimens and sorting out various problems with the equipment is greatfully aknowledged.

I would also like to thank APV Baker and Cranfield University for offering me sponsorship and support, enabling me to finish this study.

Last but not least, I would like to thank Zoe, who never failed to remind me that'' *if you try hard there is always a glimpse of light in the end of the tunnel*''.

Abstract

Extruders are used in a wide range of process industries and high reliability is essential if cost effective manufacturing is to be maintained. A critical part of twin-screw extruders is the barrel that must withstand many different wear and corrosion environments depending on the end user. For many applications the extruder barrel is a critical component and it is essential that it performs in a predictable manner, providing the necessary design life-time.
This project has addressed these aims by considering the wear/corrosion behaviour of current and potential extruder barrel materials from which a life prediction model has been developed.

A wide range of engineering materials has been evaluated in the laboratory for abrasive wear resistance using a dry sand abrasive wear test according to ASTM G 65-93. An appraisal of the tests and the applicability of the results to the in-service conditions of an extruder has lead to further testing for abrasion and abrasion-corrosion resistance of four materials, namely Mild Steel, 440C, N18 and N18+5%TiC+5%TiN.

Plastic deformation was the main feature of the damaged surfaces in the form of ploughing which has been modelled in terms of a low-cycle fatigue process. The relative hardness between material and abrasive was found to be an important parameter in controlling the rate of material removal. It has also been shown that the synergistic effect of abrasion-corrosion results in an accelerated material removal rate.

The information from these tests has been used to develop a model of the wear of extruder barrels by abrasive particles. It is shown that there is a correlation between the particle size, wear debris size and wear groove size distributions. From a knowledge of the particle flux, the particle size distribution and the loading conditions, metal recession is predicted based on a low-cycle fatigue process. The wear rates for a wide range of Fe- and Ni-based materials are predicted to better than a factor of two.

When corrosion is also present, the mechanism of metal recession depends on whether passive surface films are formed. For the Fe-based materials which exhibit direct dissolution of material, the wear/corrosion rate can be estimated by combining the metal loss rate under pure wear and pure corrosion conditions only. For the Ni-base alloys, thin passive films form in all the aqueous environments studied and corrosion rates are extremely low. However, during abrasive wear the passive films are removed and the overall metal recession rate is a combination of metal loss due to abrasive wear of the substrate and the continual formation and removal of surface passive films.

Contents

List of Figures

List of Tables

Table No **Page No**

List of symbols

H: bulk hardness
σ: flow stress
ϵ: true strain
n: work hardening exponent
θ: angle of the abrasive particle
a: half groove width
α_c: degree of wear
h: depth of cut
f: shear strength
Dp: degree of penetration
β_c: fraction of contact points
R: radius of the abrasive particle
Y: yield strength
K: wear coefficient
a_c: critical attack angle
β: proportion of material removed as wear
α: proportion of grits cutting
C: strength coefficient
L: sliding distance
V: volume of material removed
W: applied load
Cs: shape factor of the abrasive grain
ϵ_f: fatigue ductility coefficient
c: fatigue ductility exponent
$\Delta_{\epsilon p}$: plastic strain amplitude
fv_i: volume fraction of the i phase
W_i: volume wear rate of the i phase
PM: powder metallurgy
HIP: Hot isostatic pressure
OECD: Organisation for Economic Cooperation and Developement

CHAPTER ONE

1.1 Introduction

Wear is a phenomenon that is encountered in many situations varying from the home to industry. The critical study of abrasive wear is of recent interest, dating from the 1950's and involves the material loss from a surface by the mechanical impact of an abrasive harder than the surface being worn. It is the most frequent mechanism of wear met in industrial situations, leading to heavy expenditures for maintenance and replacement of industrial equipment (Fig.1.1).[1]

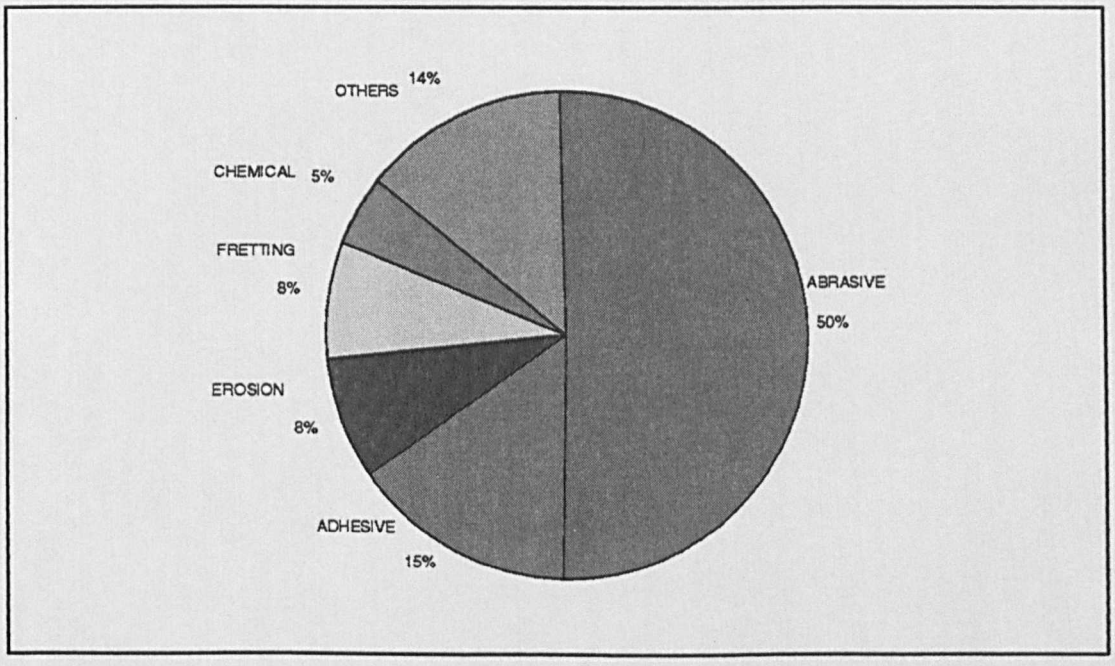

Fig.1.1 : Most frequent wear mechanisms in industry[1]

Corrosive wear, the research of which has been active for some decades involves the progressive loss of original material from a solid surface by its chemical interaction with the environment.

Wear in the food industry is considered to be due to both mechanical abrasion and chemical corrosion, though abrasive wear is the dominant mechanism aggravated by corrosion. A cooker extruder is a machine, considered as a continuous chemical reactor, which cooks and shapes a product in a single operation. Single screw or twin screw cooker extruders have the same principles of operation and can handle the same products(Fig.1.2). They are currently used in many food applications (snacks, pet foods and protein substitutes) while various other fields (sterilisation, biotechnology) seem likely candidates.

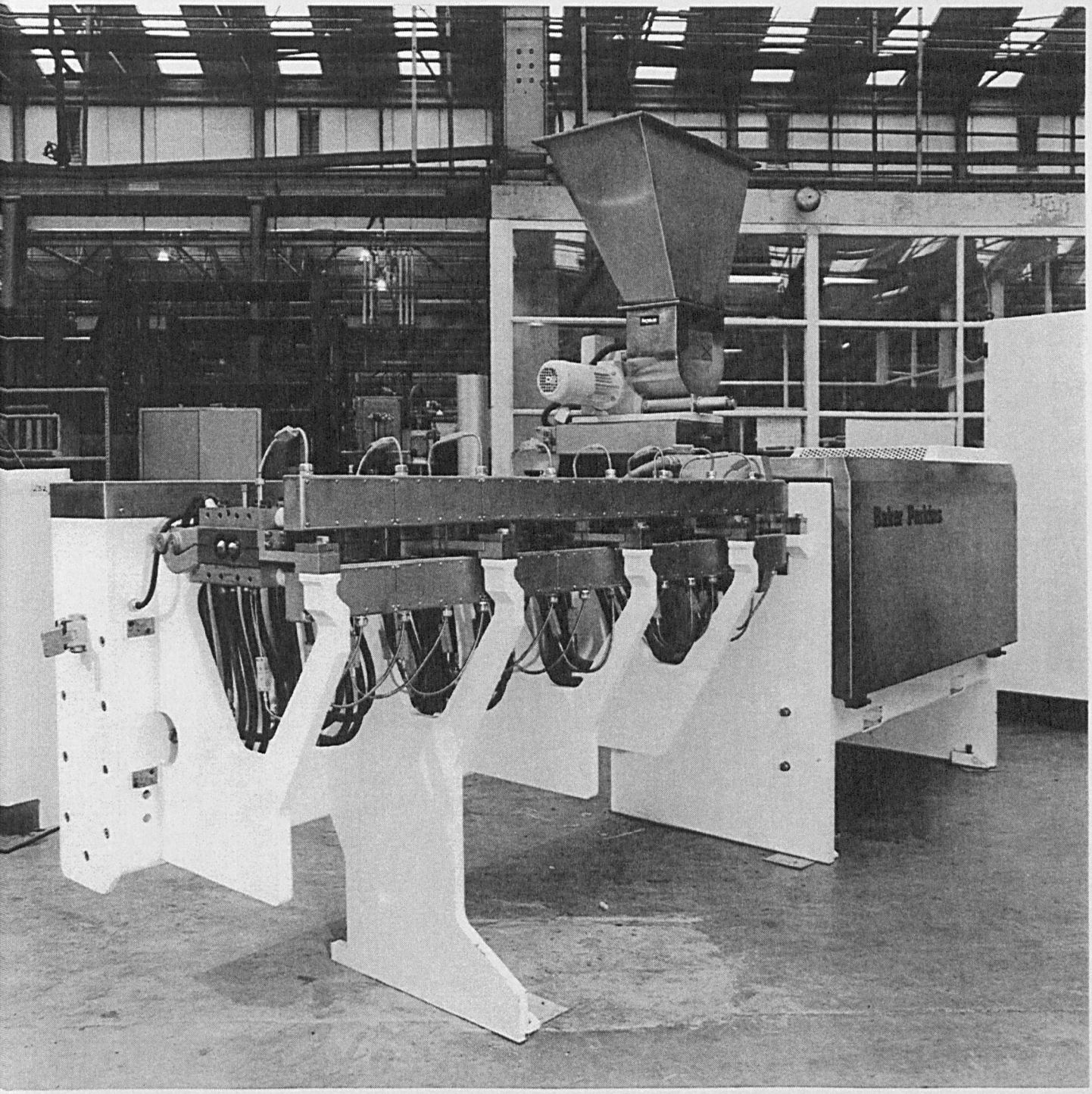

Fig.1.2 : Twin-screw extruder used in food industry

The very wide range of particle size of the raw materials to be handled along with the highly corrosive environment inside the extruder because of the nature of the materials being processed and high temperatures(500°C) and pressures(150 bar) have a direct effect on the materials, that the extruder is made of. These extreme conditions of corrosion and wear include high mechanical contact fatigue, abrasive and erosive wear and corrosion/erosion mechanisms which result from the synergistic interaction between different degradation processes(Fig.1.3).[2]

Extruders tend to produce low levels of waste product in general. Some of this waste is produced each time the extruder is started or stopped, so there are great incentives to run continuously for the longest practical period and unscheduled down time is unacceptable and costly.

A Surface Engineering approach to eliminate the combined effect of wear/corrosion that is so damaging is often the only step that can be taken. If the bulk material is decided on the grounds of strength, the component can then be coated or surface treated to overcome the tribological problems. This is the case whether the substrate be a wrought or cast or a powder metallurgy material. It is important that the most appropriate surface treatment be selected which will not cause dimensional changes, reduce the hardness and load carrying capability or impair the corrosion resistance of the substrate.
The two main requirements for the user of surface treatments and coatings are;[3] the identification of the particular surface treatment needed to solve a specific problem, and ensuring that the process can produce consistent and predictable results.

For the extruder application the most appropriate surface treatment is the deposition of a relatively thick wear/corrosion resistant coating achieved by flame or plasma spraying processes. These techniques are relatively low cost but depending on spraying parameters and coating composition, coatings of this kind may contain small levels of porosity which affects properties such as mechanical strength and corrosion resistance.

Experimental results[4] show that WC/Co based coatings in addition to WC in Ni and Ni/Cr binders do not work satisfactorily due to preferential corrosion of the cobalt binder or catastrophic failure of the coating layer(Fig.1.4).

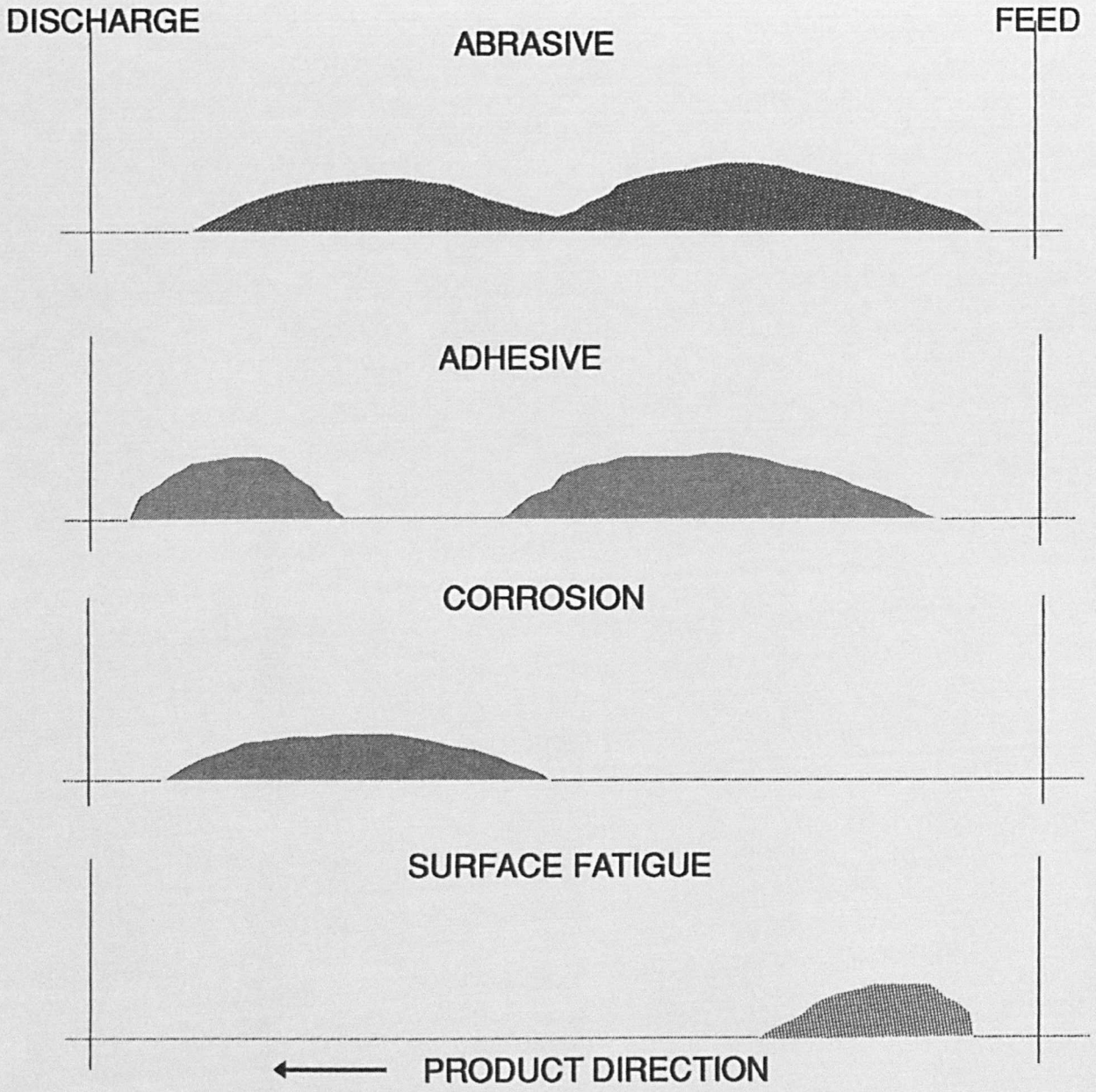

Fig.1.3 :

WEAR PROFILE INSIDE AN EXTRUDER BARREL [2]

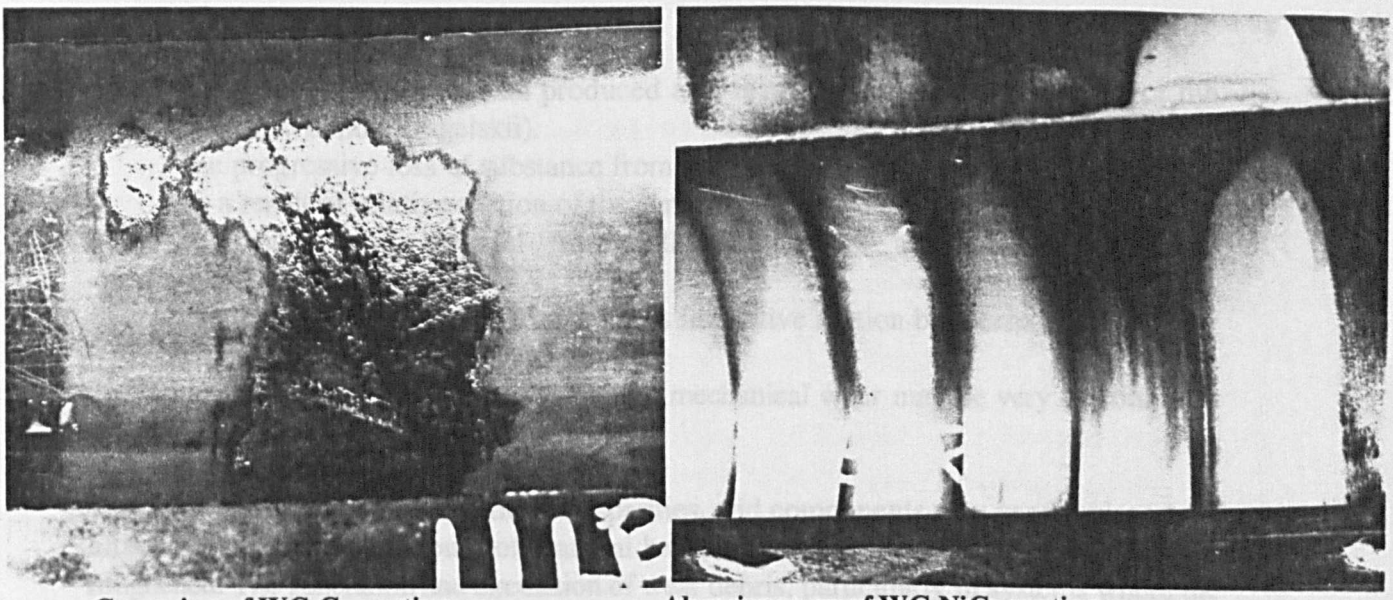

Corrosion of WC-Co coating Abrasive wear of WC-NiCr coating

Fig.1.4 : Abrasive/corrosive wear of an extruder barrel [4] (x 0.5)

Poor results were also reported[4] when a coating system based on Ni/Cr/B/Si/Fe with addition of WC particulate developed for application by a thermal spraying and fusing process was used. The quality and integrity of as-sprayed deposits were not high enough for the severe in-service conditions within the extruder.

However, APV Baker and Cranfield University have developed a new method for applying the aforementioned coatings which is based on a conventional PM and HIP approach. The selection of the starting powders and the appropriate HIP cycle enables fully dense coatings and tailored microstructures with significant improvements in service performance compared to other commercially available coatings and surface treatments. One particular application demonstrates this superiority of the new technique where conventional surface treatment(nitriding) lasted 100 h, high velocity spray coating less than 1000 h and this new process approached 20000 h in service.
A combination of solid state diffusion bonding and HIP'ing has been also reported to give corrosion and wear resistant layers[5] e.g cladding of steel valves.

1.2 Wear classification

Wear, part of the science of Tribology, is one of the three most commonly encountered industrial problems leading to the replacement of components and assemblies in engineering; the others being fatigue and corrosion. Wear is rarely catastrophic but it reduces operating efficiency by increasing the power losses, oil consumption, and the rate of component replacement.
What is important is not the cost of material removed but the total effort required to restore the original conditions. Thus, understanding the type of wear in equipment, gives us the ability to select the right materials to provide an adequate wear life.

No completely adequate definition of wear can be agreed but there follows a number of

theories that have been widely accepted :

- the destruction of material produced as a result of repeated disturbances of the frictional bonds(Kragelskii).
- the progressive loss of substance from the operating surface of a body, occurring as a result of relative motion of the surface(OECD).
- the removal of material from solid surfaces as a result of mechanical action(Rabinowitz).
- the removal of material from surfaces in relative motion by mechanical and / or chemical processes(Tabor).

The synergistic effect of such corrosion and mechanical wear may be very important in many applications.

Wear occurs by surface interaction at asperities, and components may need replacement after a relatively small amount of material has been removed or if the surface is unduly roughened. The generation and circulation of wear debris, particularly in systems where the clearances are small, may be more of a problem than the actual amount of wear. The debris may cause oil blockage, seizure or both. The presence of wear debris may also give an indication of the operating efficiency.

The classification of different types of wear can be only arbitrary and should include several factors, namely[6]:

I) the nature of the main interaction (e.g adhesive or mechanical ones)
ii) type of deformation (e.g elastic, plastic)
iii) the character of the changes in the surface layer (e.g oxidation)
iv) the character of the loading conditions(e.g sliding, rolling)

However, because of its general nature and for study purposes, it is convenient to attempt to sub-divide mechanical wear into several categories. Those that have been used, traditionally, are adhesion, abrasion, erosion, fretting and pitting.[7]

Abrasive wear arises from the cutting action of hard surfaces rubbing on softer materials. It occurs when hard particles penetrate a surface and displace material in the form of long elongated chips or slivers. An otherwise smooth surface becomes roughened with fairly regular grooves, with or without loosely attached metallic debris.

Adhesive wear occurs when one smooth surface slides over another smooth surface under pressure, providing intimate contact between asperities. The detailed mechanism by which adhesive wear occurs is still a controversial topic. The traditional explanation offered by Bowden and Tabor[8] involved the welding or adhesion of asperities followed by fracture away from the weld to remove material. More recently, Suh[9] has proposed an alternative mechanism based on sub-surface delamination.

Erosion occurs when sharp particles impinge on the surface, resulting in deformation and removal of surface material. Two main damage mechanisms contribute to erosion; abrasive and impingement erosion.

Fretting or fretting corrosion is due to a slight oscillatory motion of small amplitude between two mating surfaces under load, and its main characteristic is the

appearance of a reddish brown surface surrounded by oxidation debris.

Pitting is a result of the fatigue failure of the metal surface or sub-surface due to rolling, sliding or impacting motion. Repeated application of relatively low stresses may result in numerous pit-like cavities in the metal surface.

Other classifications proposed envisaged only two wear classes[10] : **mild and severe.** This classification is not really based on any particular numerical value of wear rate but rather on the general observation that, for any pair of materials, the increase of loading by increasing either the normal load, sliding speed or bulk temperature, leads at some stage to a comparatively high jump in the wear rate. In general, mild wear leaves extremely smooth surfaces, often smoother than the original and small wear debris particles, typically only 10^{-4} mm diameter, partially produced by reaction with the ambient atmosphere or fluid. Elastic deformation is the dominant feature in this type of wear. However, severe wear leaves the surfaces deeply torn and rough and wear debris normally consists of large metallic particles, typical dimensions being up to 10-20 mm diameter. Plastic deformation is the dominant factor in this type of wear.

Tabor[11] maintains that wear can be classified as adhesive, non adhesive and a mixture of both.
Quinn[12] accepts that the classification of wear as mild and severe is the most basic and easy to apply to any situation, despite the fact that this classification does not specify a range of wear rates for each class of wear. He also places all the other categories mentioned by other researchers as *"mechanisms of wear"*. In general, however, the severe wear processes are often two orders of magnitude more effective at removing material from the sliding surfaces.
Other classifications of wear appeared according to the type of the shape, size and composition of wear particles produced[13], showing the place of their formation(surface, volume, film) and the possible mechanisms(fatigue, plastic deformation).

Despite all the controversy about wear classification there are situations where one type changes to another, or where two or more mechanisms operate together. Wear is further complicated by other operating conditions of which fatigue, impact, high temperatures and other forms of hostile environment are the most important.

In order that the size of the problem and the enormous consequences in every aspect of life can be estimated, some recent publications are cited.
In agricultural and construction industry, 75-80% of the soil-processing machine parts become disabled due to abrasive wear and only 20-25% because of breakdown.[14]
In the automotive industry, as Fig.1.5[15] shows, engine wear accounts for about 41% of the energy losses in a car.

The "*loss of substance*" as defined by the Organisation for Economic Cooperation and Development (OECD) is of enormous economic importance. It was estimated that its cost to the British Economy in 1988 was about £2 billion.[16]
For the elimination of wear in machine parts, 822,000 tonnes of lubricating oils and greases were consumed by the UK economy in 1990 with all the financial implications and profound risk to peoples' Health and the Environment.[17]

In the UK, the engineering coatings industry turnover in 1990 was estimated to be £ 3.4 billion[18]. This was predicted to increase to over £ 5.5 billion by 2005. The major application areas are for corrosion and wear resistance. As an example, in 1990 the market value for hard facing and thermal spray coatings used mainly for thick wear resistant coatings was £ 100 million and for 2005 is estimated to be in excess of £ 160 million.[18]

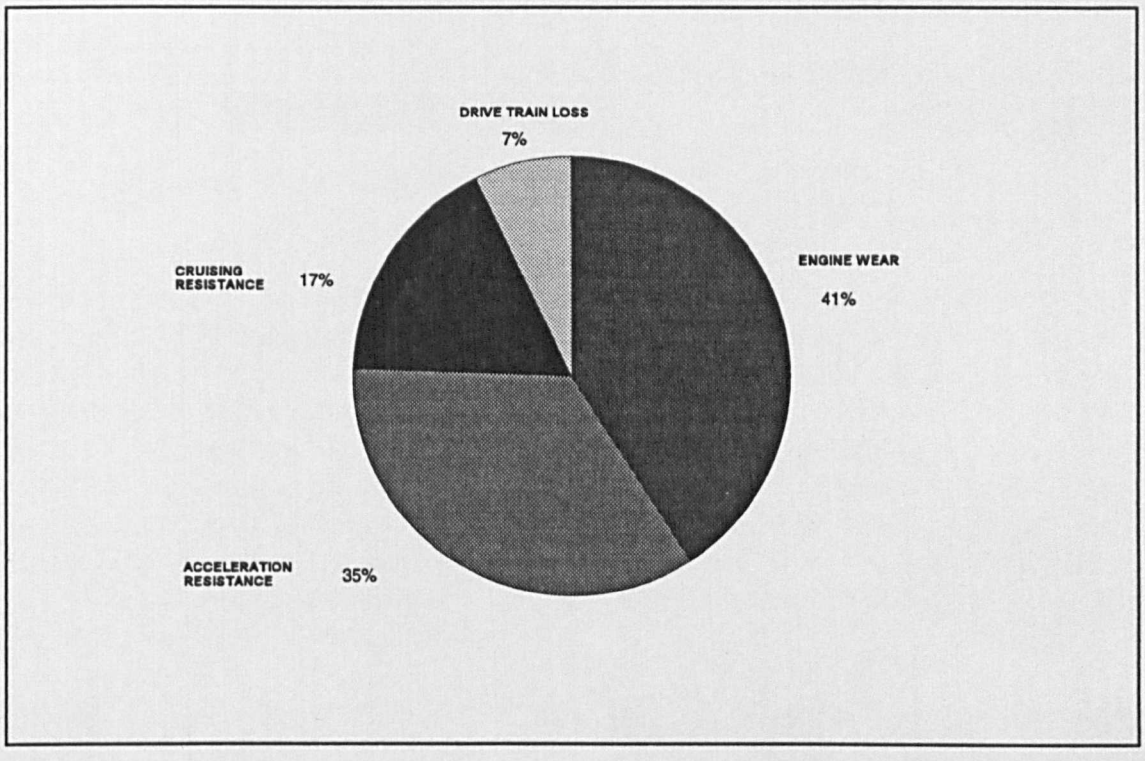

Fig.1.5 :Contribution of wear to total energy loss in a car[15]

A better understanding of tribological principles and how to apply them to reduce wear in machinery through greater control of friction, could save UK industry an estimated £1 billion annually according to a campaign launched by the Institute of Mechanical Engineers (IMechE).[19]

Last but not least, wear causes considerable human suffering, for example osteo-arthrosis. The design and development of more reliable and low wear artificial joints and heart valves could save lives.

The purpose of this study, which is sponsored by APV Baker Ltd in Peterborough, is to examine abrasive/corrosive wear both experimentally and theoretically. By understanding the basic mechanisms and controlling factors of abrasive/corrosive wear, it should be possible to provide methods by which this type of wear can be minimized and economically extend wear life of a cooker extruder.

The objectives of this project are therefore:

i) to study the abrasive wear behaviour of conventional and future materials for use in extruder barrel application.

ii)to study the synergistic effects of abrasion and corrosion on the wear behaviour of various alloys.

iii)to predict wear behaviour by modelling

The thesis covers these objectives in approximately this order. Chapter 2 considers the classification of abrasive wear, test methods, equipment, the influence of experimental variables and ways of reporting data before embarking on an extensive literature review of abrasive wear modelling in Chapter 3. Chapter 4 refers to corrosive/ abrasive wear and the effect of aminoacids. Chapter 5 presents the experimental conditions for wear and corrosion. In Chapter 6 the experimental results are cited and an interpretation of their significance in Chapter 7. Also, in Chapter 7 a proposed model for three-body abrasive wear is considered. Chapter 8 summarizes the conclusions based on the results of the present work and gives some recommendations for wear and wear/corrosion minimisation. Finally Chapter 9 gives suggestions for future work.

CHAPTER TWO

2. Abrasive wear and its classification

Abrasive wear is defined as *"wear due to hard particles or hard protuberances forced against and moving along a solid surface"*(ASTM G65-93). This definition covers several different wear modes or mechanisms that fall under the abrasive wear category e.g cutting, ploughing.

Abrasive wear processes are divided, traditionally, into two groups : two-body and three-body abrasive wear(Fig. 2.1)[20].

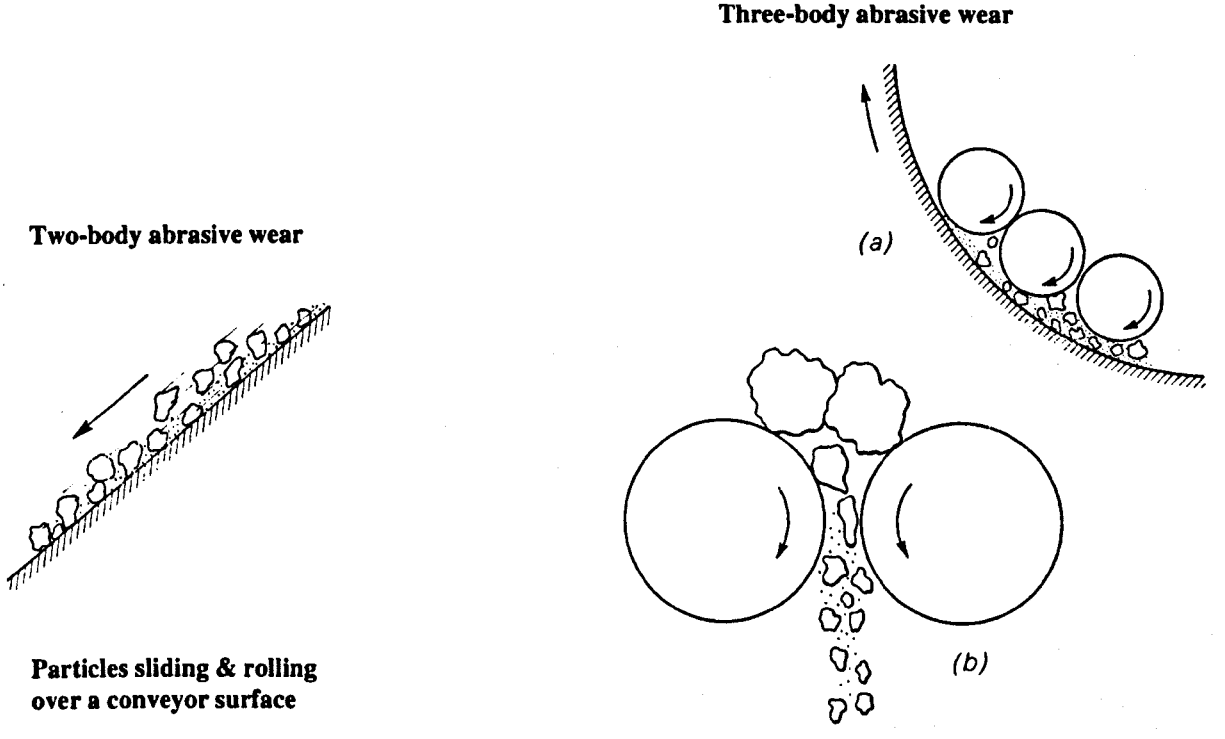

Fig.2.1: Classification of abrasive wear [20]

Two-body abrasive wear occurs when a rough surface or fixed abrasive particles slide across a surface to remove material. A grinding wheel or an emery paper polishing a solid or even a ploughshare when it first dislodges the composite soil are examples of two-body abrasive wear.

In three-body abrasive wear, the particles are loose and may move relative to one another, and possibly rotate, while sliding across the wearing surface. The grits trapped at the bearing interface can be considered as an example or as we walk on the floor, which is covered with dust particles, our shoes and the floor undergo three-body abrasion.
Two-body abrasive wear is a clearly-defined process. However, several types of three-body abrasive wear may arise. Some of these types of three-body abrasive wear are now described.

2.1 Types of three-body abrasive wear

The formation of three-bodies as reported in the literature, involves two surfaces and the abrasive particles. However, in many practical situations only one surface contacts the abrading particles or the two surfaces are so far apart that the mechanical properties of one surface have no influence on the wear of the other surface. Consequently we can define *"open"* and *"closed"* three-body abrasive wear (Fig.2.2).

closed three-body abrasive wear. This type of wear which has been studied extensively by Rabinowitz-Mutis[21] and Toporov[22], occurs when loose abrasive particles are trapped between two sliding or rolling surfaces. The particles often indent and settle into the softer surface changing its properties and influencing in that way the wear of the other surface. Often it can be eliminated by using filters or seals.

open three-body abrasive wear, when only one surface is involved, is an inherent feature of a process and has to be controlled by a suitable choice of materials. This type of wear can be further classified into one of three groups[23]: gouging, high-stress grinding and low-stress scratching. All three may occur simultaneously on a wearing part, but usually the type which predominates can be recognised.

2.1.1 Gouging abrasion

Gouging abrasion occurs when large or heavy abrasive particles contact a surface with a certain amount of impact and remove a relatively large amount of material.[24] This type of wear occurs for example in some chute liners, in impact-type pulverizers or in shovels digging into a rock pile. The stresses at the contact points are high, but the overall loading on the surface is low, and tends to be fairly uniformly distributed.

2.1.2 High-stress grinding abrasion

High-stress abrasion occurs in general under conditions of low load and high stress and the

wear situation is governed by two principal factors;[24] the properties of the abrasive particles and those of the materials against which the abrasive particles are rubbing. In service, this situation is met in various types of grinding mills (ball, rod) which are used by the mining industry to grind most metallic ores and many non-metallic minerals. In most situations the particle properties are fixed with respect to hardness and toughness, and it is the properties of the wearing metallic surfaces which must be considered in order to control or minimise the wear rate. Limiting factors of the system are the relatively low compressive crushing strength of the particles(minerals) and the yield strength of the surfaces. The broken particles are sharp and can cause deterioration of the metallic surfaces by scratching, plastic flow and microcutting.

Norman[25] has also found that the spread in relative wear rates of various materials when exposed to high-stress open three-body abrasion by hard ores or minerals does not tend to be as great as when it occurs in gouging wear.

2.1.3 Low-stress scratching abrasive wear

This type of wear occurs by very light rubbing contact from sharp abrasive particles. The stresses are due mainly to velocity and are normally insufficient to cause much fragmentation of the abrasive. Examples of this exist in solids-handling equipment such as conveyors, chutes, vibrating screens etc. Since impact is virtually absent the property of toughness as associated with gouging abrasion is not so important, the important properties being hardness together with corrosion resistance, cost and ease of replacement.

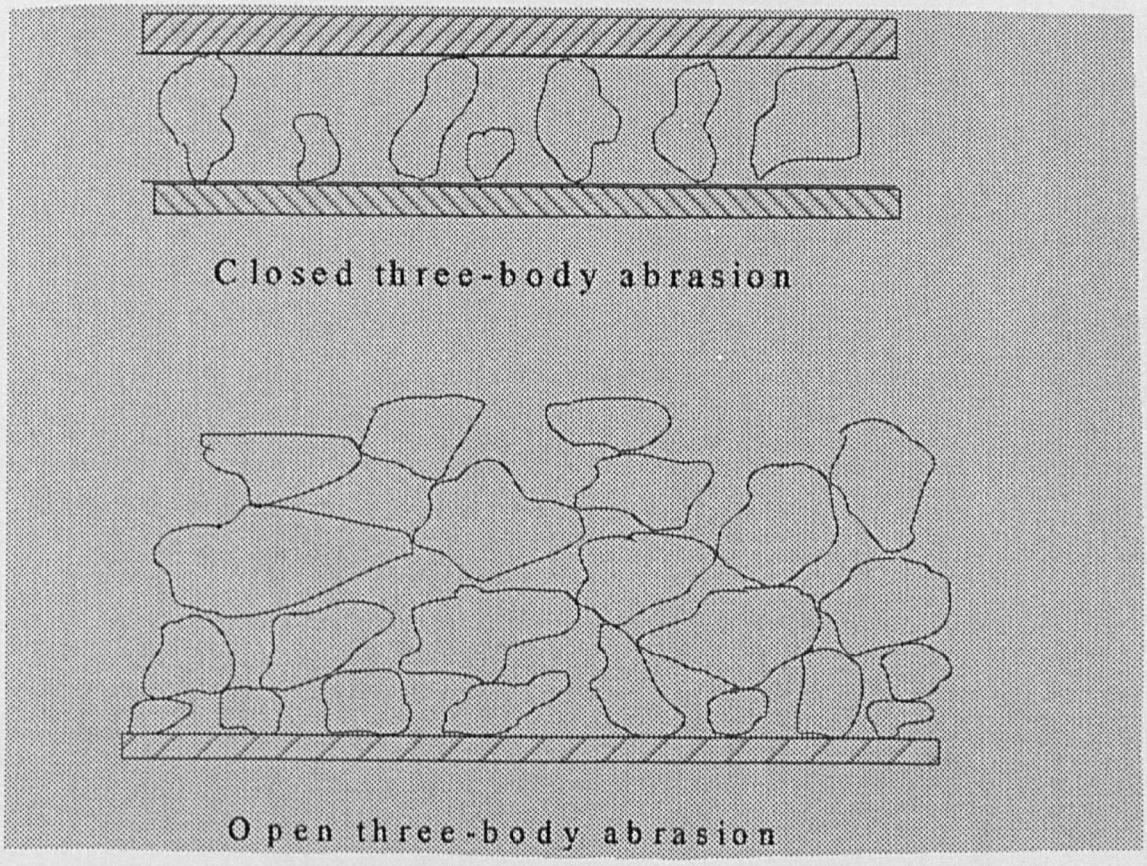

Fig.2.2 : Open and closed three-body abrasive wear

This wide classification of abrasive wear may appear elaborate since the border between different categories is sometimes diffuse. But it is worthwhile because knowing the mechanism of material removal for different types of abrasive wear then the optimum choice of wear-resistant materials can be made.

2.2 Modes of deformation in abrasive wear

Abrasive wear, being the consequence of the cutting or deformation of the surface of one body by the asperities of another, usually harder body or by harder loose particles, can involve surface interactions of two extremes. Under one set of conditions, plastic displacement of surface material may take place without the removal of material from the surface(Fig.2.3)[26,27,28]; at the other extreme, the entire cross-section of the groove may be removed(Fig.2.4)[26,27,28]. The transition between those two extremes goes through the wedge-forming mode(Fig.2.5)[26,27,28].

The first case is *plastic grooving*, often referred to as ploughing, in which a prow is formed ahead of the abrasive particle, and material is continually displaced sideways to form ridges adjacent to the developing groove. In the ideal case there is no detachment of metal from the surface and hence no overall volume loss. In practice, wear in this situation would probably occur as a result of the cyclic variation of stress in the surface layers of a solid. Ludema[29] sees abrasion in this case, if the cutting efficiency is low, as promoted by low-cycle fatigue processes, that is the repeated displacement of ploughed material by a succession of asperities or hard particles.

One important mechanistic concept to arise from the idea of cyclic stress is the delamination theory of wear developed by Suh[30]. This theory, which is only applicable in low speed sliding with no appreciable rise in the bulk temperature of the interface - in order that diffusion and phase transformation be avoided, suggests that as a rider moves over a surface and the latter is plastically deformed, dislocations are generated a finite distance from the surface. This will lead to the formation of voids which, with time, will coalesce. The end result is the creation of a crack parallel to the wear surface(Fig.2.6a,b). When this crack reaches a critical length the material between the crack and the surface will shear, yielding a sheet-like particle. This particle is plate-like with a length often exceeding 10 times its thickness. Typical dimensions are 100-200μm in length.

In a composite metal surface which is created by depositing a thin layer of a softer metal on a harder substrate, heavy plastic deformation and delamination of the substrate may be prevented. This is because in a conventional homogenious material the dislocations are formed and piled-up beneath the soft layer which exists at the outer surface of the wear track, whilst in a composite material the dislocations pile-up at the interface between the deposited metal and the substrate.[31]
Even with high stresses where there will be some transfer to or generation of dislocations in the substrate material, the composite surface will delay delamination of the substrate material.

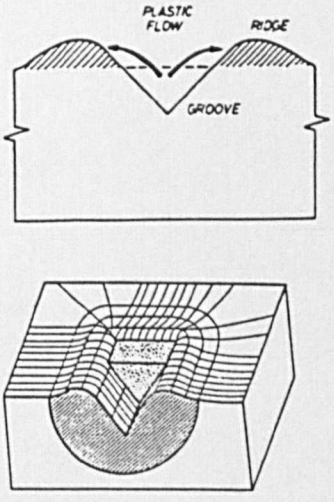

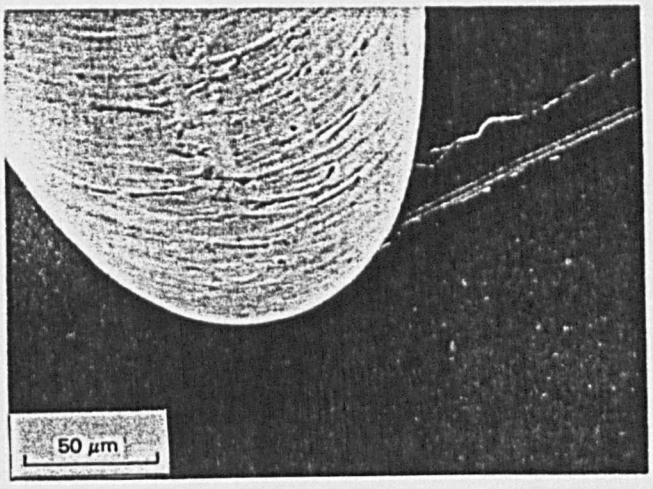

Schematic diagram **SEM micrograph**

Fig.2.3 : Ploughing - mode of abrasive wear deformation[26, 27, 28]

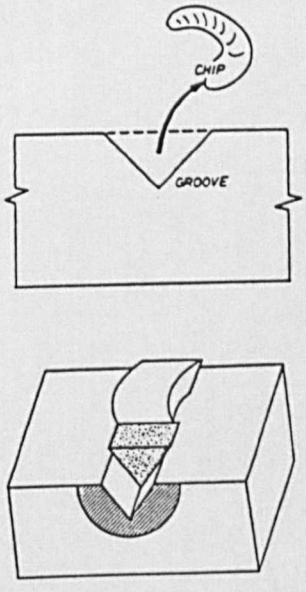

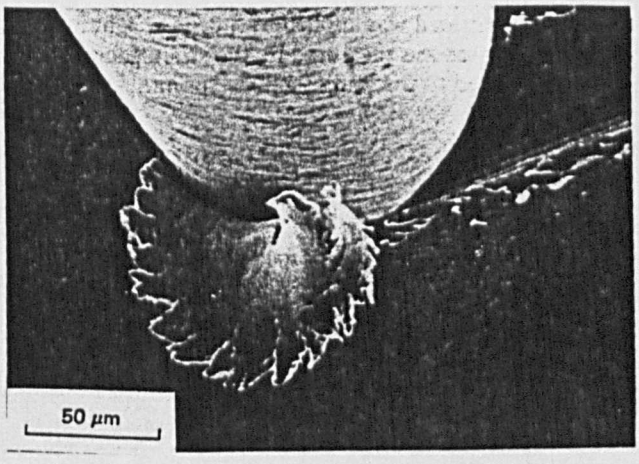

Schematic diagram **SEM micrograph**

Fig.2.4 : Cutting - mode of abrasive wear deformation[26, 27, 28]

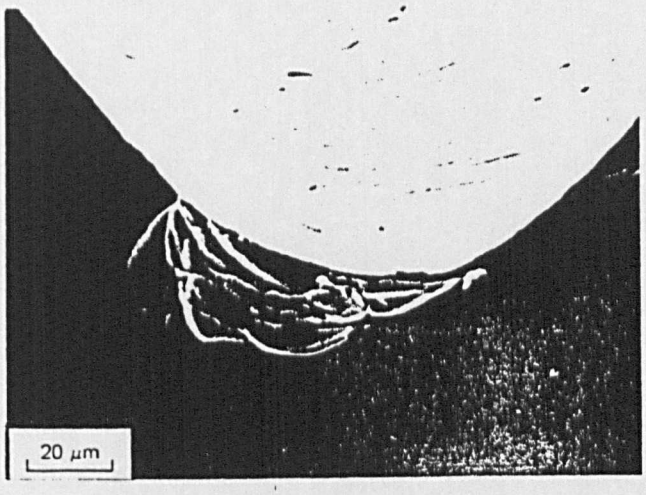

Fig.2.5 :Wedge-forming ; transition between ploughing and cutting[26, 27, 28]

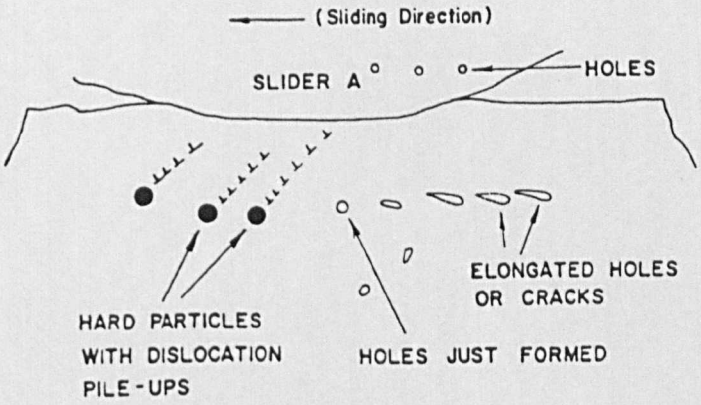

Fig.2.6a :The process of wear particle formation by the shear deformation of voids[30]

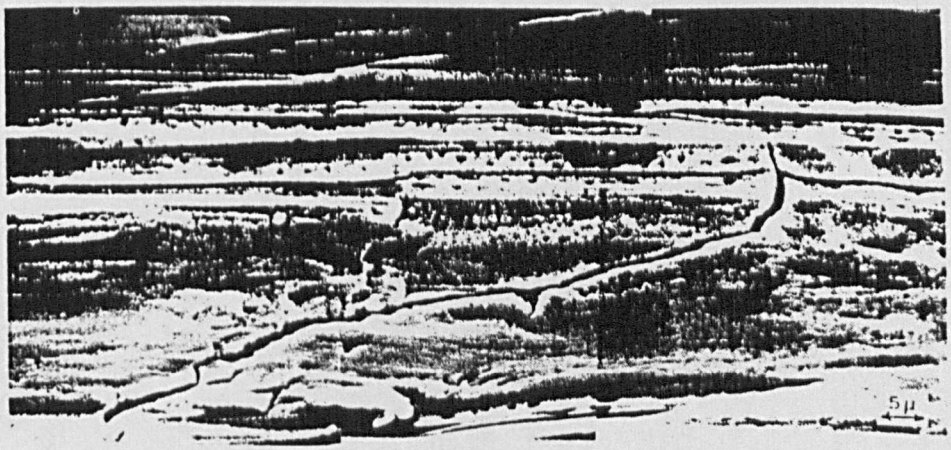

Fig.2.6b :Crack and wear sheet formation at the wear track of a copper specimen(fcc lattice)[30]

In the second case of groove formation, referred to as *cutting*, metal is fully detached from the surface by the mechanism of micro-machining. Again, we can identify an extreme case in which the volume of the groove is equal to the volume of metal in the swarf, and no ridges are left flanking the groove. Total removal of this sort would give rise to the most severe rate of abrasive wear in ductile materials.

In the transition between ploughing and cutting, that of *wedge-formation*, the total amount of material displaced from the groove is greater than the material displaced to the sides. This wedge formation is still a fairly mild form of abrasive wear and occurs when the ratio of shear strength of the contact interface relative to the shear strength of the bulk rises to a high enough level (from 0.5 to 1.0).

Challen and Oxley[32] gave another approach of these two distinct modes of deformation, ploughing and cutting, by using plain strain slip-line fields. Fig.2.7 illustrates a rigid two-dimensional wedge(an idealised abrasive particle) sliding over a rigid-plastic material from right to left. Fig.(2.7a) shows the cutting mode, in which material is deflected through a shear zone and flows up the front face of the particle to form a chip. This mode of deformation is exactly the same as that caused by a single-point tool in an orthogonal machining process, for example in lathe turning. In this mode all the material displaced by the particle is removed in the chip.
Fig.2.7b depicts the other extreme case, the ploughing mode, in which a ridge of deformed material is pushed along ahead of the particle, in much the same way that a wrinkle can be pushed along a piece of cloth lying on a table. In this mode no material is removed from the surface.

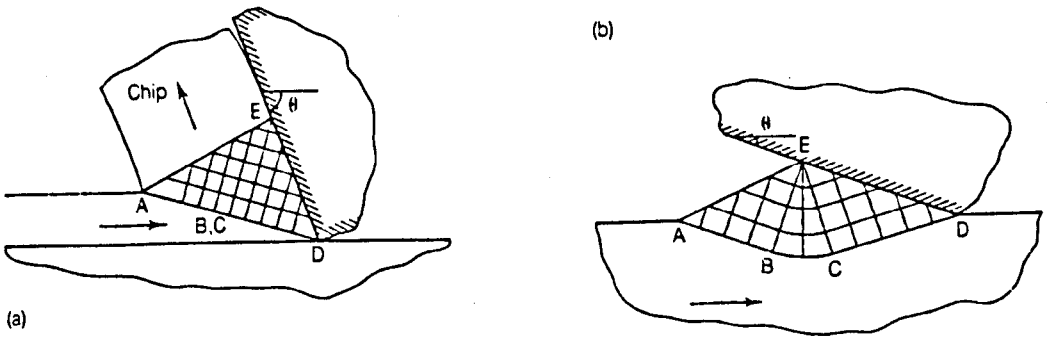

Fig.2.7 : Slip-line fields for the deformation of a perfectly plastic material caused by the sliding rigid two-dimentional wedge [32] a) cutting , b) ploughing

The idealised modes of deformation shown in Fig.2.7 are two dimensional. In practice, abrasive grit particles will cause three-dimensional flow patterns which are much more difficult to analyse, but which are nevertheless analoguous to those previously discussed.

The controlling factors for both modes are θ, the attack angle of the particle, and the ratio f between the shear stress at the interface and the shear yield stress of the plastically deforming material. The transition from ploughing to cutting, occurs at a critical attack angle θ_c which lies between 30° and 90° for most metals.[32]

2.3 Abrasive wear of brittle and multiphase materials

Abrasive wear and chip formation for brittle materials differs radically from that in metallic materials. In this case the material is mostly removed by subsurface cracks formed during the movement of the abrasive particle. These subsurface cracks eventually grow to the surface leading to high abrasive wear due to fragmentation(Fig.2.8).[26, 27, 33]

Khruschov[34] after testing a range of brittle materials found that the wear rate of brittle materials was about 11.5 times higher than the wear rate of an annealed pure metal of corresponding hardness(Fig.2.9).

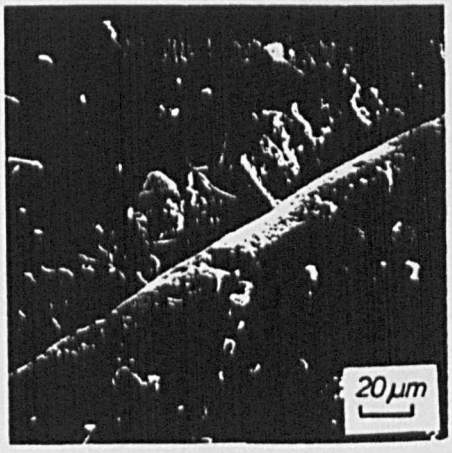

Fig.2.8 : Mechanisms operating during abrasion of brittle materials[26, 27, 33]
SEM micrograph of groove formed in high Cr white iron using Vicker,s scratch diamond

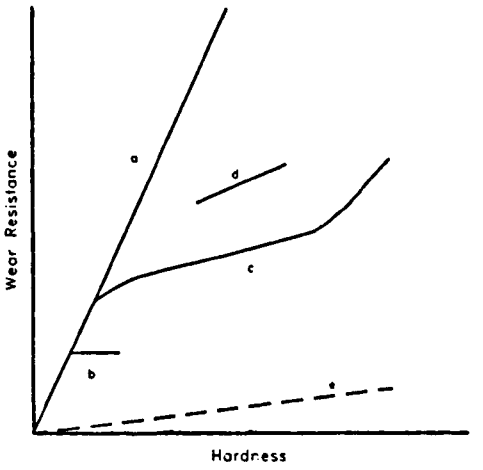

Fig.2.9 : Correlation between the relative wear resistance of some metals and minerals, and their hardness; a-pure and annealed metals; b-cold worked or precipitation hardened alloys; c-quenched and tempered steels; d-ferrous alloys with retained austenite; e-ceramics and minerals.[34]

Although plastic deformation occurs during abrasive wear of brittle materials, fracture is often the rate-controlling mechanism[35]. The mode of fracture as a result of indentation in brittle materials depends on the applied load on the indenter, the shape of the indenter, whether the indenter is sliding or static, and the environment[36]. If the indenter is spherical, fracture often occurs under elastic contact whilst at small radii of curvature elastic-plastic contact occurs because the radius of curvature has a larger effect on the plastic indentation load than on the Herzian fracture load. The critical radius for the transition from elastic-plastic indentation to Herzian fracture increases as the hardness of the material decreases and as its fracture toughness K_c increases.[37] With sharp indenters, pyramids or cones, indentation results in plastic deformation, and fracture does not occur until the indentation reaches a critical size. These plastic indentation phenomena also apply qualitatively to sliding indentation but with reduced loads required to produce fracture. In both cases fracture may be enhanced in certain environments; for example by the presence of water or humid air, or acidic solutions on glass[38].

In the abrasive wear of multiphase materials containing both ductile and brittle phases, fracture may also occur. The predominant material removal mechanism will depend on the properties of the individual phases and on their volume fractions.

Wang and Hutchings[39] in their investigation showed that both the volume fraction of the reinforcement and the size of the abrasive particle, plays a significant role for the relative wear resistance of a metal-matrix composite. For small abrasive particles, the highest volume fraction of reinforcement gave the highest wear resistance whilst with larger abrasive particles, fracture of the fibres occurred and the benefits of reinforcement were limited. They also found that for volume fractions greater than about 20% further reinforcement actually led to a reduction in relative wear resistance.

Tongjiawin et al[40] showed that for composite alloys comprising hard reinforcements (WC) in a soft Cu-Ni-Mn matrix, the wear resistance was different under two-body wear

conditions and three-body wear conditions. These differences observed in wear resistance of composite alloys under different wear conditions must be associated with the wear mechanisms. Under two-body wear conditions the abrasive, fixed to a rigid back plate, makes contact mainly with the hard tungsten carbide of the alloy which protects the matrix and relieves wear. In turn, the matrix could support the brittle tungsten carbide and prevent fracture. But for the three-body wear conditions, selective wear of the matrix and consequently digging or fragmentation of tungsten carbide occurs(Fig.2.10).[40]

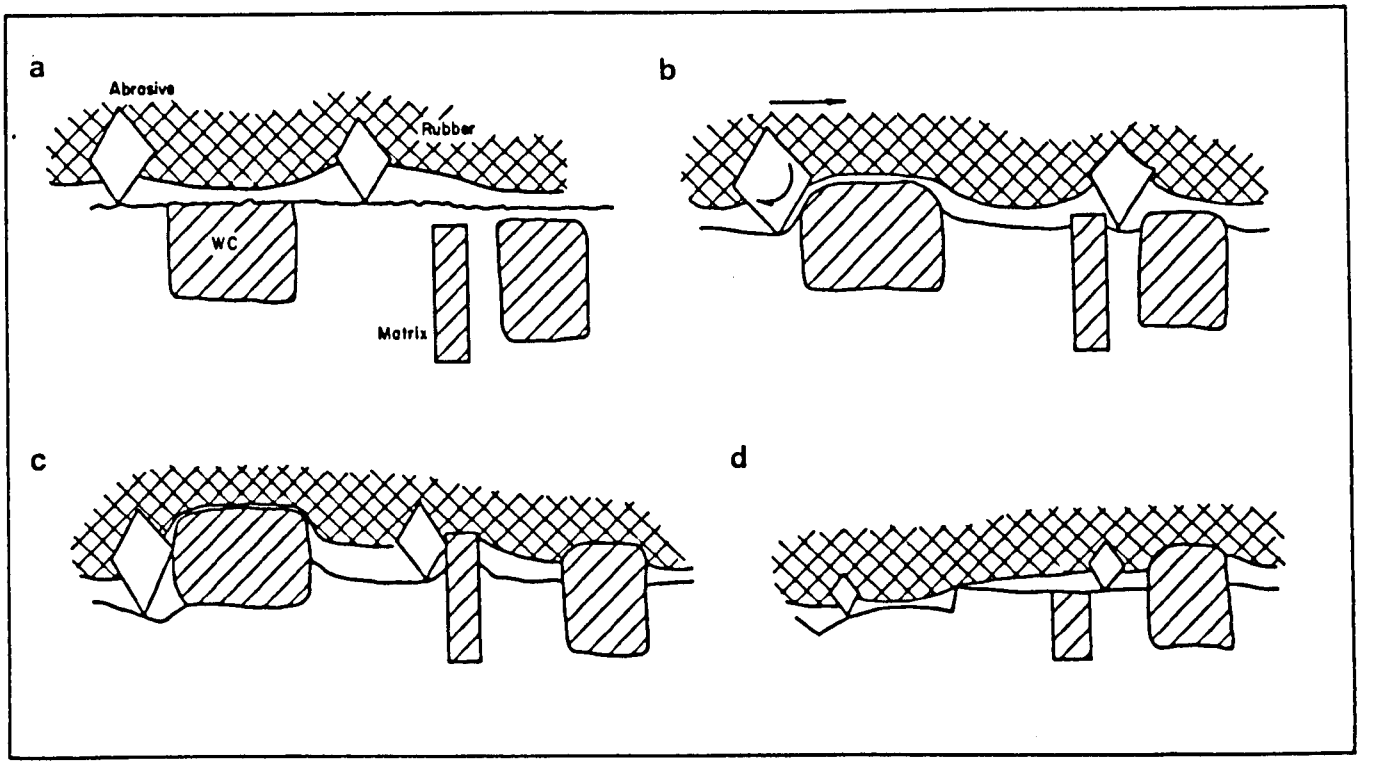

Fig.2.10 :Schematic wear process for a composite alloy under rubber wheel wear test [40]
a - b - c :selective wear of the soft matrix d:fracture of the protruded carbides

Also the difference in the distribution of load over the particles is illustrated in Fig.2.11. With compliant support(Fig.2.11a), particles in contact with regions of the hard ceramic reinforcing phase can deflect the support and therefore will indent the surface of the composite to a much smaller extent than those pressing against regions of the softer metallic matrix.

With a rigid support(Fig.2.11b), in contrast, the indentation depth of all the particles must be the same, and so a much greater proportion of the total load is carried by the particles in contact with the reinforcement. The overall normal load on the system at which fracture of the reinforcement occurs would therefore be expected to be significantly lower with rigid support of the abrasive particles than with the compliant support.

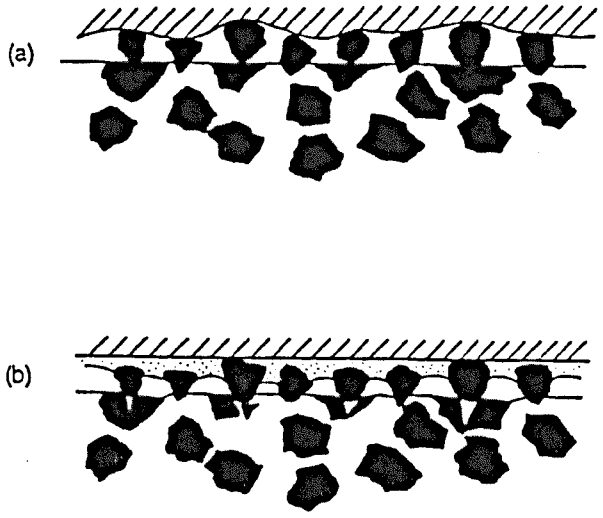

Fig.2.11 : Illustration of the effect of the compliance of the abrasive support in two-body abrasion. If the support is compliant, as at a) the particles in contact with the hard reinforcing phase can deflect the support and thus carry less of the total load than if the support is rigid b) fracture of the reinforcement will occur at a lower total load with a rigid support than with a compliant support[39]

Wang and Hutchings[39] also stressed another point which is very important in determining wear rates of metal-matrix composites. The dimensions of the contact area of each abrasive particle, compared with the scale of the reinforcement, will determine whether the composite responds heterogeneously to particle contact, as illustrated in Fig.2.12[39] or whether it acts effectively as a homogeneous solid. In the first case, shown in Fig.2.12(a), the particle contact zone is appreciably smaller than the reinforcement size, and individual elements of the reinforcement can be considered to act independently. Under these conditions a relatively high wear resistance compared with that of the matrix may result if fracture of the reinforcement is avoided. However, if the microstructure of the composite is much finer than the scale of the contact zone, as in Fig.2.12(b), then even if the reinforcing phase does not fracture it will simply be removed by ploughing and cutting along with the matrix, and no major benefits of reinforcement can be expected, apart from those associated with the small increase in bulk hardness.

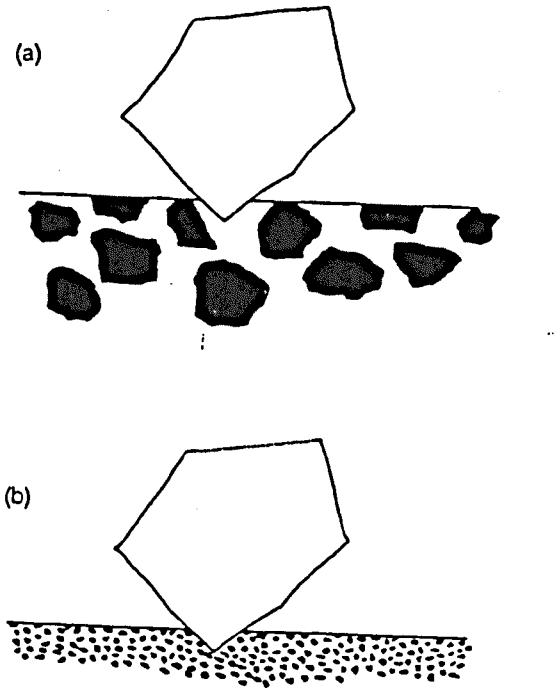

Fig.2.12 : Illustration of the importance of the relative scales of the particle contact zone and the reinforcement (a) if the particle contact area lies within individual regions of the reinforcement, the response of the composite will be heterogeneous (b) if the particle contact area encompasses many regions of the reinforcing phase the response will be homogeneous [39]

2.4 Influence of experimental parameters on abrasive wear

The incosistencies in the abrasive wear of metals determined by different authors necessitates a detailed investigation to determine the possible relationships between the abrasive wear of metals and the experimental parameters which influence the abrasive wear. The parameters can be classified as[41]: properties of the abrasive and other variables within the system.

2.4.1 Abrasive properties

The role of the abrasive is to concentrate stress, which may dominate as shear, tension or compression. Important qualities are: shape, size, orientation, velocity, load, path length and hardness of the abrasive.

2.4.1.1 Abrasive shape, hardness, orientation

Moore [42,43] reviewed the properties of the abrasive. Abrasives are usually inert oxides which

can fracture under stress to produce sharp angular fragments. He found that abrasive type and its hardness relative to the abraded surface does not influence wear resistance, except when the two surfaces have approximately equal hardness. This agrees with findings by Khruschov and Babitchev.[44] However, Nathan and Jones [45] found that even with very hard abrasives the volumetric wear still depends on the abrasive hardness.

The shape of the abrasive particle is important in that it influences the transition from elastic to plastic contact. Barwell[20] reported that wear rate is higher for *'sharp'* pointed abrasives than for *'blunt'* rounded ones. Abrasion increases as the particle becomes less platelike and thus has less chance of lying flat. Also from practical applications it is well known that sharp particles are likely to produce more chips whereas spherical particles lead to more wide-spread plastic deformation.

The orientation of the abrasive can influence the formation of wear debris. Mulhearn and Samuels[46] showed that chips are only produced when the contacting face of an abrasive grain makes an angle greater than the *'critical attack angle'* with the wearing surface. A transition from ploughing to microchip formation occurs when the critical attack angle is exceeded.

2.4.1.2 Abrasive velocity, load, path length

Larsen-Basse[47] observed that a linear relationship exists between wear rate and abrasive path length after the running-in period. Wear rate is also directly proportional to nominal load up until the load where the abrasive is being crushed. The wear rate per unit load decreases with load and is a function of the material.

Moore[42] reported that wear increased slightly with sliding speed in the range from 0-2.5 m/s.
Allen et al [48] found austenitic stainless steels to be very velocity sensitive in the range 0.02-0.45 m/s. This was not true for other grades of stainless steel and mild steel. They explained their findings in the light of the ability of microstructures to accommodate the high strains without fracture.

2.4.1.3 Abrasive grit size

The dependence of the rate of material removal on the abrasive particle size is an important characteristic in abrasive, erosive, grinding and metal cutting processes. Fig.2.13[45] demonstrates that the volume wear rate of different materials, in two body abrasive wear, increases sharply with grit size to some critical size and then increases at a reduced rate or becomes constant with increasing grit size. The same conclusion can be reached from Fig.2.14[49] for a copper specimen in three-body abrasive wear. Also Fig.2.15 [50] shows the same effect on erosion. This critical abrasive particle size is usually between 50 and 100μm. Beyond this critical abrasive size the wear rate becomes much less sensitive to the particle size. This is very fortunate because it is very difficult to filter out small particles.

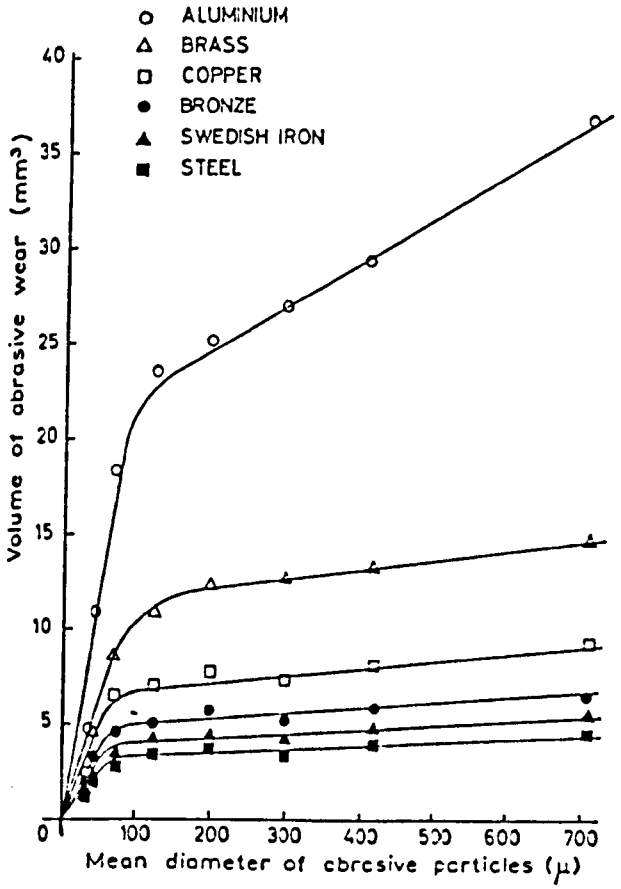

Fig.2.13: The relationship between the volume of abrasive wear and the mean diameter of abrasive particles, at a load of 2 kg, abrasive path 6m and velocity 0.5 m/s(two-body abrasive wear)[45]

This behaviour has been studied and possible explanations have been given by many investigators[51, 52, 53]. However, what is intriguing about the *size effect* phenomenon is that it does not agree with the basic theoretical model(Archard) for abrasion discussed in chapter three, according to which the wear rate should be independent of the abrasive particle size. In erosion, a theoretical model developed by Finnie[52] also predicts that the wear rate should be independent of the abrasive particle size.

A more recent modelling approach [54] using a low-cycle fatigue mechanism and a Monte Carlo simulation technique has been used to predict the effect of particle size distribution in erosion, successfully. The wide range of particle sizes, 80-600μm used and the very good fit of the measured and predicted values suggests that the abrasive particle size plays no significant role in erosion.

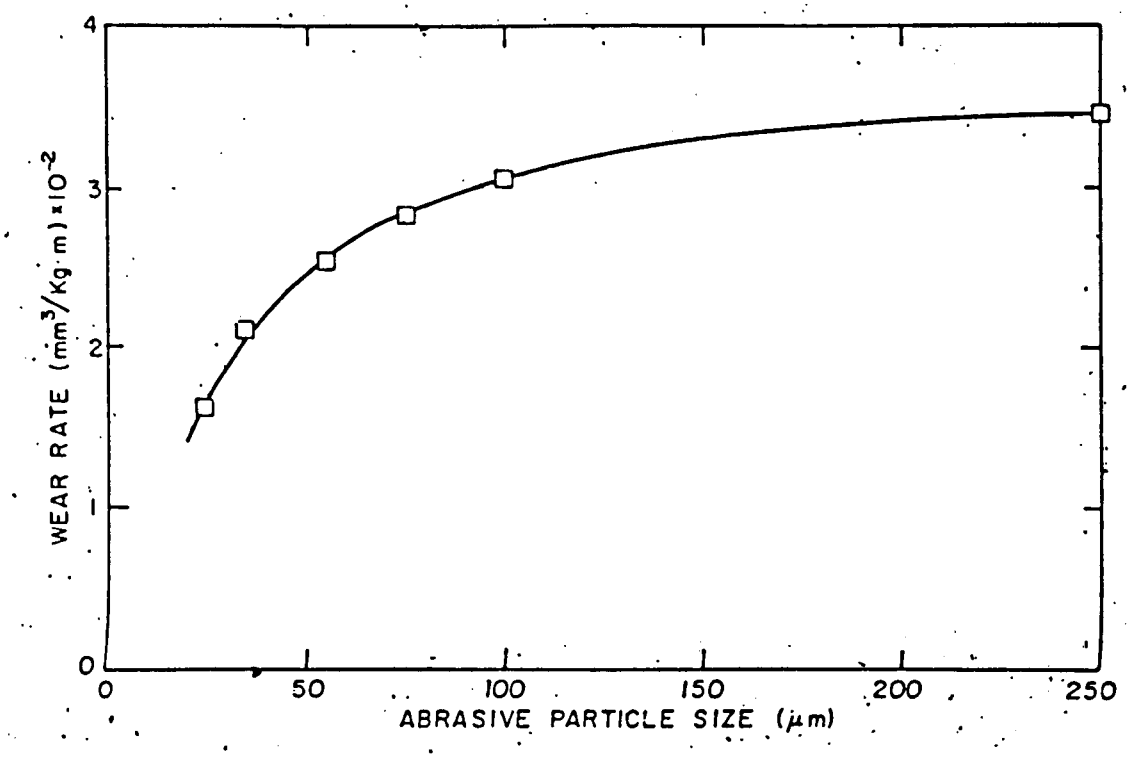

Fig.2.14 :Wear rate as a function of abrasive particle size for copper sample(3-body abrasive wear)[49]

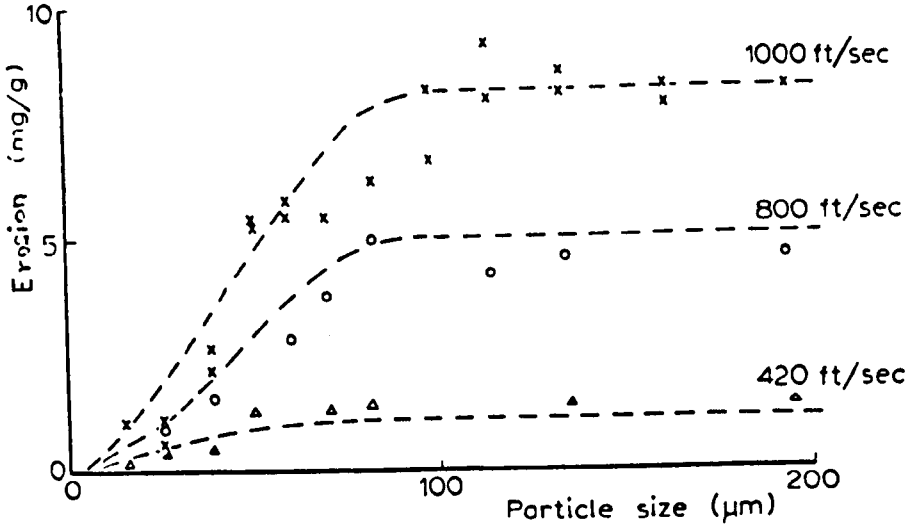

Fig.2.15 :Wear rate as a function of abrasive particle size at different velocities(erosion)[50]

Among the mechanisms which have been proposed by researchers are:

a) abrasive grit damage - Mulhearn and Samuels[46] relate *size effect* in abrasion to the abrasive grit wear and damage which as they argue becomes more intense at small grit size. Larsen-Basse[47] suggests that the size effect is due to attrition and wear of abrasive grains which lead to an increase in the fraction of the load carried by grains in '*non-cutting*' contact with the surface as the size of the abrasive particle decreases.

b) clogging - Avient, Goddard and Wilman[55] after experimenting with abrasive papers of different mean particle diameter under repeated pass condition, proposed that the *size effect* is due to the clogging of finer abrasive paper and also due to the excessive pick-up of abrasive particles by the metal surface for finer grit sizes. After clogging occurs abrasive wear is greatly reduced.

c) adhesive wear particles - Rabinowitz and Mutis[21] have proposed that the critical *size effect* is due to the interference between adhesive and abrasive particles. If the abrasive particles are smaller than the particles produced by adhesive action then the formation of adhesive wear particles prevent the abrasive from coming in contact with the material to be abraded and there is consequently very little abrasive action.

d) elastic contact - Date and Malkin[56] support the elastic contact theory which first was introduced by Larsen-Basse[47], who after observing that an increase in the applied load mainly leads to an increase of the number of grooves formed while the average groove width varied slightly, concluded that the smaller size particles are only in elastic contact with metal and thus only support the applied load without contributing to material removal.

e) ploughing - Experimenting with coated abrasives and spherical tools Malkin et al[57], have argued that the *size effect* arises because for smaller particles the material is ploughed and is displaced sideways and is not removed as chips. As the undeformed chip thickness is decreased, relatively more ploughing and less chip formation occurs.

f) high temperature - The role of heat generation due to scratching explains the *size effect* on the basis of the rise in temperature as Van Greonon[58] has argued. The abraded material softens due to heat generation caused by plastic deformation during ploughing and this softening produces the size effect because the depth of cut determines the amount of material heated and the rise in temperature.

g) abrasive tip radius - Rabinowitz[21] examined the effect of abrasive tip radius on the size effect and showed that the tip radius was not responsible for the *size effect*. Suh et al [59]feel that this phenomenon, in abrasion, was due to rounded edges of the abrasive grains.

h) strain rate effect - Larsen-Basse and Oxley[60] showed that in chip removal processes, as the depth is decreased, the strain rate is increased. This results in an increase in the flow stress of the work hardening material which in turn increases the specific cutting pressure, thus showing a *size effect*.

2.4.1.4 Evaluations of size effect explanations

As mentioned previously the size effect is not only associated with one process but it is observed in abrasion, erosion, grinding and metal cutting. It is therefore clear that any explanation for size effect should be valid for all processes because in some cases what is applied to one process is completely inappropriate to another.

Starting with the explanation given by researchers[55, 59] for size effect in two-body abrasion which was based on clogging of the abrasive paper. This explanation cannot be used as a

general one because for three-body abrasion and erosion clogging is not possible.
Other investigators[46, 47, 61] invoked the mechanism of abrasive grit damage to explain the size effect. They argued that the size effect is due to abrasive particle damage and wear which increases as the abrasive paricle size decreases. Date and Malkin[56] after an extensive study of worn coated abrasives under SEM, showed that the larger particles were damaged more. This is not unexpected because there is an increased probability of finding flaws in bigger abrasive particles than in the smaller ones. The same conclusion was reached by Tilly and Sage[62] in erosion.

Thus, if the size effect is really due to damage of the abrasive grit, then the critical size should change with change in load in abrasion and velocity in erosion. From Fig.2.16[63] it can be seen that the critical abrasive size does not change with change in the applied load.

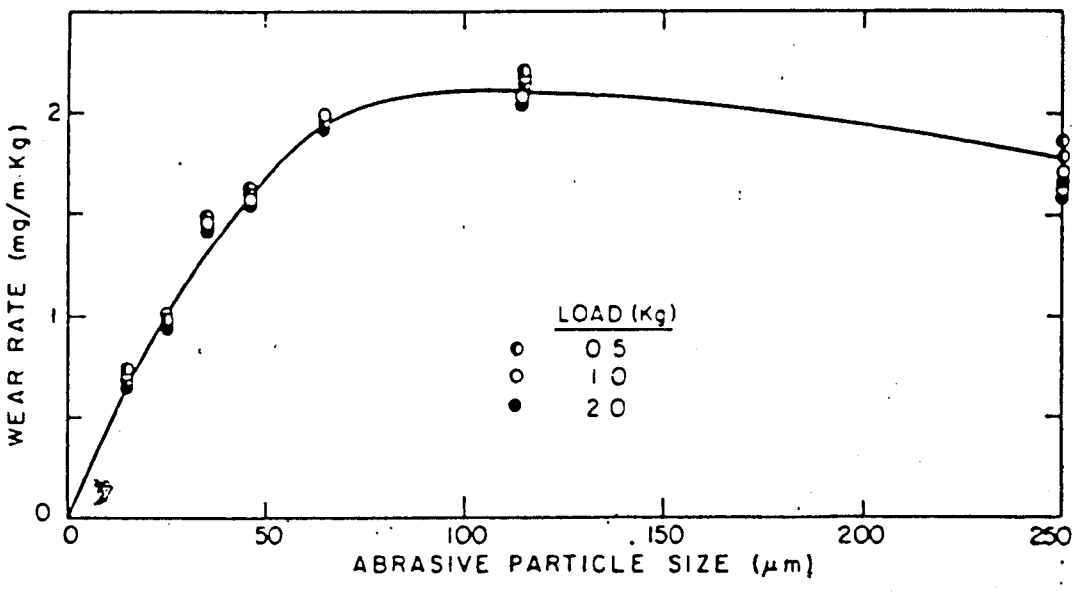

Fig.2.16 :Wear rate as a function of abrasive particle size for AISI 1020 steel samples abraded under two-body wear conditions with different applied loads [63]

In erosion, Fig.2.15[50] there is a slight increase in critical size with increase in the velocity which is attributed to the secondary erosion due to the fragmentation of abrasive particles for larger abrasive sizes rather than for smaller ones. Therefore it is clear that the size effect would still be present even if there was no fragmentation or damage to the abrasive particles. This is confirmed by single point tool metal cutting where there is hardly any damage and still a size effect is observed. As a conclusion the size effect can not be associated with the fragmentation of the abrasive grit.

The explanation given by Rabinowitz and Mutis[21] that the critical size effect is due to interference between adhesive and abrasive particles fails completely in erosion where there are no adhesive wear particles to prevent material removal by small particles.
The explanation given for elastic contact, that the smaller particles are under elastic contact and therefore they do not remove much material must be rejected because, if this is true, then by increasing the load the critical size should increase. But Fig.2.17[64] shows that this does not happen.

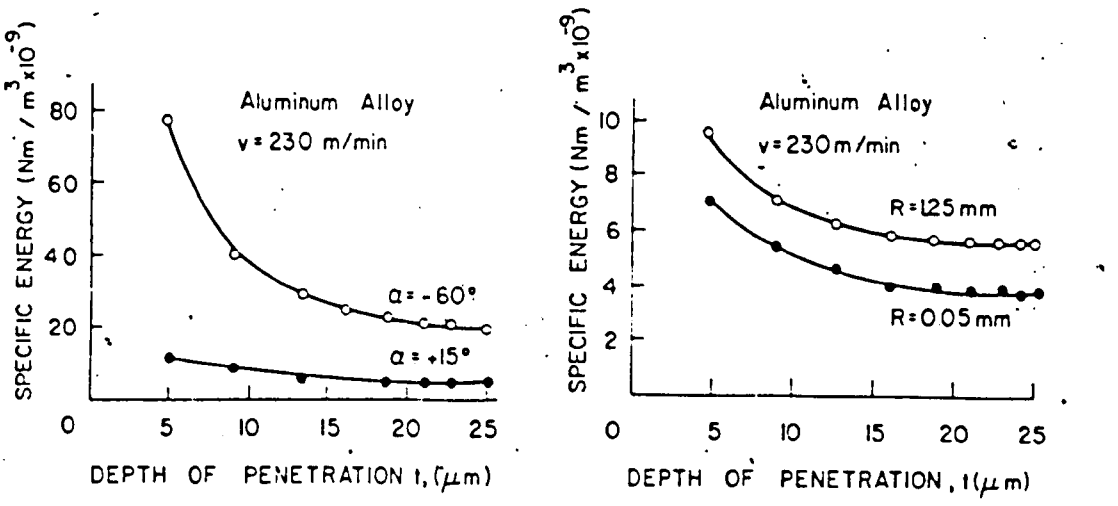

Fig.2.17 :Specific energy as a function of depth of penetration in cutting processes; (a) for pyramidal tool of rake angle x (b) for spheroidal tool of various R [64]

There is a rise in temperature in any material removal process but this seems to be a minor factor in the size effect, because if the temperature rise is the reason for size effect, then at low speeds the critical particle size should change which does not happen as can be seen in Fig.2.18.[63]

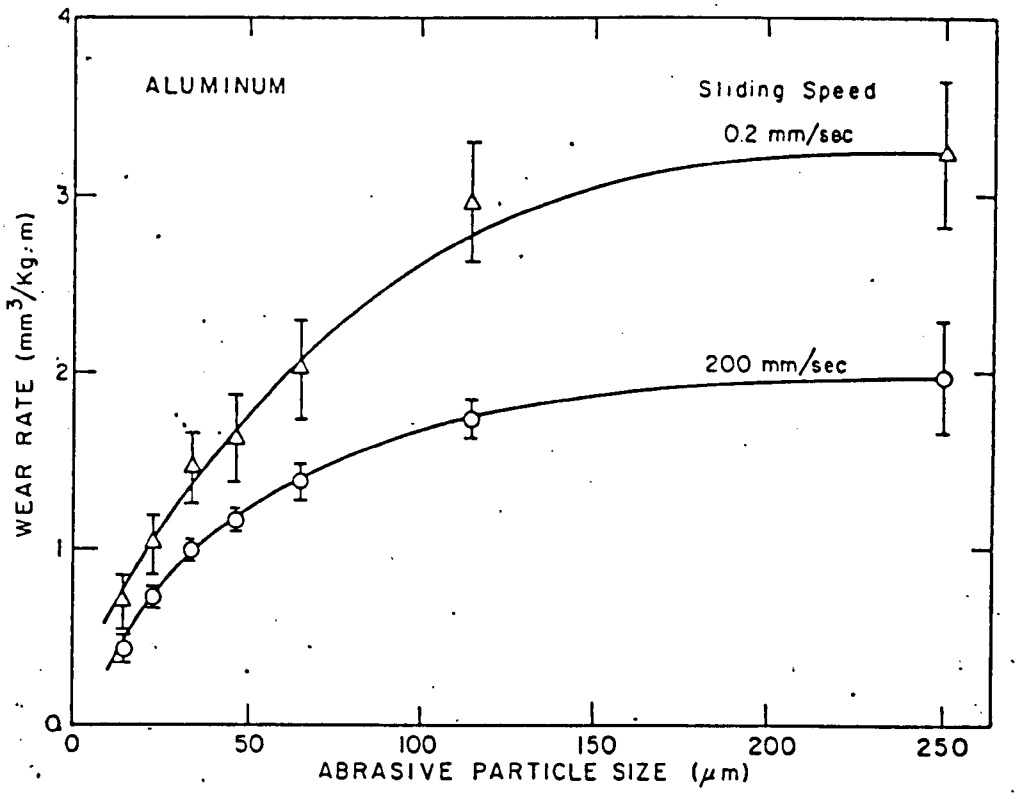

Fig.2.18 :Wear rate as a function of abrasive particle size for annealed aluminium at two different sliding speeds [63]

In refering again to Fig.2.18, the effect of strain rate on size effect can be evaluated. As the figure shows the size effect is observed at all speeds and the critical particle size does not change, though the total wear rate increases in magnitude for the lower speeds. This is evidence that the size effect can not be entirely attributed to strain rate and it seems that it only changes the magnitude of the wear resistance according to Larsen-Basse[65].

For the evaluation of the effect of ploughing on size effect, the arguments by Misra et al[63] could be recalled who looked at abraded surfaces by different sizes of abrasives under SEM for two-body abrasion. They insisted that the wear tracks look quite alike for different abrasive sizes and not much increase in ploughing was observed with decrease in abrasive size, showing that ploughing may be partly responsible for the size effect but unlikely to be a major contributor.

Finally the argument by Suh et al[66] that the size effect is due to abrasive tip radius because as they argued, finer abrasives have rounder tips and therefore they plough the material rather than cut it. If this is the case, then the critical size should change dramatically with the change of the tool tip geometry. Fig.2.19 shows loose abrasives for different sizes and an abrasive paper surface. It can be seen that most of the abrasives are not conical but of polyhedral shape, and tip geometries look similar for different abrasive size.

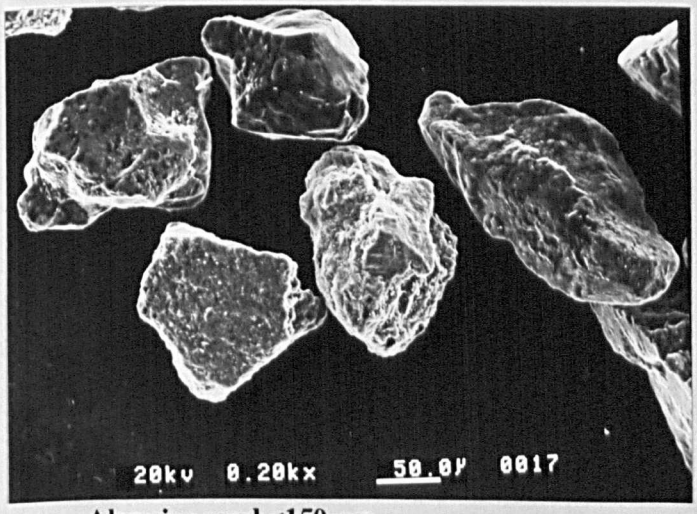

Abrasive sand <150 µm

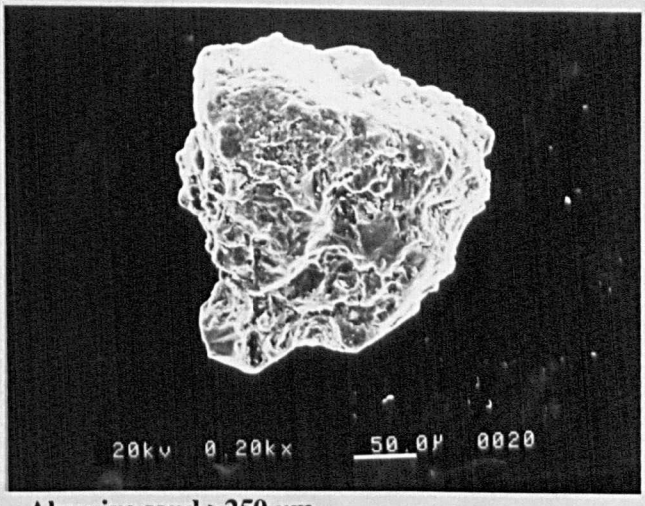

Abrasive sand >250 µm

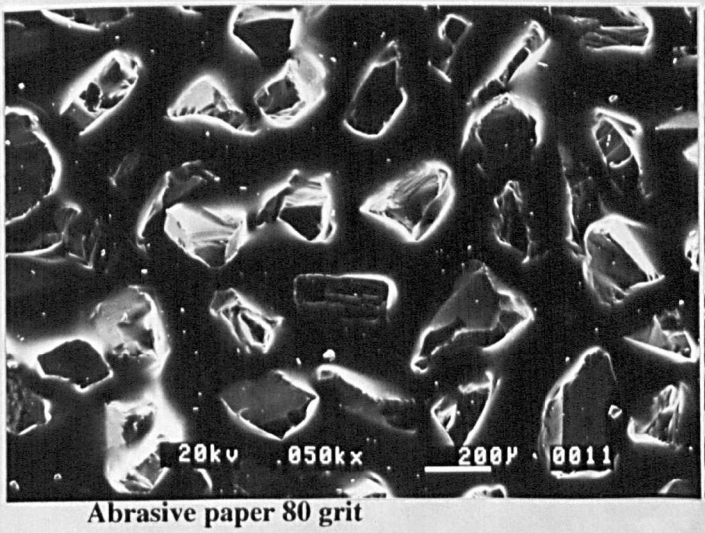

Abrasive paper 80 grit

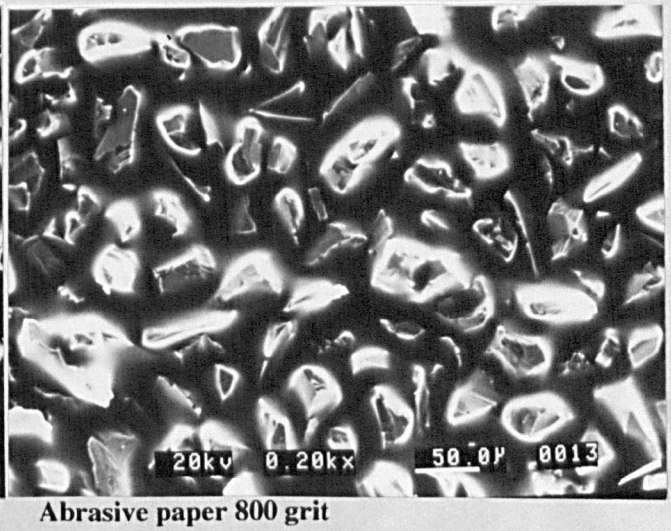

Abrasive paper 800 grit

Fig.2.19 : SEM photographs of loose abrasives and abrasive paper

Since the size effect is observed in so many processes, it should be due to some material property or rather surface properties of a material. Two explanations related to surface properties exist.
The first one is the observation by Kramer [67] that the surface layer work hardens more compared to the bulk material. This hard *debris layer* is about 50-100μm in depth. When small particles abrade the surface they only influence the hard layer while larger particles also deform the material below the debris layer. After some critical particle size, the influence of this debris layer will be slight, and therefore there will be no increase in wear rate for a further increase in particle size. The hard debris layer was contradicted by Fourie [68] who experimenting with copper, found that the flow stress in the interior becomes greater than that in the surface. Thus a soft surface layer is formed instead of a hard one, which is about 2mm deep.

The second explanation by Marsh [69] and Fischer [70] is based on the dislocation tangles near the surface. In abrasion and erosion the surface develops grooves and craters which act as notches and produce high stress concentrations under load with short range stress fields. As a consequence the surface of an abraded specimen provides an easy source of dislocations which are responsible for plastic deformation of the surface in abrasion and erosion. The pile-up of these dislocations will cause stress that will activate secondary slip systems. This, along with the tangles will cause a preferentially work hardened layer near the surface.

The observation by Moore [61] that the plastic strain near the worn surface is about 2.5% at a depth of 2.5μm for abrasion, along with the above discussion of dislocations, makes clear that the surface after abrasion will have a preferentially hardened layer around 10μm deep.[67] Small particles would only be able to influence this layer, whilst larger ones which can penetrate the hard layer will plastically deform a material which is softer than the one encountered by small particles. This means, that after some critical size, the influence of this hard layer on material removal will be slight.
From all the previously mentioned explanations of the size effect, the last one seems to be more convincing.

2.4.2 The effect of variables other than the abrasive

2.4.2.1 Load

Several investigations[45, 71] have shown that volumetric wear is directly proportional to the nominal load up to a critical load which is determined by the onset of massive deformation of the specimen or degradation of the abrasive surface. Nathan and Jones[45] found that deviation from linearity occurred at lower loads for the smaller grit sizes.

Richardson[72] reported that, although the volumetric wear increased linearly with load, the relationship was such that the wear/unit load decreases as the load increases.

2.4.2.2 Length of wear path

Experiments conducted by Nathan and Jones[45] have shown a linear relationship between volumetric wear and the length of the abrasive path with hard abrasives.
Richardson[72], has found that the shape of the curve depends on the relative hardness of the wearing material and the abrasive, because with soft abrasives the wearing material takes much longer to strain harden to equilibrium conditions.

2.4.2.3 Specimen size

In abrasion wear testing specimen size has been found to affect abrasive wear in various ways. It is usual practice to choose a specimen size such that deterioration of an abrasive grain in contact with the specimen is minimal.
Avient, Goddard and Wilman[55] have pointed out that it is important to use a short enough specimen such that the amount of metal worn off by an indenting grain is not enough to fill interstices between it and adjacent particles, which would reduce the effectiveness of the abrasive.

2.4.2.4 Abrasive flow rate, humidity

Experiments were carried out in which the flow rate was varied [73]. When two different batches of Al_2O_3 with the same specification from the same manufacturer were used, they yielded a 10% difference in wear rates. The change in wear rate was also found to be small for small changes of the abrasive flow rate, for the same abrasive material. Even when abrasive grains were collected during one run and used during a second run, this did not change the wear rate significantly.

However, when two batches of the same material but from different manufacturers were used, the wear rates were different by about 50% when tested on the same specimens. This effect was attributed to statistical differences in either shape or mechanical properties of the abrasive. Also this highlights the need to characterise abrasive particles.

Larsen-Basse et al [74] tested Cu, Al, 1040 Steel in two-body abrasion and found an increase in wear rates between 0-65% r.h.
Larsen-Basse [75] testing a number of materials in three-body abrasion by SiC abrasives, found a sharp increase of wear rates with humidity above ambient conditions while there was little effect below this point. This effect was primarily attributed to moisture-assisted fracture and self-sharpening of the abrasive grains.

2.4.3 Relationships between materials and abrasion

2.4.3.1 Mechanical properties

Numerous publications exist in the literature where researchers tried to relate abrasion

resistance to a measurable mechanical property.
Moore[42] found that elastic modulus and the elastic limit of strain are inversely proportional to the wear volumes for pure metals but not for heat treated steels.

Zum Gahr[76] identified the different properties of a material which would influence friction abrasive wear, as flow pressure or hardness, work hardening rate, ductility, crystal anisotropy and mechanical instability. Resistance to elastic/plastic strain or hardness together with work hardening determine the contact area between an abrasive particle and the material.

Richardson[77] attributed the high ductility at the abraded surface to the presence of hydrostatic pressures and compressive residual stresses.

Diesburg and Borik [78] observed how little is understood of the relationship between abrasion resistance and toughness. They showed that for wrought and cast low alloy steels, a decrease in toughness improved the abrasion resistance. A notable exception is the austenitic manganese steels where a great improvement in toughness may be gained without affecting the high stress abrasion resistance found in crusher jaws. The microstructure of these steels is known to be unstable to mechanical deformation.

2.4.3.2 Bulk hardness

Khruschov [34] in Fig.2.9 showed that the wear resistance of pure annealed metals and some alloys is directly proportional to the Vicker's hardness while different relationships apply for hardened and tempered steels.
Rubinstein[79] has shown that relative wear resistance is related to hardness by the reciprocal of the hardness of the standard material.
Richardson[72] also showed that impurities and alloying elements in the pure metals do not produce increases in wear resistance proportionate to increase in hardness.

Richardson [77] found that the surface hardness of an abraded metal is considerably higher than its bulk hardness. He suggested that the abrasion resistance of a metal might correlate better with its hardness in a very heavily worked condition.
Garrison and Gariga [80] argued that a knowledge of the surface hardness is insufficient to predict abrasion resistance.

Moore[42] pointed out that a high degree of strain hardening occurs at the surface. That is, wear is dependent on the strength of the material in its maximum work hardened state and this would be a function of its attained surface hardness. This can only be related back to bulk hardness within a narrow group of materials where the rate of strain hardening is shown to be a function of the bulk hardness- as in the heat treatment of a plain carbon steel.

Moore [42, 43] explained the limiting strength (maximum hardness) attained at the worn surfaces in terms of metallurgical structure. He suggested it is a measure of the maximum dislocation density that can be stored by the material under the stress system developed during abrasive wear and before fracture occurs. The extent of surface hardening is large for pure metals where the nucleation of cracks is limited to dislocation interactions. On the other hand, the extent of strengthening is low for martensitic steels which have a high

probability of pre-existing cracks or crack nucleation sites. He concluded that abrasive wear has to be defined more in terms of the flow and fracture properties of a material and its metallurgical structure rather than surface hardness.

Despite the inadequacies, the hardness of a material is the most important mechanical characteristic for describing the contact surface between an abrasive particle and the surface of a material. The static penetration of an abrasive particle into a softer surface is analogous to the process of hardness testing. As a conclusion, although hardness is an inadequate measure of abrasive wear resistance, it will continue to be used to predict results within a narrow class of materials.

2.4.3.3 Work hardening during abrasion

Work hardening or strain hardening is defined as an increase in hardness and strength caused by plastic deformation at temperatures below the recrystallisation temperature. Cold work is the operation of producing such deformation and the resulting permanent strain.

A measure of the work hardening ability of a material is given by the strain hardening exponent, n, normally determined from a tensile test and defined in the equation:

$$\sigma = C \epsilon^n \qquad 2.1$$

where: σ = Flow stress, C = strength coefficient, ϵ = true strain,
n = work hardening exponent

Work hardening is related to the restraint to shear or slip so pure fcc metals do not harden as extensively as bcc metals. It is also a strong function of purity. The values of the work hardening exponent 'n' can be obtained from tensile tests or obtained by indirect means using abrasive wear data.

Moore et al [81] found that the extent of strain hardening is a maximum for pure metals and is decreased by the addition of substitutional elements.

Ball [82] described the advantage in having a material with high work hardening capacity for abrasive wear resistance. He argued that a material with a moderate yield strength but high work hardening capacity is able to respond plastically to the impact loading associated with abrasion(Fig.2.20). He described how a rising stress-strain curve(the post yield region) reduces the chances of wear loss for a given stress distribution of abrasive strikes. Wear would only occur after work hardening has proceeded to the limit and ductility has been exhausted. Fracture at the surface then occurs because the imposed stresses are exceeding the maximum attainable limits in material strength and strain accommodation.

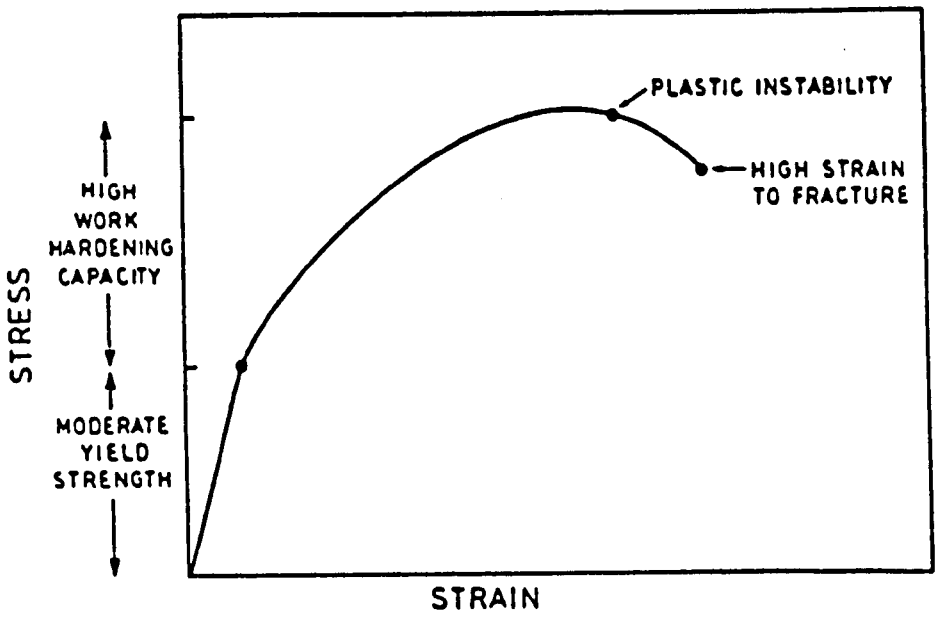

Fig.2.20 :Schematic stress-strain curve illustrating the good strength and ductility found in a material with a high work hardening capacity. [82]

Prior cold work has an effect on abrasion resistance because work hardening is inherent in the abrasion process. Avery [83] found no statistically significant benefits from prehardening by cold work under high stress abrasion, grinding or gouging conditions.
Allen et al [48] found prior cold work to be detrimental to the abrasion resistance of austenitic stainless steels.

2.4.3.4 Microstructure

Work hardening has been found to be a maximum for pure metals but alloying does increase the materials ultimate tensile strength and micro-fracture properties. The decrease in work hardening by the addition of substitutional elements can be minimised through microstructural control.
Moore et al [81] identified four classes of materials according to their response to an applied flow stress at high and low strain.

- Pure metals show the highest degree of strain hardening.

- Substitutional solid solution alloys which increase the material strength by solute atom/dislocations interactions. They strain harden less than pure metals.

- Interstitial atoms can support a high dislocation density and offer a powerful obstruction to dislocation movement but the strain hardening of the material is limited. There is an increased probability of crack nucleation and fracture.

- Precipitation and dispersion hardened alloys with very limited ability for strain hardening.

Materials with a fully martensitic microstructure do not fall within any one class but are a combination of all the above mentioned strengthening mechanisms. Bryggman [84] observed that a ferrite-pearlite microstructure had a lower specific grooving energy than the same material in a martensitic structure.

Diesburg and Borik[78] considered a tempered martensite to have the best combination of toughness and abrasion resistance for structural and constructural steels. They suggested suitable alloying additions were necessary to achieve the martensitic microstructures and ensure hardenability of thick sections.

Resistance to low-stress abrasion is best in alloy steels when the structure consists of a uniformly distributed fine carbide in a martensitic matrix containing some residual austenite.[24]

2.5 Abrasive wear testing

2.5.1 Introduction

Wear tests are generally less accurate and less reliable than tests of other engineering properties of materials or components. Because there is no universal wear test[85], wear rates are evaluated by many different procedures, each one designed to evaluate a specific type or mechanism of wear.

For abrasive wear, the testing machines should meet the following criteria:[86]

- **reliability** - that is, capable of producing wear of a certain material in a predictable and statistically significant manner.
- **reproducibility** - average results of duplicate samples should not differ by more than 10%.
- **ability to rank materials** - that is, able to achieve statistically significant differences in wear rates among different types of materials.
- **validation** - capable of accurately predicting the relative service performance of different materials.

2.5.2 Methods of abrasive wear testing

Before any test begins, the first question which has to be determined is that of the apparatus, whether it is to utilize a two-body or three-body geometry.
Thus, Kruschov and Babichev[87] have determined the wear rate of metals by processing them against a rotating surface covered by abrasive paper, while Spurr and Newcomb[88] have

studied the abrasion of metals pressed against files, emery paper and roughened metal surfaces. These experiments all measured the so-called two-body abrasive wear rate - namely, the wear rate of a body sliding against a rough, harder body.

The most common type of two-body abrasive wear tester is the simple pin-on-disc and pin-on-abrasive belt set-up shown in Fig. 2.21. [89, 45]
Abrasive, normally in the form of abrasive paper, is attached to the top surface of the rotating disk. The head of the pin specimen is held against the abrasive, usually by dead weight loading. As the disk is rotated at a fixed speed the pin is allowed to traverse radially inward during the course of the test and exposed continually to fresh abrasives. The same principle applies to the abrasive belt.

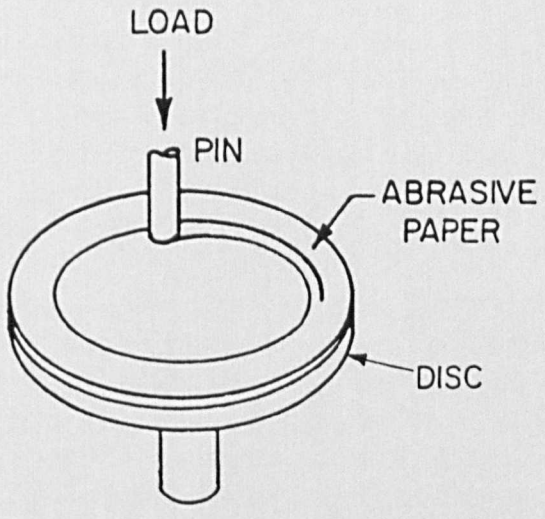

Schematic diagram of the pin-on disk test[89]

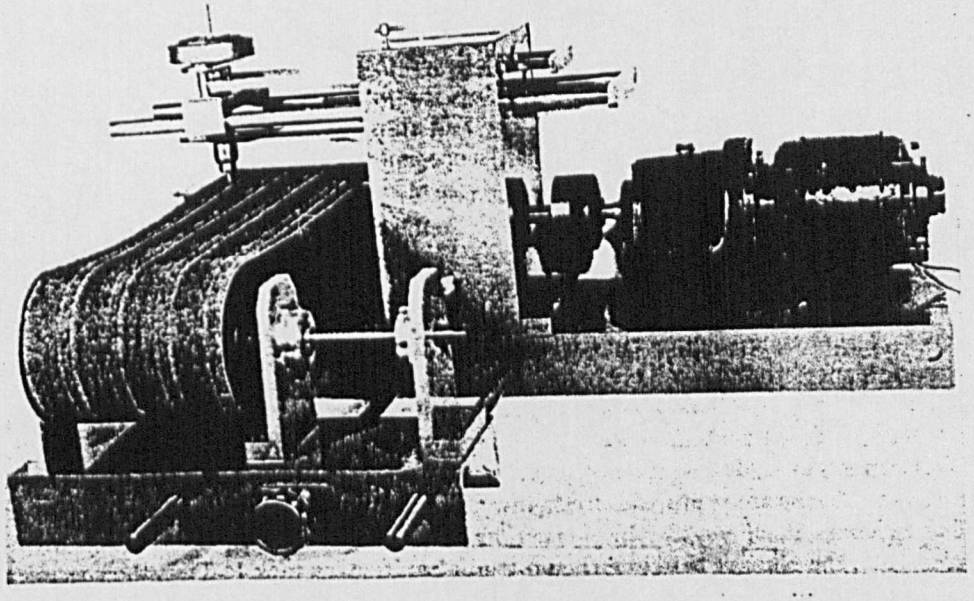

Abrasive belt in the working position[45]

Fig.2.21: Testing methods for two-body abrasive wear

For the three-body abrasive wear situation, where hard abrasive particles are introduced between smooth sliding surfaces, the most common methods used are shown in Figs.2.22, 2.23, 2.24, 2.25. [73, 90, 91, 92]

The wear test equipment in Figs 2.22, 2.23, 2.24 are used for low-stress three-body abrasive wear. The apparatus in Fig.2.22 [73] consists of a vertically mounted loading cylinder, restrained by a ball bushing to rotate but it can move freely in a vertical direction, which presses a stationary annular specimen against a rotating flat plate, while abrasive particles pass through the space between the wearing surfaces. The abrasive grit is fed from an adjustable rate dispenser into the loading cylinder and then, through holes in the bottom plate of the cylinder, reaches the top surface of the flat wear specimen. The used grits go out through two diametrically opposed slots in the annular ring of the top wear specimen.

The same principle applies for Toporov's wear tester, Fig.2.23[90], where again abrasive particles are introduced between two surfaces which are sliding over one another under load. Occasional contact of the two surfaces may also produce adhesive wear in this type of tester. It is common practice in wear testing to express wear of a tested material relative to that of a standard material. In Toporov's apparatus, the standard is tested at the same time as the material being studied.

In the Misra and Finnie tester, Fig.2.24[91], a rotating disk shaped specimen is abraded by particles flowing out of a tube. A variable- speed d.c motor allows the velocity to be controlled from 0.5 to 50 rpm. The abrasive is contained in a long plastic tube which is loaded by a dead weight through a plunger. The tube is held by a horizontal cantilever beam which has strain gage bridges for measurement of vertical and horizontal forces. An important variable is the gap between the tube and the specimen which has to be adjusted properly to keep the flow rate constant. This gap was found to be 1.0-2.0 times the abrasive particle size.

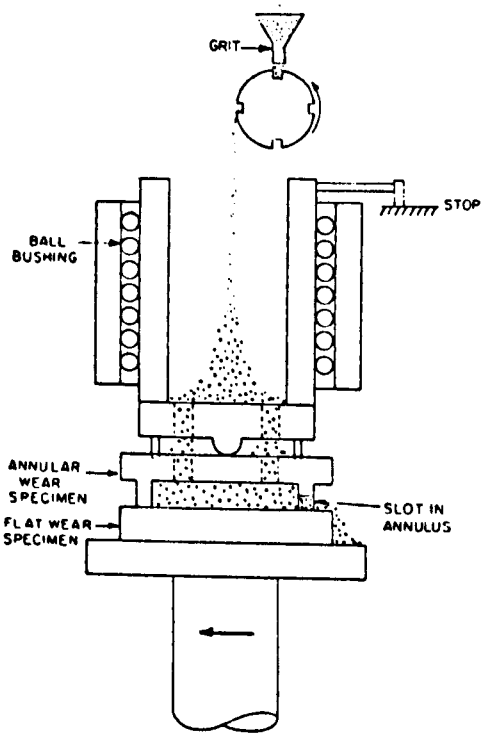

Fig.2.22: Rabinowitz low-stress closed three-body abrasive wear tester [73]

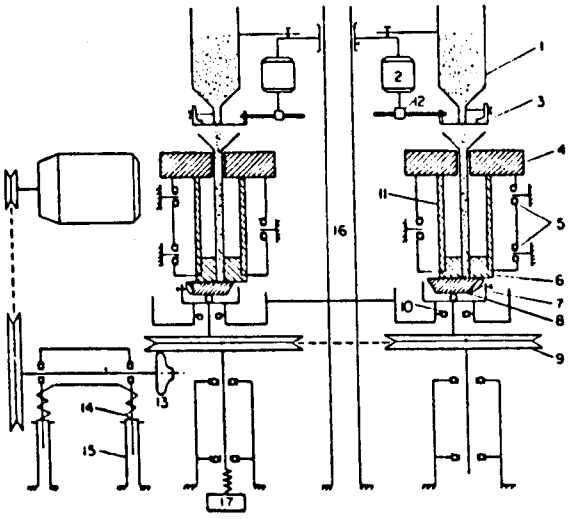

Fig.2.23: Toporov's low-stress closed three-body abrasive wear tester[90]

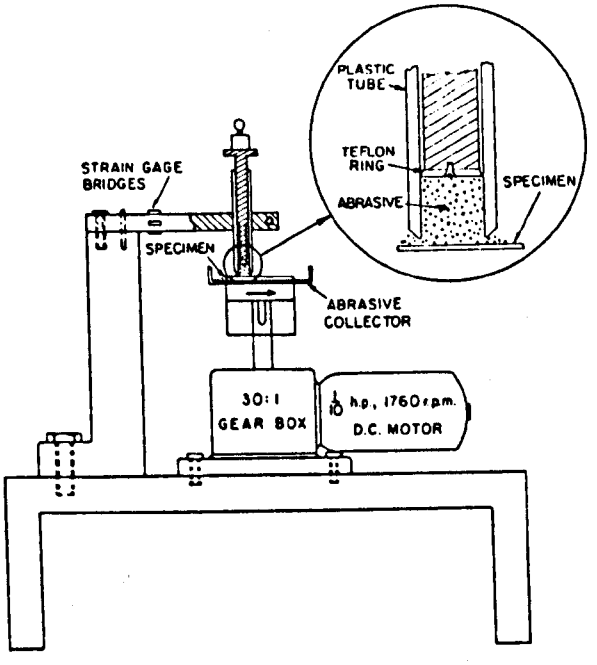

Fig.2.24: Schematic view of a low-stress open three-body abrasive wear tester [91]

The gouging category of the three-body abrasion is usually studied using laboratory-size single-toggle jaw crushers[93]. Generally, a reference material is tested during each set of tests with the wear rates of different materials being expressed relative to the reference material. The high-stress category of three-body abrasion uses a similar approach is followed. Here a convienient tester is a ball mill in which some of the balls are made from the material to be studied and some are made from the reference material[94].

The rubber wheel abrasion tester (Fig.2.25)[92], which was standardised by ASTM, has been said to produce low-stress three-body abrasion. It consists of a rubber wheel of 8 inch diameter by 1/2 in-thick steel hub with a 1/2 by 1/2 in chlorobutyl rubber tyre bonded to the rim and cured in a steel mould. The wheel is driven by a d.c motor and a gearbox which ensures that the rate of revolution remains constant under loading. The specimen is loaded against the rubber wheel through a weighted lever system. The abrasive is gravity fed from a hopper above the specimen through a chute which ensures that a uniform curtain of abrasive contacts the specimen and the wheel.
Among the many variables affecting the test, the rubber wheel surface finish and the rubber hardness were found to be variables by themselves and very important since any variation from the initial conditions will give scattered results. Also the abrasive particles may get embedded in the rubber wheel and scratch the test specimen in a manner similar to two-body abrasion.

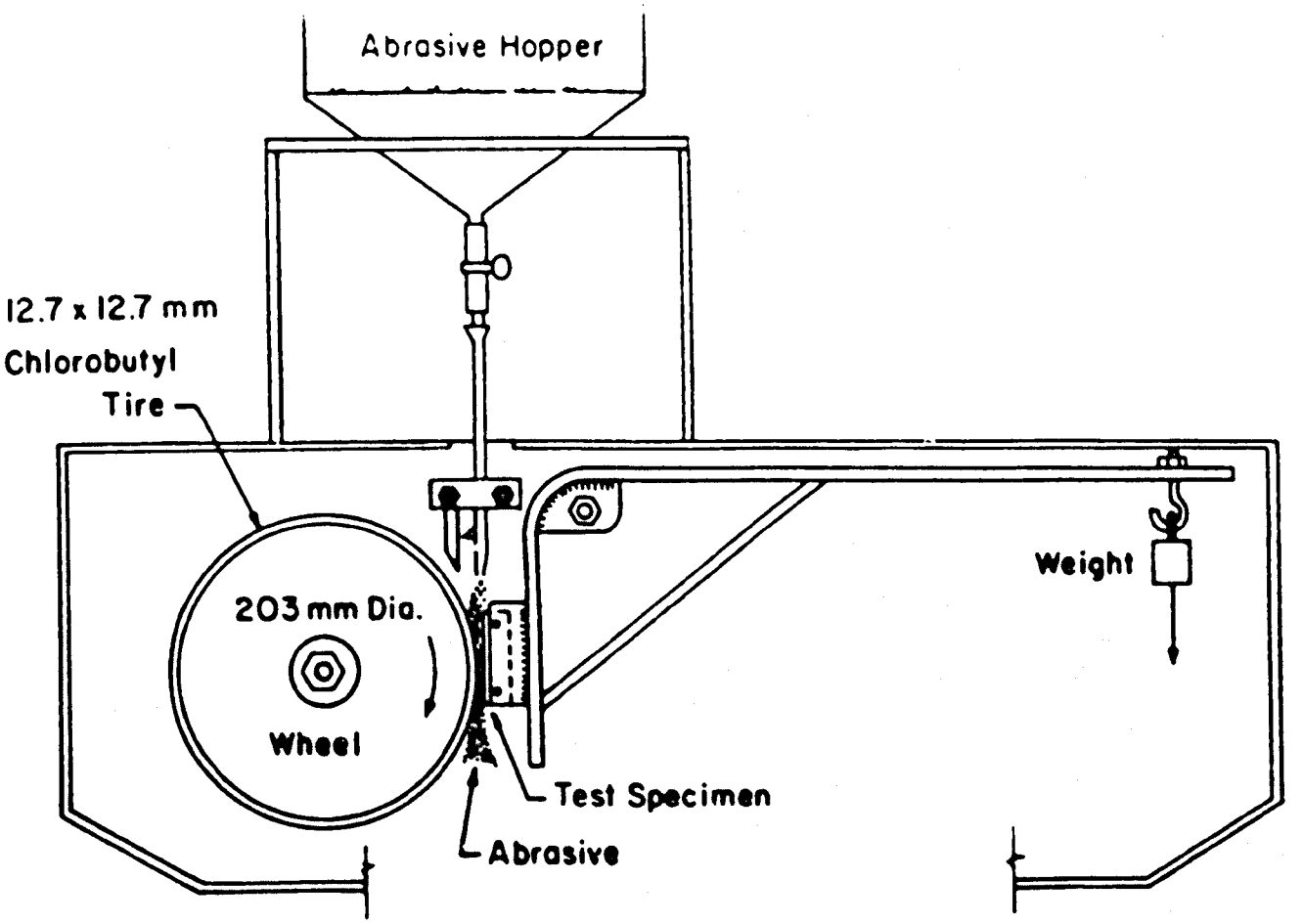

Fig.2.25: Low-stress dry-abrasive Rubber wheel Abrasion Tester (RWAT)[92]

2.6 Wear evaluation and data reporting

This is a multistep process complicated by the need for several techniques to compile the necessary wear information. These techniques range from visual judgements to metallurgical evaluations and mass/dimensional measurement[85, 92].

Visual rating has often been used, for example, in rating the mode of wear(ploughing vs cutting) and the degree of damage made.

Mass losses are the simplest to measure and, as such, give a direct quantitative indication, of wear rate. The abrasion test results should be reported as volume loss in cubic millimeters in accordance with (ASTM G65) standards.

$$\text{Volume loss } (mm^3) = {}^{\text{mass loss(g)}}/_{\text{density(g/cm3)}} * 1000 \qquad 2.2$$

Whenever a rubber wheel is used to conduct a wear experiment, the amount of scratching abrasion developed should be adjusted according to the following expression, because the rubber tends to decrease in diameter.

$$\text{Adj.vol.loss}(mm^3) = \text{measured vol.loss} * {}^{\text{wheel dia.bef test}}/_{\text{wheel dia.after test}} \qquad 2.3$$

Wear is sometimes reported as *specific wear* or ${}^{d}/_{WS}$ where d is the depth of wear; W is the bearing pressure ; and S is the sliding distance. Wear data may also be expressed as life-time in service when wear is the main determination of life-time.

Profile traces are very useful for wear evaluation. They often relate to design and analytical data and offer considerable information about a) the wear depth b) asperity effects c) geometry changes.

Metallographic evaluation yields information on changes in surface characteristics which often suggest the mechanism and origin of wear.

Wear debris is a sensitive indicator of wear mechanisms and operating conditions. When the debris from two different test devices is similar, comparable wear situations could be expected. Wear debris analysis also facilitates monitoring of wear conditions by comparing published wear data with data from actual operating equipment.

Abrasive particle distribution after the wear tests which may influence the magnitude of the wear rate and the particular wear mechanisms.

CHAPTER THREE

3. Abrasive wear modelling

3.1 Introduction

The subject of wear models is one of current and perhaps perennial interest. One can go back fifty or so years and find models for wear . In a very recent paper, Ludema and Meng[95] after searching the available literature, reported the models they found for friction and wear. They surveyed the journal Wear between 1957 and 1992 and the Wear of Materials Conferences from 1977 to 1991. They argued that from the 5466 papers they searched, the great majority were descriptive in nature. Some 20% describe a particular test, present results from the test and discuss the results, while another 10% present the solutions to a practical problem. All truly fundamental equations which were derived claimed to being complete enough to predict wear rate or wear amount with useful numerical accuracy.

A variety of meanings and expectations can be found for the term *"wear model"*.[96] In some cases a phenomenological description of the wear process is considered a model. In others a quantitative relationship for a physical mechanism is developed. Still in others the term wear model has also been applied to a qualitative description of wear behaviour and a resulting set of design guidelines. Depending on the scope desired and within the realm of possibility based on current knowledge, the question of wear modelling could be addressed under two headings; *design - oriented and fundamental level.*[97]

The design-oriented level, for design purposes, is where the models receive input on the one hand and produce output on the other hand. The input includes very well categorised data (data bank), stating parameters such as shape of abrasive, load, environment, materials and surface treatements. This type of model is often in the form of computer software and the user would enter the data bank giving values to all parameters in the projected application.

The fundamental level which, despite the fact that the connection between the input and output is again sought, is a step towards full quantification.

The first step in approaching the analytical wear modelling requires that at least two questions be asked:

a) what is the end objective of the modelling?
b) is a wear model of universal use?

The answer to the first question is that a model is useless unless it is predictive. It can not just explain past experimental results or practical observations. It must also point the way to new experiments or new approaches which follows that modelling and experiments must go hand in hand. The International Workshop on Wear modeling[98] summarised the benefits of wear prediction as follows:

a) energy savings

b) materials savings
c) design optimisation
d) failure analysis
e) predicting maintenance and repair requirements

The answer to the second question is that despite the existence of several wear models these are extremely limited in scope and applicability. What suits in one situation does not apply elsewhere or the controlling variables must be modified.

At the moment, however, the best use of a wear model is to accept it and use it with all the necessary precautions because as Tabor [99] quoted : " *it is better to predict without certainty than never to have predicted at all* ".

3.2 Literature review

In the past there have been many attempts to model the abrasive process. The process is clearly related to the interactions of negative rake tools with the workpiece. These interactions are also related to the mechanics of indentation and work hardening of material in the theory of plasticity.
A comprehensive literature review reveals that while a considerable amount of work has been conducted on two-body abrasive wear, little attention has been paid to the equally important problem of three-body abrasive wear. Selected publications which give an overview of abrasive wear are cited here along with some theoretical models developed to describe the process better.

Usually there are three steps which are followed in model development, namely observation, formulation and validation.[100]

The first step in developing a model is the observation of a worn surface. Fig.3.1shows a typical worn surface by abrasion.

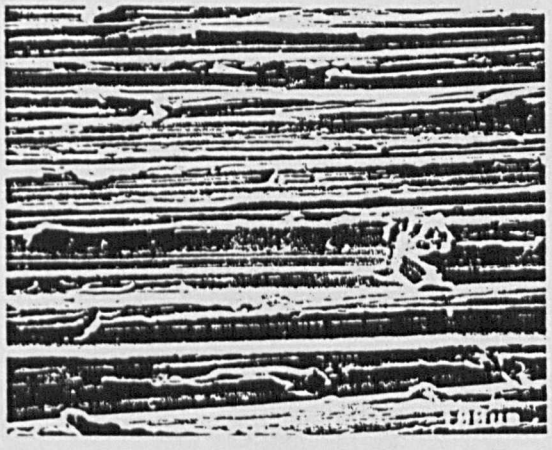

Fig.3.1 :Aluminum alloy 3003 abraded with 240 grit SiC paper [100]

It can be seen that the surface has become covered with long scratches, grooves and also some microchips at the end of interrupted grooves.

Babitchev and Kruschov,[101] investigating the basic mechanism of abrasive wear identified two processes taking place when an abrasive grain made contact with the wearing surface:
a) the formation of plastically impressed grooves which did not involve direct metal removal
b) the separation of metal particles in the form of microchips.

Avient et al[55], in their experimental studies with metals slid on emery papers observed that much of the metal displaced from the grooves remained on the metal as lateral raised ridges.

Aghan and Samuels [102] found that the extruded fins at the edge of grooves produced by rubbing can sometimes become detached forming secondary chips, although they accept that primary chips dominate in terms of metal loss.

Sakamoto and Tsukizoe[103] studied the prow formation in scratching copper with diamond cone tools. They observed that, as sliding proceeded, material removed from the groove was piled up forming a prow ahead of the tool. Then the accumulated material flowed to both sides forming the ridges.

The next step in wear modelling will be the development of a more quantitative expression (model) based on these observations of a worn surface.

3.2.1 Basic model

Rabinowitz[104] developed a simple expression for the volume of material removed during abrasion by approximating the abrasive grit by a cone ploughing a surface(Fig.3.2).

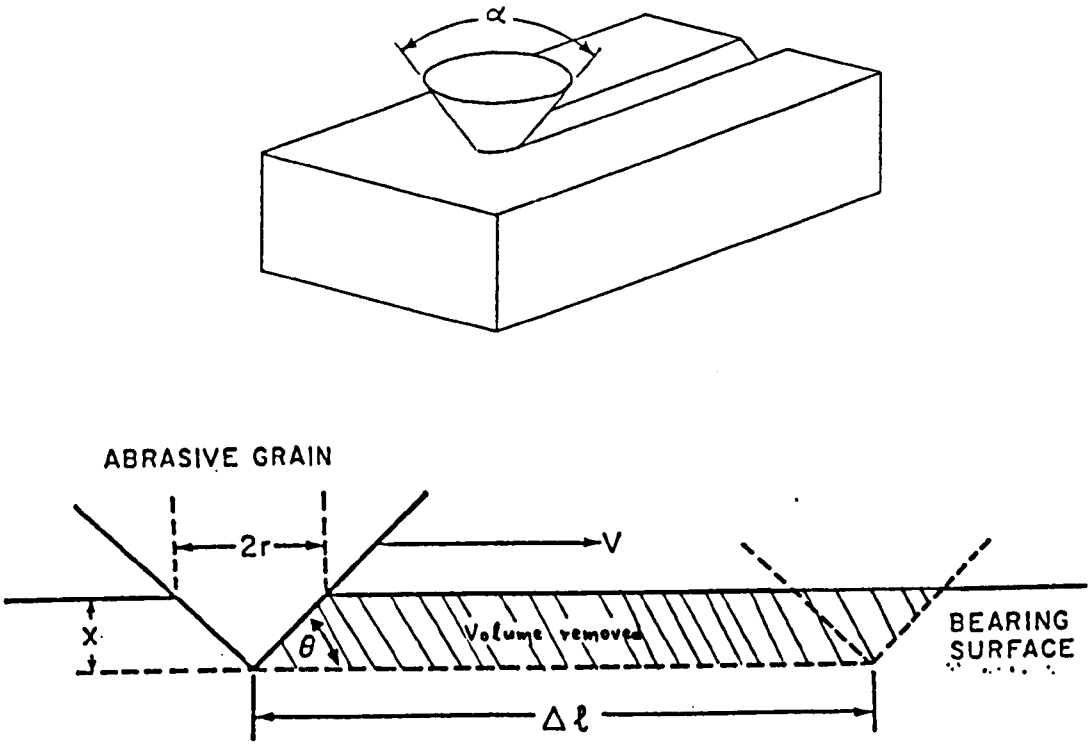

Fig.3.2 :Schematic illustration of a conical abrasive particle cutting a groove [104]

Assuming that the indentation is fully plastic, the penetration into the surface is controlled by the hardness of the material and the load.

$$W=H\pi r^2 \qquad 3.1$$

The shaded area in the Fig.3.2 shows the volume of material removed and is given by:

$$V=r^2 l\tan\theta \qquad 3.2$$

Based on an average value of the cone angle θ, the total volume removed is the result of many such individual contacts. The combination of equations 3.1 and 3.2, the total volume lost is obtained.

$$V=\frac{\tan\theta Wl}{\pi H} \qquad 3.3$$

Replacing $\tan\theta/\pi$ by K/3 the Archard's [12] well established wear law for adhesive wear results, which states that the wear volume is proportional to the applied load W, the sliding distance L and inversely proportional to the hardness, H.

$$V=\frac{K}{3}\frac{WL}{H} \qquad 3.4$$

This wear model despite its simplicity satisfies the intuitive knowledge that resistance to abrasive wear often increases with hardness.

Finally the last step to the wear modelling process is to compare this simple model expressed by equation 3.4 with experimental results.

Kruschov and Babichev [106], confirms the validity of equation 3.4 for pure metals, and typical annealed alloys when they are abraded by very hard, fixed abrasives, such as abrasive silicon carbide or alumina papers. However, there are deviations when a broader range of materials is considered, which throw some light on the wear process and on the effects of material properties.Fig.2.9 [34]

3.2.2 Deviations from the basic model

The deviations from the main deformation pattern of a wider range of materials, as Fig.2.9 shows, are all explainable relative to the model if the assumptions made by Rabinowitz are examined.

Grooves do form on the surface even for the brittle materials but only a few per cent of the groove cross section is actually removed. Much of the material is pushed into ridges along the groove sides(Fig.3.1).
The stress level which controls abrasion is much greater than the level given by a conventional hardness indentation.

For brittle materials cracks may form under the sliding indenter. The material may show some elastic spring-back after the abrasive has passed.
The abrasive can be affected significantly by the process and it may wear, crush or the environment cause moisture-assisted fracture.[74] Abrasive particles may roll most of the time, 90% of time rolling and 10% of time abrading, giving less wear than predicted by the model whilst if they are less than 20% harder than the abraded surface, they will not be able to indent it and form grooves.[104]

Mulhearn, et al[46,107] clearly indicate that the assumption of a conical indenter which removes the theoretical volume is the most serious limitation of the model. They worked both with abrasive papers and model cutting tools. They realised that the cutting angle 'α' was more important than the angle of the abrasive particle θ (Fig.3.3a). They defined '*critical attack angle, a_c*" as the angle below which no cutting, only ploughing occurs(Fig.3.3b). Then, they related these angles to the cross-sectional area of the groove. They measured the cutting angles present in sections of silicon carbide abrasive paper, and estimated the percentage of contacting grits which cut as between 7 to 10%. Finally they incorporated all this information into a model. The wear mass for the n_{th} abrasive grit was of the form:

$$m_n = \frac{\rho f_n l W}{HK\phi} \qquad 3.5$$

where, ρ is the density, l the sliding distance, W the load, H the hardness, K and ϕ are form factors for the shape of the groove, and f_n is the proportion of grits cutting.

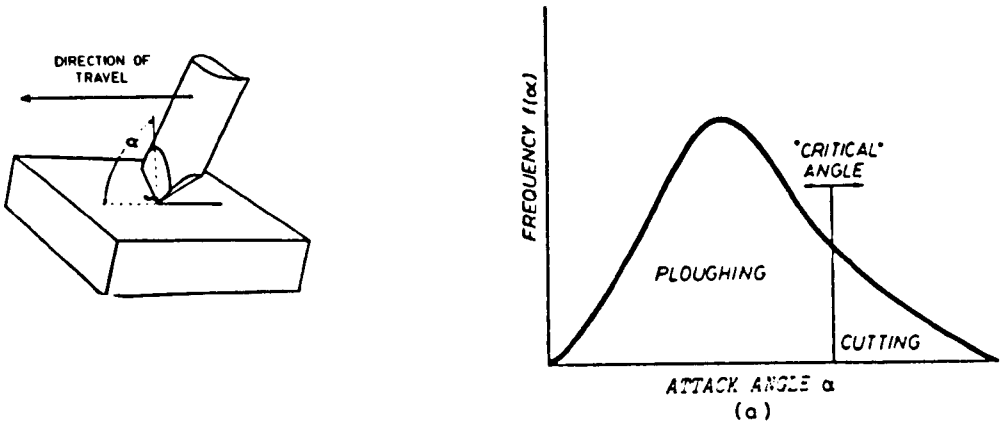

Fig.3.3 : Critical attack angle- a) definition of the attack angle b) schematic diagram showing the concept of the critical attack angle [46, 107]

Moore[108] attempted to use Archard's wear model in a more global fashion in order to handle the results of Fig.2.9 for different groups of materials. He proposed that for ductile and partly ductile materials where abrasion is a form of plastic deformation at very large levels and rates of strain, it could be related to their low-cycle fatigue behaviour. Then it would be expected that work hardening exponents would affect the abrasion resistance.

Kragelskii et al [6] have also argued that chips rarely form in real abrasive situations and that the wear is due to low-cycle fatigue of the ridge material. In this case, which appears quite possible, the above argument will still hold in general, with low-cycle fatigue stresses and strains replacing the values for single-loading failure.

Garrison et al [80] proposed a model where ploughing is incorporated into the basic wear equation for the volume abrasive wear(V) in the form :

$$V \propto \frac{L(1-f)}{H_s} \qquad 3.6$$

where,V is the volume wear , H_s is the surface hardness, L is the applied load, f is fraction of a wear groove ploughed to either side of the abrasive particle but not removed from the surface.

This approach yields results which seem to be compatible with the abrasive wear behaviour of ultrahigh strength steels but which are unrealistic for very soft and ductile materials such as copper and aluminum.

Zum Gahr [109], proposed a model which considers the detailed processes of microcutting and microploughing in the abrasive wear of ductile metals. Experimenting with steel riders of different attack angles sliding on polycrystalline metals and alloys, he reconfirmed the

different attack angles sliding on polycrystalline metals and alloys, he reconfirmed the influence of critical attack angle α_c in determining the transition between microploughing and microcutting. He also showed that work hardening, ductility, crystal anisotropy and mechanical instability play a significant role in abrasion.

Buttery et al [110] studied the grooves formed during scratch tests and from abrasive grinding. The geometry of the scratches were measured and classified in terms of three areas A1, A2, and A3 as shown in Fig.3.4.

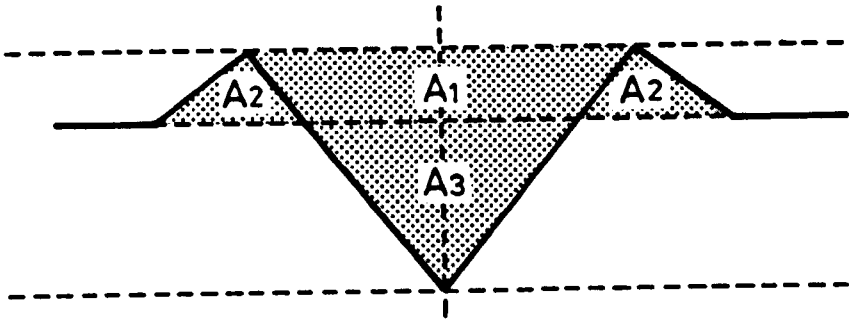

Fig.3.4 : The classification of abrasive wear scratches [110]

The scratch volume is given as (A3+A1) and the proportion of material removed as wear, β was suggested to be (A3-A2)/(A3+A1). The wear equation of the type developed by Rabinowitz(equation 3.3) was then proposed:

$$\frac{V}{l} = \frac{0.5\alpha\beta W \tan\theta}{H} \qquad 3.7$$

where α is the proportion of grits cutting, the other variables having the same definition as those in equation 3.3. They also performed some repeated scratch tests and found that the proportion of material removed increased with the hardness of the abraded surface, with softer materials the bulk of the groove material was piled-up as shoulders.

Kato et al [111] performed a comprehensive series of scratch tests in an SEM. Their studies thoroughly cover the transitions between ploughing, wedge, and cutting flows for spherical tipped and three dimensional pyramidal sliders. They defined two parameters, degree of penetration Dp=h/a and shear strength f, which determine the possible range of each wear mode on the wear mode diagram. The degree of penetration, Dp, is very useful for predicting changes of wear rate and number of wear particles in relation to wear modes.

Moore et al [112] developed simple models to assess the indentation fracture and plastic deformation of ceramics. They validated these models by testing a wide range of brittle materials on 180 and 60 grits SiC papers. They found that both mechanisms exist during abrasive wear of brittle solids but the predominant and rate controlling one differs for both different environments and different materials. Hardness is a major factor in determining wear because of the effect it has on the rate of deterioration of the abrasive particle

geometry and depth of indentation. Small abrasive particle sizes and low applied loads favour plastic deformation while large abrasive particle sizes and high loads favour indentation fracture. Delamination may also causes material removal beneath the plastically deformed grooves but to what extend is difficult to be estimated.

3.2.3 Other approaches of modeling of abrasive wear

Challen et al [32] used slip-line field theory to explain the deformation of a soft asperity by a hard one, assuming a low-cycle fatigue mechanism. They validated their models in terms of Archard's wear coefficient and showed that for very smooth surfaces and good lubrication, this can have very low values as observed in wear tests for such conditions. For rougher surfaces and less efficient lubrication, it was shown that the wear coefficient was increased dramatically.

Torrance [113], using a Vickers indenter to simulate an abrasive particle, developed an approximate mathematical model of the abrasive process. He used the slip-line field developed for a rigid wedge sliding over a perfectly plastic solid. He compared the model result with his own experimental values, and the model predicts metal removal quantities and force ratios satisfactorily.
Another finding of the model is that a rough surface should be less abrasion resistant than a smooth surface which is confirmed by practical observation that a fine ground surface is harder to hone than a coarse ground surface.[114]

Jacobson et al [115] studied the case of multiple abrasive groovings in a surface of realistic topography created by two-body abrasion. The influence of grit size, load and workpiece hardness on wear rate, specific energy, number of contacting particles and wear surface topography are predicted. The validity of the model is also demonstrated by comparing it with results of other investigators. The model is restricted to pure microcutting without material displacement to the sides of the groove. It also provides a basis for the separation of geometrical and materials parameters.

Halling[116], produced a wear equation for systems in which surface films exist. In this model contact may occur between the asperity and both the film and the substrate material. He insisted that his wear equation is appropriate to a wide range of tribological contacts since, apart from deposited films, films are often present because of environmental contamination (oxidation, corrosion) and /or because metallurgical structure changes produced by energy released during rubbing.

3.2.4 Modelling of abrasive wear behaviour of multiphase microstructures

Abrasive wear may involve variously-shaped particles impinging upon microstructurally complex targets, consisting of several phases. These multiphase materials are widely used in engineering applications where wear resistance is paramount. A sub-group of multiphase

materials are composites which are often described as artificially manufactured multiphase materials with constituents from different material groups e.g., ceramic reinforcing phases in a metal or polymer matrix.
As new manufacturing techniques emerge which require materials with good wear resistance, there is great demand for better understanding of how to predict and increase a composite's wear resistance.

In the literature, there are quite a few publications on the abrasive wear resistance of multiphase materials.[117, 118, 119] It has been shown that a multiphase material often exhibits wear properties widely different from those of its constituents. For a composite material not only the wear properties of the matrix and reinforcing phase, but also the size, shape, volume fraction and distribution of the phases influence the wear resistance.

Wang and Hutchings[39] reported on transitions in wear behaviour of alumina-fibre reinforced aluminium associated with the size of the abrasive grits. They derived an expression for a critical abrasive grit size, above which the fibres fractured and thus lost most of their improving effect. Many studies deal with the influence of abrasive grit size, and of the size and volume fraction of the reinforcing phase on metal matrix composites with ceramic particle fillers.[118, 119]

Some attempts have been made to predict the wear resistance of multiphase materials by using rules of mixtures which describe the wear resistance in terms of the material's constituents.

Kruschov [34] mathematically described this approach, arguing that the wear resistance of such a material is a linear function of the volume fraction of the phases present.

$$W^{-1}=\sum_i fvi W_i^{-1} \qquad 3.8$$

The IROM (inverse rule of mixtures) model, described by equation 3.8, is only valid when each phase shows a wear rate proportional to the applied load e.g ductile metal systems. However, when hard phases and ceramic materials are involved the IROM model cannot be applied because the wear rate is non-linearly related to the load.[120]

It has been pointed out [119] that while IROM better describes structures which consist of phases with very different properties, the LROM (linear rule of mixtures) rather describes a combination of very similar phases. The existent model which describes this rule is :

$$W=\sum_i fvi W_i \qquad 3.9$$

Zum Gahr[119] confirms the LROM for the description of ferrite-pearlite behaviour in a two-body pin-on-paper abrasion test. He also found that ferrite-martensite system conforms

better with IROM and that M_7C_3 carbides in high chromium white irons showed a modified IROM-type relationship.

Another point which can have significant effect in multiphase systems is the particle-matrix interfacial bond strength.[118] The total abrasive action on such systems is considered to be the macroscopic sum of each microscopic effect produced by an individual abrasive grain.

Many of the commercial alloys used for their good abrasion resistance contain large, hard alloy carbides which contribute to wear resistance by directly obstructing the cutting action of abrasive particles. Carbides should be as large as the grooves produced by the abrasive particles so as to resist being gouged from the matrix. If they are considerably smaller than this, they should be uniformly distributed and as fine as possible so as to dispersion-strengthen or precipitation-harden the matrix. Large carbides should be supported by a strong matrix, such as tempered martensite, or their outer edges will fragment and their effectiveness will be lost.
Another point which must be stressed here is that carbides should not be in the form of continuous networks through which brittle cracks may easily propagate.

Other researchers have found upper and lower limits outside which the wear resistance of a composite cannot be expected to fall.[121, 122] The upper limit corresponds to a linear relation between the wear resistances of the matrix and the reinforcing phase.
Axen and Jacobson[123] presented a model for the upper and lower limits for the wear resistance of composites. Their experimental results confirmed that the wear resistances of composite materials do fall between such extreme values.

Axen and Lunberg[124] produced a model of wear in intermediate(I) mode. Intermediate mode wear proceeds between two wear modes which correspond to upper and lower limits for the wear resistance which can be expected for a multiphase material.They introduced the concepts of equal linear wear rate of the phases(EW) and equal pressure on the phases(EP) in order to describe the upper and lower limits of the wear resistance respectively. This intermidiate model is based on Archard's equation and a weighted average of the pressure distributions for the two extreme modes. The pressure distribution over the phases decides which wear mode will dominate. They insisted that the predictions of the model have been confirmed by experimental results for different multiphase materials.

3.3 Assessment of the wear modeling

After reviewing the literature on wear modelling, it appears that apart from some cases, most of the work done on the abrasive process is experimentally based. These experiments suggest that an abrasive particle may be modelled as a spherical, conical or pyramidal tool.

In several experiments, single point tools have been used to simulate abrasive grits in negative rake angle cutting. In comparison to ordinary metal cutting, which is positive rake angle cutting, the effective rake angles of the abrasive grits are predominantly negative. As the tool advances, the material in front of the tool piles-up and a chip is formed or the material is ploughed or both. The *"critical attack angle"* as defined by Mulhearn et al[46],

seems to determine which action is the dominant. This is because if the rake angle is between positive and a certain negative value, the tool forms a chip. For more negative rake angles, some of the material in front of the tool flows upwards over the tool face to become a chip and the other flows downwards to rejoin the work material. At very high negative angles the tool does not form a chip and the material flows under and to the sides of the tool.

In multiphase microstructures the abrasive wear situation is complicated by the combination of phases and constituents with different properties. The rules of mixtures only describe the contribution of each phase/constituent to the total behaviour which is considered as an oversimplification, because it assumes that the wear rate of each phase/constituent was obtained under the same experimental conditions. Thus the rules of mixtures are not useful in the quantitative prediction of industrial wear rates, but instead are useful as a laboratory tool in the development of abrasion-resistant materials.

Moreover, these rules of mixtures only describe the volume fraction effect without taking into consideration the microstructural size. But as experimental work shows[121], the relationship between the size of the reinforcing phase and the groove size is an important parameter which must also be considered. This reinforcing effect of a reinforcing phase seems to be more effective when the microstructure is larger than the groove size allowing in that way the hard phases to act as real barriers instead of only reducing the plastic deformation on the overall material surface. Furtheremore, if the bond strength between the phases is a potential weak point, a coarse microstructure avoids high stresses at the interface.

As a general assessment on the wear modelling, the following conclusions can be drawn:

i) the most striking aspect of all equations in the literature is the great number of variables cited.
ii) most equations contain constants which are ambiguous among the parameters and constitute the "numerical bridge" between values calculated from the variables in derived equations and values measured in experiments. Some of those constants are assigned to represent specific quantitative phenomena that are not readily measurable.
iii) experiments to verify models seldom prove their point very clearly and it is questionable how useful they are when so many confusing factors are present.
there is lack of visible progress whatsoever towards a more universally accepted wear equation and the reason is that most authors cite mechanisms, modes or processes of wear for their model and there is little agreement on the meaning of the terms.

It can also be added as a final point, that a new approach for future wear modelling is needed. This approach says that all published experimental work, should be completely described so that other researchers can duplicate the experiments and obtain similar results. The presently available wear equations should be used only as a reference but not relied upon.

CHAPTER FOUR

4. Corrosive wear

4.1 Introduction

Wear and corrosion, as materials degradation phenomena, are linked in significant ways and result in enormous costs to the industrialised nations from the materials and energy consumed, lost productivity, contamination of process streams and of the natural environment, and in industrial accidents. It is reported that corrosive wear is responsible for 5% of the wear encountered in industrial situations.[1]

The wear due to abrasion, adhesion and fatigue can be explained in terms of stress interactions and deformation properties of the mating surfaces, but in corrosive wear, the dynamic interaction between environment and mating material surfaces plays a significant role. [125]
Wear and corrosion can involve a number of mechanical and chemical processes. The combined action of these processes can result in mutual interaction beyond the individual contributions of mechanical wear and corrosion. The interactions among abrasive wear,sliding wear and corrosion can significantly increase total material losses in aqueous environments, thus producing a synergistic effect.

4.1.1 Nature of corrosive wear

Corrosion is a chemical or electrochemical process in which surface atoms of a solid metal either react with or dissolve in a substance that contacts an exposed surface. This is the result of metals seeking their lowest energy state which thermodynamically is the oxide for all non-precious metals. Usually, the corroding medium is a liquid substance, but gases and even solids can also act as corroding media. In some instances, the corrodent is a bulk fluid ; in others, it is a film, droplets, or a substance adsorbed on or absorbed in another substance. Corrosion can dissolve one phase and leave another as loose debris, or can dissolve one phase and leave another phase exposed and susceptible to wear.

Corrosive wear occurs where a body is subject to wear within a corrosive environment. In most cases, a rapid form of wear or material loss results. The corrosive and wear functions may be intimately linked together, as shown schematically in Fig.4.1. [24] One or both of the types of attack on the original surface may be very low, and one or other may be missing completely, and the overall process is likely to be dominated by corrosion of worn surfaces and wear of corroded surfaces, neither of which can proceed faster than the other.

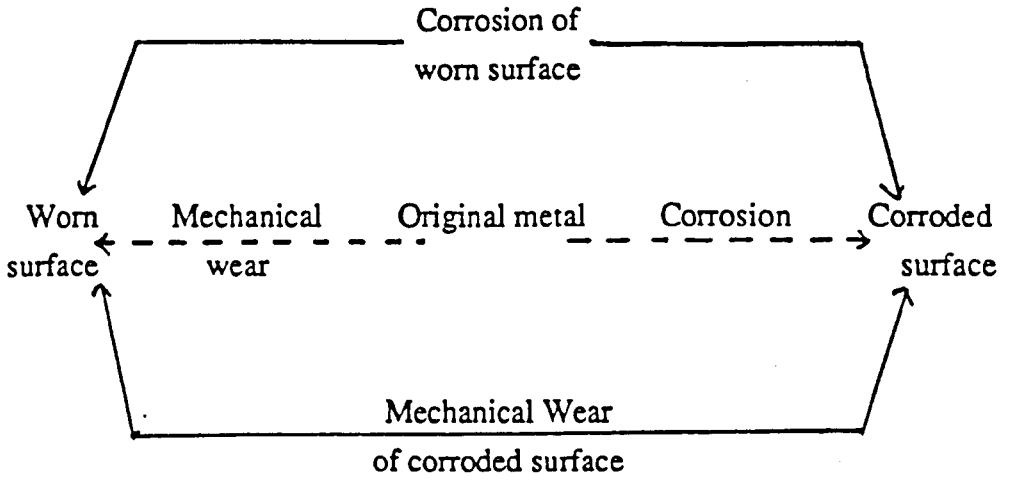

Fig.4.1 : General mechanism of corrosive wear [24]

Because the wear rate of a corroded surface will often be higher than that of an uncorroded surface, and the corrosion of a worn surface will often be higher than that of an unworn surface, the total rate of loss of material in corrosive wear can be high and the resulting problems can be very serious.
This happens because a worn surface has, in comparison to a smooth, polished surface, a greater surface area and a greater dislocation density and degree of work hardening. It is in a higher state of disorder and has a lower average atomic coordination. Thus the physical and chemical activity of an abraded surface is higher and there is an increased probability of reaction.

Oxidational wear as developed by Quinn[126] is a mechanism of mild wear in which protective oxide films are formed at the real areas of contact, during the time of a contact, at the contact temperature. When the oxide reaches a critical thickness(ξ), usually 1 to 3 μm as experimental and microscopic evidence have shown, [127] the oxide breaks up and eventually appears as wear particles. These oxides are preferentially formed on plateaux, which alternately carry the load, as they reach their critical thickness, and are removed.

The oxidational mechanism does not explain why the plateau breaks up at a thickness(ξ). It simply states that when the contacting plateau finally breaks up, another plateau elsewhere on the surface becomes the operative one and the virgin surface beneath the original plateau is now free to oxidise at the general temperature of the surface.

A corrosion resistant substrate material is usually protected by a passive layer, for example a thin oxide film, or generates one after initial exposure to a corrosive medium. This self-limiting film is easily removed by abrasives and, if subsequently regrown, causes a much greater material loss than would occur by undisturbed corrosion(Fig.4.2). [128] Corrosion under abrasive conditions can also be accelerated by such factors as the anodic potential of a small break in a self-limiting film as compared to the rest of the passivated surface.[129] Passive films are usually brittle and will break up easily under abrasive impact, leaving the substrate material mechanically undisturbed. However, if the abrasive loading increases, or the corrosion film is too thin, then the underlying metal will be abraded and the wear

mechanism will revert to a purely abrasive mode.

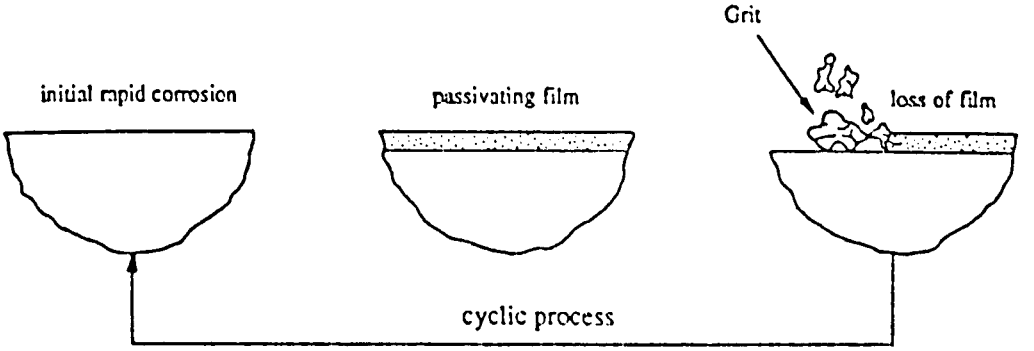

Fig.4.2 : Model of corrosive wear [128]

4.1.2 Abrasive corrosive wear

Metals are continually subjected to oxidation or corrosion during their useful life and this cannot be separated from the abrasive wear process. A comprehensive review of the literature reveals that many researchers have studied and tried to quantify the wear-corrosion synergism.

Allen et al, [130] in recognising the detrimental influence of corrosion, studied the abrasive-corrosive wear of stainless steels. They tested, in the laboratory, various ferritic, martensitic and austenitic stainless steels and the results were compared with the testing of similar materials in-situ in a gold mine. They found the stainless steels to show superior abrasive-corrosive resistance than the majority of the proprietary abrasion resistant alloys. Their high abrasion resistance was explained in terms of the materials ability to accommodate high strains by the stress induced transformation and the consequent high work hardening rate. Schumacher[131] also found in wet ball mill tests that the stainless steels with the highest strain hardening capacity were the most effective in resisting abrasive-corrosive wear.

Bachelor et al [128] studied mild steel, zinc and magnesium under simultaneous abrasion and corrosion and compared results with static corrosion and dry abrasion tests(Fig.4.3). Sulphuric acid was used as the corrosive medium at room temperature. Their results imply that : when the rate of corrosion is less than the rate of abrasion (time based), a weak synergism between corrosion and abrasion may occur, and the life of materials may be estimated by only dry abrasion data without any significant error. However, when the undisturbed corrosion rate becomes greater than half the time based dry abrasion rate, then synergism of 100% between corrosion and abrasion occurs and estimation of material life can not rely on dry abrasion rate or dry abrasion rate plus undisturbed corrosion rate. The abrasion-corrosion rate can be four times larger than the corrosion rate even when the abrasion rate is negligible. They also explained the rapid rate of corrosion-abrasion and negligible dry abrasion by suggesting that the rolling of grits over a surface is far more

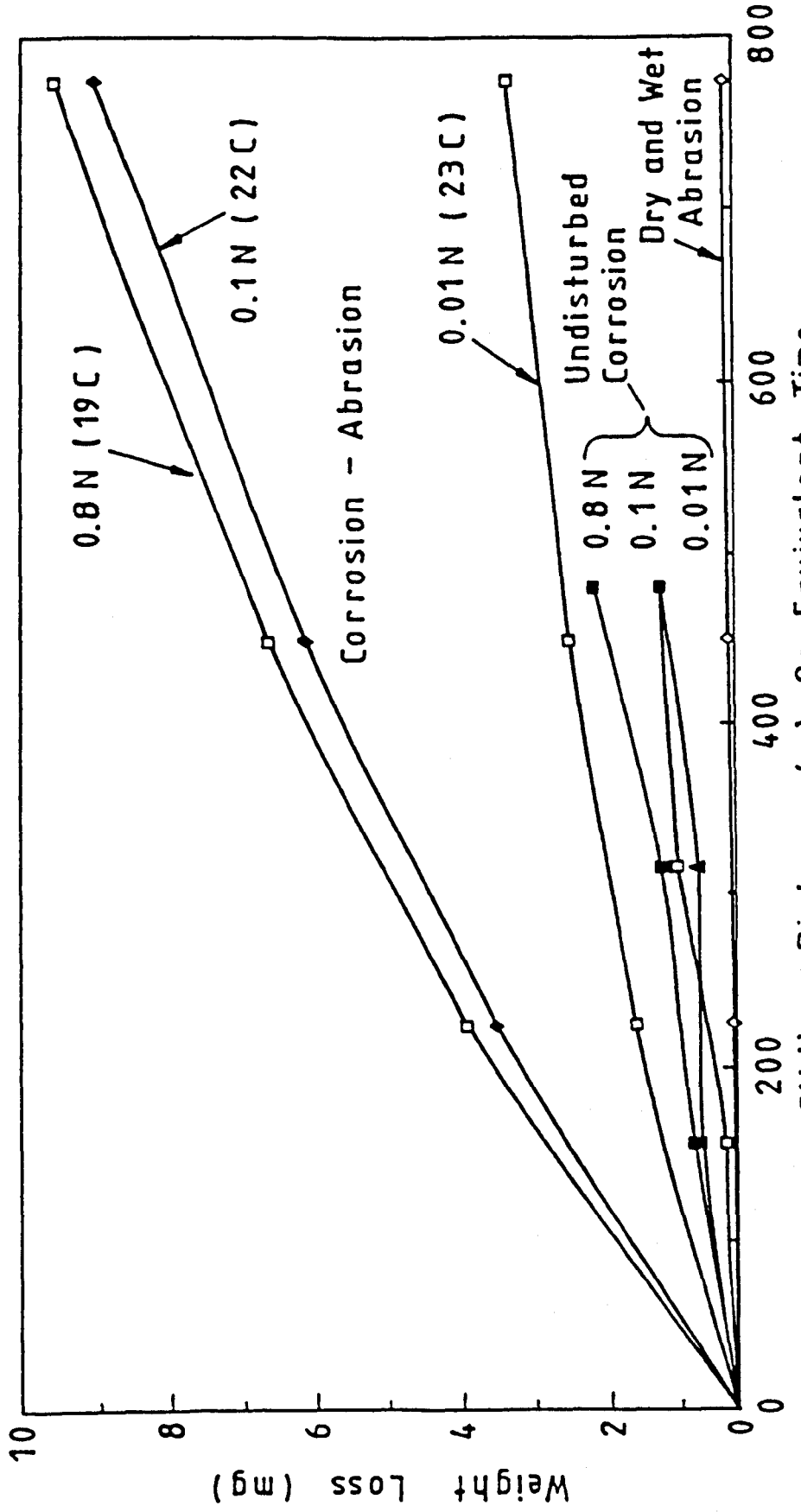

Fig.4.3 : Three-body abrasion-corrosion of steel [128]

effective at removing a brittle corrosion product film from the steel surface than at wearing away the steel itself. [132]

Further evidence for synergism between corrosion and abrasion was gained by Ball et al [133] where deformation zones associated with abrasion had accelerated corrosion of the substrate; hardness also proved to play no role in the relative wear resistance of the materials tested.

Jia-Lin et al [134] tested a new cast-in composite material composed of a chromium-alloyed matrix reinforced by WC particles for wear-corrosion in a water-sand medium containing various concentrations of sulphuric, hydrochloric and nitric acids.
The results showed that weight losses of specimens, wear-corroded in acid-sand media were about 2 times greater than those of specimens wear-corroded in a water-sand medium, and that the abrasion dominated the wearing process. The severity of wear-corrosion in the presence of acid solutions caused the matrix to wear-corrode preferentially. In particular, the boundaries around the WC particles which stood in relief to the metal matrix(Fig.4.4).[134]

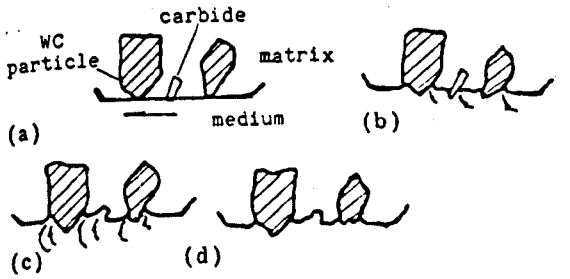

Fig.4.4 : Schematic diagram of wear-corrosion process : a) beginning b) matrix preferentially wear-corroded c) erosion, turbulence d) WC particles broken [134]

As the particle boundaries and their matrix were attacked, the adjacent metals were weakened. Finally the matrix failed to support the WC particles and they fell out.

Stott et al [135] carried out laboratory work to examine the influence of corrosion on wear of cast iron diesel engine cylinder liners in sulphuric acid solutions, in an attempt to validate reports[1,136] that wear increases as the sulphur content of the fuel is increased. The examination of wear scar topographies and morphologies of the specimens and the surface topography of areas of some liners taken from service has indicated selective corrosive attack of microconstituents in the cast iron. There was no doubt that the products of this attack along with carbonaceous particles resulting from combustion or partial combustion of the residual fuel or lubricating oil or hard foreign matter introduced with the induction air abraded the surfaces and largely contributed to the overall wear loss increase. In a 10% sulphuric acid solution, the applied potential influences the rate of degradation under wear conditions.

The contribution of corrosion to the abrasive-corrosive wear of high-carbon, low-alloy steel(HCLA), commonly used for grinding balls, was evaluated in 15% quartz slurries. [137] The magnitude of the synergistic effect of corrosion and abrasion was determined for

various conditions of applied load, hardness and pH. It was found that the synergistic effect is considerable, even if the corrosion component of the wear is small. The macro-removal of metal particles, producing the synergistic effect, may be considered to result from the initiation and propagation of pitting and microcracks assisted by anodic corrosion. Corrosion of HCLA steel also increased with higher load and lower pH. The magnitude of the corrosive-abrasive wear is determined essentially by pure abrasion and the synergistic effect.

Noel et al[138] studied the interactive effects of abrasion and corrosion on mild steel specimens as a function of abrasive load, corrosion time and the frequency of abrasive-corrosive treatments. The specimens were sequentially abraded on a pin-on-abrasive belt machine and corroded by exposing the abraded end to flowing water containing chlorides and sulfates at pH=6.7. An increase in load had only a slight incremental effect on the volume loss due to corrosion in the abrasive-corrosive wear of the steels. As load was increased, the volume loss due to abrasion increased, and since volume loss due to corrosion remained the same, the percentage of volume loss due to corrosion decreased. The test results imply that when abrasive wear occurs continuously under high loads in a corrosive medium, the percent corrosion effect is negligible. For a low load and infrequent abrasion in a corrosive medium, the percent corrosion effect can be very high. There is a definite *"frequency effect"*, that is, the greater the frequency of corrosion-abrasion for a set period of corrosion time and abrasion distance, the greater is the volume loss. This greater volume loss is due to the very high rate of corrosion attack during the initial exposure to the corrosive environment each time a new test is run. The initial high rate of corrosion is due to the increased internal energy resulting from high dislocation densities in the near surface region. The corrosion rate decreases with time as the deformation layer is removed. The research was thus able to specify some basic guidelines for material selection in mining environments but the authors did not generalise their approach or quantify the synergism.

Watson et al[139] studied a commercial 13.5% Cr white cast iron sample and the individual constituents(matrix, M_7C_3 and M_3C carbides) of a white cast iron to determine the role of each phase in the degradation processes of wear, corrosion and wear-corrosion synergism. The synergism results from these studies for the components of the white cast iron sample showed that corrosion plays a significant part in the sliding wear of cast iron in the neutral sulphate environment of 1N Na_2SO_4. The carbide phases appeared to undergo most of the degradation. However, once these phases broke down very high wear rates resulted. The matrix probably undergoes corrosive attack and works as a sacrificial anode due to galvaning coupling with the components of the cast iron.

Very recently Madsen[140] developed penetration rate equations for quantifying each of the degradation processes(wear-corrosion), providing useful engineering data on the synergism between wear and corrosion.

The development of abrasive-corrosive wear resistant materials encompasses a combined study of abrasive wear and corrosion. Their synergistic action has been observed to systematically increase wear in many tribological systems. However according to Dunn, [141] who has identified about seventeen relationships between abrasion, impact and corrosion that could significantly increase wear damage in wet and aqueous environments, it is very difficult for the magnitude of the synergism to be estimated.

4.1.3 Identifying the nature and cause of corrosive wear

Depending on the environment and circumstances of operation which determine the type of surface film formed (oxide, oxycarbonate, chloride etc), the nature and cause of corrosive wear can be identified[126]. The wear debris in corrosive wear tends to be finely divided and fully reacted, with very little or no unreacted metal present. The existence of such debris is not a definite indication of corrosive wear, because in abrasive wear it is possible for the wear debris to be fully transformed before or after removal from the surface.

The worn surface will be fairly smooth, but the total loss of material can be very high. There will often be traces of corrosion on the worn surface, and it is important for the surface to be examined as soon as possible, before atmospheric corrosion can confuse the issue.

In the context of the present work it is important to define the environment in the twin-screw extruder, which is used in the food and chemical industries. Corrosion is of particular concern for good processing applications and constitutes a major problem. The construction materials used in the food industry have to meet the following technical requirements: [142]

- it has to be resistant to a humid CO_2 atmosphere, possibly polluted by sulphur compounds
- it has to be resistant to cleaning and disinfection
- it should not release any undesirable substances, especially where taste and/or odour are concerned.

Twin screw extruders are used in the manufacture of food and plastics. The most critical component within an extruder, which determines the operational efficiency, is the extruder barrel which must resist extreme conditions of corrosion and wear. [143] These conditions result from the synergistic interaction between different food additives such as aminoacids, β-carotene and salts in operational temperatures of up to 500°C.[4]

The selection of specific food additives for incorporation into commercial food products is based on the characteristics of the food requiring modification and the suitability of a particular additive, in terms of both its effectiveness in the food item and its cost compared with possible alternatives. [144] Also one of the main problems during selection, is a possible interaction between the additive and the metalic materials that the processing equipment is made of, which is a concern among others of this study.

4.2 Effect of other additives appropriate to food extrusion

4.2.1 Aminoacids

There are more than 200 different aminoacids known to occur in nature.[144] Most of the natural aminoacids are the α-aminoacids which contain carboxyl and amino functional groups bonded to the same carbon atom. The L-cysteine aminoacid with chemical formula $CH_2(SH).CH(NH_2).COOH$ was used in this work.

Aksut and Bilgic[145] have investigated the inhibiting effect of aminoacids on the corrosion of Ni and Co. The work for Ni was conducted in 1N H_2SO_4 and for Co in 0.5N H_2SO_4. The results for Ni showed that inhibition effects of aminoacids were most pronounced at low pH values while for Co they do not have a significant effect as corrosion inhibitors and in fact, in one case the values calculated by the linear polarisation method actually showed a slight acceleration of corrosion.

The effect of L-cysteine aminoacid on the corrosion of Co and Ni which are used as alloy additives in stainless steels and superalloys will be investigated in this study.

CHAPTER FIVE

5. Experimental procedure

The experimental techniques for wear and wear/corrosion which have been used and developed in this dissertation are presented in six main subsections. The emphasis will be on low-stress closed three-body abrasive wear tests using the rubber wheel (ASTM G 65-93). A 440C wheel was also employed to conduct dry abrasive, and wear/corrosive tests with abrasives.

5.1 Materials

A wide range of materials was tested in this investigation, in order that the more suitable candidates for the extruder application could be selected. Their chemical composition is shown in Appendix A.

All the materials which were tested were obtained as large billets, small specimens or manufactured in the laboratory. The presentation of those materials selected for further investigation follows, while the reasons for this selection will be discussed in the results chapter.

a) Mild steel (EN 3B)- wrought. This was used as a reference material and the performance of all the other materials has been recorded relative to this. Specimens were machined from commercial flat bar and tested in the as-received condition.

b) 440 C - heat treated - which is a typical barrel/screw material produced by casting. It was provided by APV Baker.

c) N 18 - Nickel-based superalloy produced by hot pressing of metal powder compacts. The starting powder for N18 consisted of spherical particles in shape and an average particle size of 75μm and it was provided by Tecphy-France.

d) N 18 - with ceramic particulate additions(TiC,TiN), produced by hot pressing of metal powder compacts. The same N18 powder was used, manually mixed with TiC and TiN particulates of an average size of 5μm, provided by HCST - Germany.

5.2 Specimen manufacture

The specimens were manufactured using different routes in order that the different microstructures produced be tested for wear and wear/corrosion behaviour.

Although the specimens can be any convenient size, the majority of tests were made with samples having the following dimensions:

Thickness : 3-6.5 mm (ASTM 3.2-12.7 mm)
Width : 20-25mm (ASTM 25 mm)
Length : 40-50mm (ASTM 76 mm)

According to ASTM G 65-93 standards, specimen size is not critical. The only requirement is that the length and width should be sufficient to show the full length of the wear scar as developed by the test.
The specimens were initially ground in order that the test surfaces be parallel and then polished on 800 and 1200 grit SiC paper.

Similar specimens and procedures were used for the preparation of the specimens that were tested on the 440 C wheel.

Specimens provided or manufactured for corrosion tests were prepared following a similar procedure to the wear tests specimens. However they were cut to smaller dimensions:

Thickness : 2-5 mm
Width : 10-18mm
Length : 25mm

5.2.1 Wrought and cast materials

Specimens were machined to size directly from the raw materials. Care was exercised to ensure that the test surfaces were parallel, and therefore the specimens were ground before the final polishing procedure.

5.2.2 Hot pressing

Hot pressing is a powder metallurgy technique where high density metal powder compacts with controlled microstructures can be produced. This method refers to an application of both an elevated temperature - at about 80% of the melting point -and a high pressure to the powder mass. Fig.5.1 shows the equipment set-up and Fig.5.2 the schematic diagram of the hot pressing machine used in the laboratory for the present study.

The metal powder was filled into a graphite mould which gives the compact a fixed shape and pressed in a high purity argon environment. In order to avoid contamination of the powders, the walls of the graphite tooling were sprayed with boron nitride(BN). Also, because most metal and metal alloy powders react strongly with the oxygen of the air, a controlled environment of high purity argon must surround the material at elevated temperature throughout the entire hot-pressing cycle. A typical cycle is shown in Fig.5.3.

Ni and Co-based superalloys exhibit superior creep resistance at high temperatures under loads encountered in service. However this reduces the capacity of superalloy powders to deform plastically during hot consolidation. This means that higher temperatures and pressures or longer times under load are required to achieve high density.

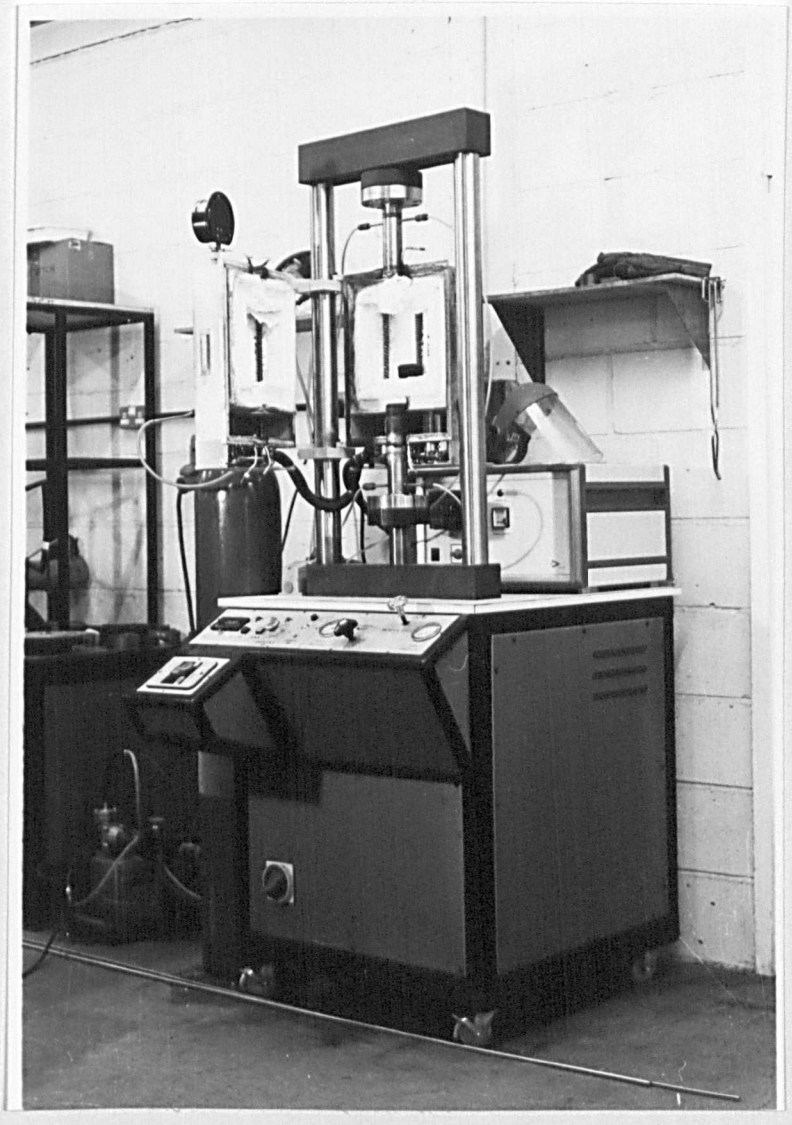

Fig.5.1 : Set-up of the Hot-pressing machine used in the laboratory

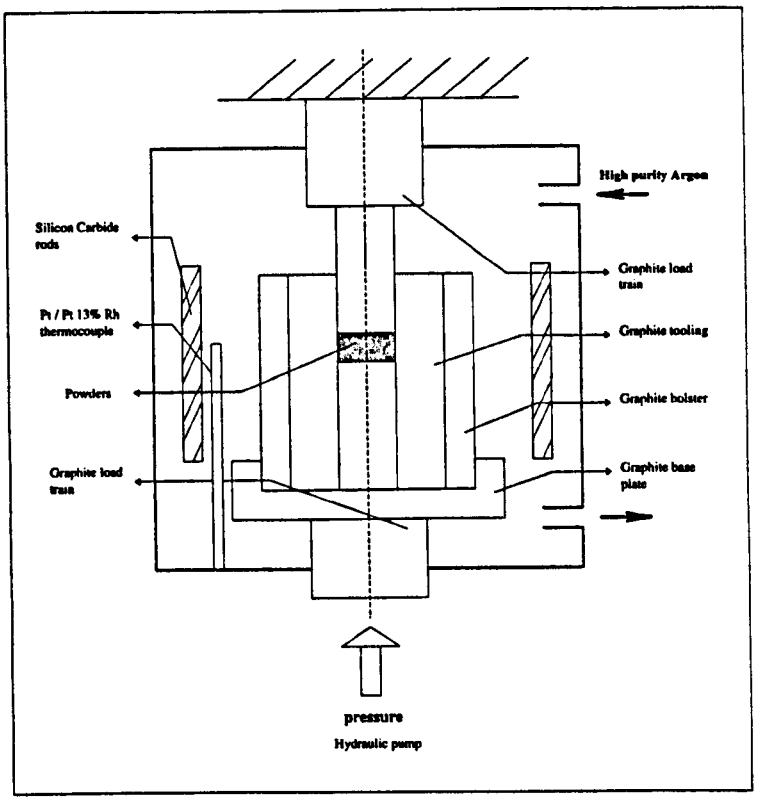

Fig.5.2 :Schematic diagram of the Hot pressing equipment

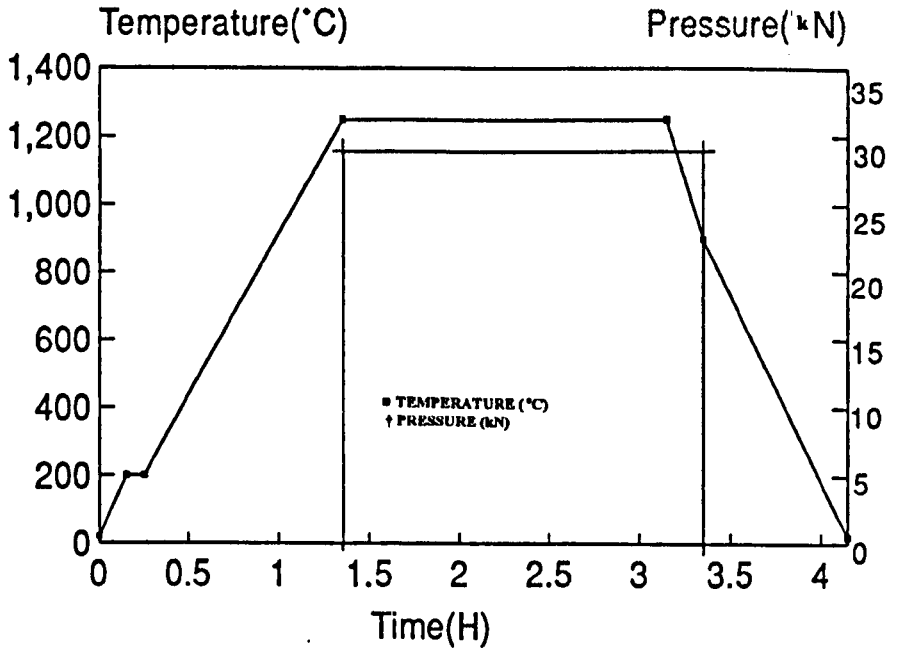

TEMPERATURE(°C)	20	200	200	1,250	1,250	900	20
PRESSURE(kN)	0.01	0.01	0.01	0.01	30	30	0.01

Fig.5.3:Graphical presentation of conditions for hot pressing

5.2.3 Hot isostatic pressing (HIP)

This materials processing technique uses the effect of high isostatic gas pressure at elevated temperatures to consolidate the particles of a powder part or to remove porosity of a finished part. The dense and well bonded structure which results may consist of a single material or a combination of different materials.

The capacity of the furnace for the particular Hipping machine used in this project has been ϕ 80mm x 170mm long. Pressure was applied uniformly using an inert gas, argon, at a maximum pressure of 2000 bar and maximum temperature of 2000°C, which are controlled independently by a microprocessor control facility.

The metal powder was filled in a can made from 316 stainless steel metal sheet, evacuated to approximately 10^{-1} bar and at 200°C, crimped and sealed using TIG welding. Initial can dimensions to produce a finished part from encapsulated uncompacted powder must account for a machining allowance, powder/can interaction and dimensional shrinkage. After the processing cycle the stainless steel can was removed and the Hipped metal machined to final dimensions.

5.2.4 Heat treatment

Tool steels and superalloys must be processed to develop specific combinations of wear resistance, resistance to deformation and fracture under high loads or elevated temperatures. In order that these properties be achieved, a proper heat treatment is critical. Some of the materials tested in this project were also heat treated. Their heat treatment cycles are given in Appendix A.

5.3 Corrosion testing

Corrosion, a materials degradation process can be defined as the interaction between a material and its environment. The problem in extrusion is usually the aqueous environment which exists during the process and comes in contact with the stationary and moving parts of the equipment. However the real question about corrosion is not whether it will happen but how fast and in what form. Thus corrosion kinetics must be studied.

Two kinds of corrosion tests were conducted in the laboratory:

a) A 3 vol.% sulphuric acid solution (pH=0.7) was prepared using grade 98% sulphuric acid(Merck) diluted with appropriate quantities of distilled water. These tests were carried out at room temperature (18-22°C) and at different exposure times.

b) A AEW-Middlesex horizontal electric furnace was employed for the high temperature aqueous corrosion experiments. The temperature inside the furnace was chosen to be 90±5°C, following temperature measurements during the wear tests which indicated

that this would be a realistic value. However, it should be remembered that the actual surface temperature during wear should be higher than this value. The corrosive medium was again a 3 vol% sulphuric acid solution. The steps followed to run the test were :

- the specimens were cut to dimensions
- a 3mm dia. hole had been drilled in the upper corner, which allowed the sample to be suspended on a platinum wire
- each specimen was polished on 800 and 1200 grit SiC paper, cleaned with alcohol and dried
- the specimens were weighed to the nearest 0.0001g and immersed in a 1000 ml Pyrex beaker
- at different time intervals they were removed from the solution, furnace dried for 2 minutes and reweighed.

The corrosion rate was calculated based on the weight change data and the original surface area.

5.4 Wear testing

5.4.1 Mechanistic studies

Mechanistic studies give an opportunity to examine in depth, the particle/surface interaction, reveal the mechanisms involved and correlate them to the actual wear tests. They can be divided into :

a) indentation tests

Indentation experiments were carried out to simulate the abrasive action of the single sand grains and quantify the damage produced on the surface. The following steps were followed :

- a new surface was used to simulate the abrasive wear tests (rubber wheel)
- based on the dimensions of the wear scar and the average particle size of the sand, the quantity of the sand expected at any particular moment abrading the surface was calculated along with the total applied load
- a piece of rubber of similar hardness to the rubber wheel(Dry Sand Abrasive Test-DSAT) was used and it was pressed against the surface of the specimens having the abrasive particles in-between
- three loads were used(44.5-127.5-197.5N) taken from the range of loads used in the main wear tests

b) scratch tests

Scratch test studies employed individual or a small number of abrasive particles and were carried out in the same laboratory environment using the rubber wheel. The conditions of the test were similar to those used in abrasive wear tests:

-speed of the wheel set at 200rpm
-two different loads of 44.5 N and 197.5 N
-three different particle sizes

The purpose of these tests was to trace the path of each individual particle along a specimen surface and quantify the damage produced by well characterised particles. The size of a wear groove was quantified by measuring its width, depth and length.

5.4.2 Dry abrasive wear tests - Rubber wheel

The device used to conduct low-stress abrasive wear tests and the schematic diagram of this tester are shown in Fig.5.4. The procedure employed is that described in the approved ASTM G 65-93 standard test method developed by Committee G-2 on Erosion and Wear.

The test sample was loaded against a chlorobutyl rimmed steel wheel through a weighted lever system. Four hardness readings were taken on the rubber approximately 90° apart around the periphery of the wheel using a Shore Durometer tester and the hardness was found to be A 60±1. A range from A 58 to 62 is acceptable according to ASTM standard. The diameter of the rubber wheel was measured before and after each test and thoroughly examined for any visual defects and any abrasive sand adhered to the surface was brushed away.
After each set of tests had finished the rubber wheel was machined, with the intention to produce a uniform surface that will run tangential to the test specimen without causing vibrations on the lever arm or leaving an uneven wear scar on the specimen.

The specimen holder is attached to a lever arm to which weights are added, so that a force is applied along the horizontal line of the wheel. The theoretical force applied on the specimen was found by using the formula:

$$F(N) = W\ g\ (L/l) \qquad 5.1$$

where : W = load applied on the lever arm(kg)
g = 9.81m/sec^2
L = length of the lever arm
l = length from the specimen holder to the lever arm
(in this case : L/l = 2.5)

(a)

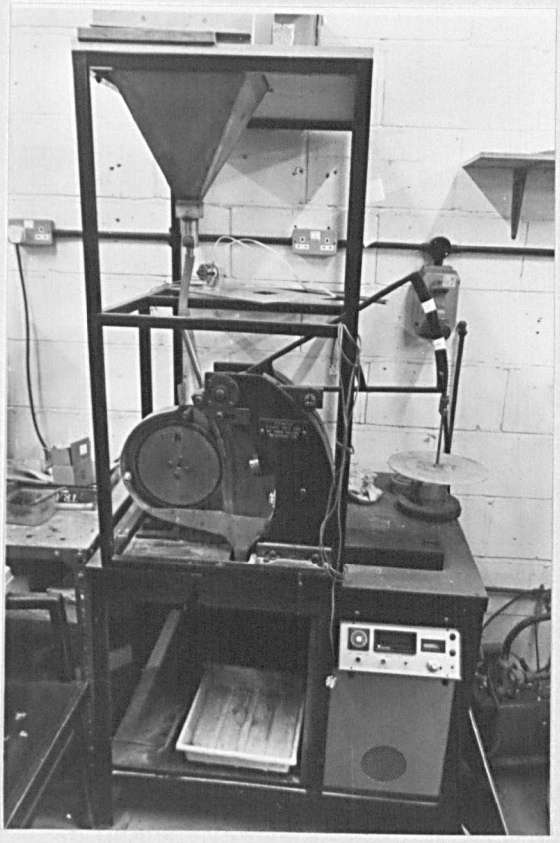

(b)

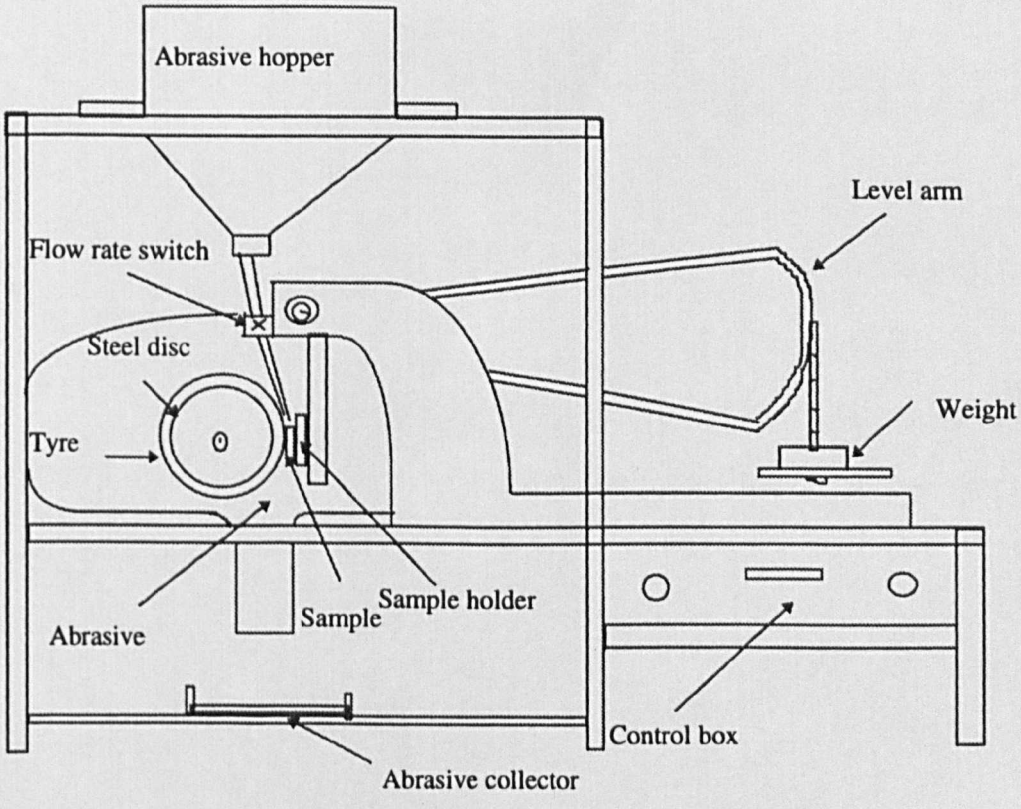

Fig.5.4 : Dry abrasive wear tester
a) equipment set-up b) schematic diagram

The system was then calibrated using a spring-balance to measure the actual force and correlate this with the theoretical value for a given mass.

The wheel is driven by a 1 HP d.c motor through a 6:1 gear box to ensure that the full torque is delivered during the test. The rate of revolution was set to 200 rpm (ASTM 200±10rpm) and should remain constant under load. This was not the case, as the calibration of the wheel rotational velocity revealed. Therefore the number of the wheel revolutions was monitored during each test using a counter. This was taken into consideration when calculating wear rates.

The abrasive silica sand is gravity fed from a hopper to the interface between the specimen and the wheel. Its shape was angular and the particles' size 100-350μm while the ASTM standard specifies semirounded particles of a size 212-300μm. The hardness of the sand was taken to be about 700Hv. The reported range is 600-800 Hv. [108] The moisture content of the sand was regularly checked and found to be less than the maximum recommended by ASTM standard (0.5 wt%).This checking consisted of measuring the weight loss after heating a sample of sand in the furnace to approximately 120°C for 1 h.
All abrasion, scratch and indentation experiments were conducted with silica sand of the same specification obtained from Laboratory Equipment Service Ltd in Bedford.

The hopper was calibrated to deliver a sand rate of 250g/min (ASTM standard 250-350g/min) in the form of a sand curtain. From the very first test it became apparent that while the proper shape of the sand curtain was achievable, the flow rate was not constant. It was then decided to collect and weigh the sand at the end of each exposure period. A plastic container was used for this purpose. The effect of this variability on the data was considered for the presentation of results.

The actual test consisted of the following steps:

- the surface of the specimen was polished using 800 and 1200 grit SiC paper
- prior to weighing the specimen was cleaned with alcohol and dried
- the specimen was weighed to the nearest 0.0001g(ASTM procedure C)
- the specimen was positioned in the holder of the rig
- the revolution counter was set to 200 rpm
- the sand flow was started and a short time allowed for the flow to become uniform
- the specimen was engaged on the wheel, trapping sand between the wheel and the specimen
- each test was run for 40 minutes
- the specimen was removed and reweighed at given time intervals. Tests from the second interval onwards were conducted on the same wear scar. Every new specimen followed the same procedure.
- care was taken to replace the specimen back in the holder after each removal such that the wear scar was at the same location.

All experiments reported here were conducted in a laboratory with no provision for temperature or humidity control. However, there are not large variations in temperature and humidity. Typical values are 18-22°C and about 70% r.h.

The abrasion test results were reported as mass loss in grammes or volume loss in cubic millimetres. The mass loss was converted to volume loss according to:

$$\text{Volume loss}(mm^3) = (\text{mass loss}(g)/\text{density}(g/cm^3)) \cdot 1000$$

There was no need for *"the adjusted volume loss"* to be calculated since there were no measurable dimensional changes of the rubber wheel(diameter, thickness) after the end of each run.

5.4.3 Dry abrasive wear tests-440 C wheel

Considering that metallic screws and paddles run against the barrel in an actual extruder, it was decided to replace the rubber wheel with a 440 C wheel. Tests were undertaken with abrasives to study dry abrasive wear process and compare results with those obtained using the rubber wheel.

The test conditions and specimen preparation were similar to those for the rubber wheel, except that only two loads (44.5 N and 197.5 N) were used. A new ground 440 C wheel was used for each set of tests.

Sand from the tests was also collected and weighed by placing a plastic container underneath the 440 C wheel.

5.5 Wear/corrosion testing - 440 C wheel

It is clear that the testing of materials for dry abrasion resistance alone is not likely to provide a satisfactory guide for the selection that is to be used in a corrosive environment like that existing in an extruder. Consequently a series of experiments was conducted to investigate the influence of metal-environment interactions on the rate of material loss under wear conditions.

5.5.1 Abrasive/corrosive wear testing - 440 C wheel

A similar device to that used for dry abrasion testing was used to conduct wear/corrosion tests. A close-up of the wheel set-up is shown in Fig.5.5. The tests were designed so that the abrasive wear and corrosion occur simultaneously. The corrosive medium was tap water, and various concentrations of H_2SO_4(0.3-3-30 vol%). As one of the main ingredients processed by an extruder is aminoacid, it was decided one test to be conducted with 3vol% H_2SO_4+10wt% L-cysteine Aminoacid.

The test conditions and specimen size and preparation were similar to the tests with dry abrasion.
Each complete test was undertaken for 1 h with the specimen weighed every 15 minutes.

The abrasive sand was collected underneath the 440 C wheel, furnace dried for 2 h at 150°C and then weighed.

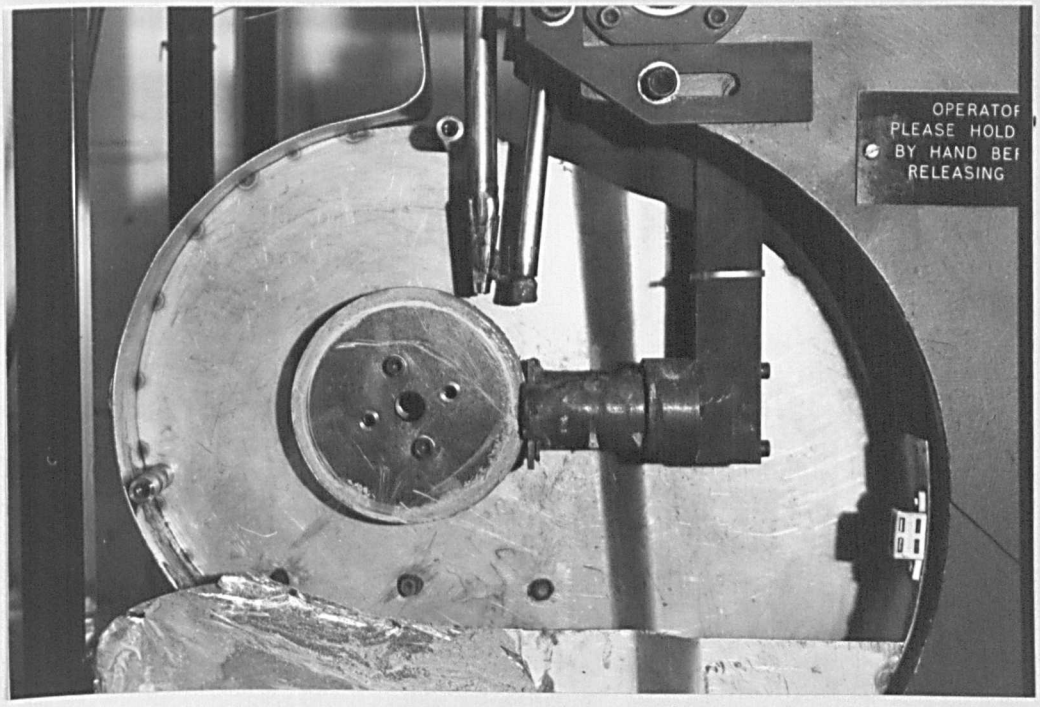

Fig.5.5: A close-up of the wheel set-up for wear/corrosion tests

5.6 Characterisation studies

5.6.1 Materials

A microstructural examination was carried out on all the test specimens. The magnifications used when taking photographs were standardised wherever possible to enable comparisons to be made directly between the different materials.

A Nikon optical microscope was used to examine the microstructure of different materials in the etched condition and the surfaces just before the wear tests (unetched).

The bulk hardness of the specimens was measured using a Vickers-Armstrong Ltd. diamond indentor set at 20 kg load. Results are quoted as Vickers hardness numbers(HV 20) and were the mean values of five indentations.

Microhardness measurements were taken at the worn surfaces of the specimens and underneath in cross-sections to determine if local work hardening had taken place. A Matsuzawa Seiki Co. microhardness tester was used with a 300 g load for 15 seconds.

Results are quoted as Vickers hardness numbers (MHV 0.3).
All the results recorded were the mean values of three indentations.

The densities of the experimental materials which were used to convert weight loss into volume loss, were determined by the Archimedes method.

A Malvern 2000 laser analyser was employed to analyse the size distribution of the abrasive sand before and after wear tests.

5.6.2 Wear and Wear/Corrosion tests

After each test was completed, the specimens were cleaned with alcohol and dried. Then they were Au/Pd coated and the worn, worn/corroded surfaces examined under the SEM microscope.
Alternatively, some specimens were sectioned and polished for a more detailed microstructural investigation of the area under the wear scar.

A Cambridge Stereoscan 250 MKII Scanning electron microscope(SEM), which was interfaced with an energy dispersive x-ray (EDX) analysis was used to examine the worn and worn/corroded surfaces in more detail. Different locations of the wear scar were studied; the abrasive entrance and exit ends and mainly the centre of the wear scar where most of the stresses apply.
Also the area underneath the wear scar of the sectioned specimen was studied for cracks or other possible damage morphologies which would provide useful information on the material removal mechanisms.

X-ray photoelectron spectroscopy(XPS) and depth profiling by ion etching were used to study the corrosion products formed on the materials, after wear and wear/corrosion tests. The XPS apparatus is an Escalab II - V.G Scientific Ltd. standard commercially available equipment.

XPS is a technique for examining the elemental composition and, in some cases, the compound compositions of the surfaces to a depth of 4 to 5 atomic layers. In addition, sputtering a method for removal of material from a surface by positive ion bombardment, is a useful tool for surface cleaning.

The surface layer compositions were examined by taking depth profiles, which involves sequencial etching and surface analysis. The objective was to analyse the composition and the thickness of the films formed on the wear/corrosion scar and original area(corrosion only) of the specimen.

For the examination of the worn surface of the 440 C wheel in the dry/wet abrasion tests, a replica technique was successfuly used. Suitable replicas can be quickly made by pressing softened, thin cellulose acetate sheet on to the surface of the wheel and moistened with acetone. After the removal of the acetate sheets from the surface, they were carbon coated and examined on the SEM.

Abrasive sand particles used in the test were also examined by SEM before and after wear tests for possible damage. The wear debris on the particles was examined, and individual phases of the wear debris were identified by EDX analysis.
Wear debris analysis develops an additional source of information concerning the wear process beyond that provided by wear surface analysis and subsurface examination. It is important to study the process by which material is actually removed from the wearing surface as contrasted to the processes that lead to only surface damage and deformation. The size and morphology of the debris particles can be directly related to the worn surface topography. Further, even though surface groove formation is the prominent process used in theoretical modelling, it seems very likely that careful study of debris can be proved valuable for abrasive wear modeling.

At the completion of dry abrasive wear(rubber wheel) test and dry sliding wear(440 C wheel) with abrasives, the sand collected was spread out on a clean sheet of paper and a magnet passed several times over it. This enabled a sufficient quantity of wear debris to be collected for examination. The sand coming from materials without magnetic properties was sieved and enough quantity of wear debris was collected for examination. Also wear debris particles were identified on sand particles by using EDX analysis on the SEM.

Wear debris from wear/corrosion experiments was collected but because of the length of time required to thoroughly dry the sand before collection could take place, it was thought that any information would not have been reliable.

After the collection, the wear debris particles were placed on glass slides, sputtered with Au/Pd prior to SEM examination.

A Joyce-Loebl Ltd. image analyser was used to measure the size distribution of the wear debris particles. The same analyser was also used to measure the number of the indents made by sand particles on the samples during indentation tests.

CHAPTER SIX

6. Experimental results

An evaluation of the abrasion-corrosion wear results for the standard tests and the general trends and relationships will be presented in this chapter. A comprehensive table of the abrasive wear results for all the materials tested will be found in Appendix B. The results are expressed as wear rates against load. The tests each lasted for 35 minutes and the specimens weighed every 5 minutes.
The materials were grouped according to their production process while the reference material, mild steel(M.St), appears in all groups for comparison purposes.

6.1 Presentation of materials

The four materials, M.St, 440C, N18 and N18++, which are presented here were selected for further investigation as they were considered to be representative materials for present and future extruder applications.

Fig.6.1a shows the typical microstructure of the reference material, mild steel, which consisted of ferrite (light) and pearlite (dark, about 19vol.%) grains. Its bulk hardness was HV_{20} =230, the measured density 7.9g/cm^3 and it will be sort-coded M.St.

Fig.6.1b shows the microstructure of the heat-treated 440C stainless steel which consisted of primary and secondary carbides(light islands and particles, (about 6vol.%) in a matrix of tempered martensite. Its bulk hardness was HV_{20}=720, the measured density 7.6g/cm^3 and it will be sort-coded 440C.

Fig.6.1c shows the microstructure of N18 which was produced by hot-pressing at 1190°C and 30KN pressure. N18 is a multiphase material with uniform microstructure which consists of small eutectics and hard Cr carbides(M_7C_3) dispersed in a softer Ni matrix. Its bulk hardness was HV_{20} =380, the measured density 8.00g/cm^3 and it will be sort-coded N18.

Fig.6.1d shows the microstructure of the N18+5wt%TiC+5wt%TiN(about 15vol% particulates in total) which was produced by hot-pressing at 1230°C and 30KN pressure where the large white areas were Ni and Co rich, surrounded by small areas of eutectic and dispersed Ti.
The same N18 powder was used, manually mixed with TiC and TiN particulates of an average size distribution of about 5μm. The ceramic particulates were provided by HCST-Germany. The bulk hardness of the material was HV_{20}=520, the measured density

7.22g/cm^3 and it will be sort-coded N18++.

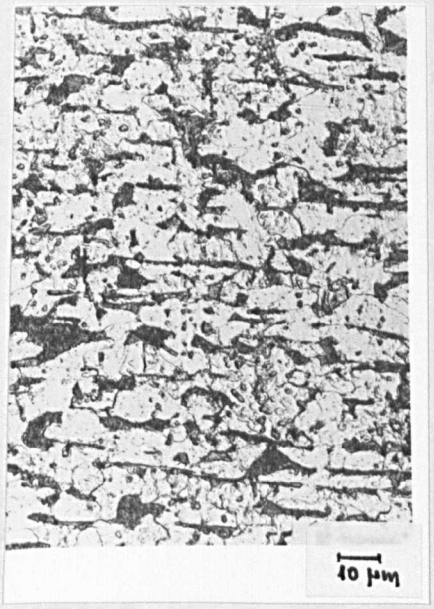

a) M.St - Etched in 2% Nital

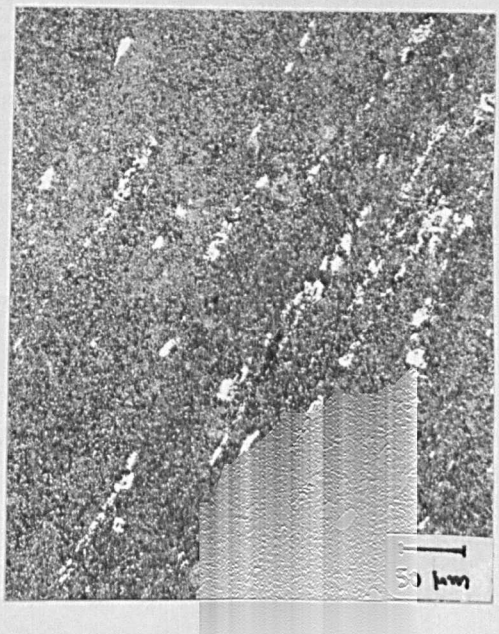

b) 440 C - Etched in Villela's reagent

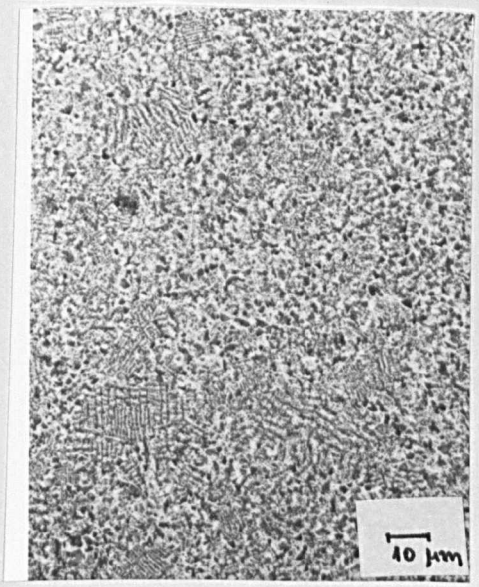

c) N 18 - Etched in Marble's reagent

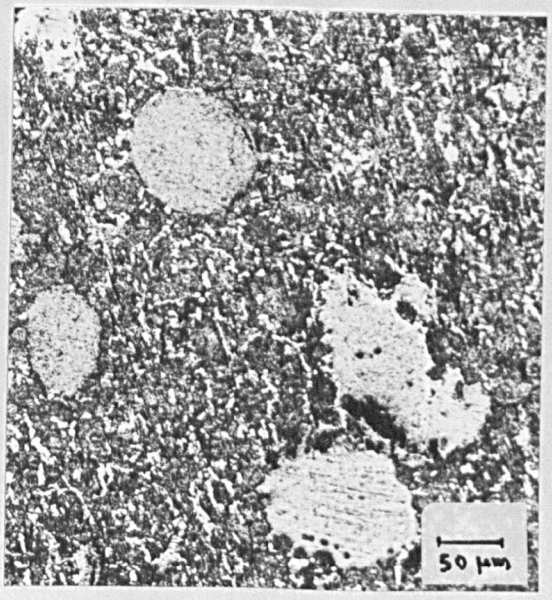

d) N 18++ - Manually mixed
Etched in Marble's reagent

Fig.6.1 : Microstructures of the materials chosen for further investigation

Fig.6.2a shows a general view of fresh abrasive silica sand where sharp angular(Fig.6.2b) and rounded particles(Fig.6.2c) coexist. An average percentage was, 25% rounded and 75% angular particles. As Fig.6.2d shows the particle size distribution, appears to be bimodal.

The average particle size was about 199μm and the mean roundness factor of the angular particles was calculated to be 0.65 which varied from 0.5 to 0.75. Larger particles tend to have lower shape factor. This shape factor was calculated as the ratio of the smallest dimension to the largest one.

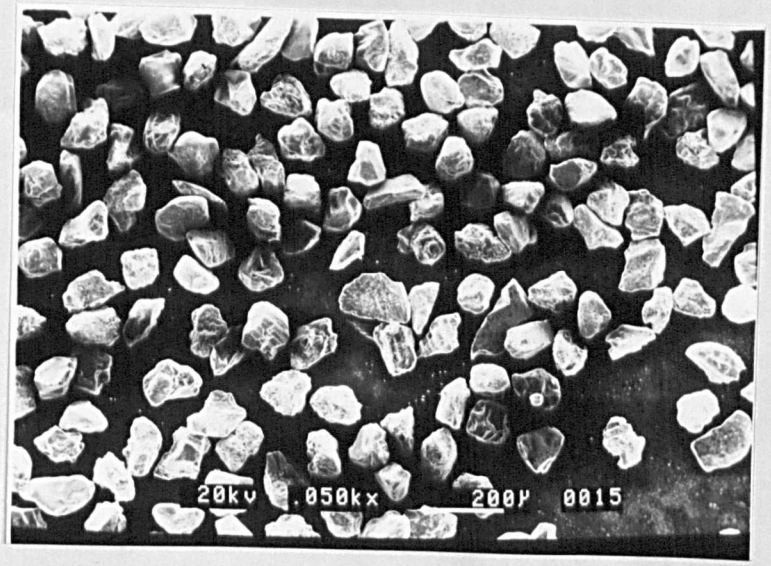

a

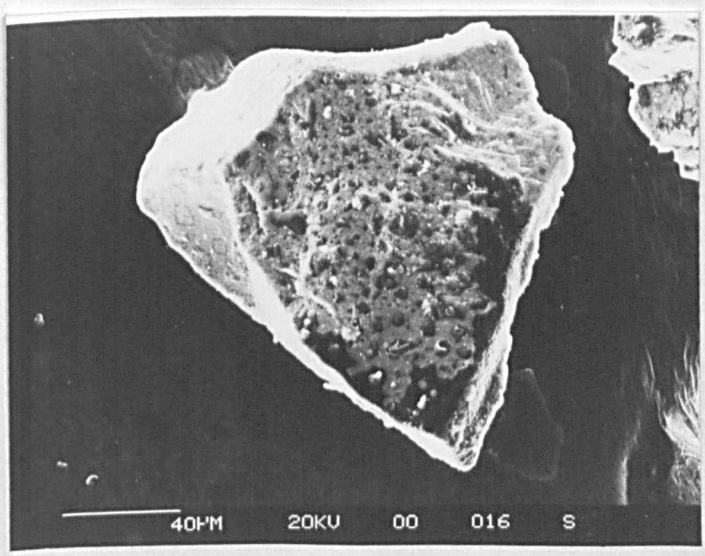

b

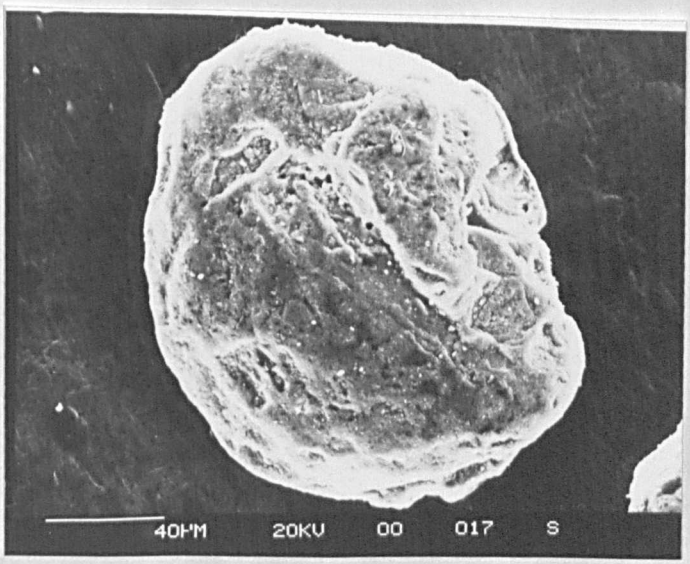

c

Fig.6.2 : SEM photographs of fresh abrasive silica sand. a) general view b) close-up of a sharp angular particle c) close-up of a rounded particle

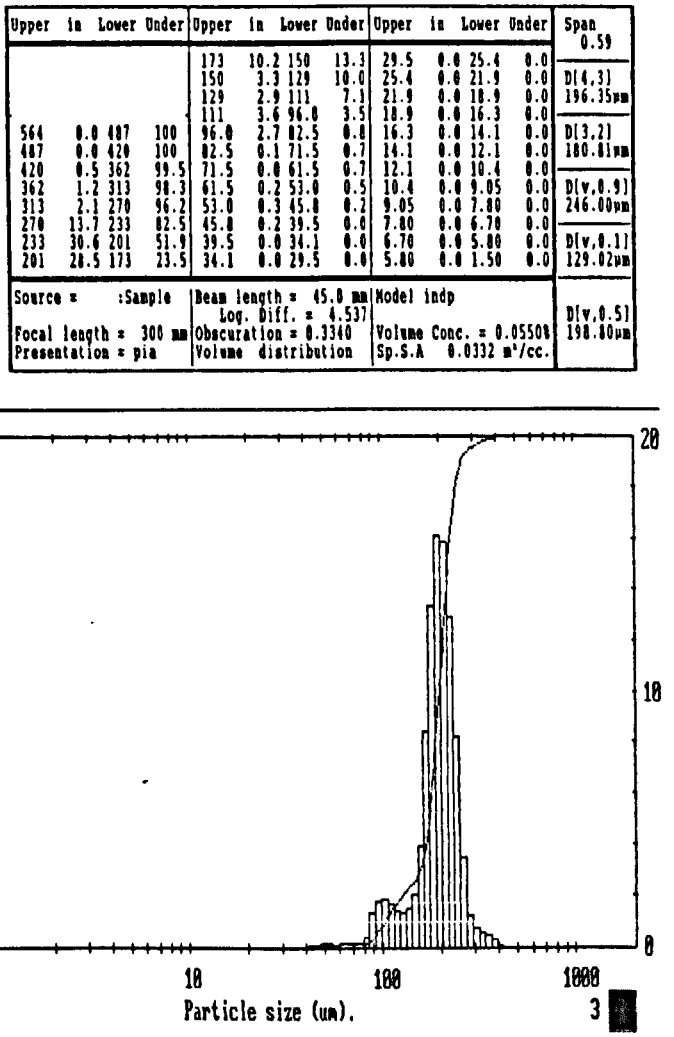

d

Fig.6.2 : continued- d) Particle size distribution of fresh abrasive silica sand.

6.2 Wear tests

6.2.1 Calibration of the wear rig

Before the actual wear tests started the wear rig was calibrated and the following results obtained. These calibration results illustrate the problems during experimentation and how the experiments should be undertaken.

Fig.6.3 and Fig.6.4 show all the calibrations done on the wear rig. The main problem encountered during the tests was the fact that as the load increased the wheel revolutions decreased and consequently the sliding distance kept changing.

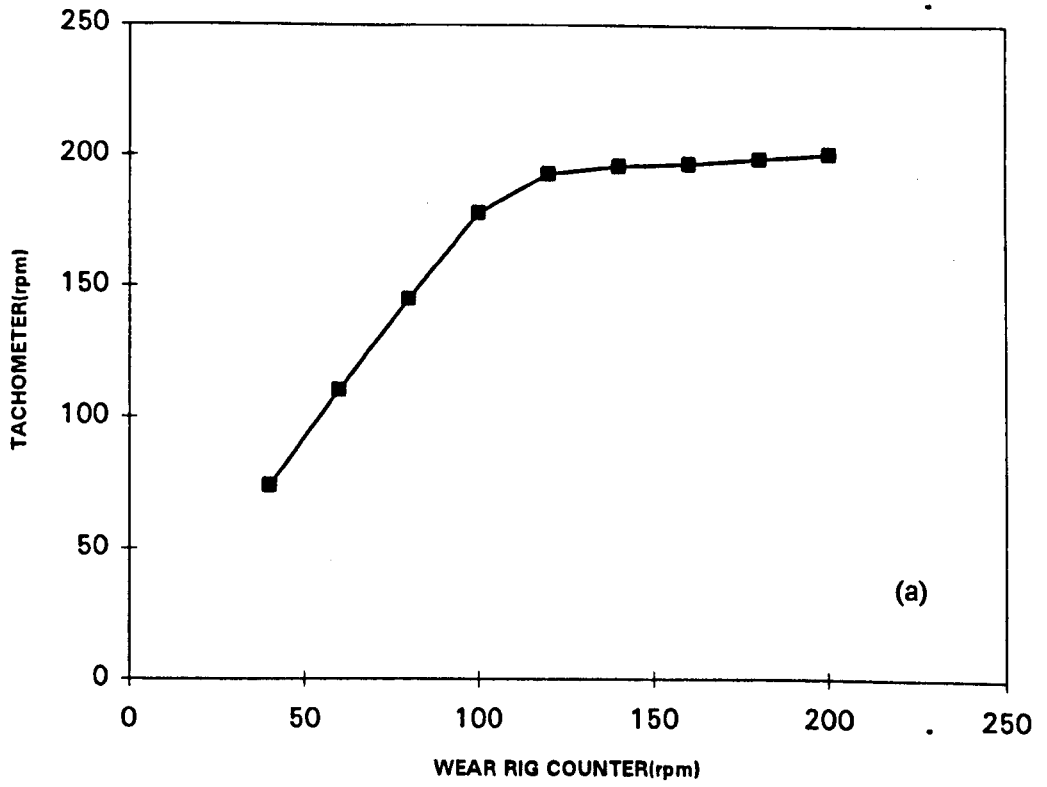

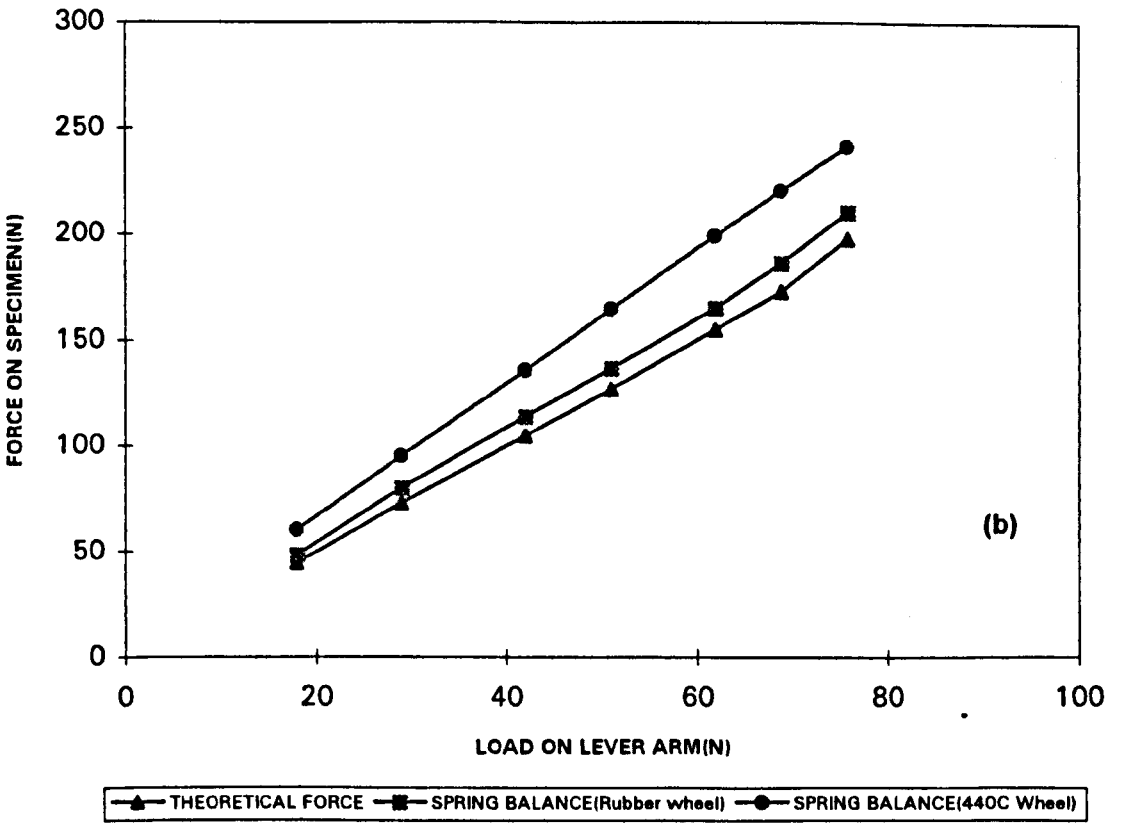

Fig.6.3 :Calibration of the wear rig: a) revolutions of the rig counter vs revolutions of the tachometer applied on the wheel b) theoretical force applied on the specimen vs measured force by using a spring balance.

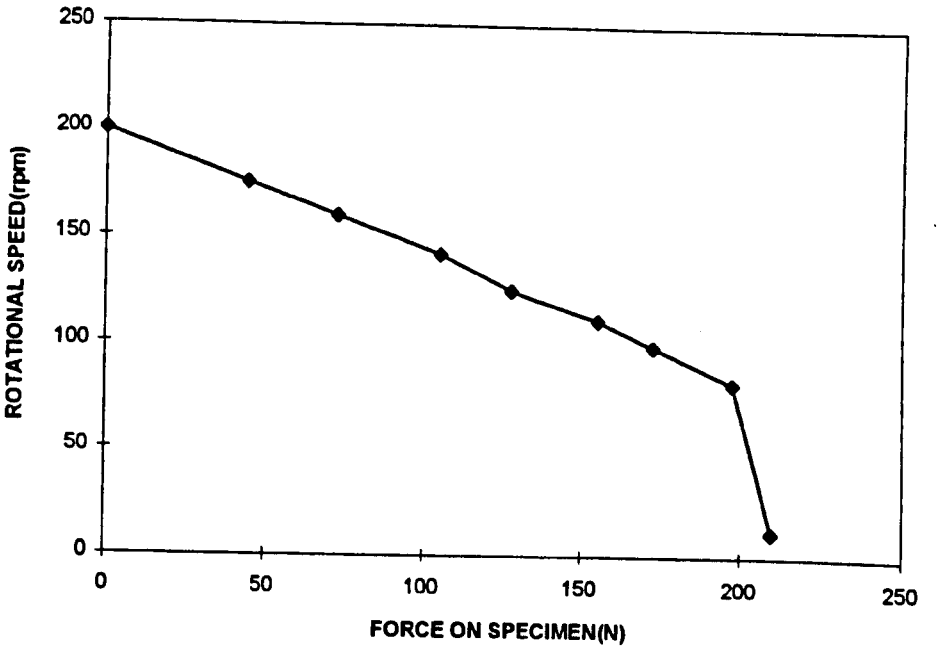

Fig.6.4 :Calibration of the wear rig- Change of the rotational speed with the applied load

From the graphs in Figs.6.3 and Fig.6.4 along with the fact that the hopper was not consistent in delivering the same amount of sand, as mentioned in chapter five, the following conclusions can be drawn:

- the test may be started with a preset speed of 200rpm because, without load, the rig counter coincides with the tachometer reading(Fig.6.3a).
  However, this is not the case under load, which means that the revolutions of the rig counter should be monitored at the end of each test.
- the real force on the specimen is slightly higher than the theoretically calculated(Fig6.3b).
- the maximum force on the specimen should be less than 200 N, otherwise the wheel comes to a complete halt(Fig.6.4).
- the mass of sand should be measured at the end of each test due to the variability of delivering rate.

6.2.2 Reproducibility of data

The reproducibility of data was checked for mild steel which was used as a reference material for comparing the abrasion behaviour of pure metals and alloys.
Five mild steel specimens were prepared from the same available stock under similar conditions. They were then tested for 3-body abrasive wear on the same wear rig, in a period of three months, by the same operator under nominally identical operating conditions. The same range of loads, abrasive sand and duration were used.

The results in Fig.6.5 show an extremely good reproducibility for all the loads tested. Even a slight variation at the highest load is within the ASTM allowable error of 5% for this sample size.

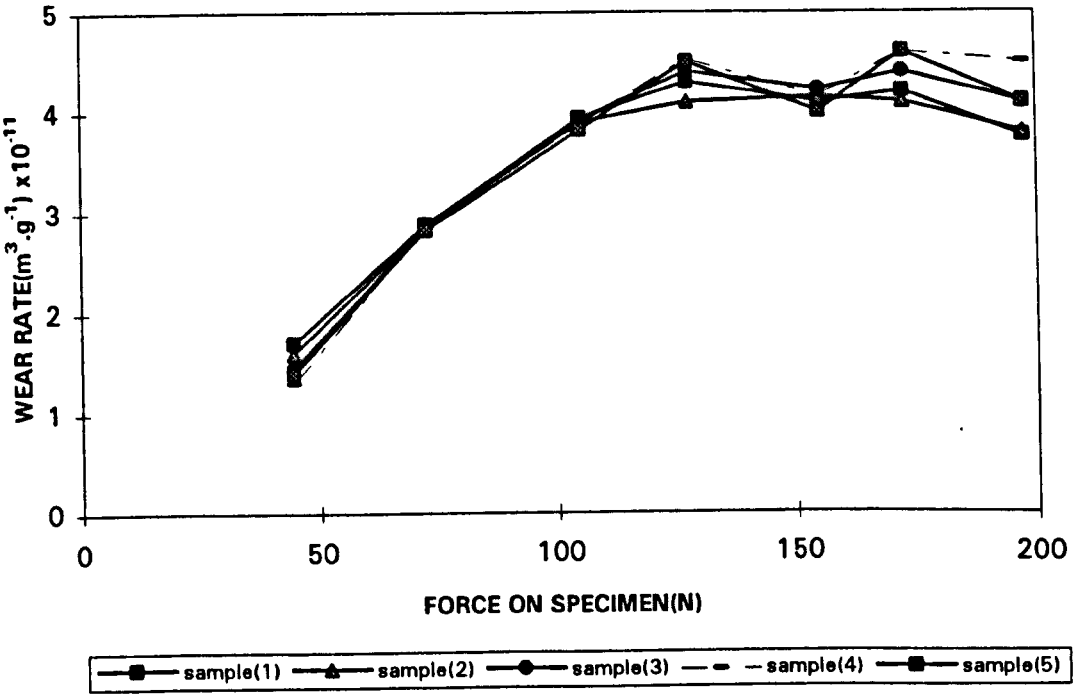

Fig.6.5 : Reproducibility of data for the reference material M. St - Dry abrasive test with rubber wheel. Test run for 35 min. in total and the specimens weighed every 5 min. interval

6.3 Dry sand Abrasion wear tests - Rubber wheel

6.3.1 Wear behaviour

The wear volume of the four selected materials for further investigation as a function of mass of sand taking part in the abrasive process has been plotted in Fig.6.6, at a range of applied loads of 44.5N, 127.5N and 197.5N. An approximately linear increase in the volume wear, with some evidence of "running-in", for all the materials was observed. The 440C showed the best wear behaviour while the N18 competing with the M.St. for the worst.

Fig.6.7 also shows a typical range of wear rates of the same materials as a function of mass of sand abrading the surface. The test time intervals and the applied loads were the same. As can be seen from the plots after an initial running-in period the wear rates for all the materials became nearly stable. Again the 440C showed the best wear behaviour and the N18 and mild steel the worst. At low loads M.St was no different from N18++.

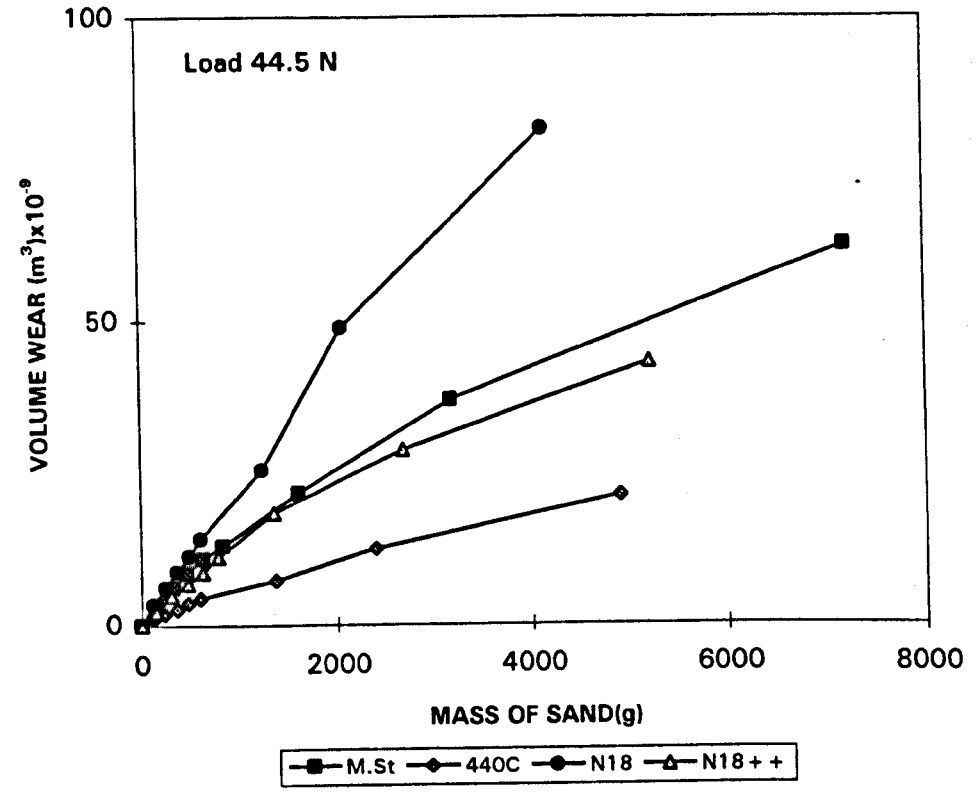

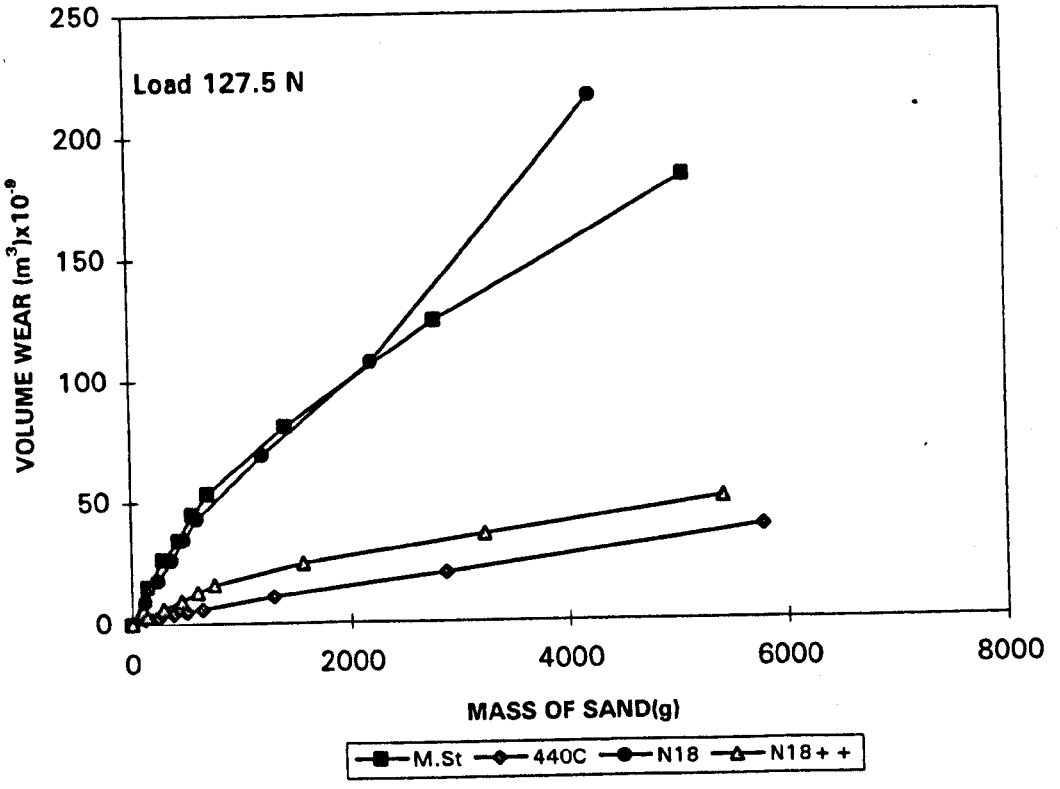

Fig.6.6 : Rubber wheel abrasive wear tests expressed as volume wear vs mass of sand. Comparison of different materials at different loads. Tests run for 40 mins in total and specimens were weighed at different time intervals

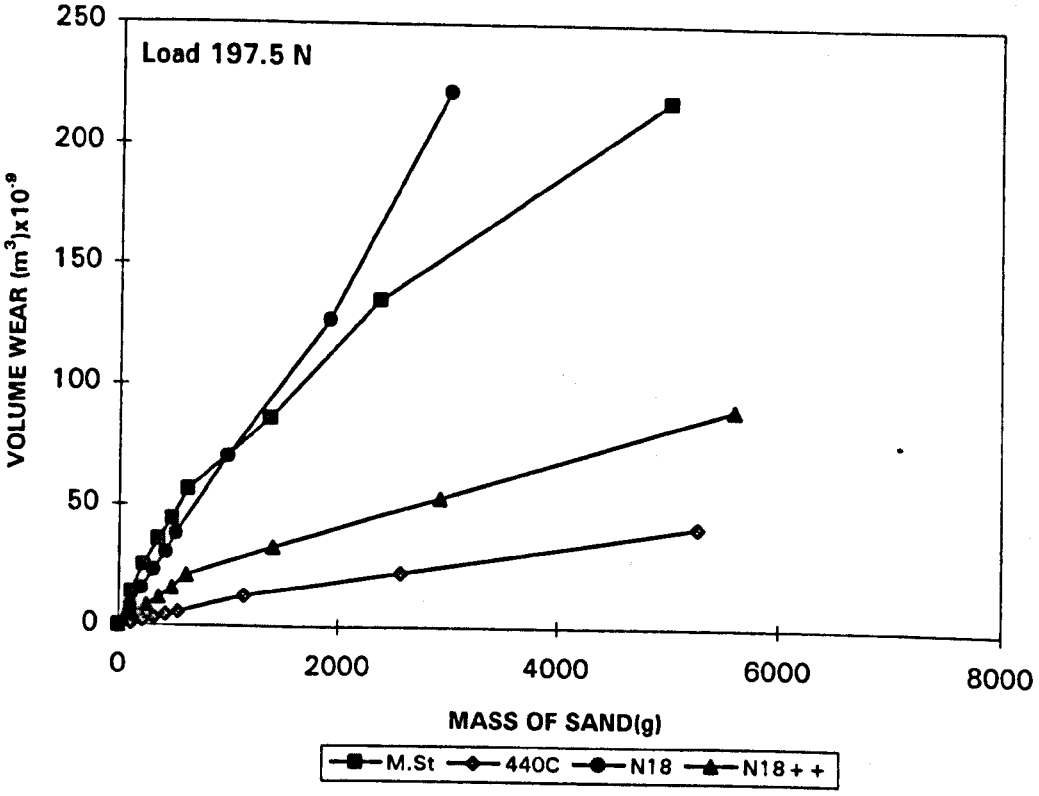

Fig.6.6 : continued

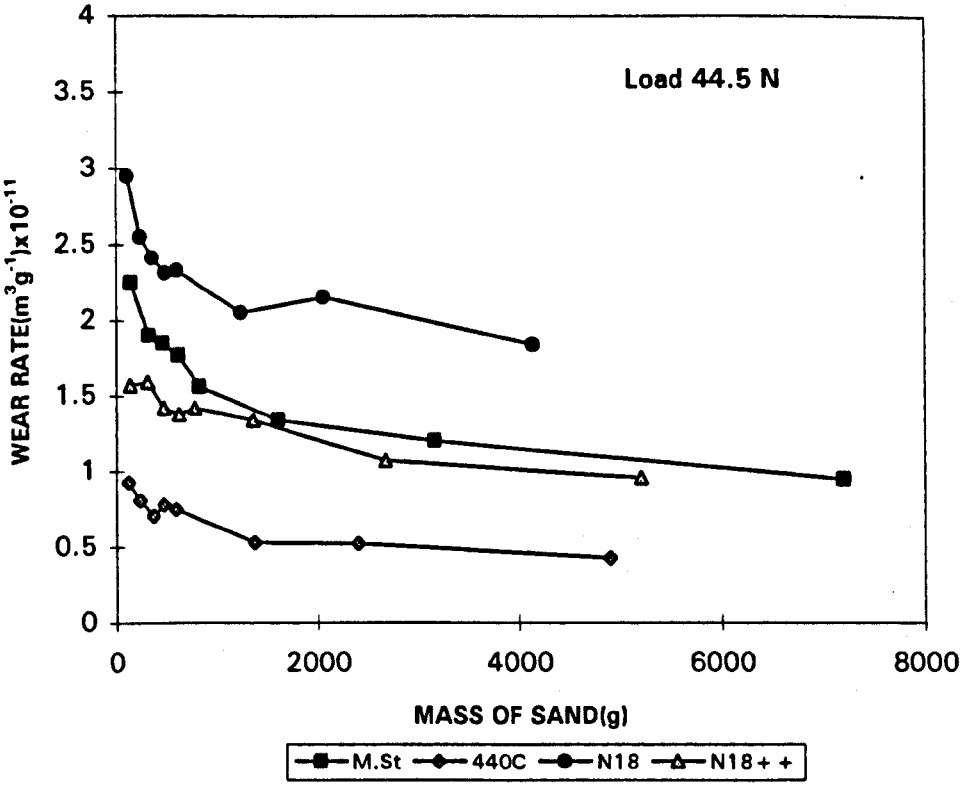

Fig.6.7 : Dry abrasive wear with rubber wheel. Results expressed as wear rate vs mass of sand. Comparison of different materials at different loads. Test run for 40 mins in total and specimens weighed at different time intervals

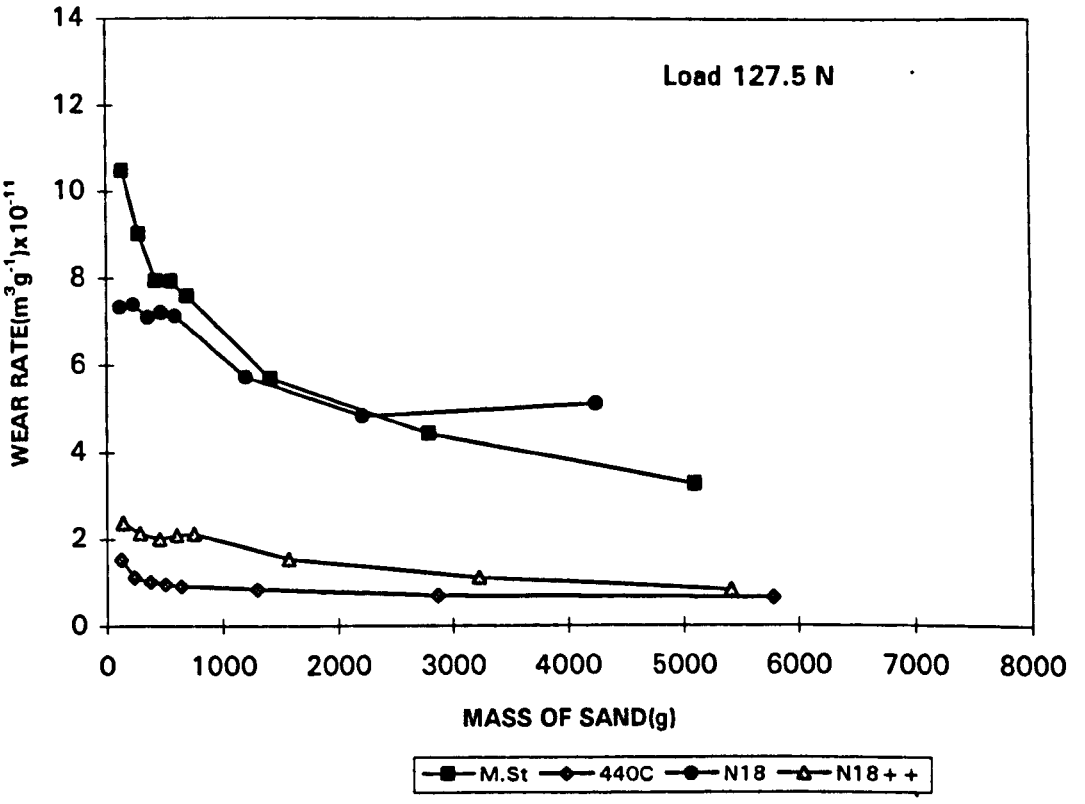

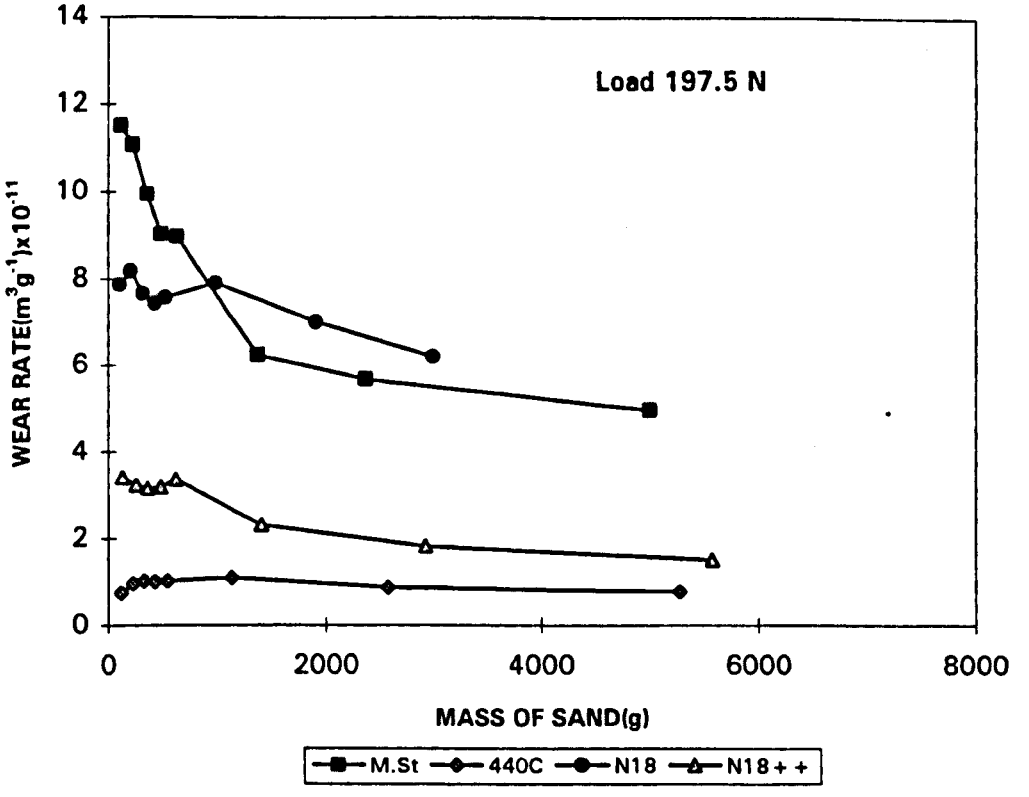

Fig.6.7: continued

Both Fig.6.6 and Fig.6.7 indicate that two trends exist; the materials with the higher bulk hardness(440C and N18++) showed better wear performance under these specific test conditions. The exception was N 18 that despite its higher hardness, compared to M.St., showed high wear rates.
These graphs also show the effect of the load on the abrasive wear since all the materials at 127.5 N and 197.5 N gave higher wear rates compared to those at 44.5 N by a factor 2-3.

6.3.2 Wear surface and subsurface

Scanning electron and optical microscope photographs of the specimens for all the materials were taken starting with the surfaces before tests, the wear scars as they appear on the specimens, the worn surfaces, a cross-section in the middle of the wear scar and subsurface examination. An example for M.St is shown in Fig.6.8.

The wear scars of all the materials tested appeared similar in shape(rectangular) although it is clear that they differ in dimensions. Two main areas can be identified(Fig.6.8b); a small entrance-exit area(coloured differently, white-black) and the main area consisting of parallel grooves. It is evident that the abrasive grains do not maintain a continuous sliding motion across the wearing surfaces. Initially, as the sand enters the interface between the rubber wheel and the specimen, most of the grains are rolling rather than sliding and the same happens as the sand exits(Fig.6.9a,b). However, at the centre of the wear scar the appearance of the grooves indicate that most of the abrasive particles are sliding across this region. This behaviour may be due to the variation of the contact pressure along the wear scar. At the sand entrance-exit zones the contact pressure is small. At the centre zone the contact pressure will have reached a maximum value so that the abrasive grains are forced more deeply into the rubber enabling them to slide rather than roll in this area. Also, initial wear surfaces show short parallel grooves, whilst steady state wear surfaces show long parallel grooves.

The surface hardness of the material seems to play a significant role as to the proportion of particles that are sliding or rolling. Fig.6.9c shows the worn surface of 440 C which is a very hard material and as can be seen a substantial number of particles seem to roll even at the centre of the wear scar which results in creation of pits instead of long grooving.

The shapes of the cross-sectioned wear scars look quite similar for all the materials tested though differing in depth(Fig.6.10a). The depth for the 440 C and N 18++ can hardly be identified. There is also evidence in Fig.6.10b that the hard phase(particulates) in multiphase materials is standing proud and supports the load whilst the matrix wears away. This can also be seen in the cross-section in Fig.6.10c in comparison to the cross-section of M.St(Fig.6.10d). This comes as a confirmation of the better wear behaviour these materials showed during the tests.

Plastic deformation and some cutting was the main features of all the materials tested which caused the roughening of the surface with little or heavy subsurface deformation(Fig.6.11a,b,c,d).

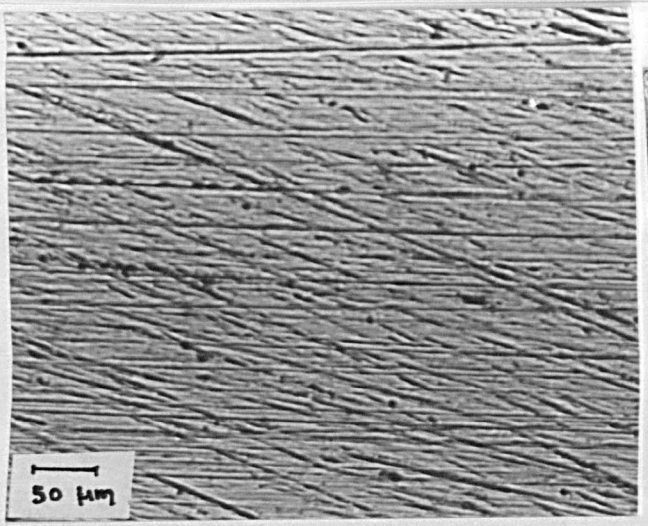

a

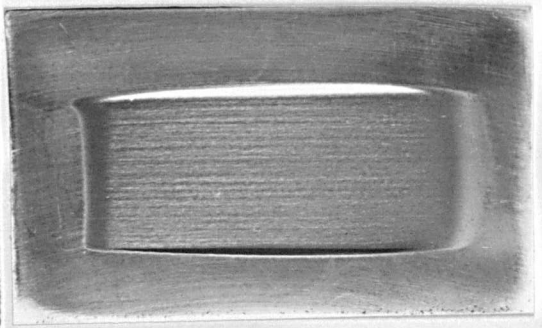

b

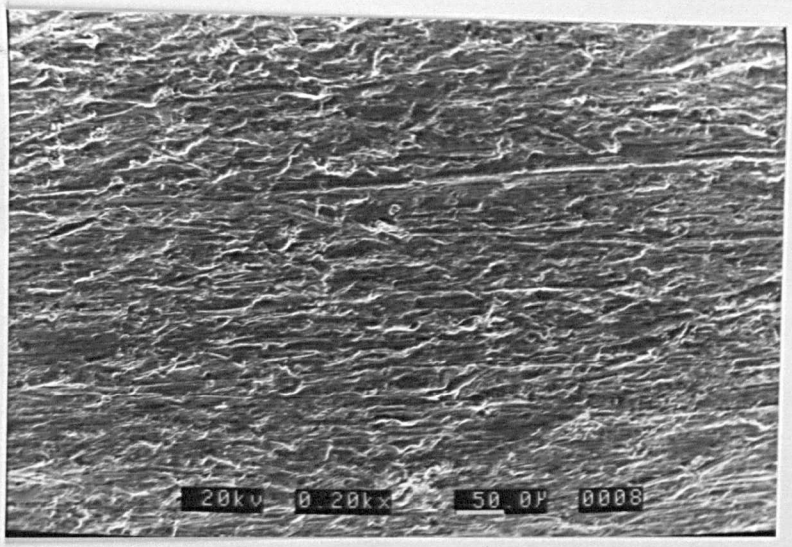

c

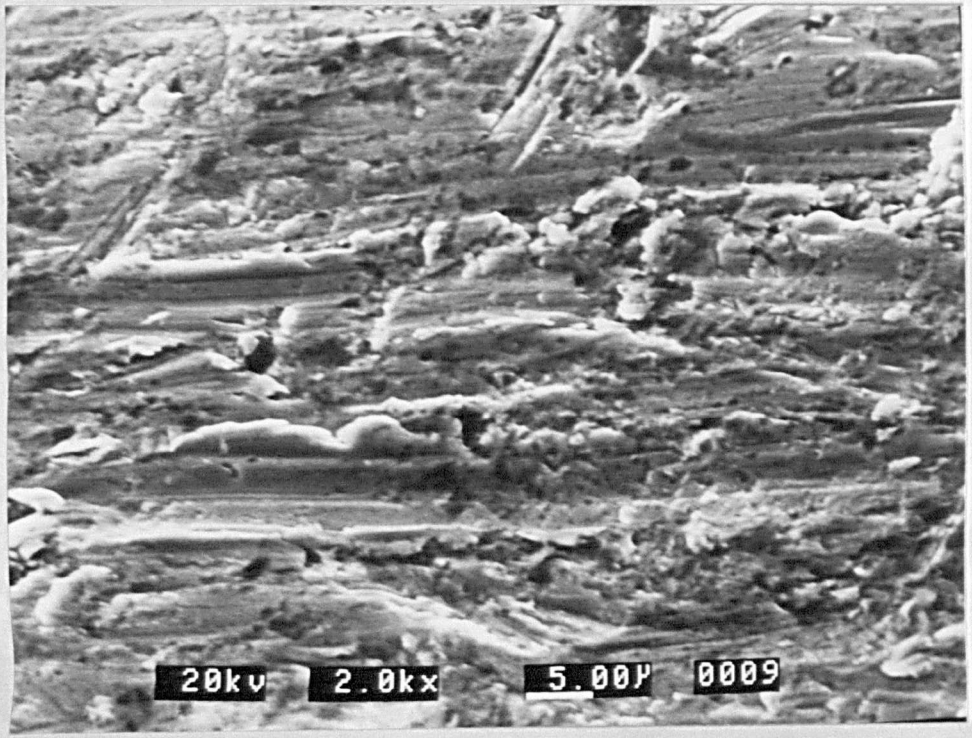

d

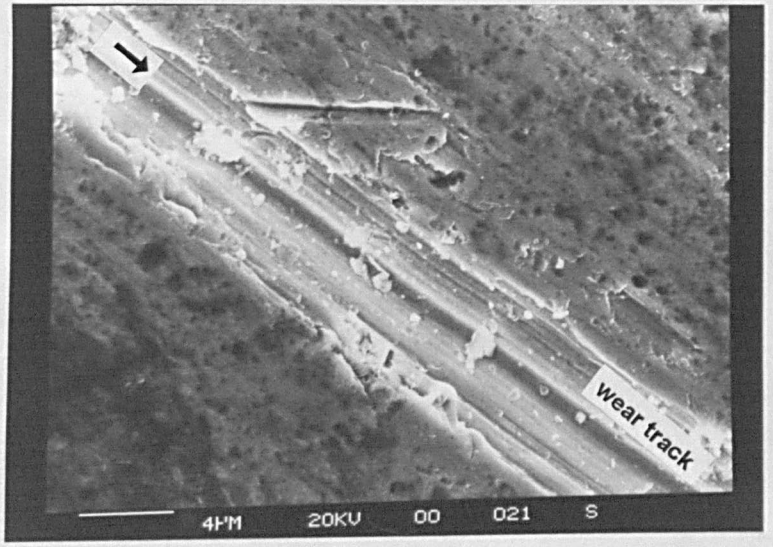

e

Fig.6.8 : Optical and SEM photographs of surface morphologies of M.St after dry abrasive wear tests(40 mins at 197.5 N) - rubber wheel

a) surface before tests b) wear scar on typical specimen X 2 c) appearance of the worn surface(tilt 40°) d) appearance of the surface at the centre of the wear scar e) close-up of a groove

a

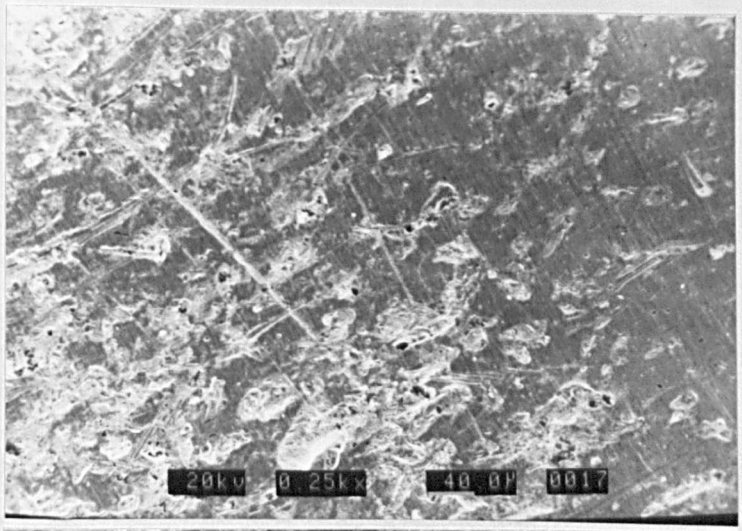

b

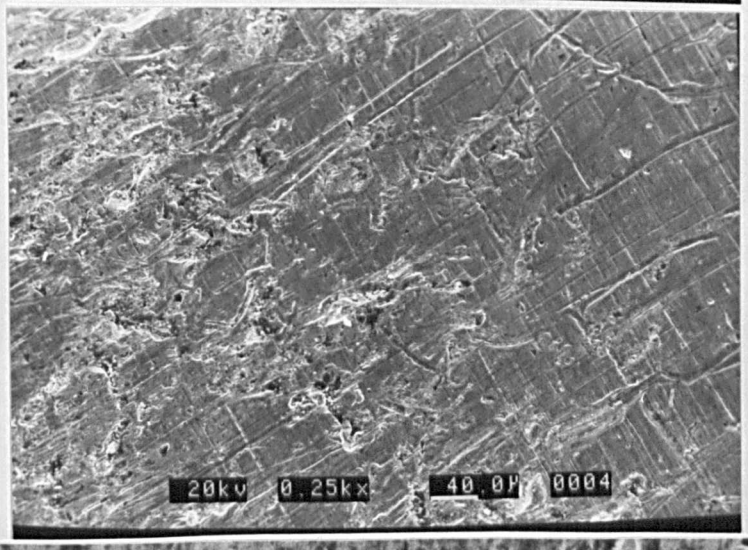

c

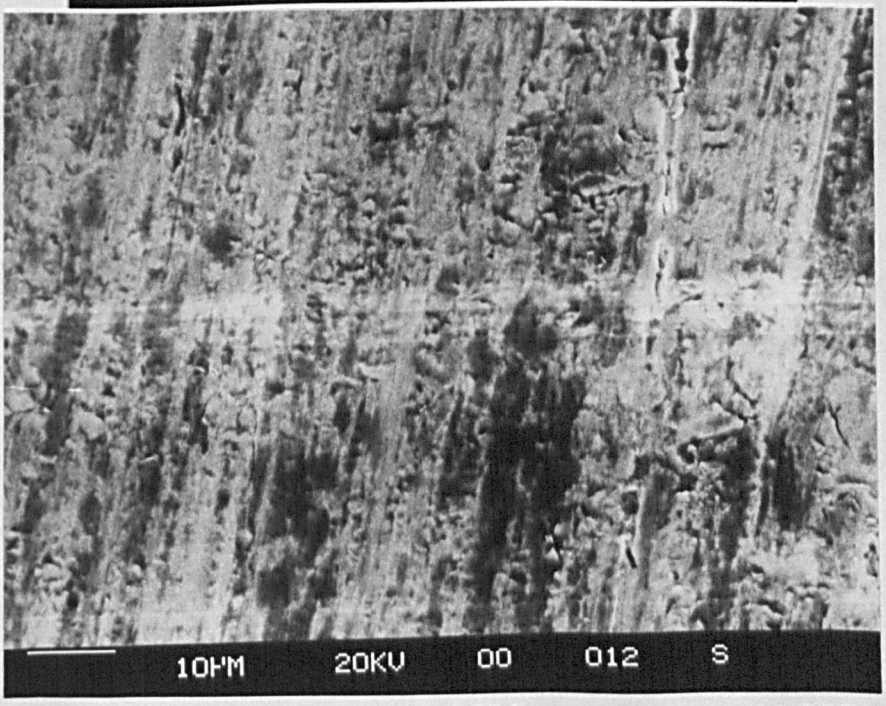

Fig.6.9 : Rubber wheel dry abrasive wear tests. a) M.St entrance area and b)M.St exit area of the wear scar shown in Fig.6.8b c)440 C - area at the centre of the wear scar

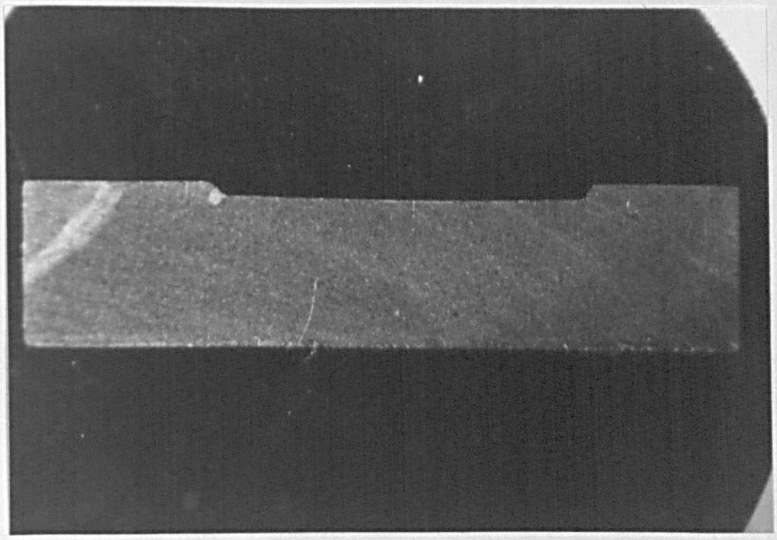

a

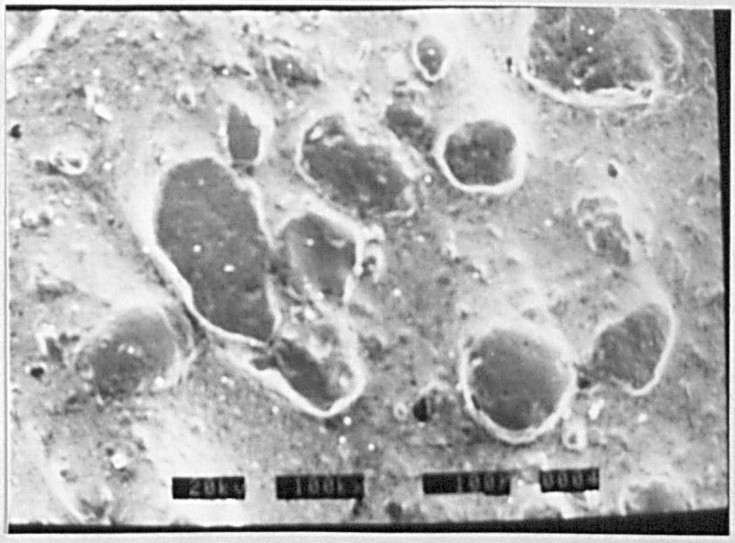

b

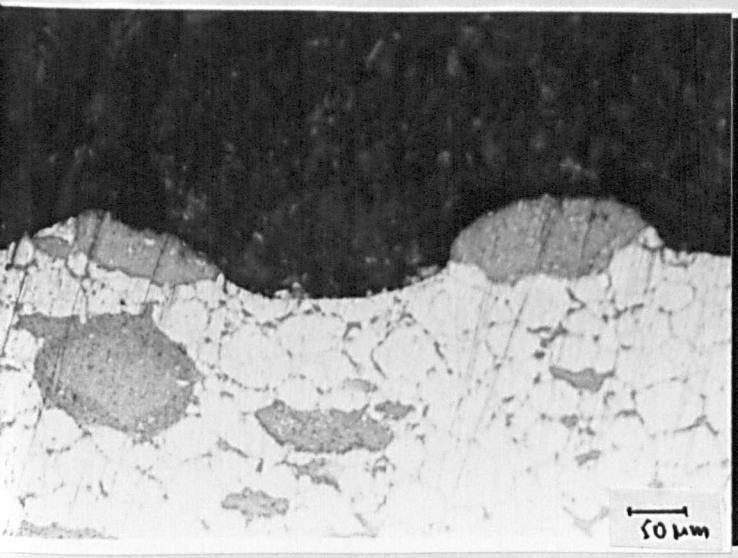

c

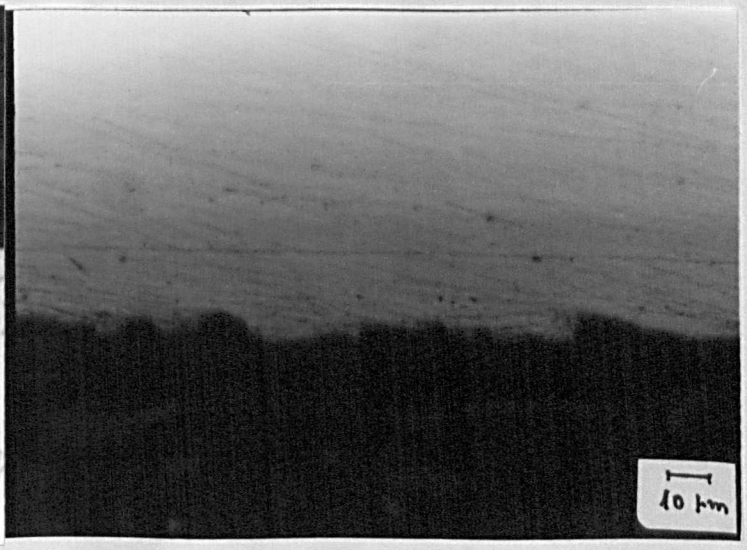

d

Fig.6.10 : Dry abrasive wear tests run for 40 mins-197.5 N - Rubber wheel. a) Typical cross-section of a wear scar (M.St) (X 1.5) b)worn surface of N18++ showing the matrix and the rounded carbides c) cross-section of N18++ showing the particulates standing out in relief above the surrounding worn matrix d) cross-section taken of the wear region of a M.St wear specimen

The formation of pits on the worn surfaces is also indicative of a high level of plastic damage on the surface.

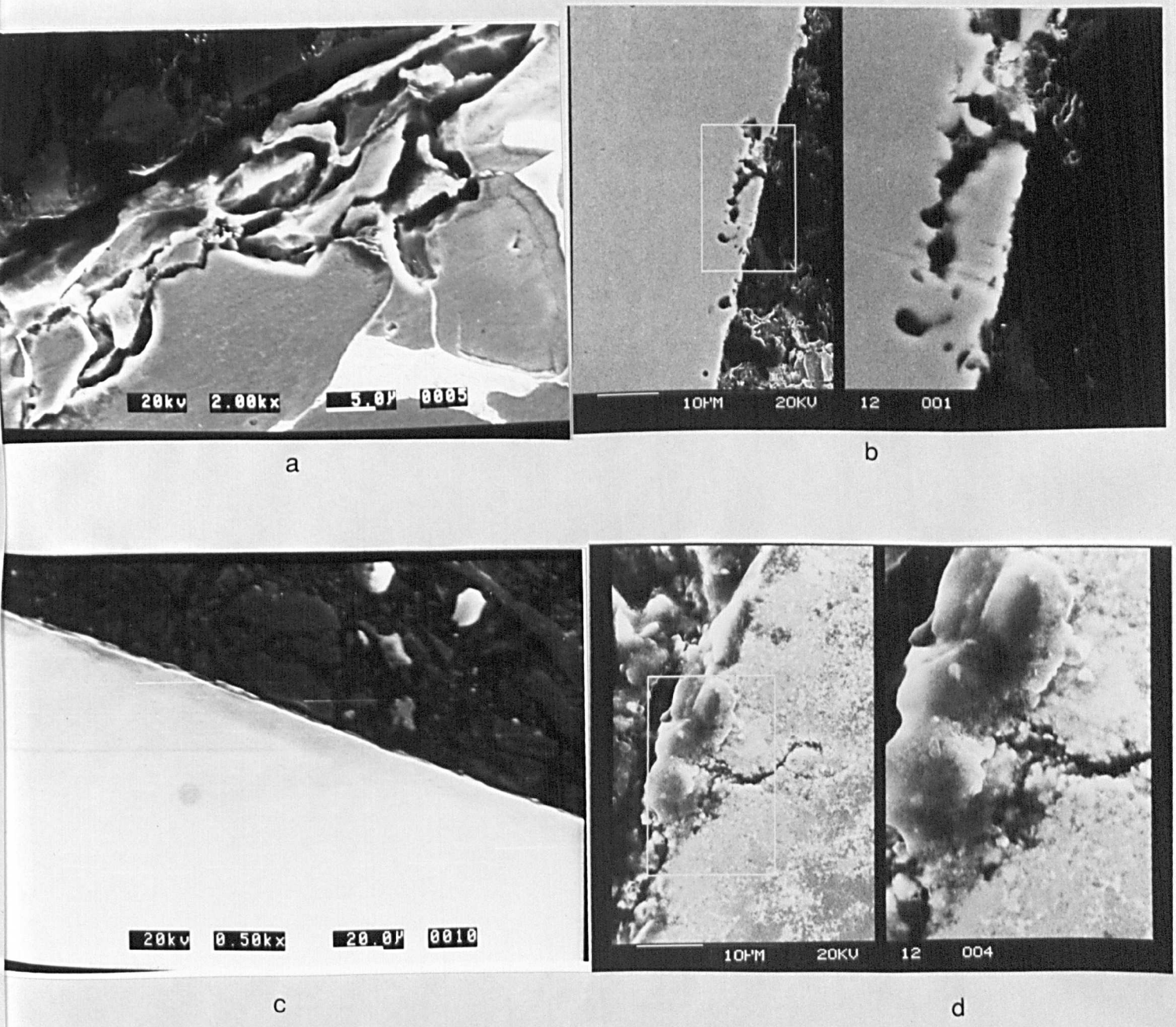

Fig.6.11: Dry abrasive wear tests run for 40 mins at 197.5 N-Rubber wheel Subsurface deformation a)M.St b) 440C c)N18 d)N18++

A micro-hardness profile for all the materials tested is shown in Fig.6.12. The specimens exhibited a two phase structure consisting of a matrix phase and a carbide phase. The M.St specimen(ferrite-pearlite) showed no appreciable variations in hardness due to the fact that the two phases have nearly similar hardness(MHV 190-230).

For the rest of the specimens, the carbide phase gave readings in the 1100-1300 MHV range, whilst the matrix readings were much lower depending on the materials.
The hardness was measured directly on the wear track surface and through the substrate in order to give information about microstructural changes and possible mechanisms involved during the wear process. No increase in the final superficial hardness or other hardness variations have been observed in all cases which shows that there was no more hardening of the worn surface.

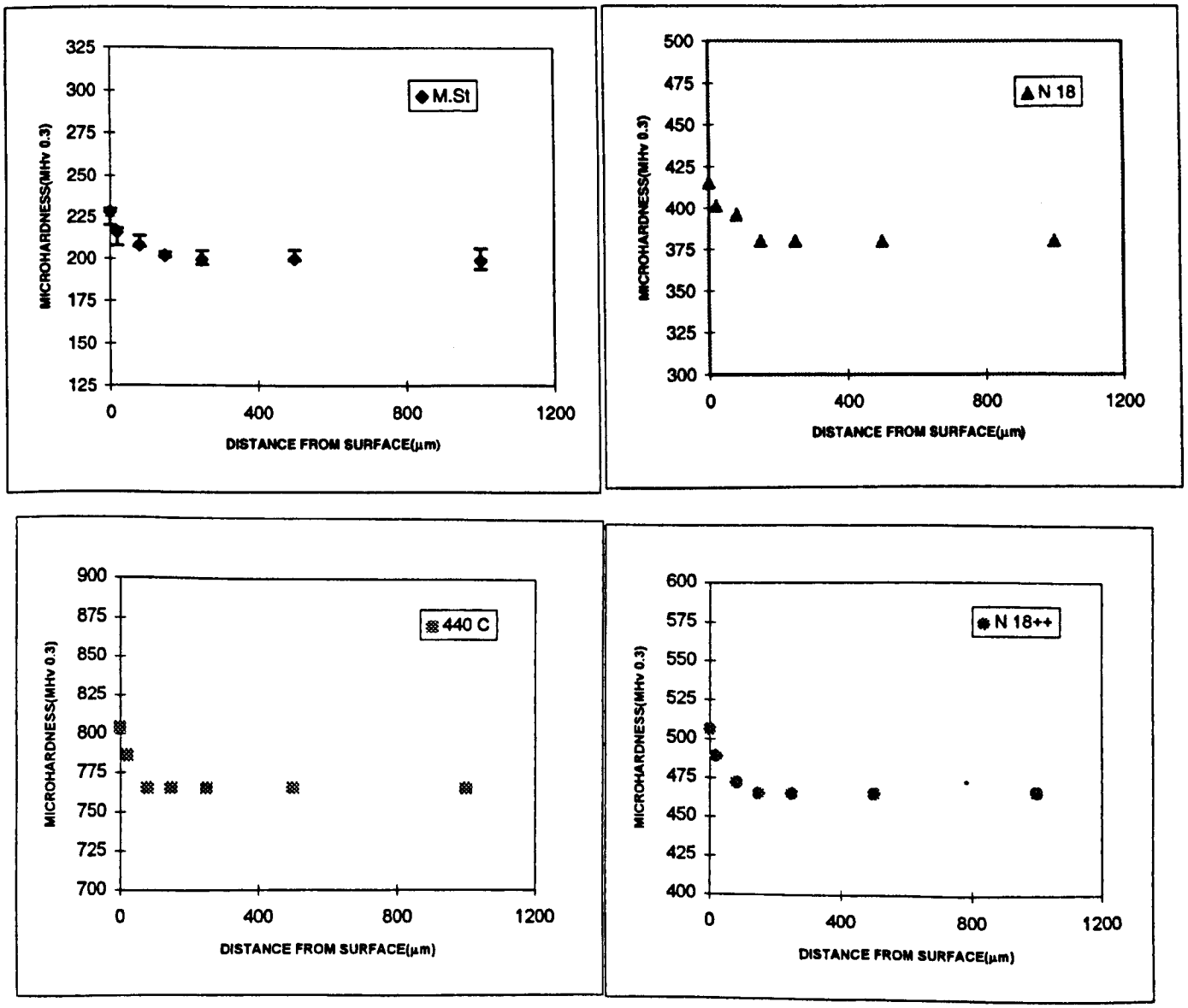

Fig.6.12 : Profile of microhardness indentations underneath the wear scar for all the materials tested

Figs 6.13, 6.14, 6.15, 6.16 present metallic wear debris particles as they are collected and separated from the sand (ferrous materials) or detected between sand particles(non ferrous materials) using EDX analysis. Some debris particles were also found stuck on the sand particles.
It is clear that according to the size and morphology of the debris particles, different mechanisms exist which will be analysed in the discussion chapter. The softer materials(M.St and N18) gave machining chips and platelets. The harder materials(440C and N18++) gave only platelets. Also for M.St and for the range of loads applied, there is no difference in the size and morphology of the debris particles.

Fig.6.17 shows the worn surface of M.St tested at 197.5 N and room temperature. The surface consists of bright grooved regions and grey areas. The existence of some oxygen in the spot analysis is consistent with high surface temperature although no oxide films are detected on the Auger.
The appearance of Si(spot analysis) is also indicative of the embedment of sand particles or pieces of broken sand on the worn surfaces.
Analytical results from spot analysis for worn surfaces and wear debris particles are presented in Appendix B.

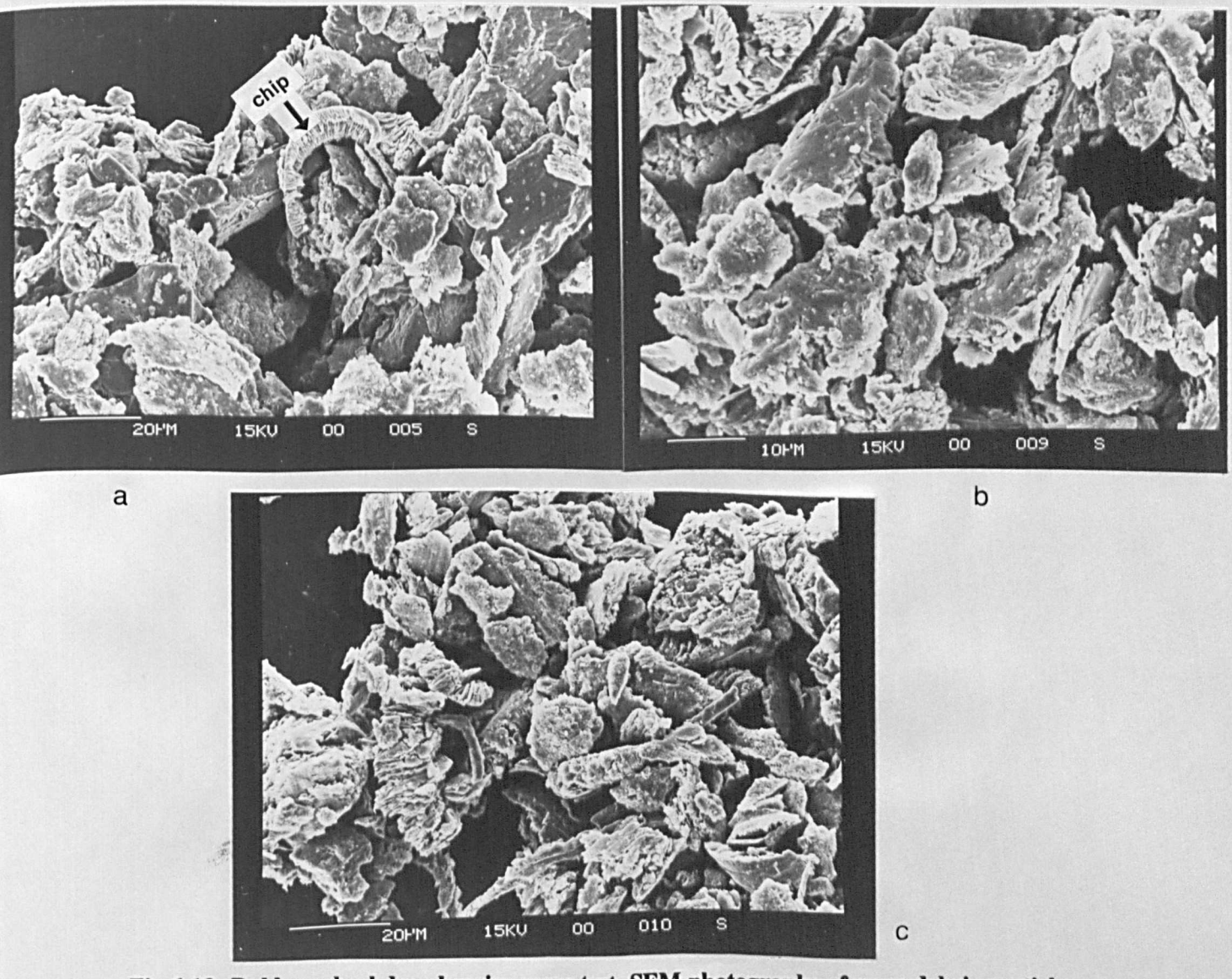

Fig.6.13: Rubber wheel dry abrasive wear test. SEM photographs of wear debris particles, showing the morphology of the particles and the range of sizes encountered.
a) M.St at 44.5 N, b) M.St at 127.5 N and c) M.St at 197.5 N

d

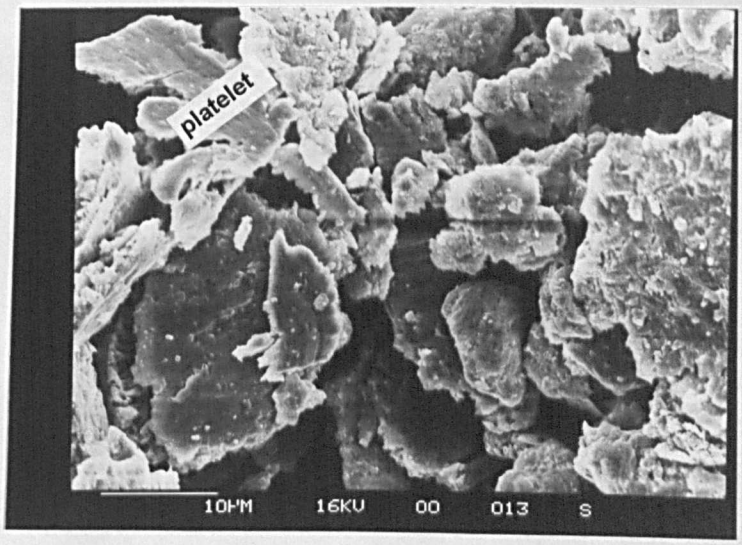

e

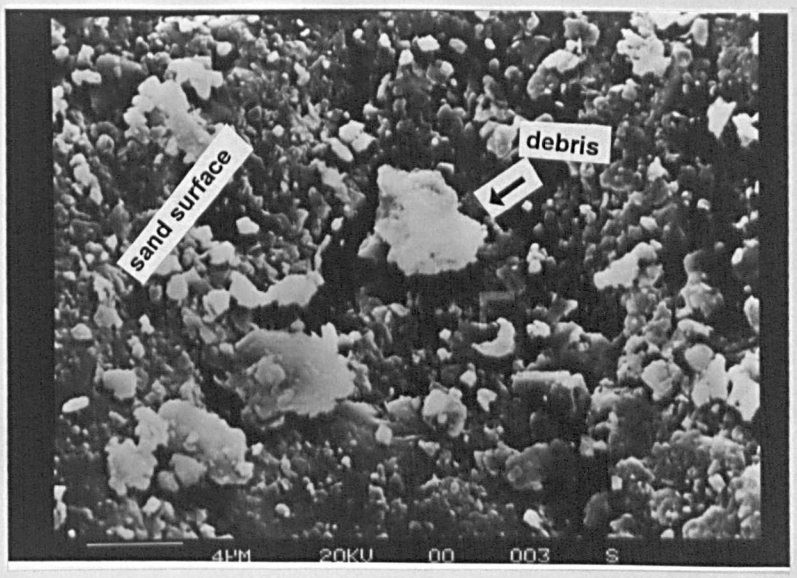

Fig.6.13 : continued .

d) higher magnification of platelets

e) debris particle stuck on sand particle

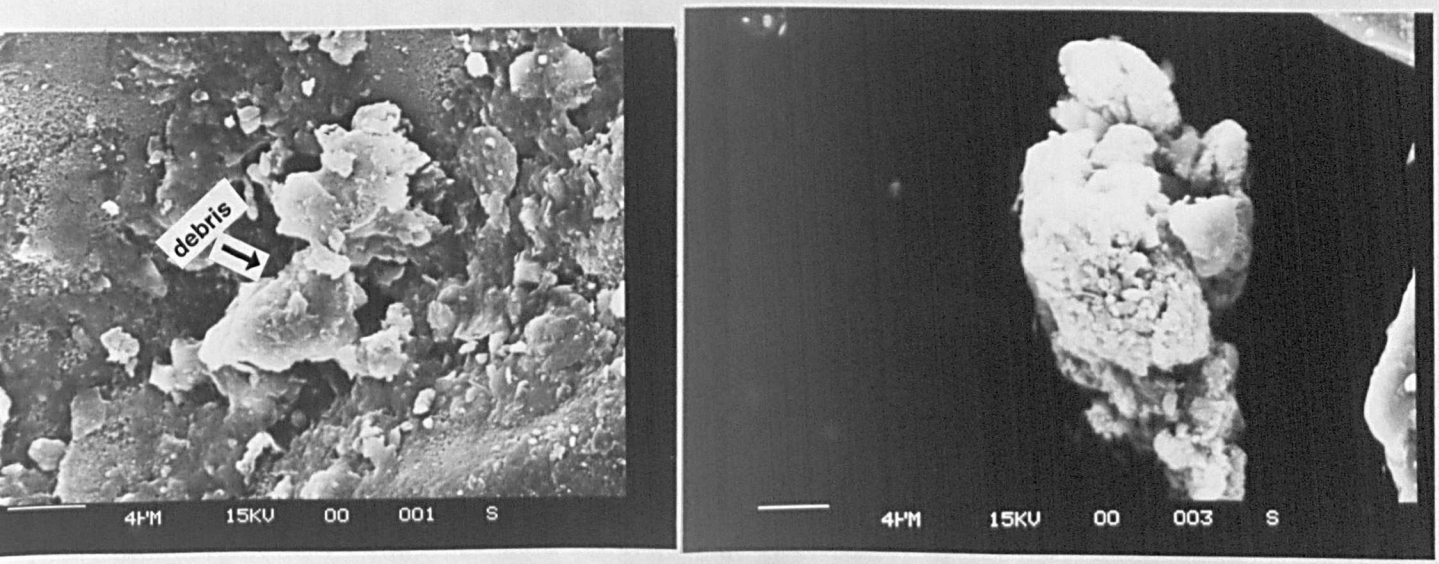

a b

Fig.6.14: Rubber wheel dry abrasive wear test. SEM photographs of wear debris particles, showing the morphology of the particles. a) 440C- spherical wear debris particles on sand and b) 440C- wear debris between sand particles.

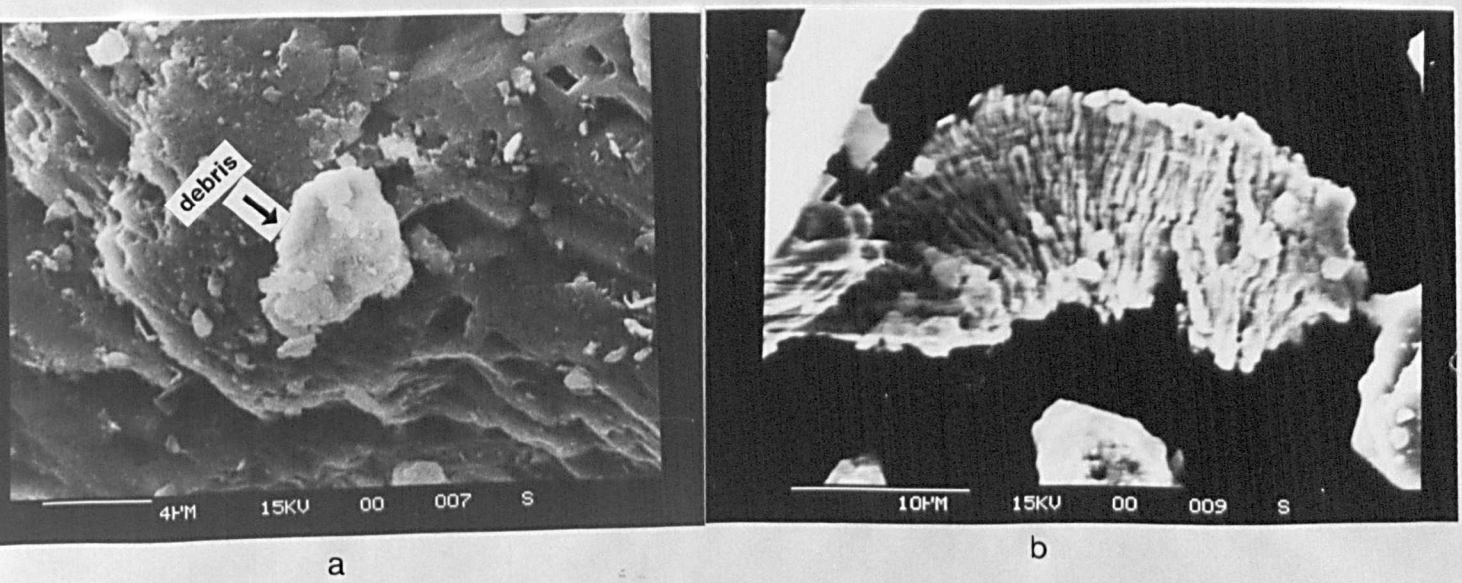

a b

Fig.6.15: Rubber wheel dry abrasive wear test. SEM photographs of wear debris particles, showing the morphology of the particles. a) N18- spherical wear debris particles on sand and b) N18 - wear debris between sand particles.

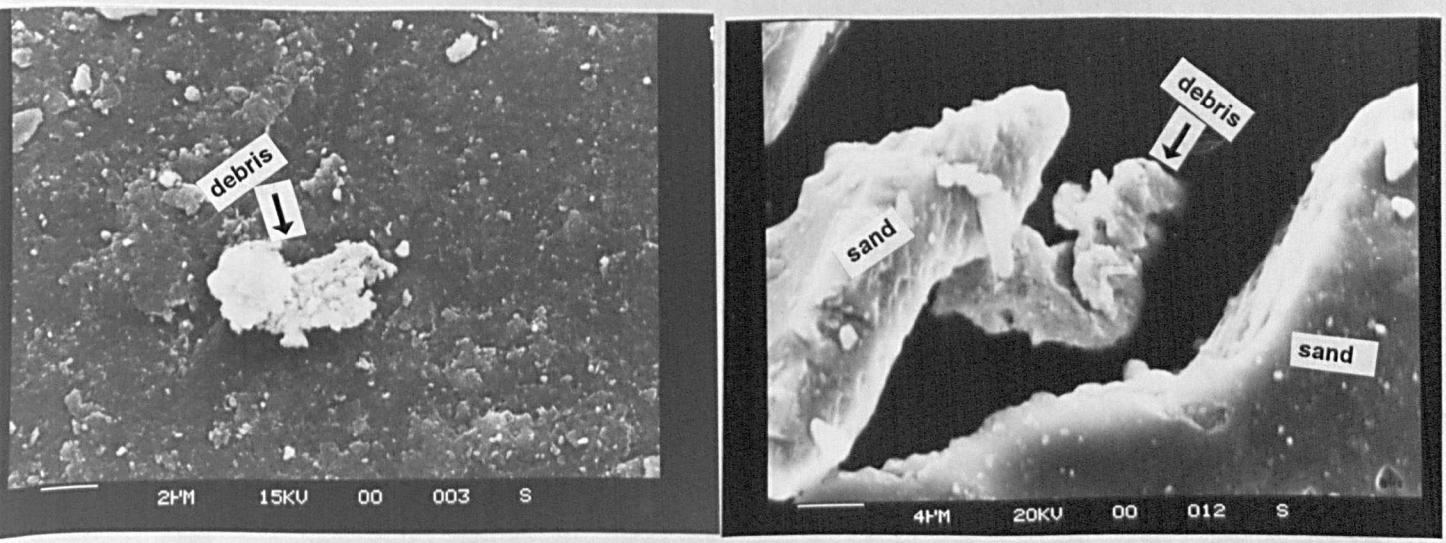

Fig.6.16 - Rubber wheel dry abrasive wear test. SEM photographs of wear debris particles, showing the morphology of the particles. a) N18++ spherical wear debris particles on sand and b) N18++ wear debris between sand particles.

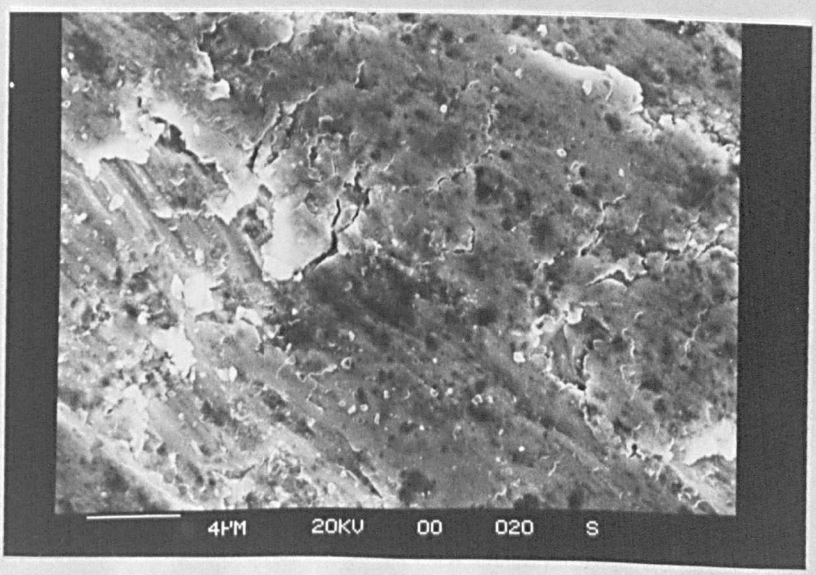

Fig.6.17 :Dry sand abrasive wear test- Rubber wheel. Appearance of the surface of M.St tested at 197.5 N and room temperature.

6.4 Dry abrasive wear tests - 440 C wheel

6.4.1 Wear behaviour

The wear results obtained with the laboratory dry-abrasion test rig, when the rubber wheel was replaced by a 440C wheel, for the same range of selected metals and alloys and expressed as volume loss(weight loss/density) against mass of sand abrading the surface are presented in Fig.6.18a,b. The test time intervals were the same as with rubber wheel and only two loads, 60 N and 240 N were used. As can be seen from both figures, in the start they cross over but then after some incubation period the materials behaved differently which could be related to different work-hardening rates.

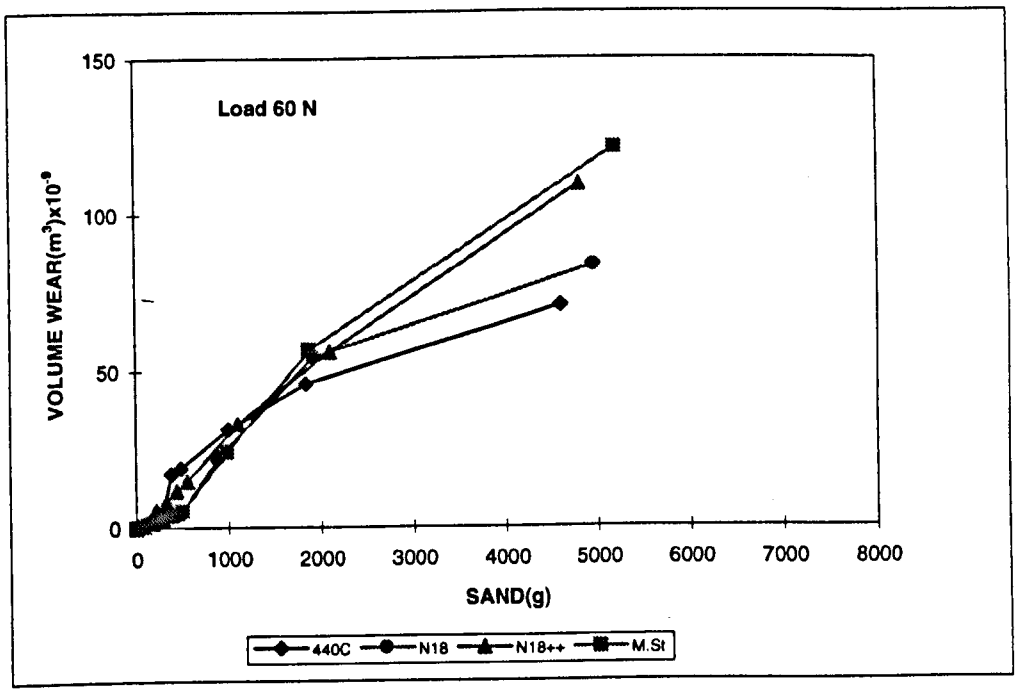

Fig.6.18 : Dry abrasive wear tests against 440C wheel expressed as volume loss vs mass of sand abrading the surfaces. Tests run for 40 min. in total and specimens were weighed at different time intervals a) 60 N

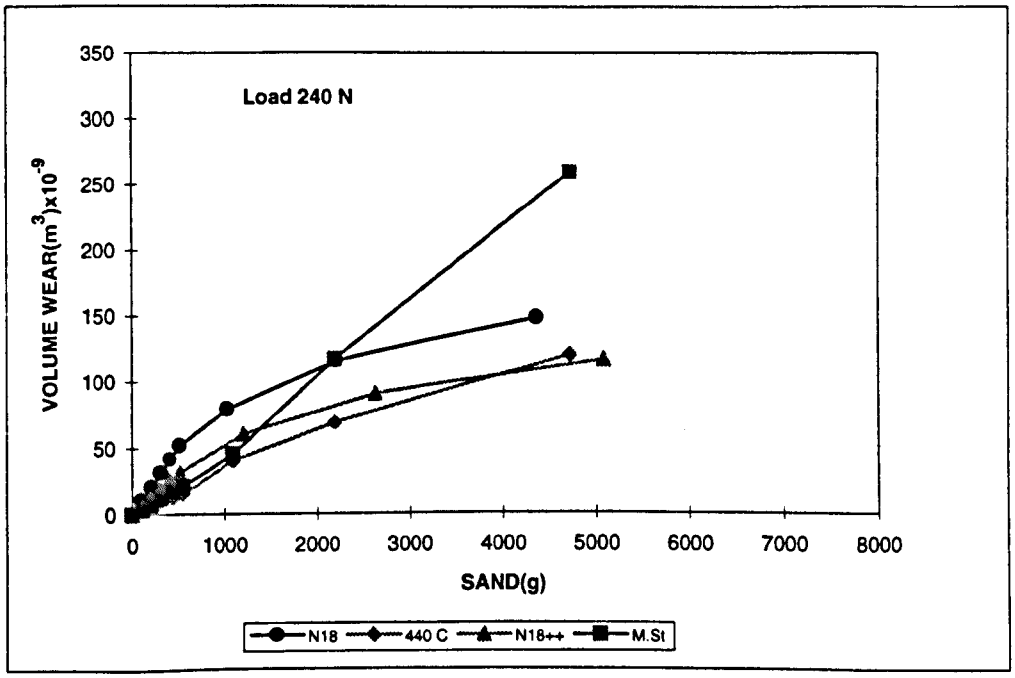

Fig.6.18 : continued b) 240 N

However, following an incubation period, all the materials showed a 'linear' increase in wear under steady-state conditions, with M.St and N18 competing for the worst wear behaviour. This is similar to the trend observed in the dry sand rubber wheel abrasion tests although the volume wear is typically 2-5 times higher compared to rubber wheel.

For comparison purposes the test undertaken under simple 440C wheel and the results(Appendix B) show, as expected, that the presence of abrasives increases the wear rates by a factor of up to 100.

6.4.2 Wear surface

The morphology of the worn surfaces of the M.St and N18++ specimens are shown in Fig.6.19a,b. It is obvious the extensive damage both surfaces have suffered; loose wear debris particles can be seen on the worn surface of the M.St specimen. The worn surface of N18++ shows the hard particles standing in relief of the matrix. Where there are no hard particles the matrix is slightly grooved.
Fig.6.20 is a replica of the worn surface of the 440C wheel. It can be seen that there is a roughening of the surface and it is abrading away according to the microstructure which consisted of the matrix and hard carbides.
Fig.6.21a,b shows the morphology of the wear debris particles collected during the tests and the range of sizes encountered.

It should be noted that a fine dust was produced while the test was running. This dust consisted mostly of fine bits and shards of silica sand. This appears to be the result of the crushing and fracture of the silica sand at the maximum shear stress zone in the middle of the specimen. This is evident in the sand particle distribution after the tests, Fig.6.22 which suggests that some break-up of the big particles during the wear process does occur. This did not happen with the Rubber wheel tests where the particle size distribution after tests was similar to that appeared in Fig.6.2d.

a

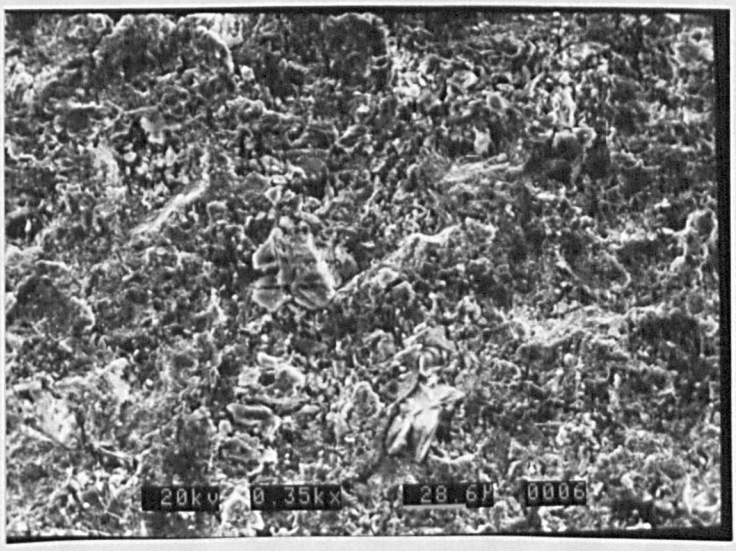

b

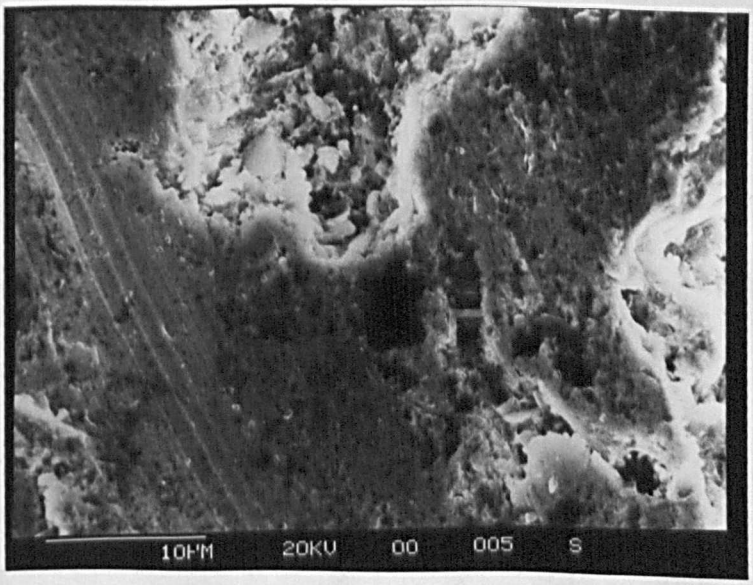

Fig.6.19 : Dry sand abrasive wear tests run for 40 mins at 240 N - 440C wheel. Morphology of the worn surfaces a) M. St specimen b) N18++ specimen

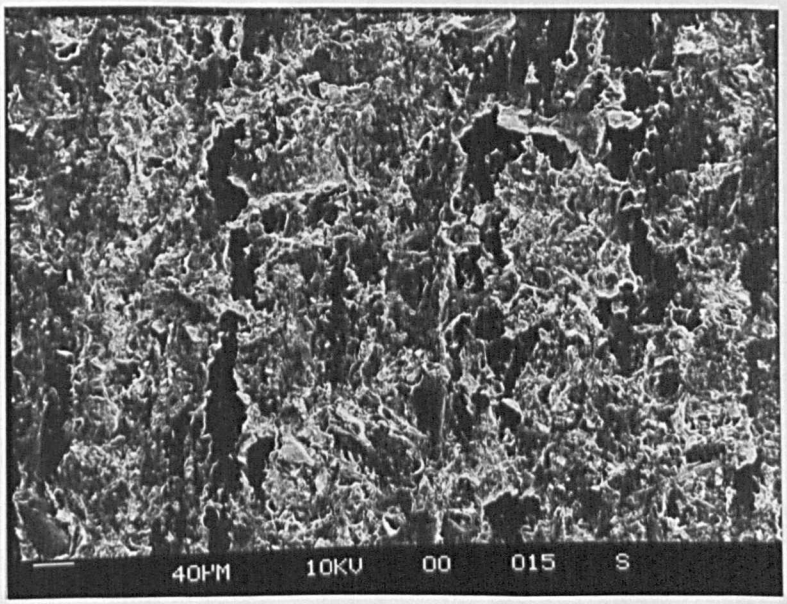

Fig.6.20: Dry sand abrasive wear tests run for 40 mins at 240 N - 440C wheel. Replica of the worn surface of the 440C wheel.

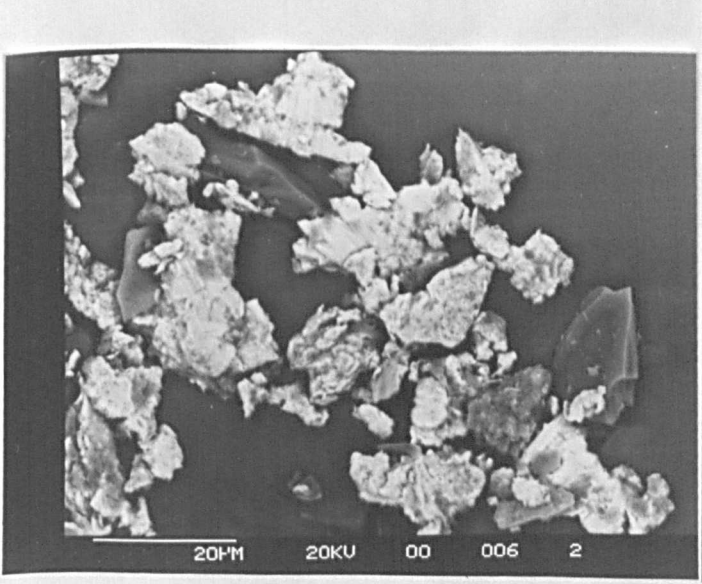

a

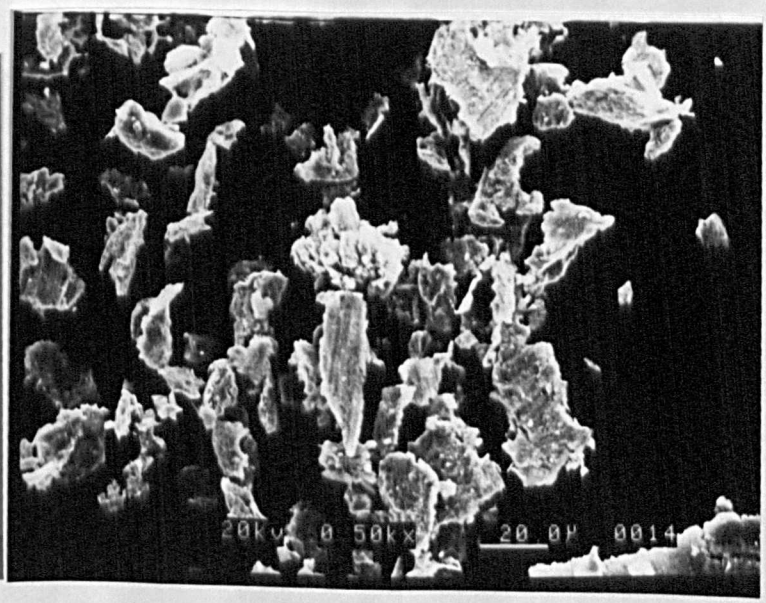

b

Fig.6.21: Dry sand abrasive wear tests run for 40 mins at 240 N - 440C wheel. Morphology of the wear debris particles.

a) back-scattered photograph-wear debris of M.St . Darker areas are sand particles.

b) back-scattered photograph-wear debris of 440C. Darker areas are sand particles.

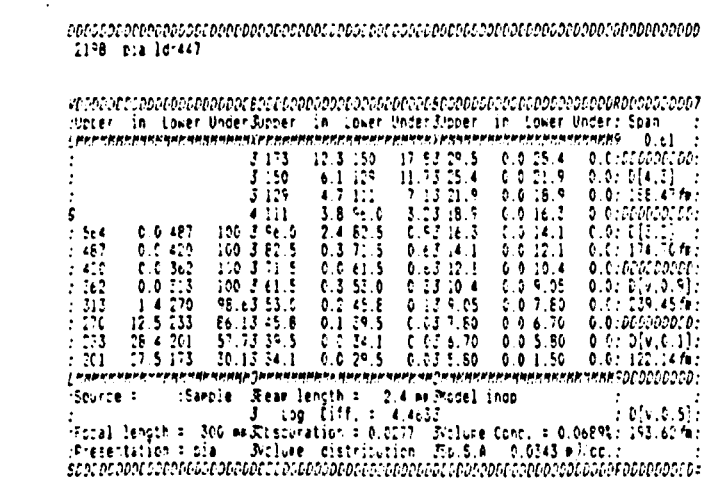

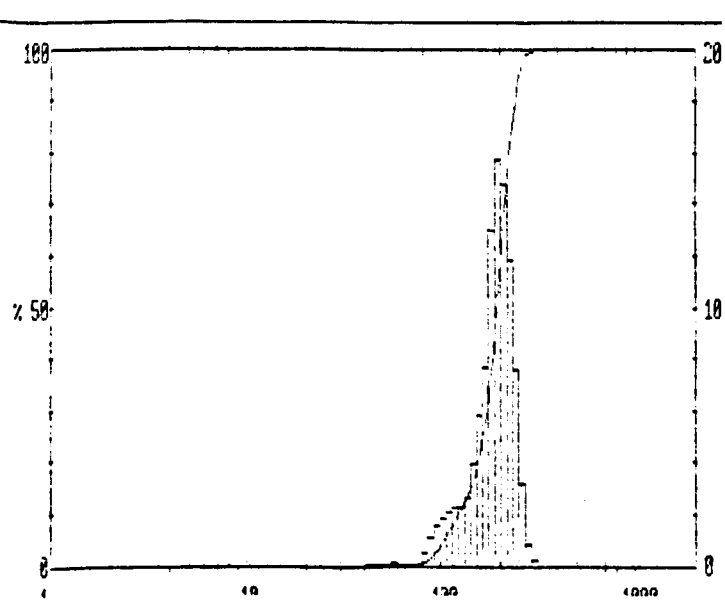

a

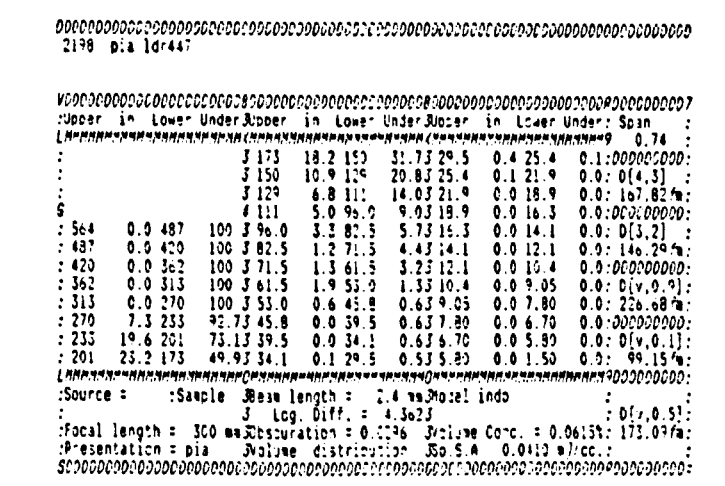

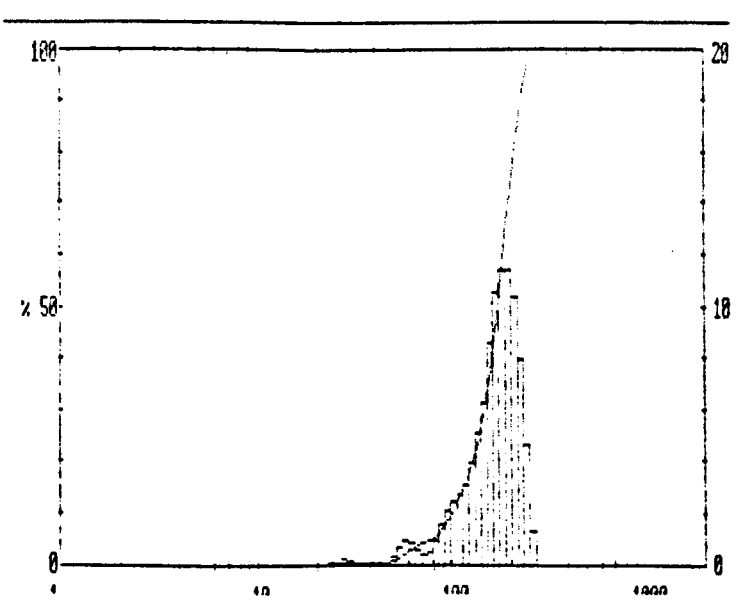

b

Fig.6.22 :Dry sand abrasive wear tests - 440C wheel. Abrasive particle size distribution after tests. a) M.St and N18 b) 440C and N18++

6.5 Corrosion tests

The results of all the experimental materials tested for corrosion in different environments are shown in Fig.6.23. The corrosion rates are expressed as material loss per unit surface area against time. Because of the big difference in corrosion rates and for better clarity, the ferrous and Ni-based materials are presented in separate graphs.

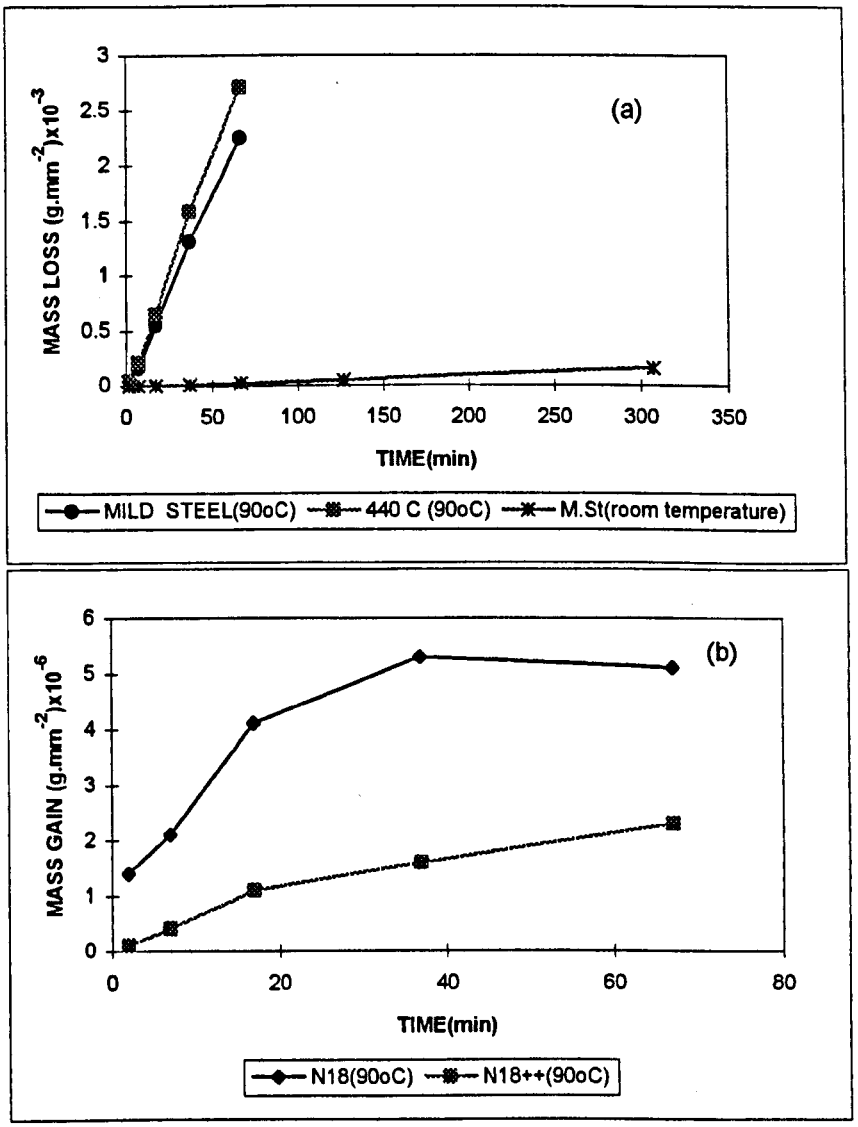

Fig.6.23 : Corrosion rates for the materials tested in 3vol% H_2SO_4 at 90±5°C and room temperature a) iron-based materials(exhibited material loss) b) Ni-based materials(exhibited material gain)

The corrosion results show a significant weight loss for the Fe-based materials(M.St and 440 C) and a very slight weight gain for the Ni-based alloys(N18 and N18++) when tested in acidic environments at 90±5°C. It is worth noting that during the dissolution of the ferrous metals(M.St, 440C), hydrogen bubbles evolved from the solution.

At room temperature and for the same environment only M.St showed a weight loss. The other materials showed no detectable weight change.
Also, all the materials were tested in H_2O at 90±5°C and the results showed no weight change.

Fig.6.24 shows the roughened and heavily pitted surfaces of 440C and M.St corroded for 67 mins in 3vol% H_2SO_4 at 90±5°C with extensive cracking over the entire surface. The oxygen peak on the surface of M.St specimen, spot analysis in Appendix B, suggests the existence of an oxide which was identified to be Fe_2O_3. Also the slight weight increase for the Ni-based alloys was due to formation of a thin NiO film on the surface as identified by Auger results, in Appendix B. It was very difficult to measure the thickness of that film.

a

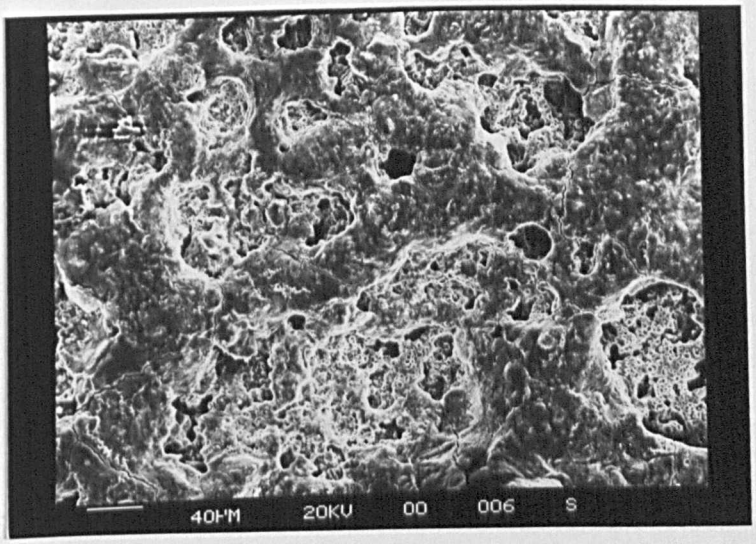

b

Fig.6.24: SEM photograph of 440 C specimen showing the surfaces of a) 440C and b) M.St after they were corroded for 67 minutes in 3vol% H_2SO_4 at 90±5°C.

6.6 Abrasive/corrosive wear testing- 440 C wheel

The introduction of corrosion at the same time as abrasion had a profound effect on the volume of the material loss and wear rates. To avoid confusion, because of the number of environments and loads used, the results for different materials are presented separately. As a basis to compare the effects of various solutions on the materials tested, experiments were conducted initially with water as the corrosive medium, followed by different concentrations of sulphuric acid and finally a solution of sulphuric acid and aminoacid.

6.6.1 Mild steel

Fig.6.25 presents abrasion/corrosion data for M.St in a range of different solutions. As can be seen there is a linear increase of the corrosion-induced wear loss for all the different environments without an incubation period.
The minimum weight loss of a specimen appeared in 3vol% H_2SO_4 solution at both loads whilst the weight losses of specimens tested in all the other solutions were significantly greater. At 240 N all the materials showed higher wear losses by a factor of 2-3 compared to 60 N.
It must also be mentioned that the surface of the specimen tested in 30vol% H_2SO_4 appeared reddish after the tests which is indicative of Fe_2O_3 oxide formation.

To obtain a better understanding of what was happening in the wear track, the specimens tested in 3vol% H_2SO_4 at 60 N and 240 N respectively that gave the lowest material loss, were examined on the SEM. The SEM photograph in Fig.6.26a is a general view of the wear/corroded surface showing a preferential channeling of the surface. The next SEM photographs in Fig.6.26b,c,d are all taken from inside the wear track and suggest that the track surface was highly roughened and it is not dissimilar from the corroded surface of M.St in Fig.6.24. Also grooves made by individual particles can be very clearly seen.
The SEM photographs in Fig.6.26e,f depict the damage of the wheel surface and the considerable general corrosion outside the wear track.

Spot analysis, Appendix B, of the M. St wear/corroded surface shows possible embeddment of sand particles on the surface. The existence of Cr in the spectrum suggests the transfer of material from the 440C wheel on to the specimen surface.

Auger results, in Appendix B have shown that the Fe_2O_3 oxide is more likely to be formed on the surface of the specimen in all the different environments. First a standard was used to identify the oxide peak on the spectrum and then the spectra of the specimens were compared against the standard.

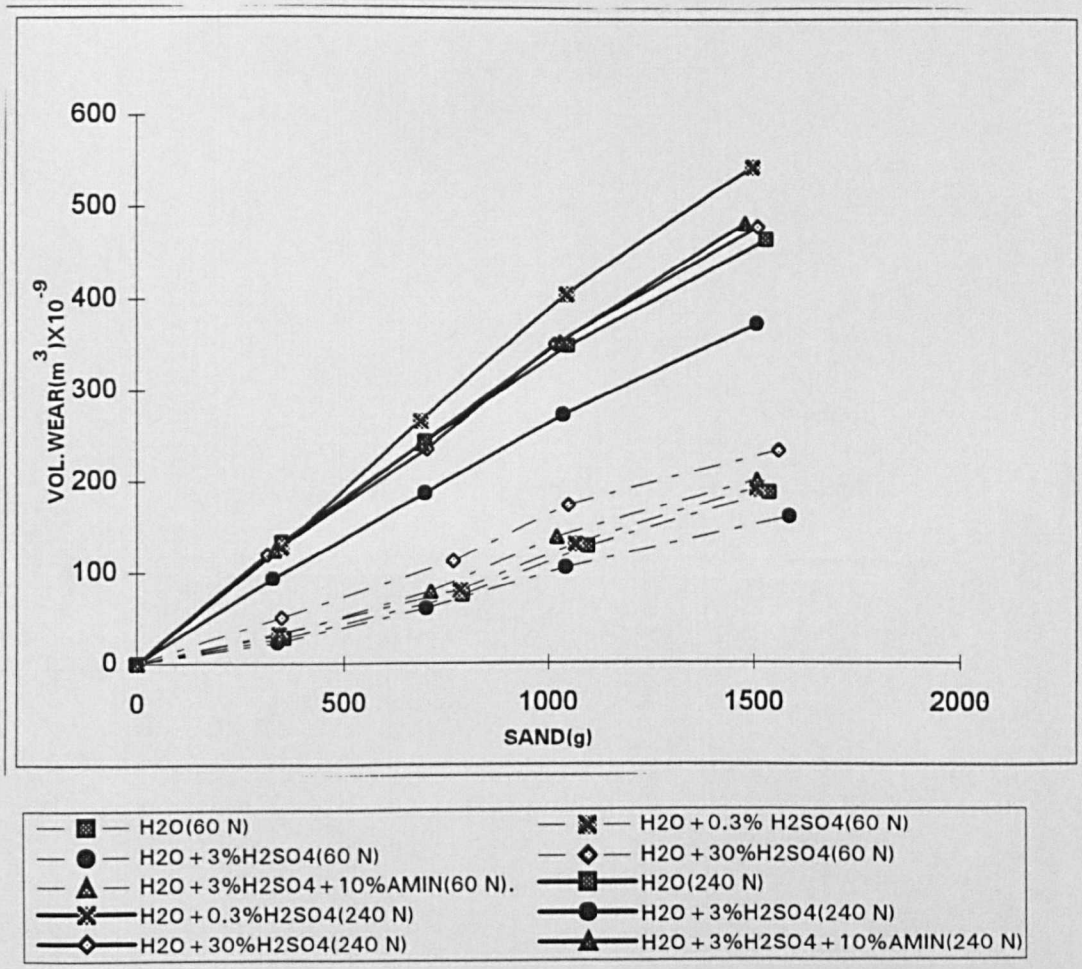

Fig.6.25: Abrasion/corrosion of M.St in a range of different solutions expressed as volume loss vs mass of sand abrading the surface. Each test was run for 1 h with the specimens weighed every 15 min.

a

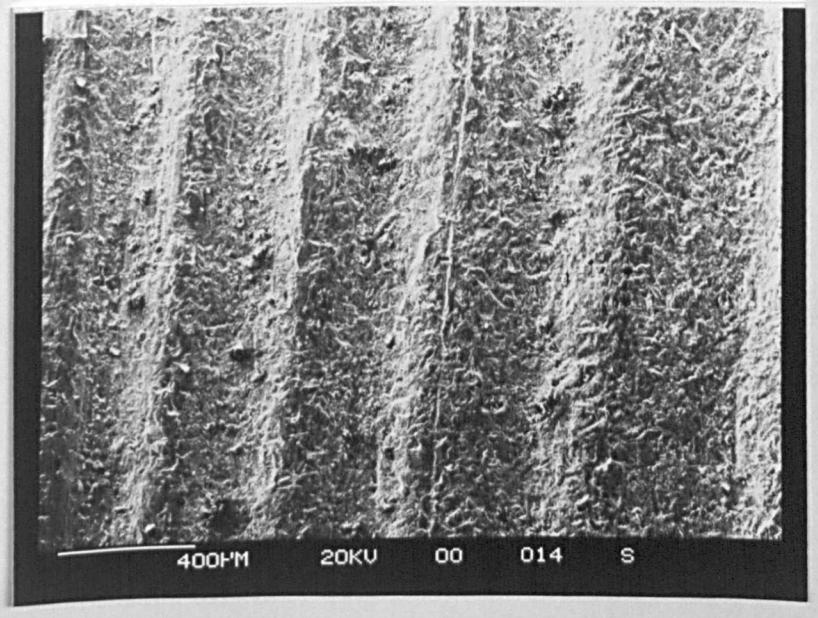

Fig.6.26: SEM photographs of M.St abraded/corroded in 3vol% H_2SO_4 solution. Test run for 1h and the specimens weighed every 15 min. a) general view of the surface showing preferential channeling.

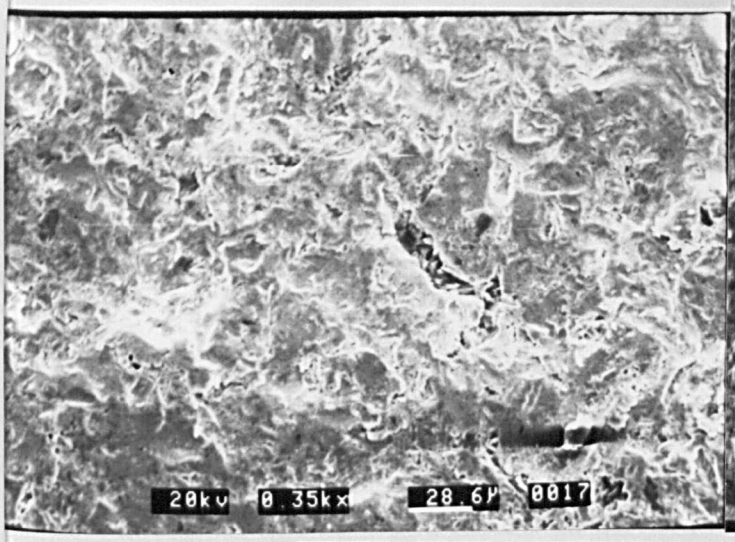

b

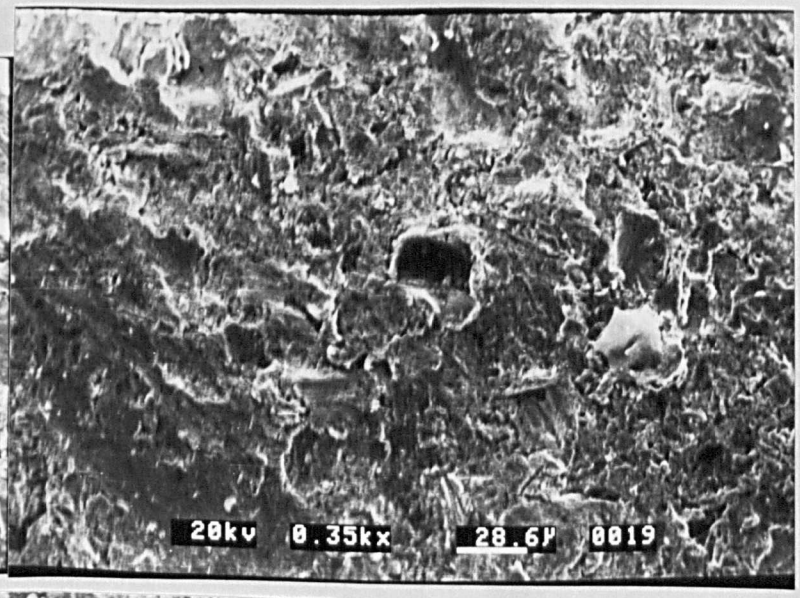

c

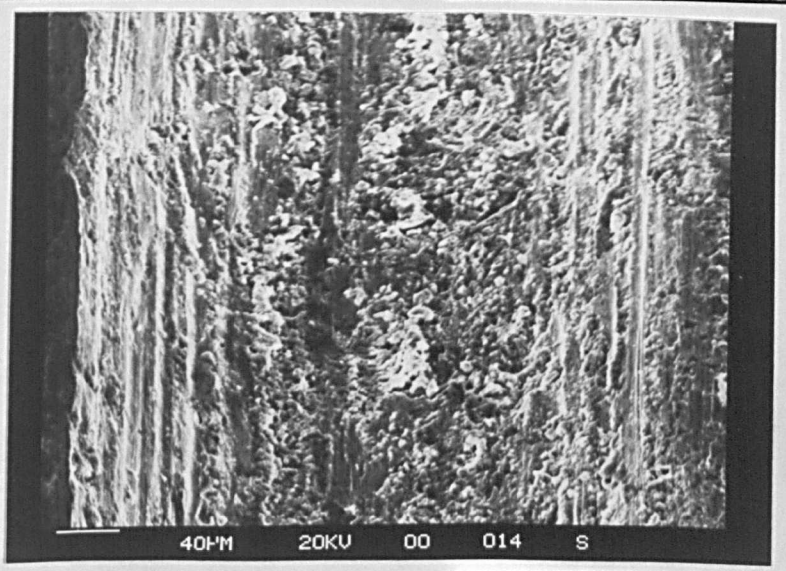

d

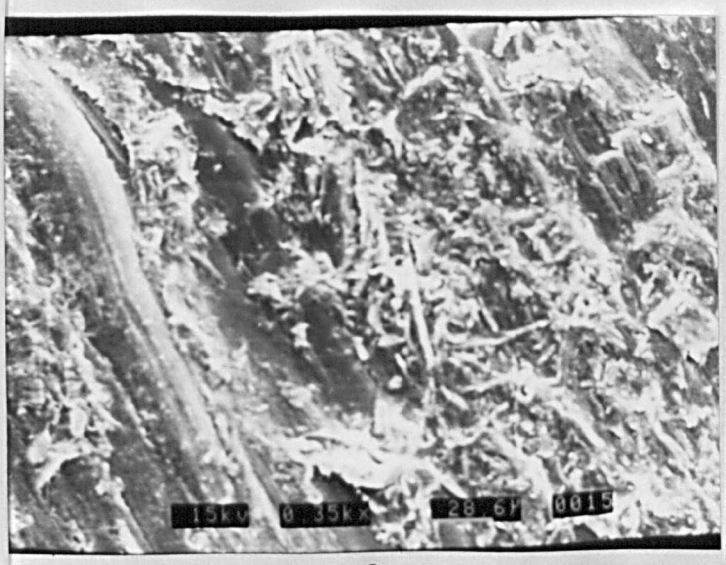

e

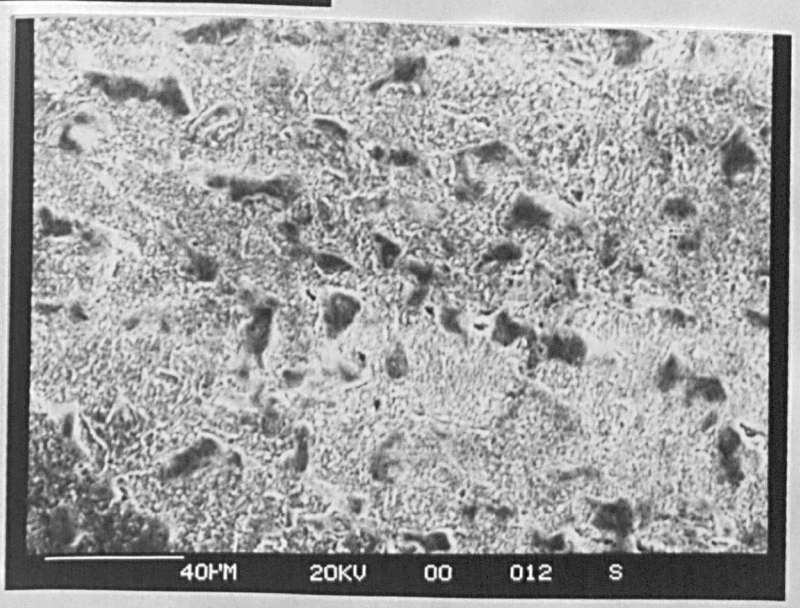

f

Fig.6.26: continued. View from inside the wear track b) 60N and c) 240N
d) individual grooves
e) replica of the worn surface of the 440C wheel
f) surface of the specimen outside the wear track

6.6.2 440 C

Fig.6.27 shows the abrasive wear of 440C after operating in solutions of H_2O and sulphuric acid of different concentrations.
The results show that there was little, if any, difference in volume of material loss for the various solutions. At 240N the volume loss was higher by a factor of 2 compared to 60N.

The SEM photographs in Fig.6.28 show specimens tested at different loads in 3vol%H_2SO_4+10wt% L-cysteine aminoacid as a corrosive medium. The surfaces were highly roughened at both loads, and covered with corrosion products. Similar was the appearance of the 440C wheel after the tests(Fig.6.28c).

Spot analysis Appendix B of the wear/corroded surface of the specimen in 3vol%H_2SO_4+10wt% L-cysteine aminoacid suggests the embeddment of sand particles and probably oxidation of the surface. The existence of hard Cr carbides limited the grooving and plastic deformation of the surface.

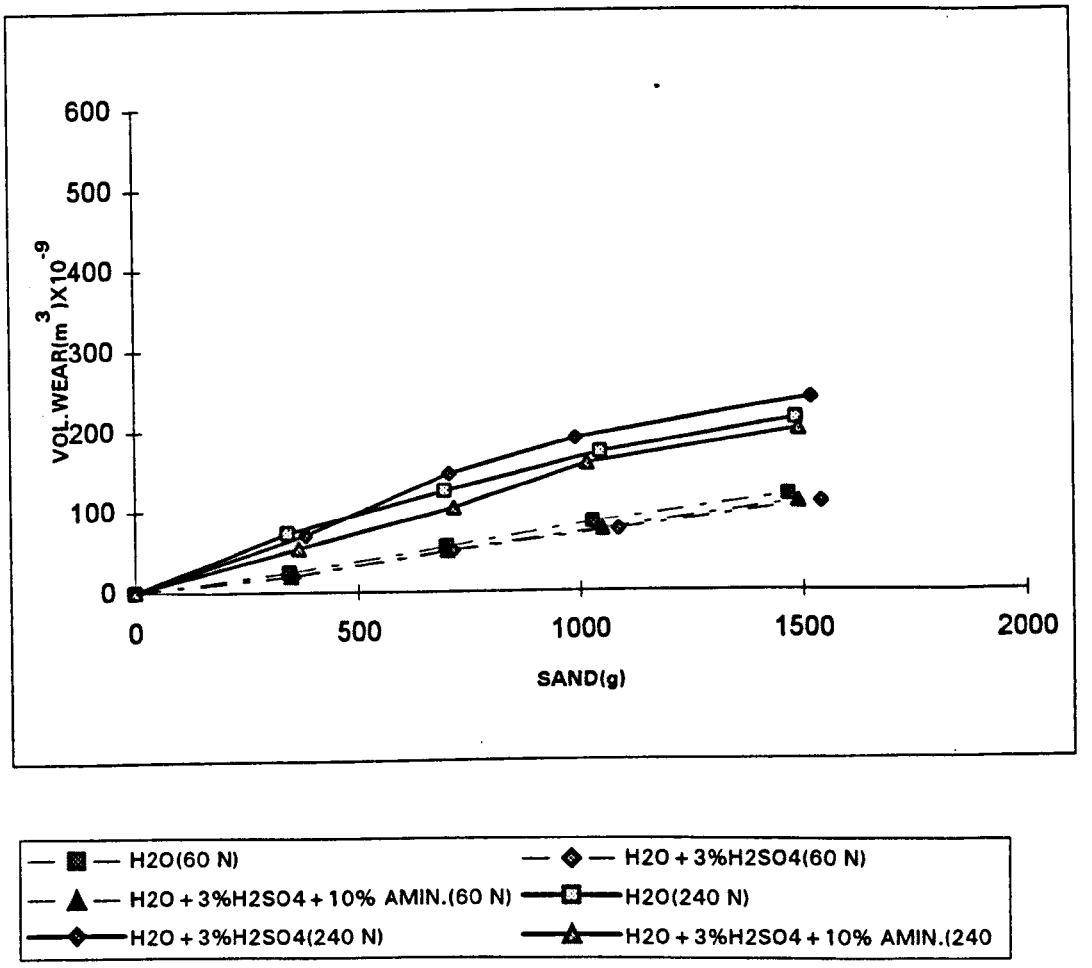

Fig.6.27 : Abrasion/corrosion of 440C in a range of different solutions expressed as volume loss vs mass of sand abrading the surface. Each test was run for 1 h with the specimens weighed every 15 min.

a

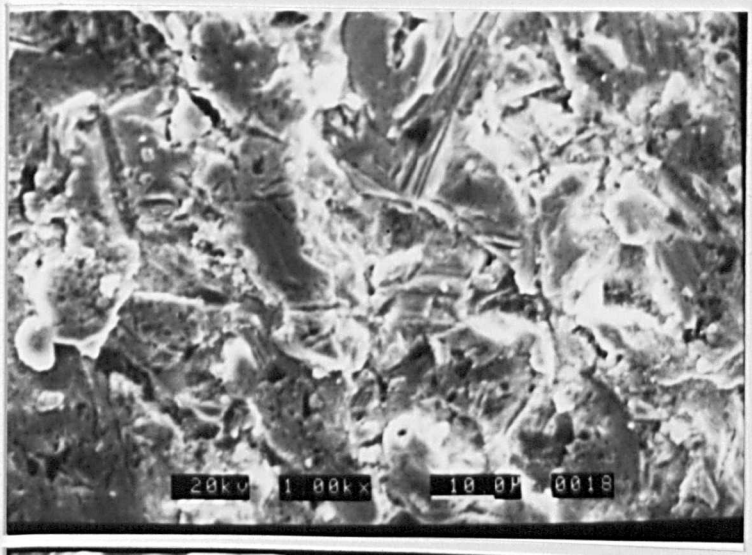

b

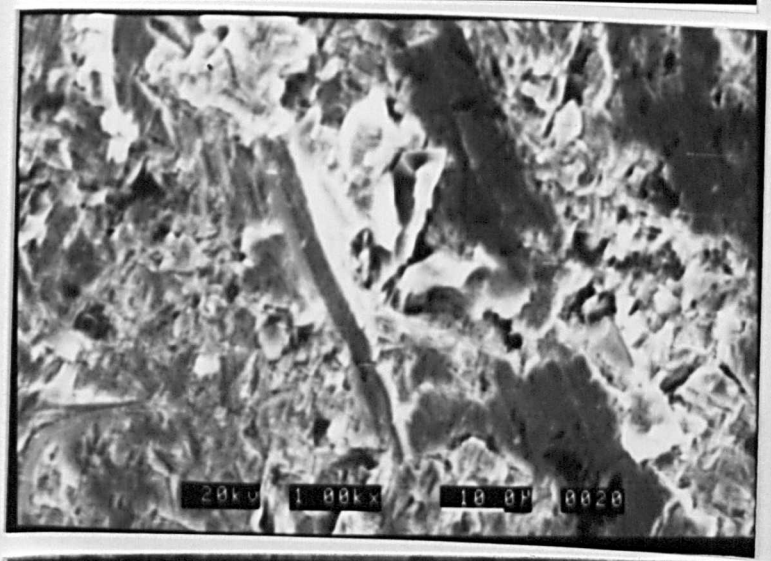

c

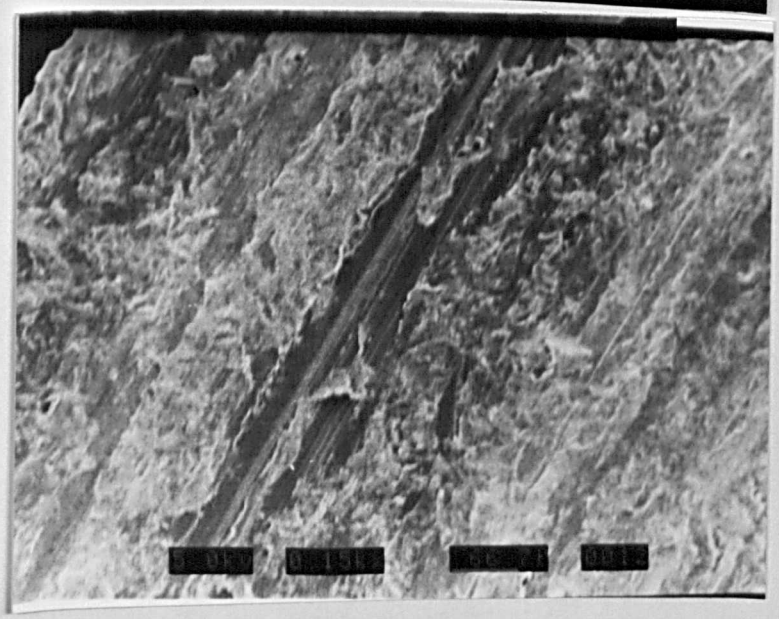

Fig.6.28 : SEM photographs of 440C specimen surface abraded/corroded in H_2O+3vol%H_2SO_4+10wt%L-cysteine aminoacid. Test run for 1h and the specimens weighed every 15 mins.
a) 60 N b) 240 N c) replica showing the surface of the 440C wheel after tests (240N)

6.6.3 N 18

The wear/corrosion data for the Ni-based alloy(N 18) tested in the same range of solutions are presented in Fig.6.29.A linear increase in metal loss was observed with the lowest corrosion induced wear loss occuring for 3vol% H_2SO_4 at both loads. The H_2O at 60 N and the 3vol% H_2SO_4+10wt% L-cysteine solution at 240 N gave higher wear rates.

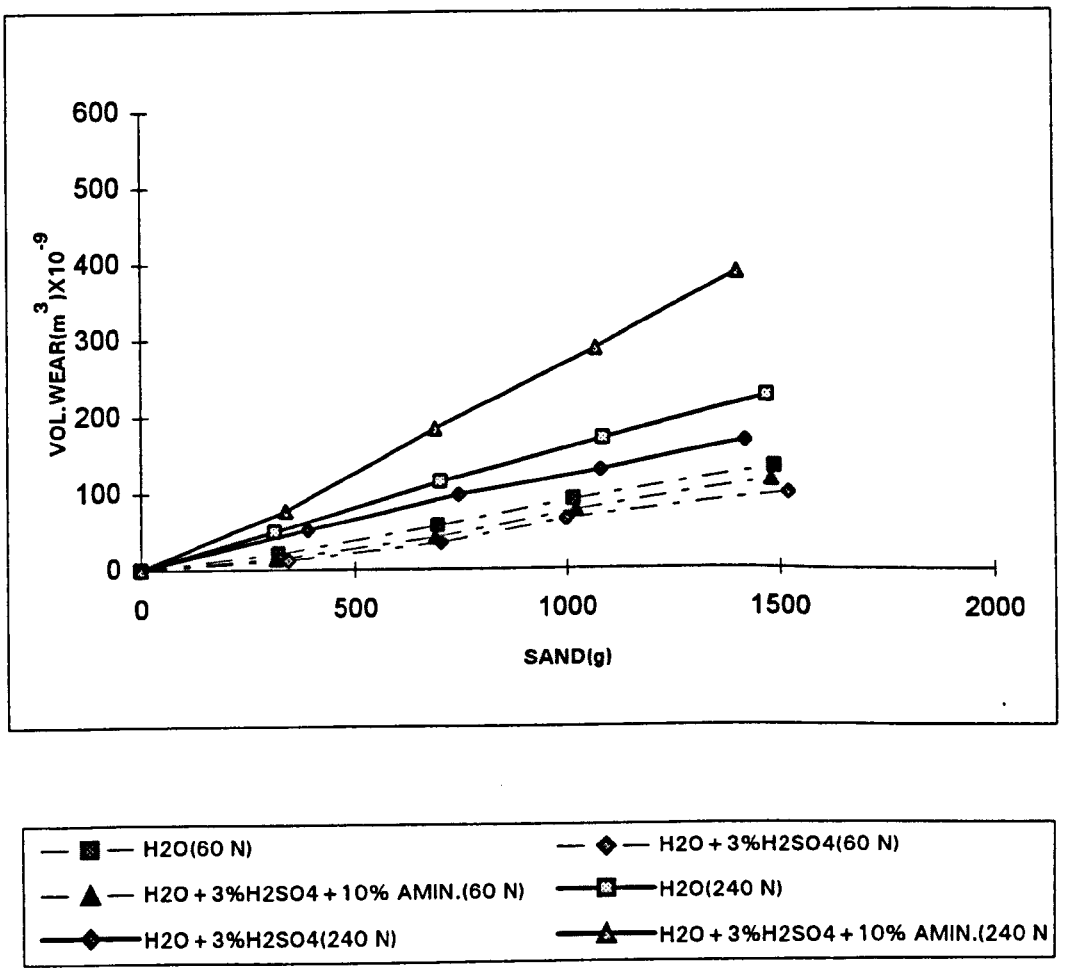

Fig.6.29 : Abrasion/corrosion of N 18 in a range of different solutions expressed as volume loss vs mass of sand abrading the surface. Each test was run for 1 h with the specimens weighed every 15 min.

Fig.6.30 shows an exceptionally heavy build-up of oxidation products on the surface of the specimens at both loads and the surface of the 440C wheel. It can be said again that the wear/corroded surface of the specimens at both loads looks similar compared to the corroded surfaces in Fig.6.24. In the replica there are dark areas standing proud, while light areas appear depressed.

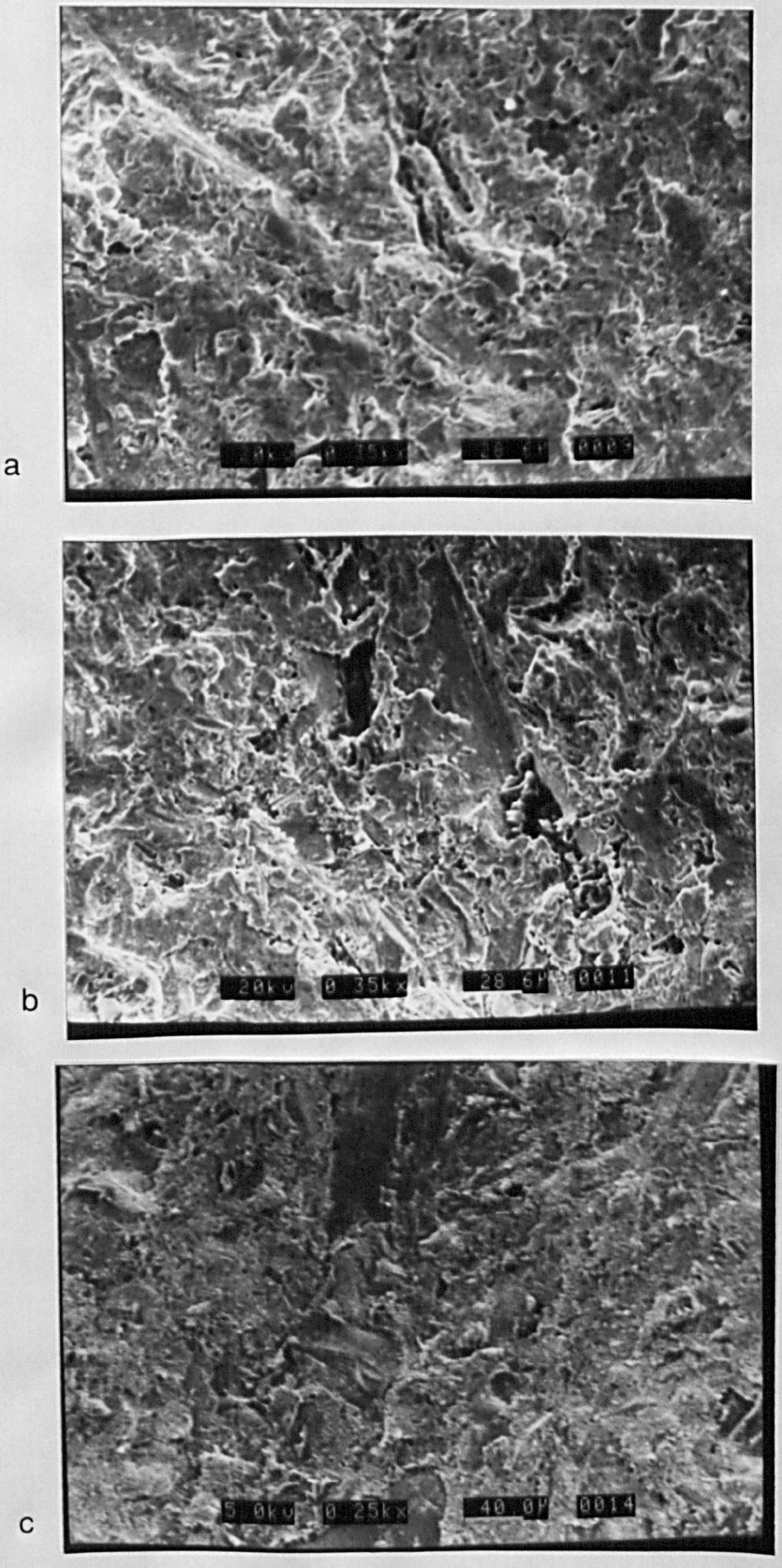

Fig.6.30 : SEM photographs of wear/corroded surfaces in 3wt%H_2SO_4 solution. Test run for 1h and specimens weighed every 15 min.
a) 60 N b) 240 N c) surface of the 440C wheel after tests.

6.6.4 N 18++

Fig.6.31 shows data obtained for the same Ni-based alloy(N 18) reinforced by the presence of hard TiC and TiN particulates.
The same pattern of results as with the plain N 18 was produced except that at 60 N the 3vol%H_2SO_4+10wt% cysteine solution gave lower material loss.

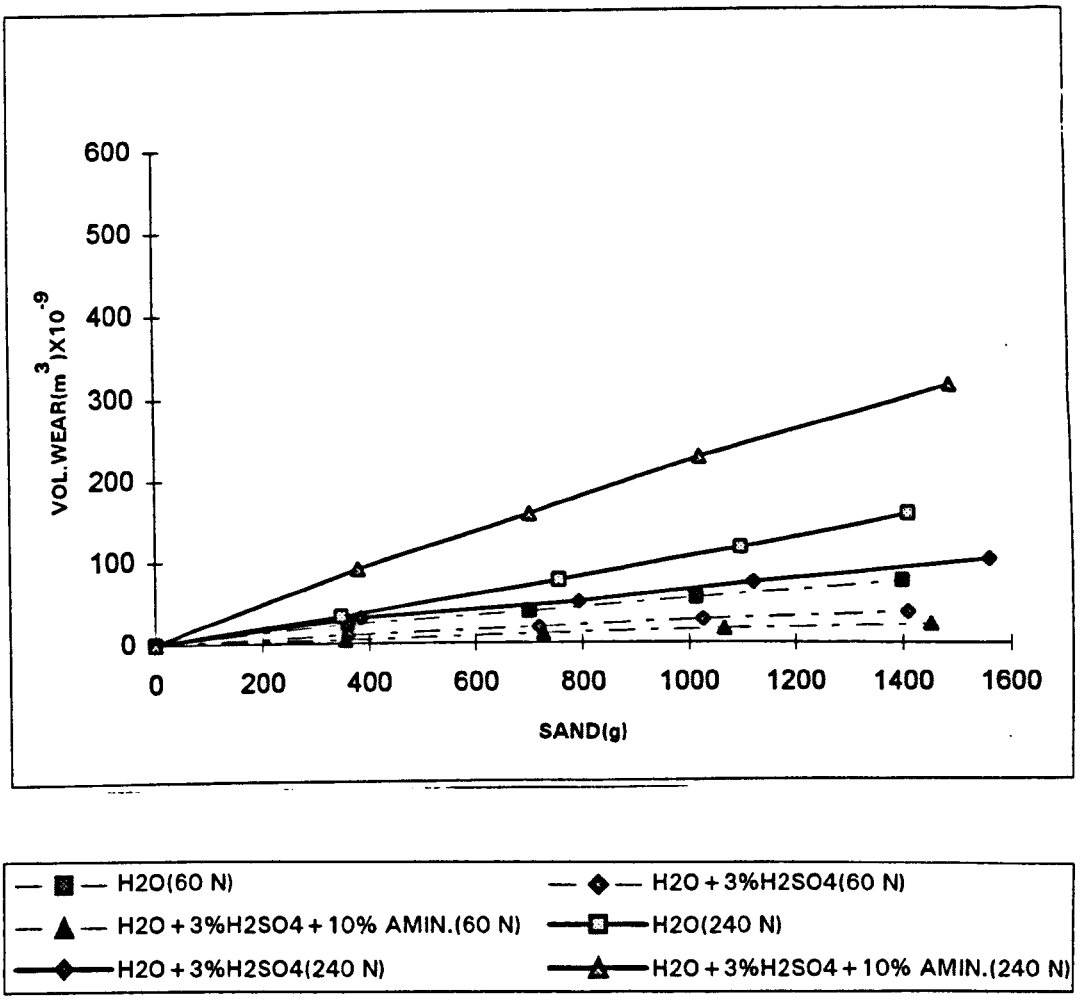

Fig.6.31 : Abrasion/corrosion of N 18++ in a range of different solutions expressed as volume loss vs mass of sand abrading the surface. Each test was run for 1 h with the specimens weighed every 15 min.

Fig.6.32 shows regions at the centre of the wear track for N18++ specimens wear/corroded in different solutions. The same highly roughened pattern of surfaces appeared for specimens and the wheel surface as well.

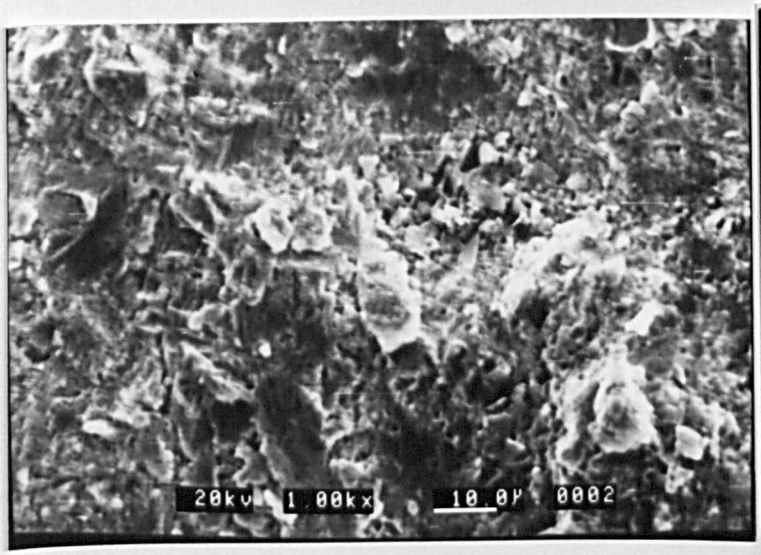

a

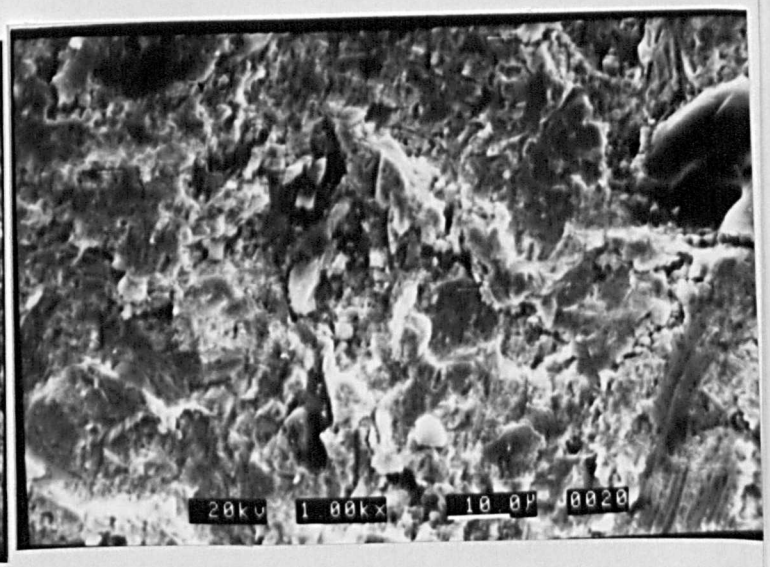

b

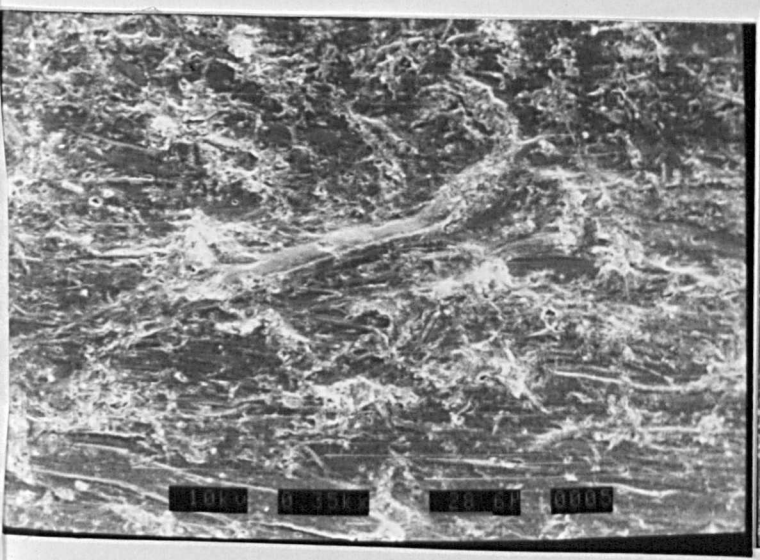

c

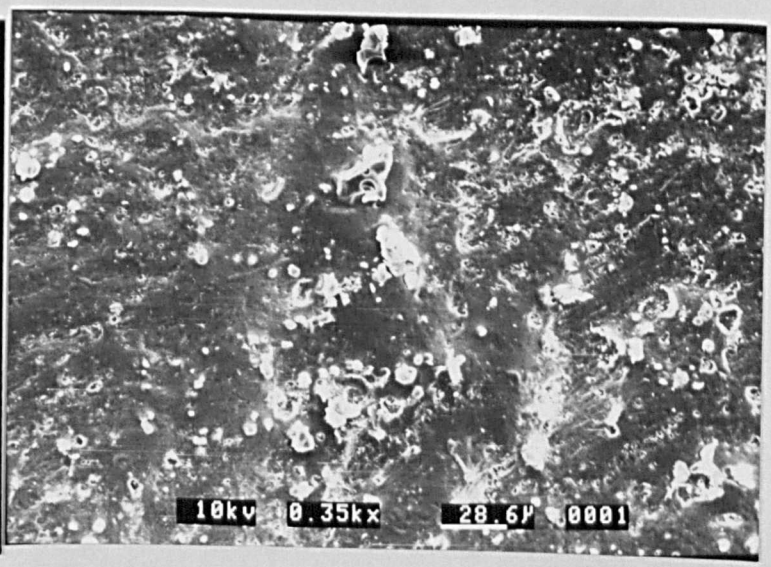

d

Fig.6.32: SEM photographs of N18++wear/corroded in different solutions. Test run for 1h and the specimens weighed every 15 min.
a) 3vol%H_2SO_4+10wt%Amin.(240 N)specimen surface and b) wheel surface(240 N)
c) 3vol%H_2SO_4(240 N) specimen surface and d) wheel surface(240 N)

For comparison purposes and in order to show the effect of abrasion on wear rates the reference material M.St was also tested for sliding/corrosive wear and the results are presented in Appendix B. The 3vol% H_2SO_4+10wt% L-cysteine solution gave the lowest wear loss at both loads. These results appeared to be one order of magnitude lower compared with the results in Fig.6.25 (abrasion/corrosion of M.St).

6.7 Comparative presentation of results

The intention of this section is to summarise all the wear (rubber wheel and 440C wheel) and wear/corrosion results previously presented.
Fig. 6.33, Fig.6.34, Fig.6.35, Fig.6.36 show the volume of material loss against the abrasive sand that took part in the wear process. Most of the materials tested on the 440C wheel gave much higher volume loss. The exception was N18 at 240 N which gave higher volume of material loss when tested on rubber wheel.

The volume of material loss appears to be about one order of magnitude higher in the wear/corrosion tests compared with dry abrasion. The ferrous materials(M.St, 440C), where there is a direct dissolution of the material, seem to behave in a similar manner in the three different environments(H_2O, 3vol%H_2SO_4, 3vol%H_2SO_4 +10wt%L-cysteine). However, for the Ni-based alloys which form a protective film on the surface, the environment clearly affects the results especially at high load.

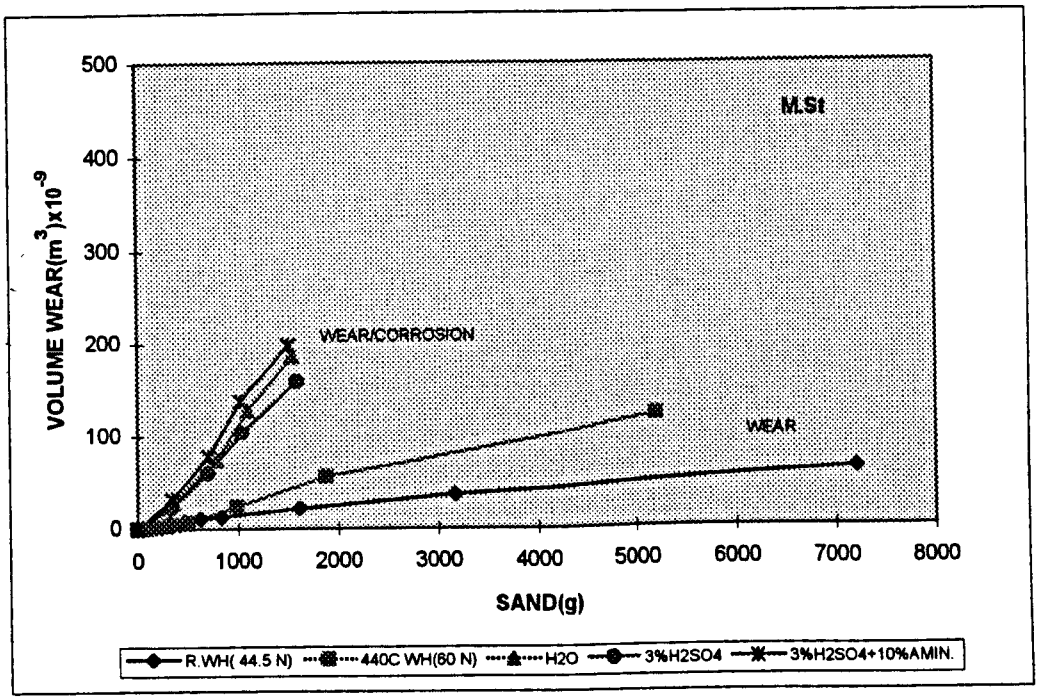

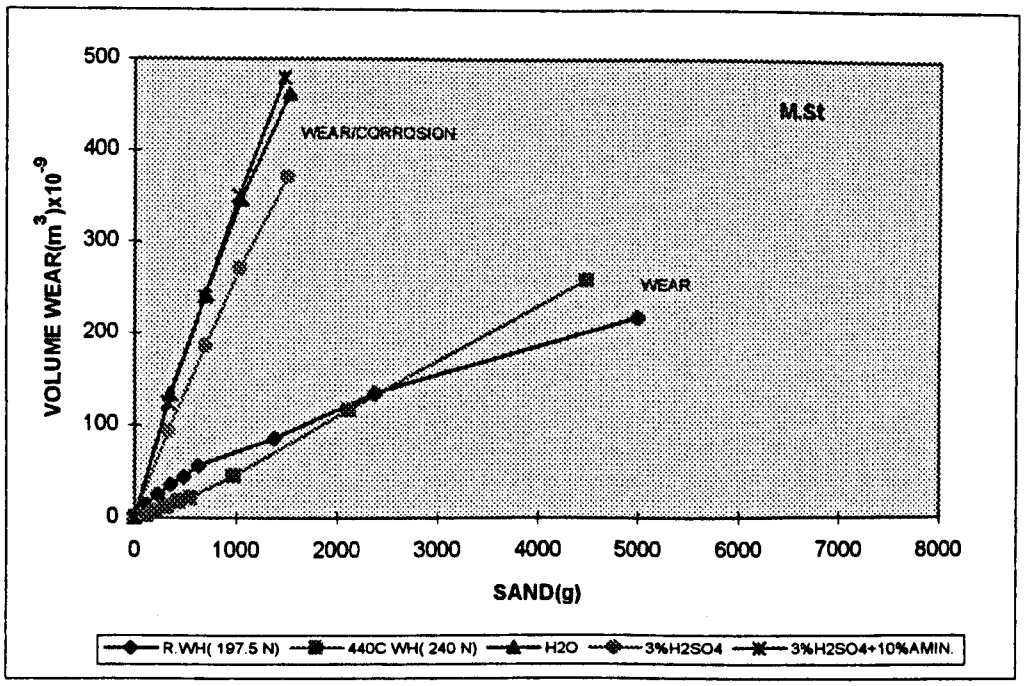

Fig.6.33 : Comparative presentation of results for M.St tested in different environments

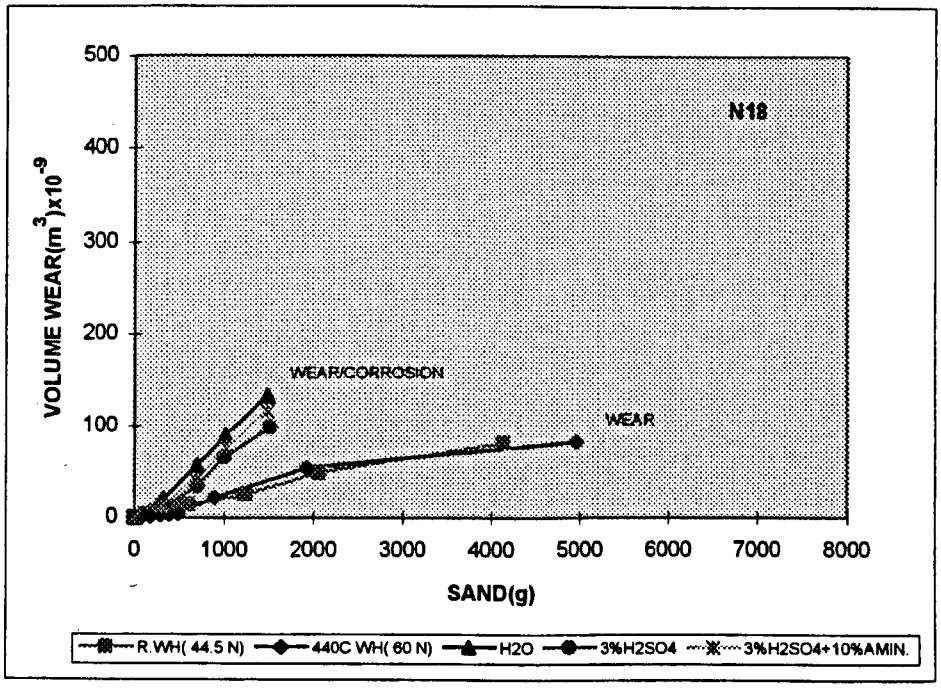

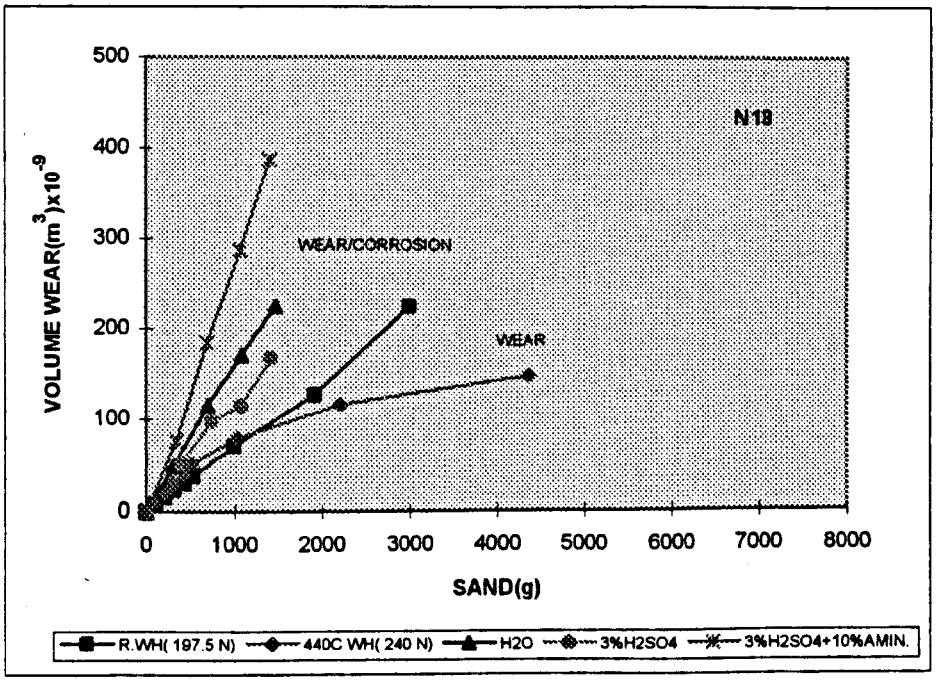

Fig.6.34 : Comparative presentation of results for N18 tested in different environments

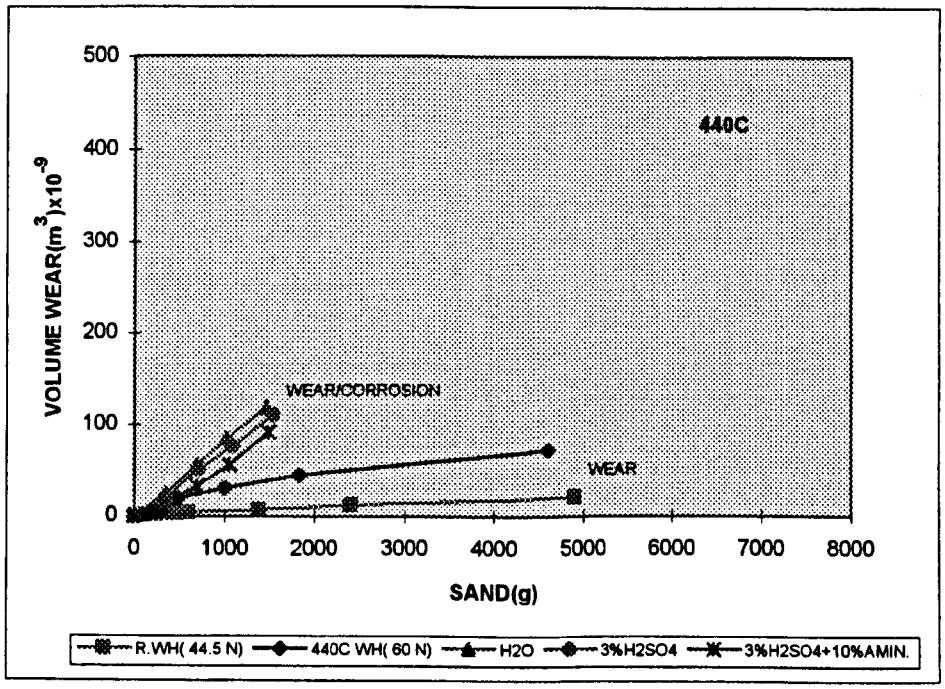

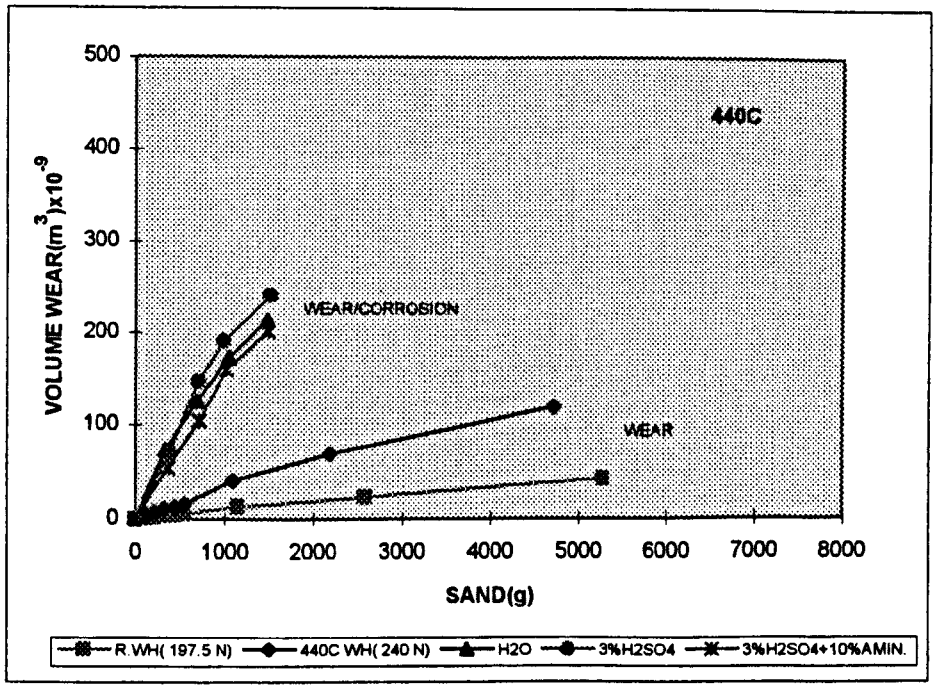

Fig.6.35 : Comparative presentation of results for 440C tested in different environments

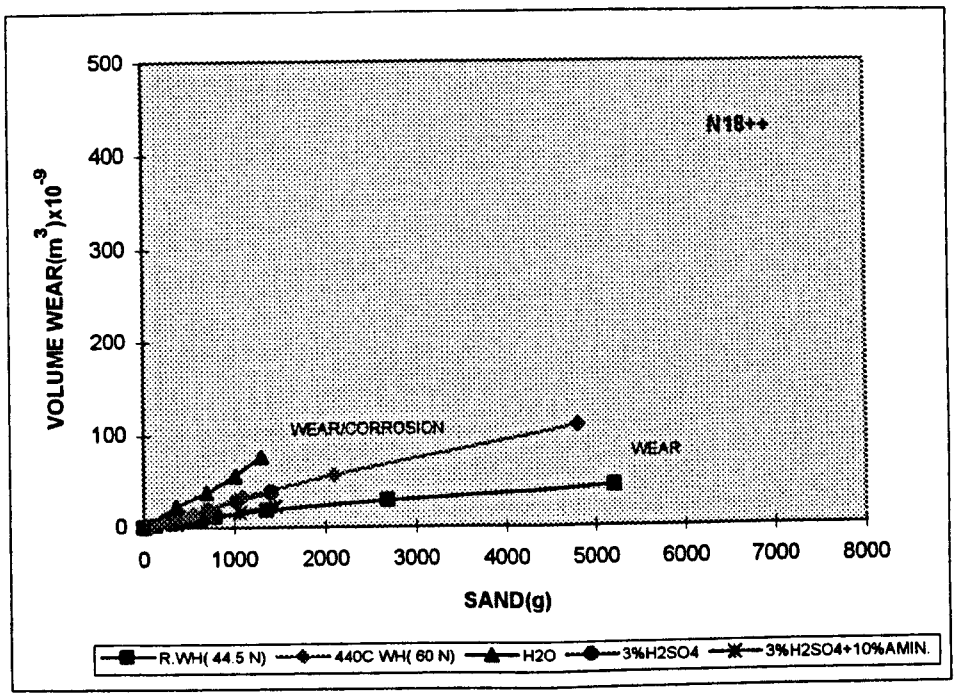

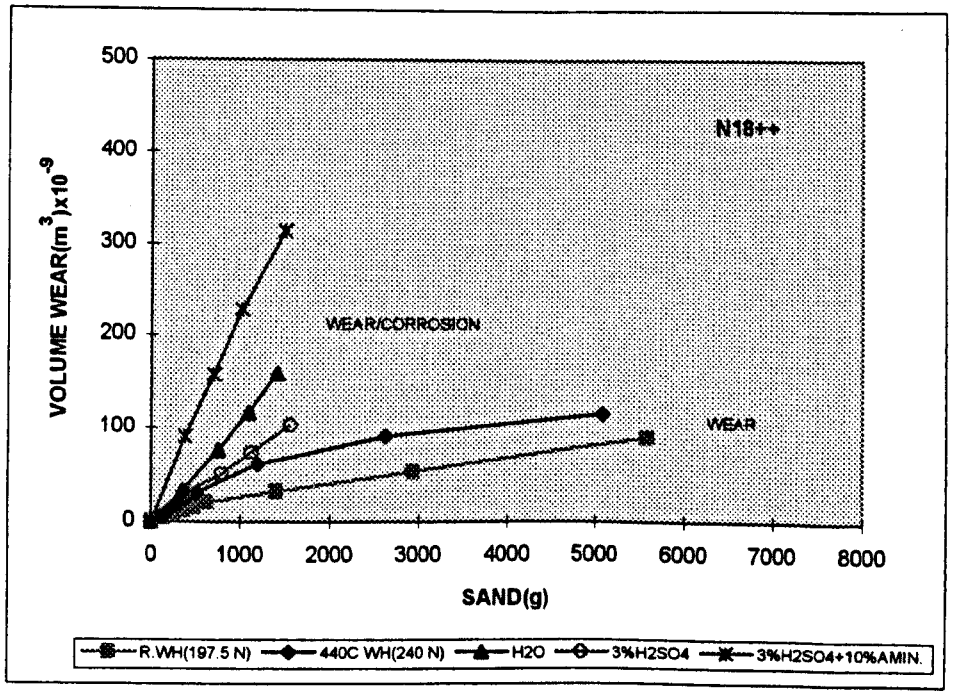

Fig.6.36 : Comparative presentation of results for N18++ tested in different environments

6.8 Indentation tests

A simulation was undertaken to assess the abrasive action of individual particles. Sand of the same particle distribution as for the dry sand abrasive test was used, in order to quantify the damage produced on the surface of the reference material, M.St. Although this test is a static one, the features of damage on the specimen surface can be related to the dynamic process which is abrasion.

Fig.6.37 shows a range of photographs taken by the optical microscope after the tests at different loads.

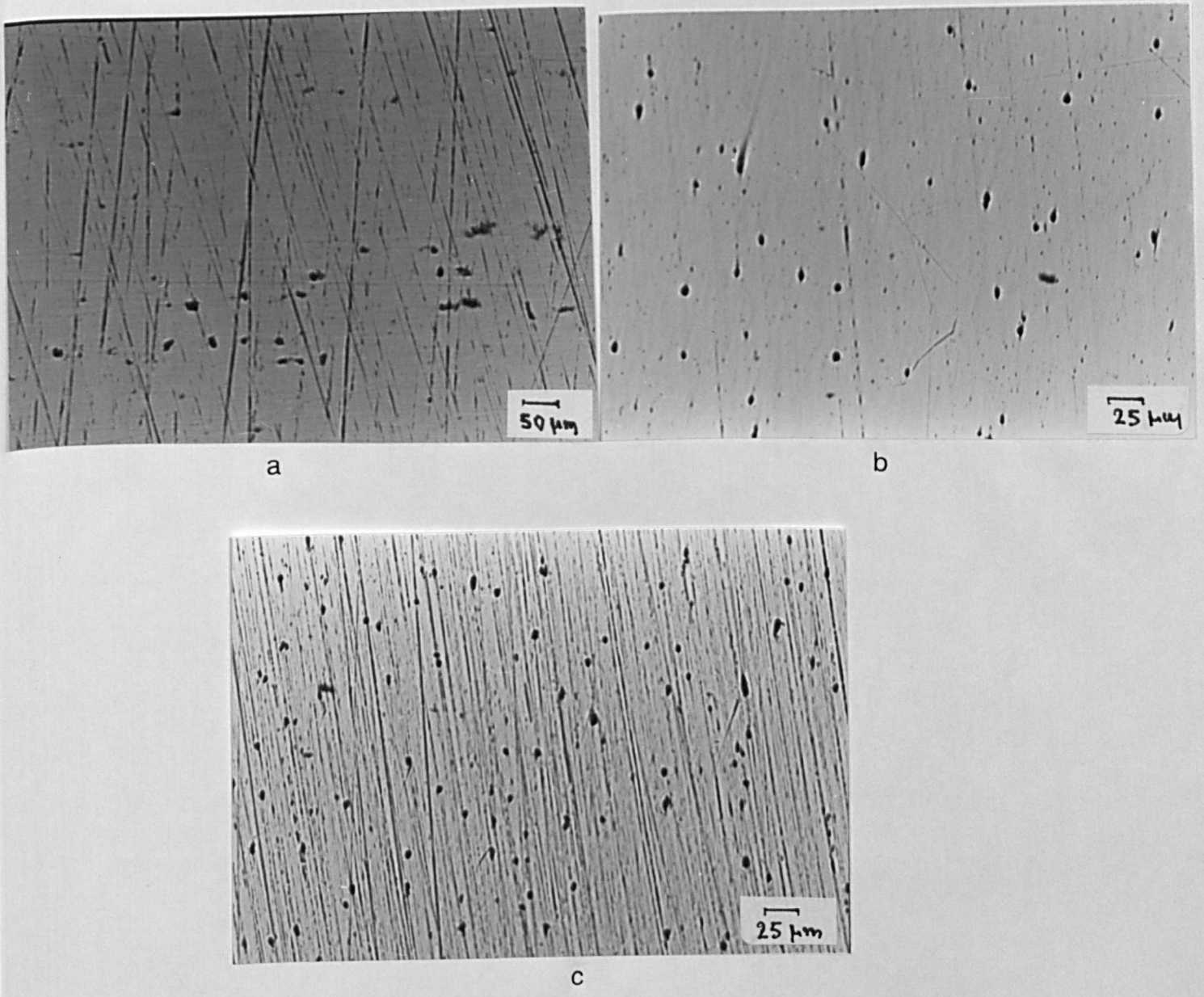

Fig.6.37: Optical photographs showing the indents on M.St specimens made by abrasive particles of similar size distribution as those used in the wear experiments.
a) 44.5 N b) 127.5 N c) 197.5 N

The indents on the surface are made by sand particles of the same size distribution as those used in the actual wear tests. As can be seen from the photographs the number of indents increases with the increase of load which suggests that during the test the load determines how many particles take part in the wear process.

Fig.6.38 gives the mean number of indents per surface area at different loads as they were counted by using the image analyser. The low values of indents per surface area assumes that only a fraction of the sand distribution actually contributes in the wear process. The estimation of this value could be very significant in determining the wear rates.

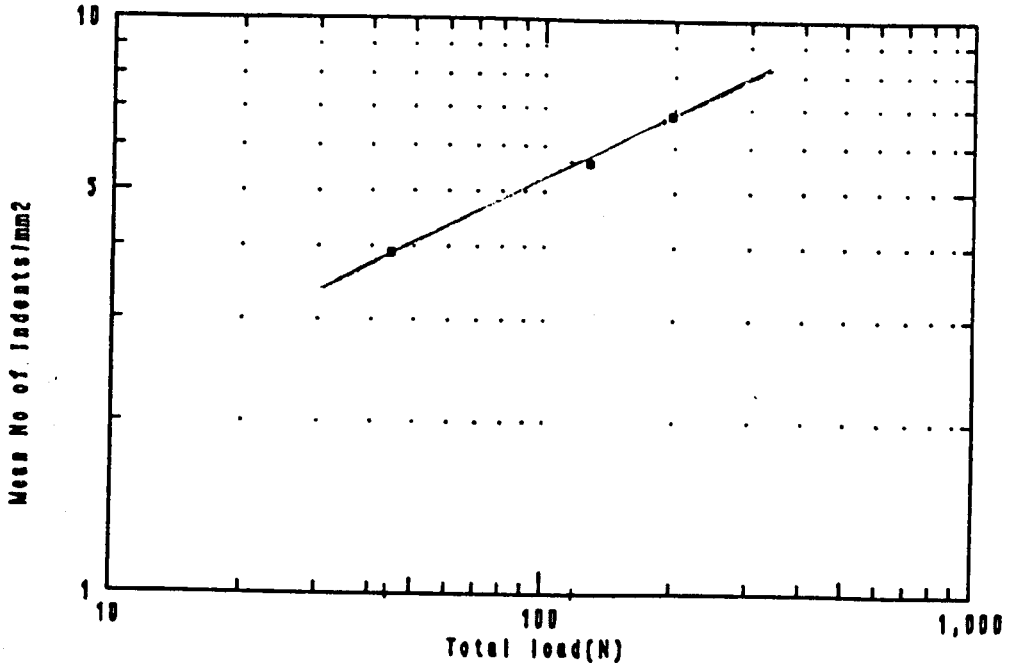

Fig.6.38: No of indents per surface area as related to load applied.

6.9 Scratch tests

The single-pass scratch test results will be presented according to the size of the sand particles abrading the specimens' surface, and the load applied. All specimens exhibited similar features of deformation although differing in severity.

Fig.6.39 and Fig.6.40 show that the single scratches produced extensive ploughing similar to that in Fig.6.8d. It is evident that ploughing has caused considerable displacement of material to the sides of the groove, indicating that the entire groove volume is not directly removed.

Wear debris particles can be seen on the scratch groove ridges which suggests that some material removal of the ploughed material occurs. It is evident from the photographs that the size of the grooves increases with the increase in load. Also, the depth of the grooves changed with the different loads,the higher the load the bigger the depth, as the

measurements in the image analyser showed.

Fig.6.41 shows the damage produced on the specimens from 250µm sand particles at two different loads.

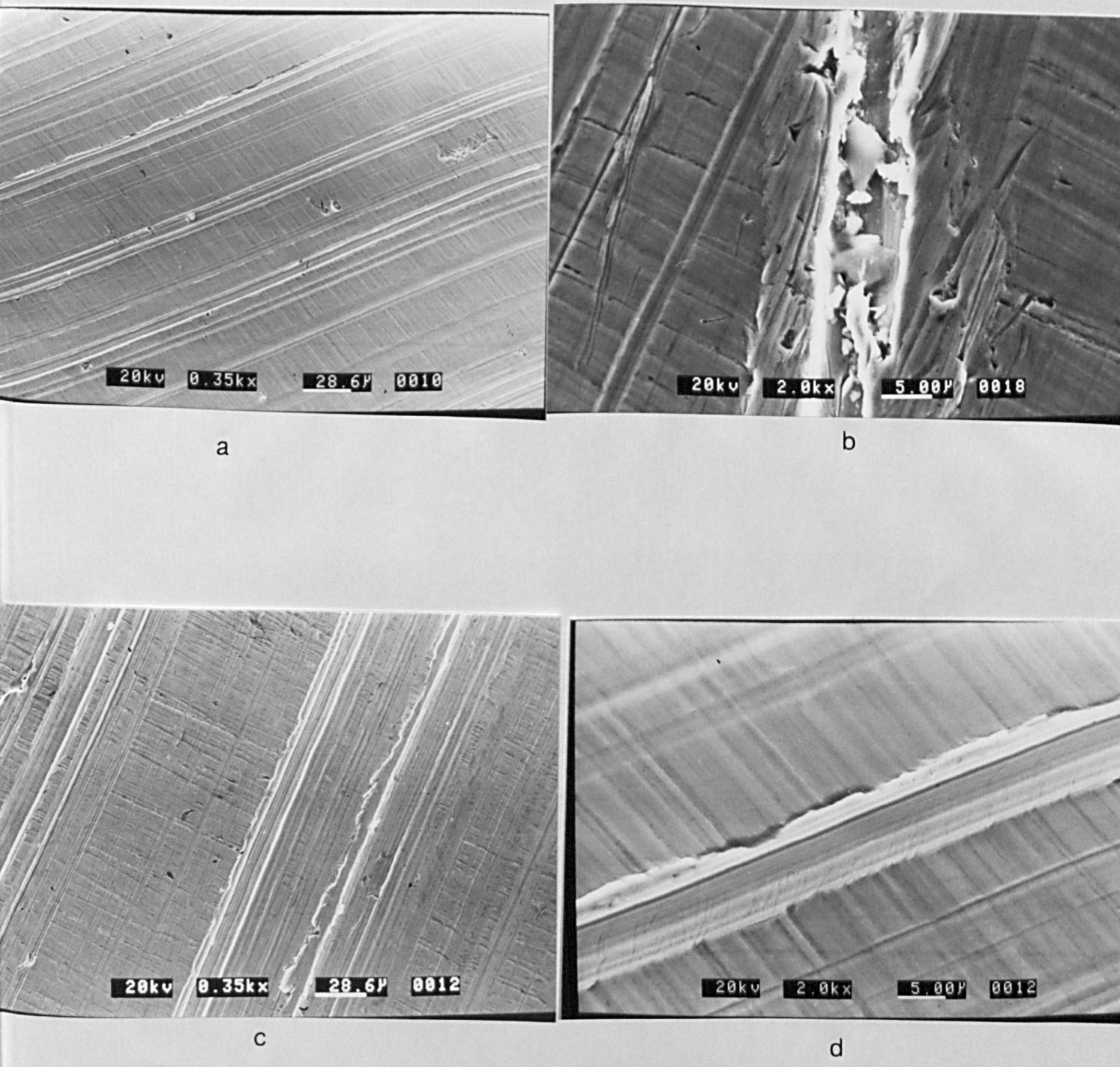

Fig.6.39: Single-pass scratch tests of M.St showing the formation of grooves and the associated deformation by dry abrasion.
a) and b) mean particle size 125µm; load 44.5 N
c) and d) mean particle size 125µm; load 197.5 N

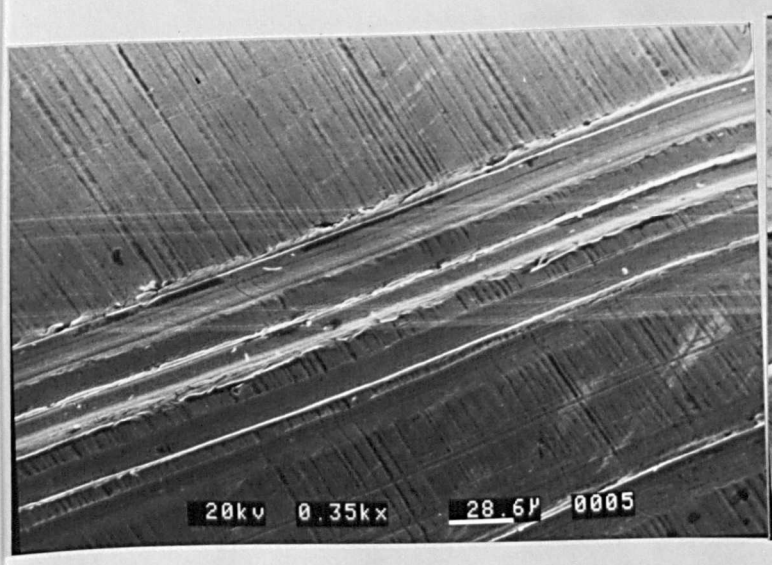

a

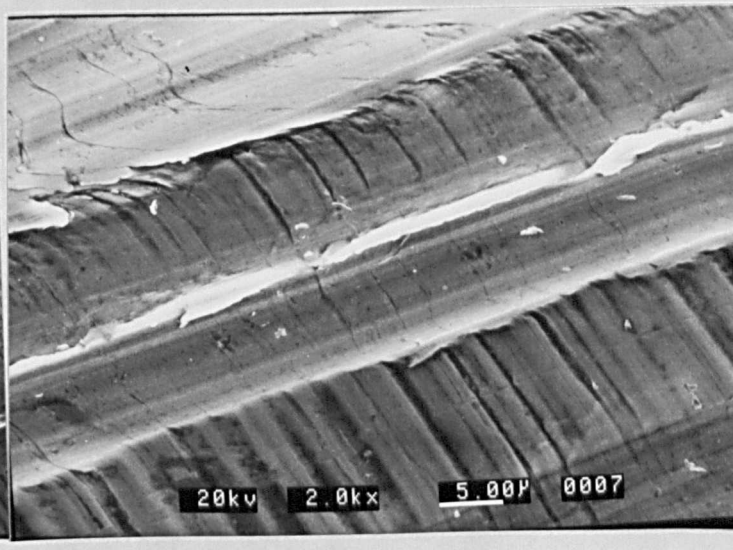

b

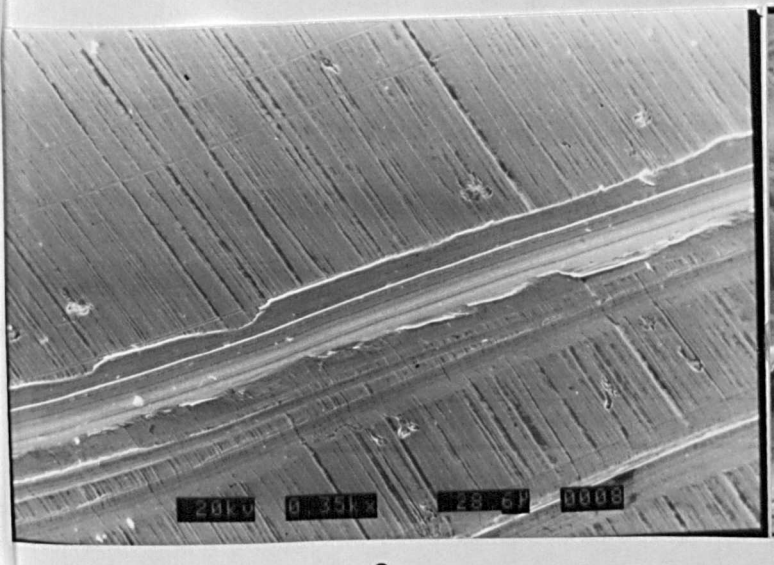

c

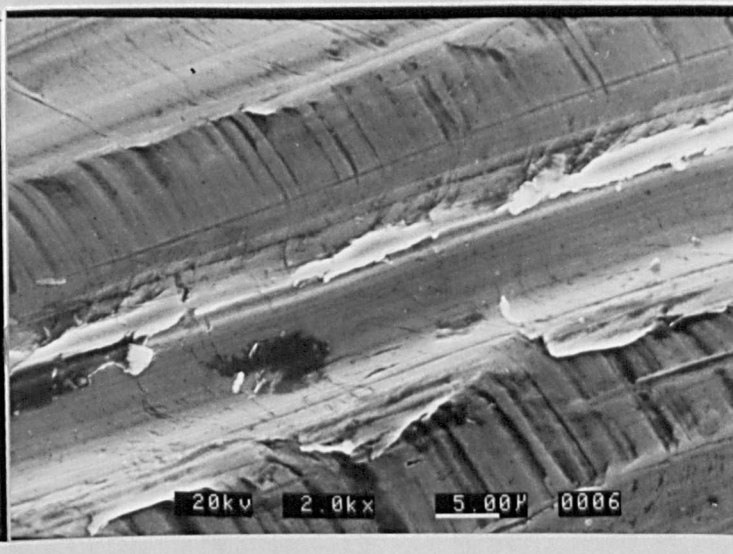

d

Fig.6.40: Single-pass scratch tests of M.St showing the formation of grooves and the associated deformation by dry abrasion.
a) and b) mean particle size 250µm; load 44.5 N
c) and d) mean particle size 250µm; load 197.5 N

a

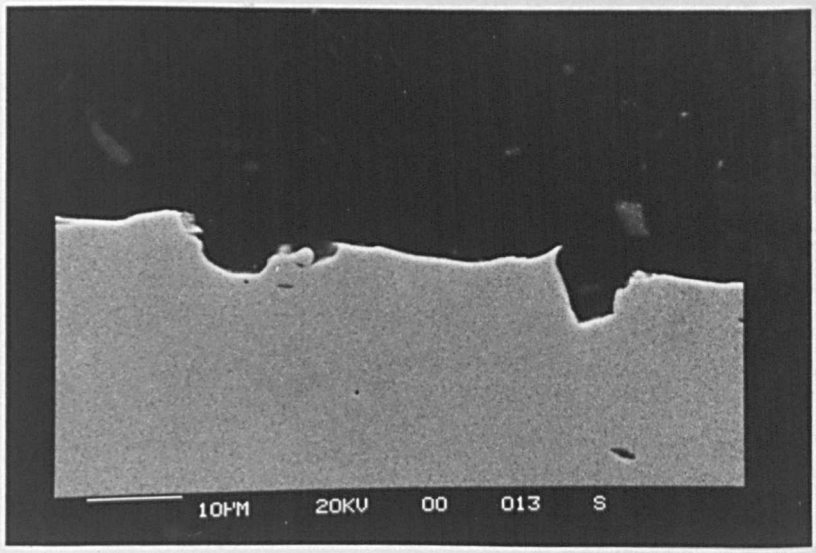

b

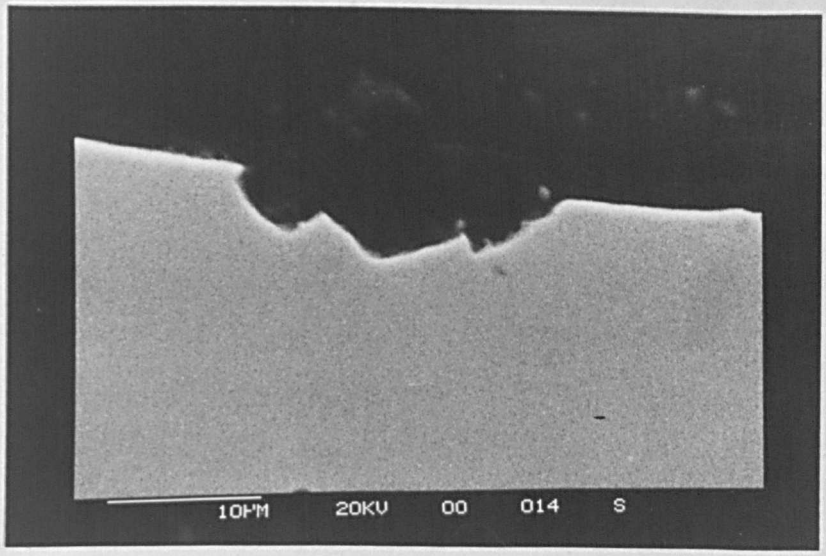

Fig.6.41: Cross-section of the specimens after being scratched by sand particles of 250µm a) 44.5 N b) 197.5 N

CHAPTER SEVEN

7. Discussion of results

The complexity of wear is emphasised by the number of factors required to describe it. The major factors influencing wear are of three types:

- Metallurgical factors such as bulk hardness, toughness, microstructure and chemical composition.
- Variables connected with surface finish of the contacting materials, applied load, the velocity of relative motion, and temperature.
- Other factors such as the existence of surface films(oxidation, corrosion), which modifies the wear behaviour of the surface.

In the present research some factors and their relevant variables are either fixed or controlled during experimentation (temperature, surface finish), whilst others such as different materials and environments are investigated to study their effect on the wear and wear/corrosion of the system.

In the discussion concerning the previously presented results some major questions will be considered, namely the reproducibility/reliability of data, effect of the main variables on the wear rates, surface and wear debris morphologies after wear tests and their implications on wear mechanisms, influence of different environments (dry, wet), and finally the significance of wear rates on equipment performance.

7.1 Reproducibility / reliability

In abrasion testing, it is often expensive to obtain multiple data points. When this occurs, the investigator has to use some criterion for choosing a minimum acceptable sample size for a meaningful result. It is important to have confidence in the reproducibility of the results at any time during experimentation and as it is common practice in all engineering applications, a 95% confidence level is sought out.

In this investigation, a set of five M.St specimens was tested for dry sand three-body abrasive wear under nominally identical conditions and the results are presented in Fig.6.5. The reproducibility of the results obtained was 4.3% which is within the ASTM allowable sampling error of 5% for this sample size and coefficient of variation of 6%.

Comparison of the particle size distribution before and after the tests, Fig.6.2(the

distribution was similar), indicated that there was no breaking-up of the abrasive particles after the tests and the slight variation of the results at the highest load can be attributed to the many variables within the system (e.g different batches of sand, different sand flow rates etc).

However, the use of a range of different loads and in general the similar results obtained, could be taken as confidence that the results are reproducible and the test procedure reliable.

7.2 Main variables

According to Archard's basic wear relation, equation 3.4(page 43), the main variables in the wear process are: load, bulk hardness and test duration (time, path length, amount of abrasive). The effect of these major variables will be considered briefly.

7.2.1 Load

With most materials wear loss in the tests using the rubber wheel increases in approximately a linear manner with load as predicted by most wear models [44,45](within the range of loads possible with the rubber wheel) until the system reaches a steady state. Then, the wear loss either remains constant or decreases with increasing load as has been reported [1] depending on the conditions i.e oxide films, structural collapse of the material due to gross plastic deformation. The results in the present study, and for the loads used show that steady state wear was reached quickly.
However, it is hazardous to try to extrapolate wear rates or even to assume that the ranking of some materials will remain constant beyond the range of loads tested.

When the load is high enough to fracture the abrasive particle and create new sharp points, wear can increase. However, as the particle size distribution after the tests showed(rubber wheel), there was no appreciable break-up in the large particles to justify any increase in wear. However, the tests using the 440C wheel showed that there was a change in the particles size distribution, indicating that the abrasive was being broken down. As discussed later, the modelling results suggest that this did not have a significant effect on the wear process.

The effect of applied load on wear rate under three-body wear conditions is shown in Fig.7.1. The trend of increasing wear rate with applied load for all the loads used in the test is clear from this figure. With the rubber wheel the materials appeared in two groups. Those with high hardness showed low wear rates and those with low hardness gave high rates. It seems that with the compliant rubber wheel and for the same load the materials hardness and the matrix reinforcement plays a significant role in determining wear rates. However, with the 440C wheel which is less compliant, all the materials gave wear rates higher by a factor of 2 or more.

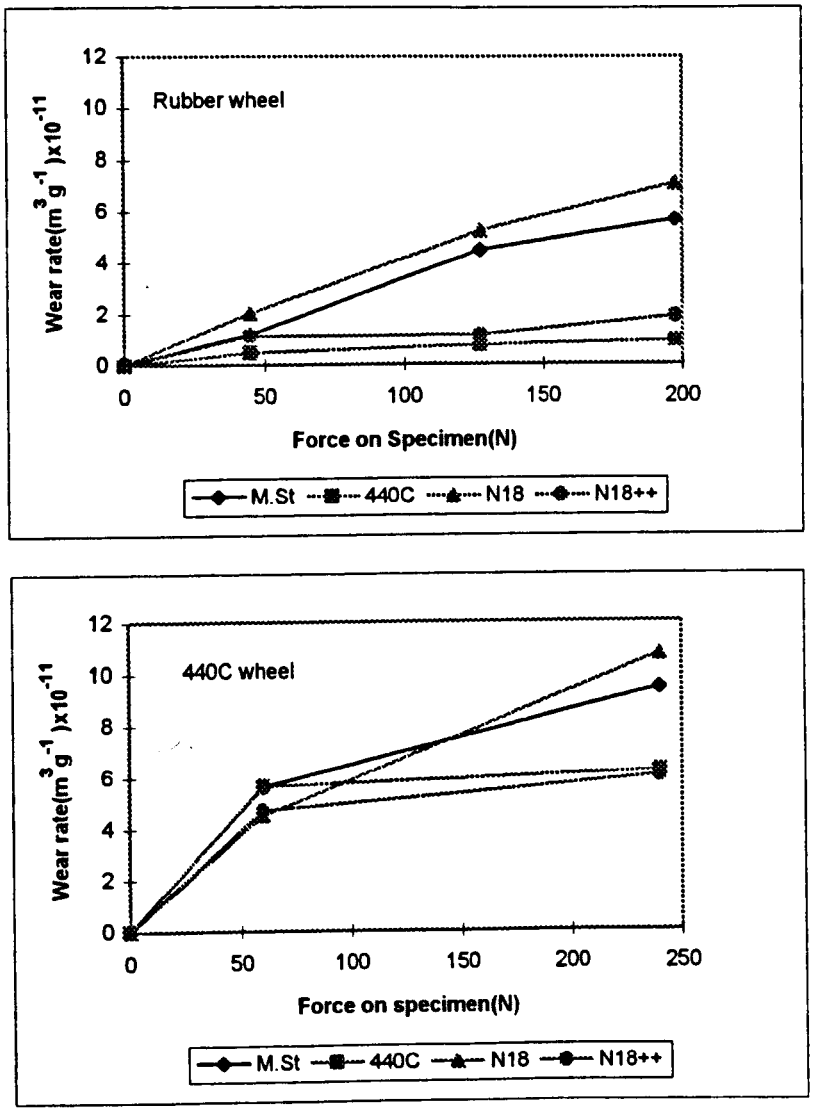

Fig.7.1 :Effect of load on the wear rates of materials with different values of hardness.

7.2.2 Effect of hardness

It is recognised that hardness is probably an important property influencing wear rates, but whilst it is generally agreed that wear rates tend to decrease with hardness, there are exceptions as well. In this work, 440C follows the rule but the reference material M.St is an exception.

Indeed, 440C showed the best wear behaviour of all the four materials tested with very low wear rates. This can be atributed to high carbon content(1.2%) and the heat treatment which gave the martensitic matrix and high hardness(720 HV). A noticeable increase of the surface hardness, as Fig.6.12 shows, might have played a role as well, but not a great deal.

Mild steel on the other hand is an exception because despite its low hardness(230 HV), it showed a reasonably good wear behaviour compared with the other tested material N18

with higher hardness(380 HV). Since there was little apparent work hardening during the test, the good performance of M.St could be attributed to the higher ductility, which means that more abrasive particles are needed to generate each wear debris particle.

The decreased wear rates of 440C can also be explained by the surface-abrasive hardness interaction. Kruschov and Babichev [44] reported that wear is independent of the abrasive hardness when this was very much greater than the hardness of the wearing material. But as the hardness of the wearing material approaches that of the abrasive, wear drops sharply. The contacting asperities will still do damage and cause wear but the mechanisms change. The number of passes over a given area increases drastically and contact fatigue becomes important. Silica sand used for this experiment has a hardness of about 600-800 HV and 440C about 720 HV.

N18++ behaved similarly despite the fact that it is less hard than 440C. This good wear behaviour could be attributed to the large size and volume fraction of the reinforcement and the fact that with the compliant rubber wheel the abrasive particles in contact with the much harder(1300 HV) reinforcement can deflect the support and indent the surface of the composite to a much smaller extent than those particles pressing against regions of the softer metallic matrix(Fig.6.10c).
However, with the 440C wheel all the materials gave wear rates that were a factor of 2 higher and there is not as great a difference between materials of different hardness.

The above mentioned cases have shown that hardness may give a guide to improved wear resistance, but that is all. The real answer to improved wear resistance lies in changing the dominant wear mechanism, which might be triggered by increasing hardness.

7.2.3 Test duration

It is useful when experimenting with materials to identify their relative wear resistance, to keep the test running and weigh the specimens at different time intervals. This enables the effect of variables, such as amount of abrasive and path length to be identified.

In this work it was found that a linear relationship exists between volumetric wear and wear rates when they are plotted against the amount of sand used(Fig.6.6 and Fig.6.7). Similar linear relationships exist if they are plotted against time or path length. Fig.6.7 also shows that for the harder materials(440 C and N18++) steady state wear is attained more rapidly than for the softer ones(M.St and N18). According to Richardson [146] this depends on the relative hardness of the wearing material and the abrasive or could be also due to the rate and magnitude of strain hardening. This strain hardening is more noticeable with the harder materials than the softer ones, as Fig.6.12 shows.

7.3 Structure after wear tests-Mechanisms

Several mechanisms have been proposed to explain how material is removed from a surface during abrasion.[147] These mechanisms include thermal phase transformation, plastic

deformation, fracture or fatigue but because of the complexity of the abrasion no one mechanism completely accounts for all the loss.

There is no clear evidence that any thermally induced phase transformation took place during the wear tests of the materials under investigation. The highest temperatures measured, using a thermocouple placed on the back side of the specimens at about 0.5mm away from the wearing surface, were between 90-130°C. The temperatures on the contact surfaces were expected to be higher but not high enough to change the microstructure of the material. If temperatures high enough to cause phase transformations occurred, they had to be restricted to an extremely thin superficial layer, mainly on the specimen's wear track inducing thermomechanical phase transformations. No evidence of this behaviour has been seen.

Mechanisms of abrasive wear can involve both near-surface plastic deformation and brittle fracture. Both of them can operate simultaneously even for materials thought of as ideally brittle.[148] This deformation is caused by friction at the contact interface. The high shear stresses introduced by abrasion into the surface and the energy of the frictional work expended, is largely accounted for by the plastic work done in the deformed substrate region. Plastic deformation is responsible for phenomena like void formation, crack nucleation and propagation and other chip or particle formation processes.

The appearance of the abraded surfaces of the different specimens was generally that shown in SEM photographs presented in the results section(Fig.6.8d and 6.9c). Two significant aspects of the surface morphology were observed:

- long grooves aligned in the sliding direction representing displaced metal
- small dispersed craters or craters concentrated at some areas on the abraded surfaces and small cracks transverse to the sliding direction.

The significant differences observed in wear resistance of the different materials tested under different wear conditions can be associated with the wear mechanism. Observation by SEM of the worn surfaces and wear debris, indicates that the predominant wear mechanism for the materials is ploughing and some cutting which respectively form plastically deformed flakes and cutting chips as shown in Fig.6.13.

Those types of wear debris particles have been identified and described by Bowen and Westcott.[13] Ribbon-shaped particles which have large aspect ratios, usually are curved and even curly and all have the characteristics of machining chips produced by a vee-point tool. The production of machining chips suggests that the following criteria are met :

- the hardness of the abrasive should be several times that of the workpiece surface which is the case with M.St and N18.
- some of the abrasives come in contact with material having a rake angle less negative than a certain critical value(α_c), characteristic of the specimen material.
- the depth of cut ratio Dp=h/a is $\geq$ 0.4 according to Kato's diagram.[149]

The existence of plate-shaped wear particles has been the basis for the development of the delamination theory of wear by Suh.[30] Those particles have lateral dimensions ranging from tens to tenths of a micrometes and thickness is typically one tenth of the lateral dimensions.

They are produced when local plastic deformation of the surface material(Fig.6.8d) results in crack initiation in the near subsurface region(Fig.6.11).
Other mechanisms [150,151] have also been proposed for the generation of plate-like particles but in this work only Suh's explanation will be considered.

7.4 Modelling of abrasive wear

Modelling is important in order to predict component life reliably. It should enable both material properties and external variables to be linked.

Starting with the dimensionless wear coefficient K given in chapter 3 which is of fundamental importance and widely used in modelling. This very simplistic approach assumes nothing about mechanisms, material properties other than hardness, or abrasive properties. However, the coefficient provides a valuable means of comparing the severity of wear processes in different systems. The range of values for three-body abrasive wear is typically $0.5x10^{-3}$ to 5×10^{-3}. [21]

Fig.7.2 compares theoretical values evaluated from Archard's basic relation, equation 3.4(page 43) by using a mean value for $K=2.5x10^{-3}$ and with experimental values from three-body abrasive wear tests(Rubber wheel) in this study. The two other lines show the scatter of the results if the upper ($5x10^{-3}$) and lower ($0.5x10^{-3}$) values for K were used. Also, for comparison purposes the experimental values from the 440C wheel tests and the theoretical (using the mean value for $K=2.5x10^{-3}$) are presented.

Considering the normal scatter of experimental data, there is good correlation between the theoretical model and the experimental results and the prediction is better than one order of magnitude.

7.4.1 Modelling material behaviour during the dry sand abrasive test-rubber wheel

As observation and experimental evidence show, abrasion is a deformation process producing wear particles by some mechanism inducing fracture. Different materials give different wear rates which may vary by orders of magnitude. Even with the same materials this is the case when the operational parameters are changed.[152]
In this work an attempt was made to predict the wear rates of the four different materials under examination. Since the abrasive wear is a dynamic process, variables are changing with time. Variables like hardness, grit radius, load, etc must be closely studied and quantified in order to monitor the progress of wear in a particular situation.

A comparison between the abraded surface and wear debris of the soft materials (M.St , N18) with those of the harder ones (440C, N18++) illustrates the differences between a cutting and ploughing mechanism of groove formation. Both mechanisms were in evidence from the wear debris of the softer materials examined, though cutting is a very minor part, and only ploughing occurs for the harder materials.

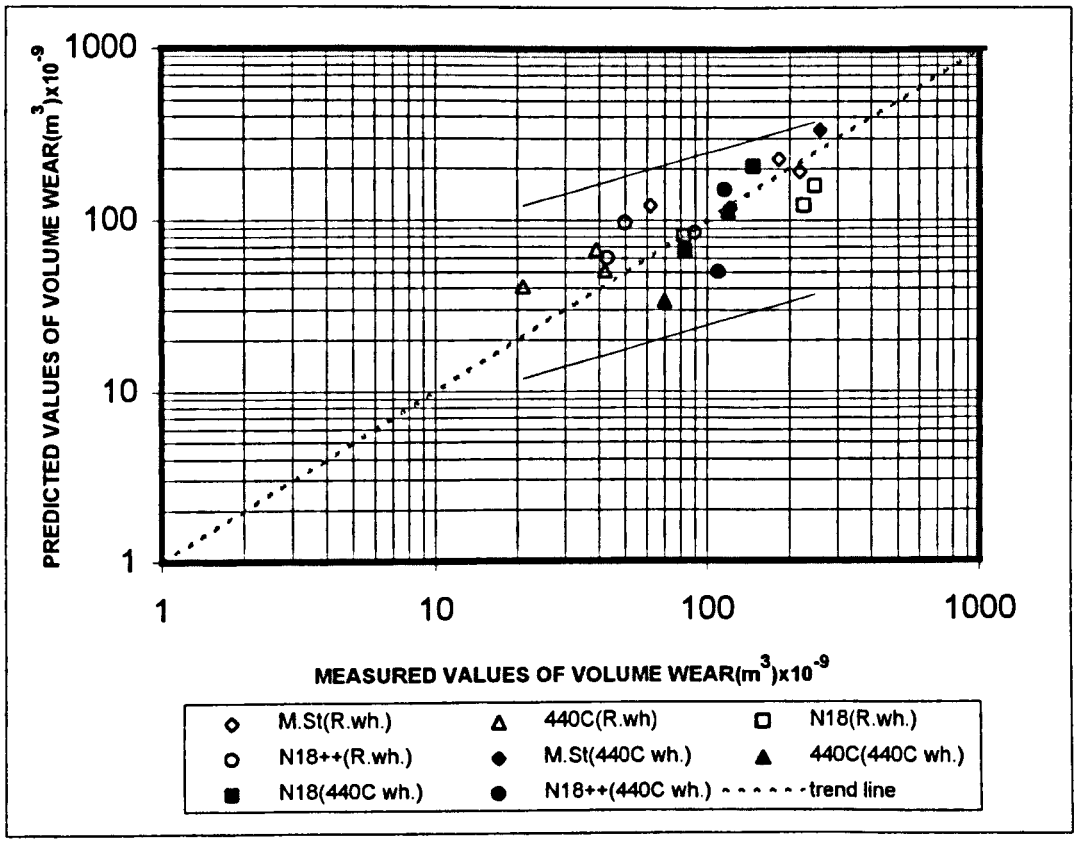

Fig. 7.2 : Theoretical vs experimental volumetric wear measured on different materials at different loads. Test were carried out by using a rubber wheel and 440C wheel.

The majority of models in the literature consider cutting as the only mechanism of material removal and these may be used to predict wear.[30,153,154,46]

Cutting leaves a groove with no ridges. It involves only the shearing off of material immediately ahead of the abrasive. Fracture is by the growth of shear cracks through the most strain-hardened material. So the first assumption was that cutting was the predominant mechanism of material removal, even though wear debris analysis suggested otherwise.

By using Kato's wear equation for cutting,[149] the wear volume can be calculated as follows.

$$V=\alpha_c \beta_c \frac{WL}{H_v}\frac{1}{C_s}$$

where:

- V: volume wear(mm^3)
- W: normal load(N)
- L: sliding distance(mm)
- C_s: shape factor of the abrasive grains(the mean value: 0.65 was used for the calculations- this value was determined by measuring the aspect ratio width/length of the angular particles- range of values 0.6-0.75)
- α_c: degree of wear(mean value: 0.25 was used for the calculations and it was estimated by measuring the grooves on the wear scar.

θ_c: fraction of contact points(taken from Kato's experiments: 0.45)
H_v: Hardness of the material(N/mm^2)

Table 1 presents the results along with experimental values from rubber wheel wear tests.

Load (N)	Theoretical(mm^3)	Experimental(mm^3)
44.5	8255	62
127.5	15447	183
197.5	13093	218

Table 1 : Presentation of theoretical and experimental results for volume wear of M.St. Theoretical results calculated by using Kato's wear equation for cutting.[149]

The above calculations of volume wear gave large numbers which had no relation with the reality of the experiments and tend to confirm that cutting is unlikely to be the dominant wear mechanism.

Another approach was to calculate the depth of penetration (Dp=h/a) for all four materials and loads. The results obtained were compared with Kato's wear diagram for rigid-plastic bodies. This diagram is a plot of degree of penetration against hardness, and the results of the present work were in the ploughing area (Fig.7.3)[149] giving values of around 0.006-0.03. Statistically it might be that a few large particles cross the ploughing-wedge transition line and cut some chips, which is evident in the wear debris photographs, but this is very limited.

In conclusion, the cutting mechanism is unlikely to be the predominant mechanism of material removal. This is consistent with the appearance of the worn surfaces and the wear debris which, apart from a few chips (cutting wear), consisted of platelets (ploughing).

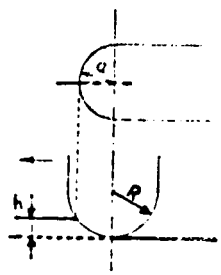

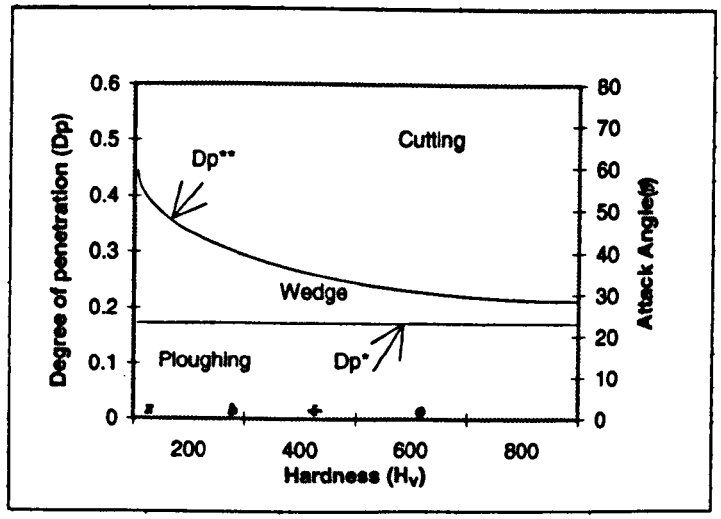

Fig.7.3: a) A contact model between a hemisphere and a flat surface in sliding [149]
b) Wear mode diagram :Dp*, critical degree of penetration, which corresponds to the transition from the ploughing mode to the wedge-forming mode Dp :critical degree of penetration which corresponds to the transition from wedge-forming mode to the cutting mode. Results from experiments for, M.St : 0.006-0.07, 440C : 0.003-0.03, N18 :0.006-0.06, N18++ : 0.004-0.03**

Ploughing is synonymous with some penetration (h/a values not deep compared with cutting) and extensive plastic flow of material laterally to the sides of the abrasive groove. Fracture is by ductile tearing and fatigue of the ridge material. Fig.7.4 shows overlapping grooves which result in fatigue of the plastically deformed material of the ridges.[155]

The observation of the wear debris particles created, in relation to the large number of abrasive particles taking part in the process is a strong indication that more than one particle is required to generate one piece of wear debris. It is difficult to correlate groove width, wear debris size and particle size, although intuitively one could expect those parameters to be related. The fact that their size distributions are all log-normal as Fig.7.5 shows, suggests that this is the case. In this work it could be assumed that there is a direct relationship between particle size, groove width and wear debris size such that the size of particle, groove width and debris particle can be equated to a given probability. This assumes that the complete particle size distribution takes part in the wear process although as discussed previously, the smaller particles may in fact contribute little to the material removal process.

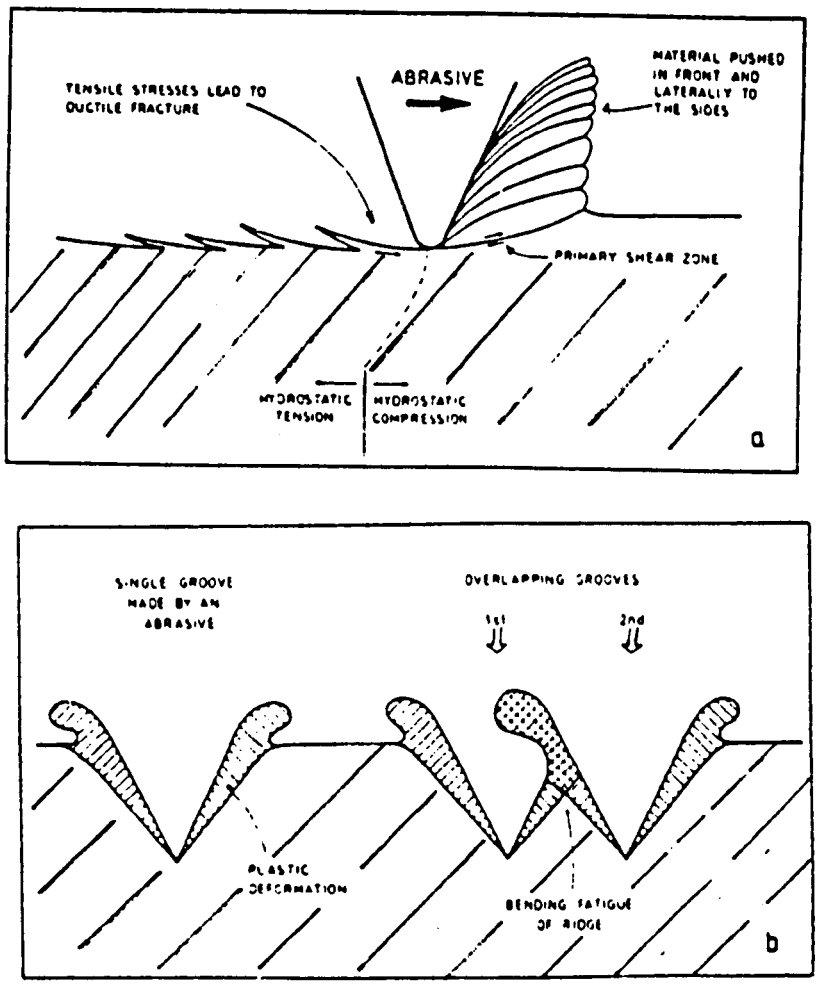

Fig.7.4: a) A predominantly ploughing mechanism is associated with a low material strength and the ductile fracture of the highly strained metal. b) Overlapping grooves result in fatigue of the plastically deformed material that make up the ridges. [155]

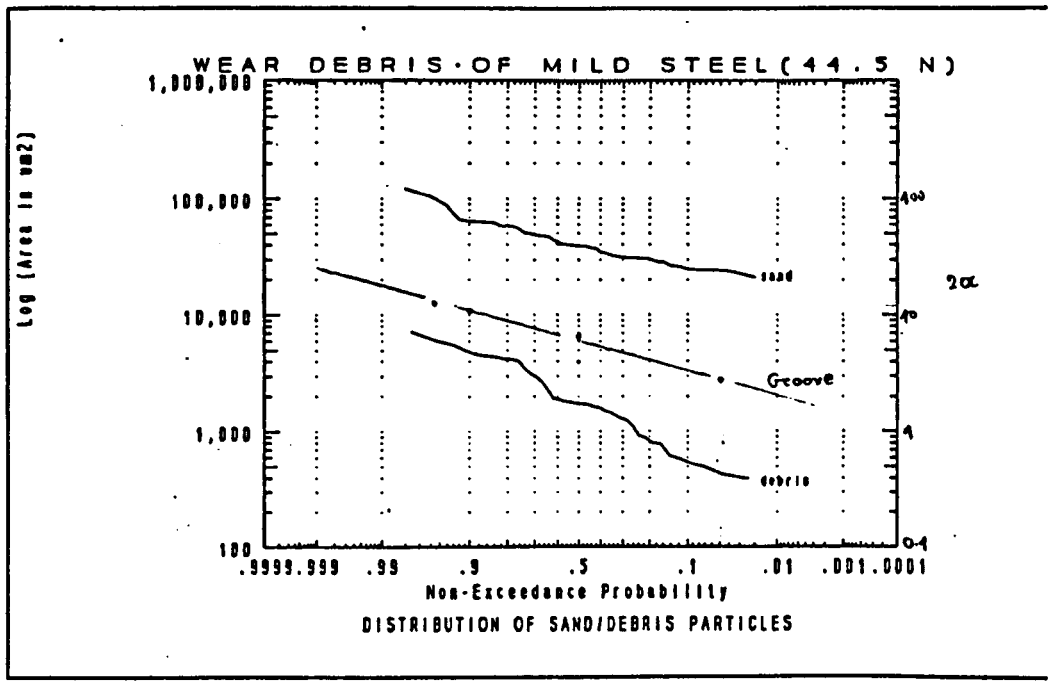

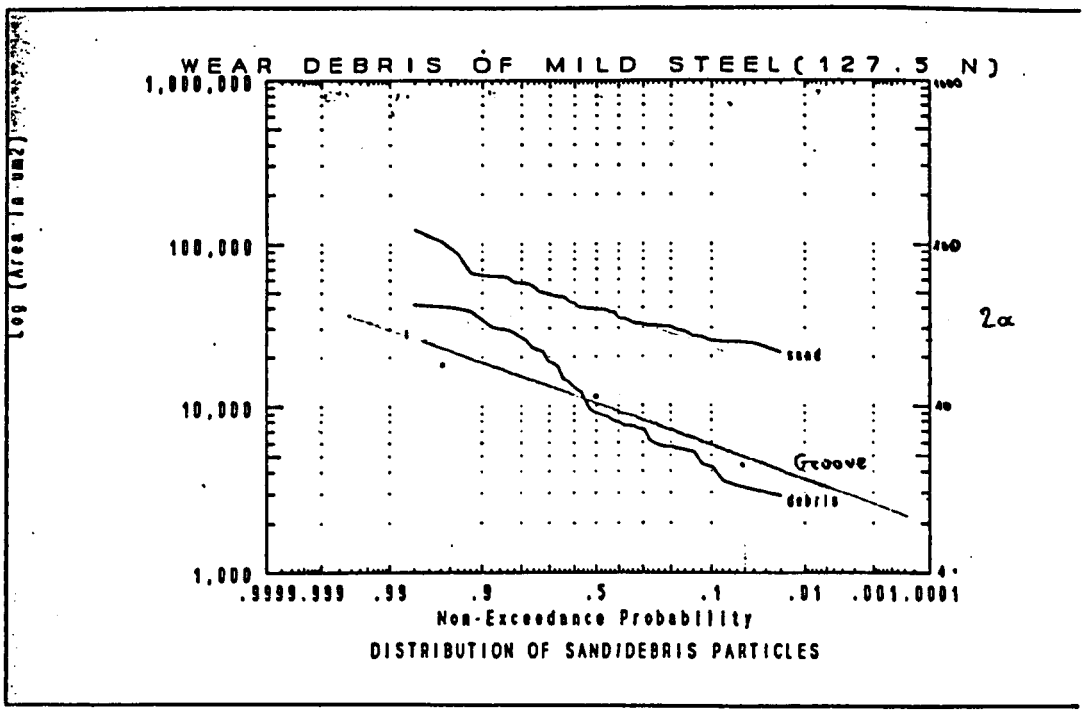

Fig.7.5 : Correlation between particle size distribution , wear debris size distribution and groove width(2a) for M.St- Rubber wheel. Nominal load 44.5N and 127.5N

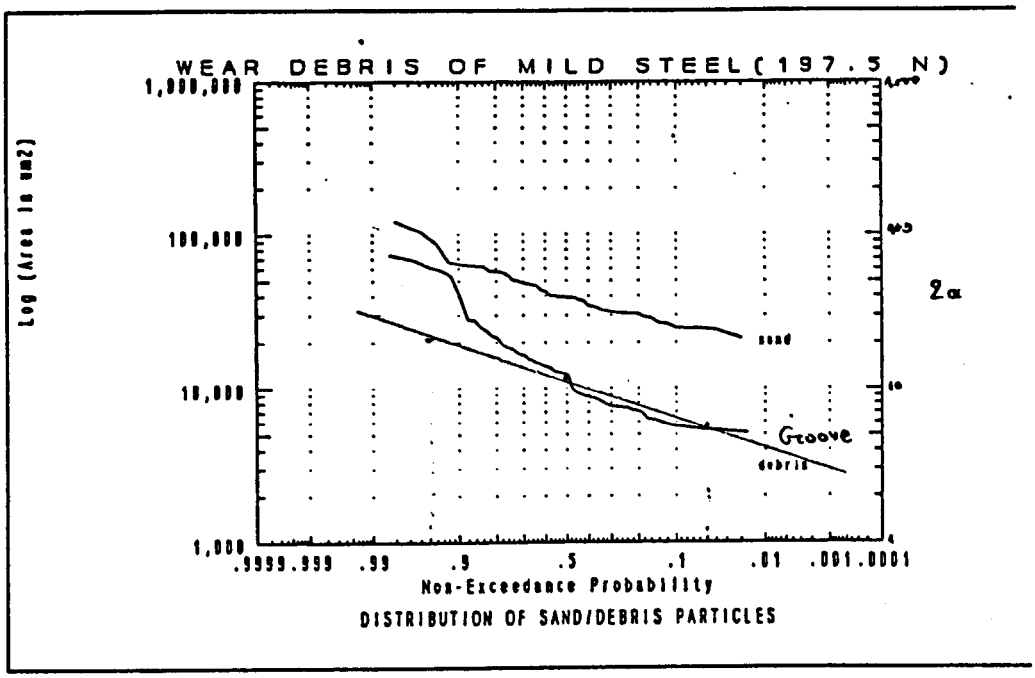

Fig.7.5 : continued for 197.5 N

Initially one may assume a delamination type of process as suggested by Suh et al. [156] According to this process, as the cyclic loading takes place on the surface, substrate cracks are generated parallel to the surface and when the crack reaches a critical length which depends on the material, the material between the crack and the surface will shear, yielding a sheet like particle. It is not possible to calculate wear rates using Suh's wear equation as it appears below because certain parameters are not known. It must also be said that Suh's model was developed for sliding wear and it will be assumed that the same approach can be used here.
According to Suh's model the wear rate is given by :

$$W=N\,(S/So)\,A\,h$$

where :

W:	volume wear
N:	No of wear sheets/layer
S:	total sliding distance
So:	critical sliding distance to remove a layer
A:	average area of a delaminated sheet
h:	thickness of a delaminated sheet(from experiments 0.5 - 2.5μm)

However, working back from the experimental wear rates one can calculate the number of particles needed to generate each piece of wear debris. Table 2 presents the results and shows that more than one particle is required to remove one piece of wear debris.

Another very simplistic approach to demonstrate the large number of particles required to generate one piece of wear debris is by taking an average size(50%) of wear debris from the probability plots, Fig.7.5 and also using the experimental wear rates to calculate the number of particles needed to generate one piece of wear debris.The results are presented in Table 2 and very clearly demonstrate that several particles are required to generate each wear debris particle.

M.St	Suh's wear equation	Average debris size
Load(N)	Abrasive particle/plate	Abrasive particle/piece of wear debris
44.5	12	50
127.5	3	15
197.5	3	15

Table 2: Calculated number of abrasive particles needed to generate one piece of wear debris using Suh's wear equation and an average debris size.

The results in Table 2 clearly indicate that a fatigue based mechanism should be appropriate to describe the wear process as suggested previously by Ludema[29] and Kragelskii.[157] They both take the view that plastic contact in asperity interactions is far less important than elastic contact and argue that, even if the initial contact is plastic, this soon changes to elastic contact with repeated loading, presumably because of strain hardening. For this reason, they explained wear in terms of cyclic stresses below the elastic limit and modelled in terms of high cycle fatigue(HCF). They also considered the case where the stresses are above the elastic limit and then a low-cycle fatigue(LCF) mechanism applies. This process is responsible for the fracture of the material displaced to the sides of the abrasive groove. Very little information appears in literature regarding LCF modelling. However, results from this work indicated that this approach could be appropriate and therefore could be followed in predicting the removal of the ploughed material.

7.4.2 Approach to modelling low stress abrasive wear using a low cycle fatigue model

In the context of the present work high stress abrasive wear relates to high h/a ratio and 'cutting' dominated wear mechanism, whilst low stress abrasive wear is consistent with localised plastic damage and 'ploughing'. As a consequence of ploughing, grooves are formed on the material surface with ridges of highly strained material in both sides of the grooves. The cyclic stresses imparted by a continuous supply of abrasive particles can therefore be considered in terms of a LCF process. The abrasive-metal interaction must be quantified and the loading conditions identified.

The particle size distribution as presented in Fig.6.2d, suggests that there is a wide range of particles from a few microns up to 500μm. Some of those particles are loaded and some others not, depending on the load applied, as Fig.7.6 shows.

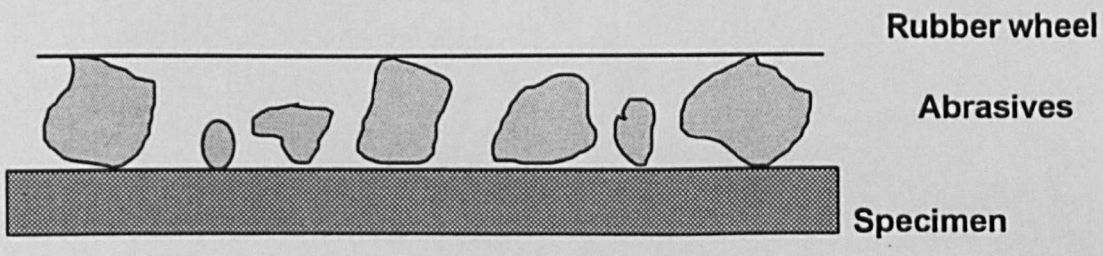

Fig.7.6: Possible loading of the abrasives during wear process

With the rubber wheel, which is compliant, a high proportion of particles is loaded which may be even higher under dynamic conditions. This proportion, as Fig.6.38 shows, was increasing with increased load. Also the fact that the particle size distribution did not vary after each test, for all loads, indicates that there is no break-up of the particles during the process.

The wear grooves as they appeared on the test specimens and scratch tests were measured and their width (2a) was plotted on probability paper. An example for M.St(197.5 N) is given in Fig.7.5 along with tabulated values of 2a for all the four materials in Appendix C.

Fig.7.7 is a plot of groove width(2a) against load(N) for an average particle size(2R) of about 200μm. There is a relation between size of indentation and load for spherical indenters which is expressed by Meyer's law: [158]

$$W = K (2a)^{n}$$

where K and n are constants for the material under examination.

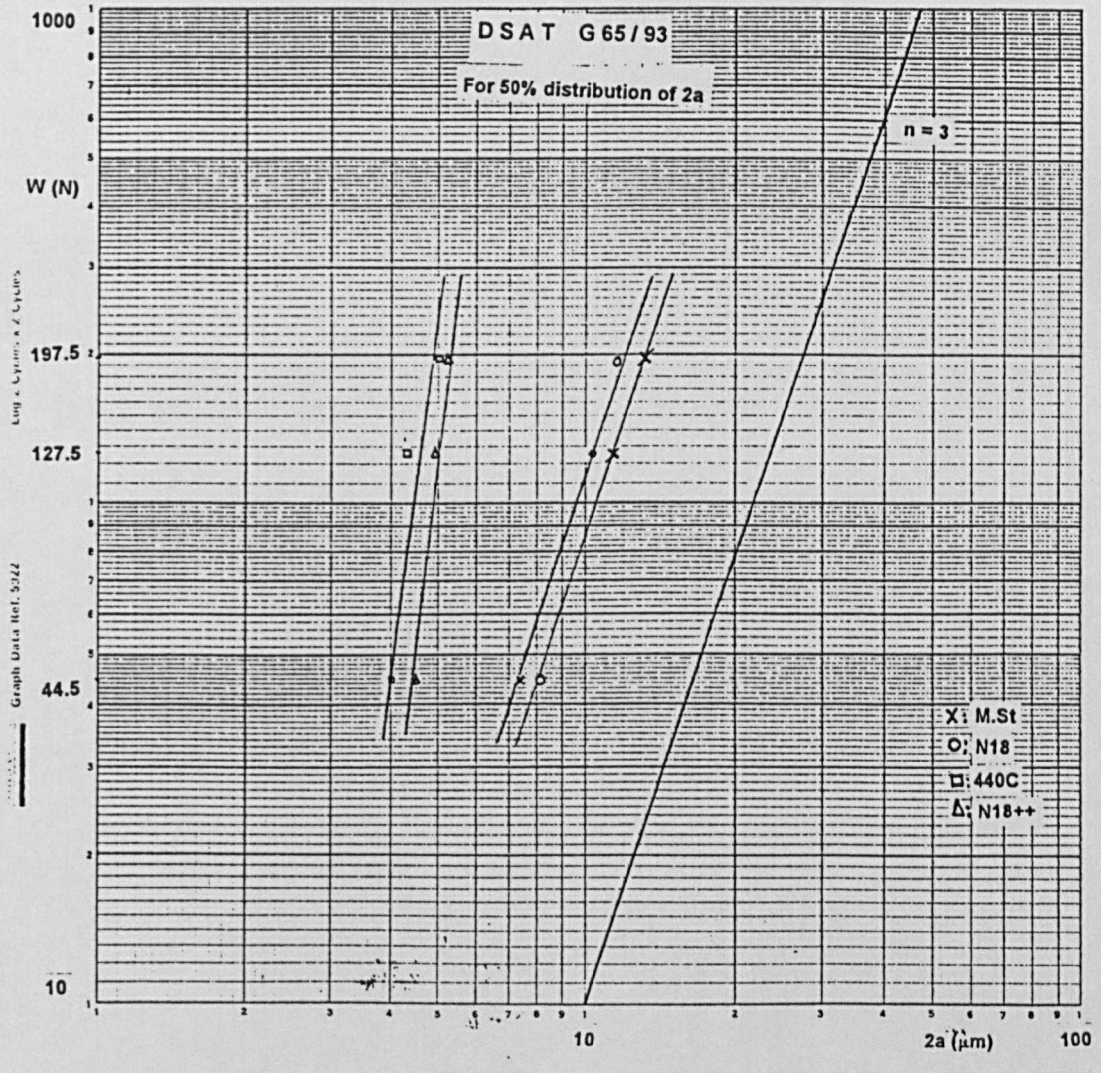

Fig.7.7 : Dry sand abrasive wear tests. Plot of groove width (2a) vs load(N).

When the values for load(N) and 2a are plotted on logarithmic ordinates, a linear relationship was observed and the slope expresses Meyer's index n. The values of the index n are between 2 and 2.5 for work-hardened and annealed metals respectively. [158]However, for small loads which give small indentations, the value of n increases towards about 3, which is the case in this work.

Fig.7.8 is a plot of groove width(2a) against hardness(Hv). Hardness is a very important parameter in determining the size of indentation. This figure shows that the materials form two distinct groups according to their hardness, and although they have the same slope, it suggests that the relative hardness between abrasive and material surface is very important. There is a transition for the abrasive, at about 400-550Hv where materials with relative hardness less than this value(M.St, N18) showed higher groove size whilst materials with relative hardness more than this value(440C, N18++) showed smaller groove size. This is consistent with all the published data which considers the relative hardness of the abrasive and the metal and suggests that good abrasion resistance is observed when the metal is at least 0.8 times the hardness of the abrasive.

This graph could be useful in predicting values of 2a for a given material hardness and indicates that simple indentation tests can be used to predict approximate values of 2a using the relation:

$$Hv = P/\pi a^2$$

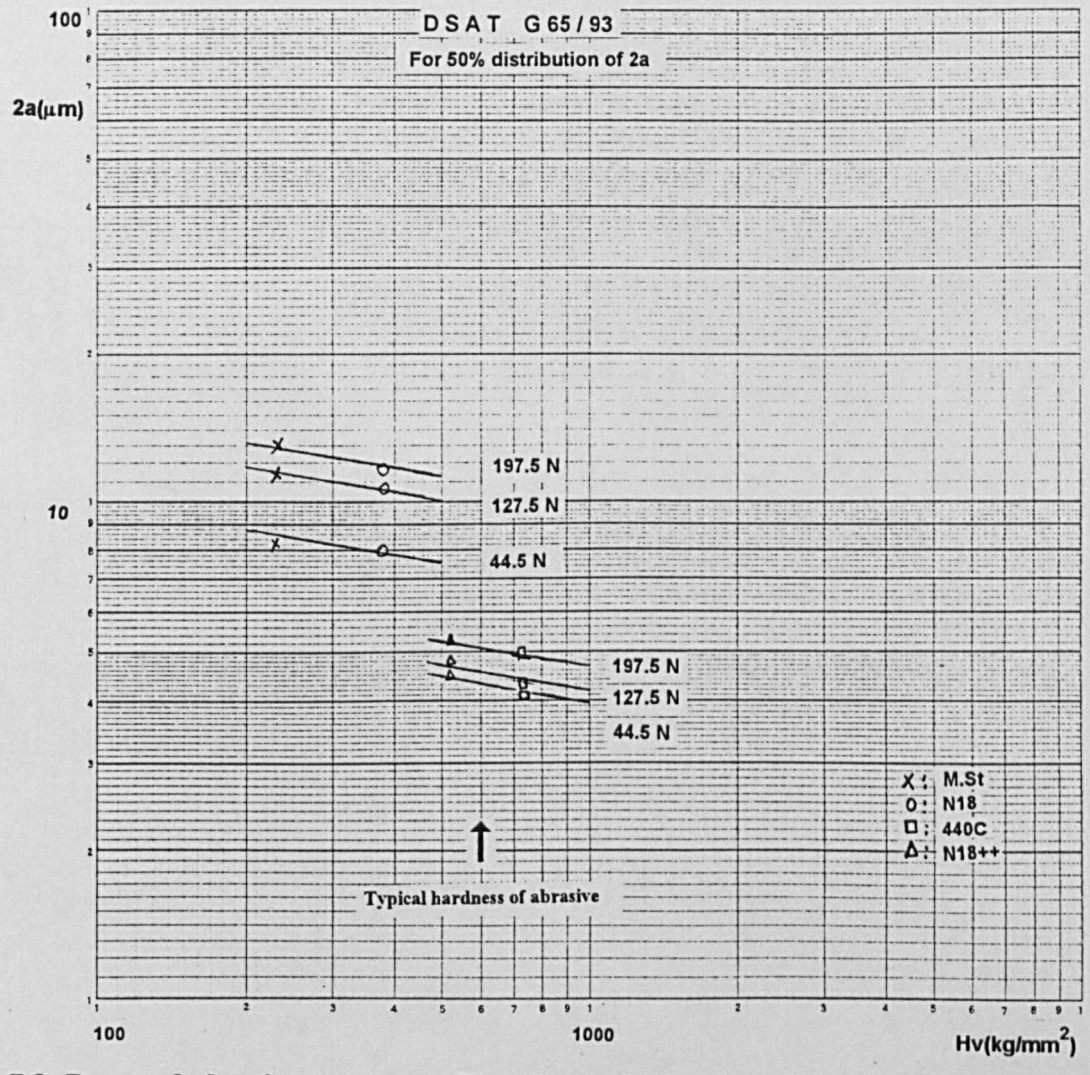

Fig.7.8 :Dry sand abrasive wear tests. Plot of material hardness(Hv) for different loads vs groove width(2a).

Using low-cycle fatigue theory, that is relatively high stresses and low number of cycles($<10^4$) to failure, the number of strain reversals to failure can be obtained as a consequence of the Coffin-Manson relation: [159]

$$\Delta\epsilon_p = \epsilon_f (2N)^c$$

where:
- $\Delta\epsilon_p$ = plastic strain amplitude
- ϵ_f = fatigue ductility coefficient [160]
- 2N = number of strain reversals to failure
- c = fatigue ductility exponent

The fatigue ductility exponent 'c' is calculated from the work hardening exponent 'n' according to the equation : $c = -1/(1+5n)$ [161]

Table 3 gives the values for ϵ_f and n which were used in the model to calculate metal recession of the materials under investigation. The values for N18++ were obtained from tensile tests undertaken as part of a parallel research programme.

	M.St	N18	N18++	440C
ϵ_f	0.2	0.17	0.07	0.07
n	0.3	0.26	0.26	0.26

Table 3 : Typical values for ϵ_f and n for the materials under investigation.

The plastic strain ϵ_p is determined from Tabor's approximation : [158]

$$\epsilon_p = 0.2\ a/R$$

where: 2a=groove width, R= radius of the abrasive particle

The particle size distribution will be important because this will determine the number of particles which will be loaded. A realistic model must then take account of the particle size distribution effect. The important stages in developing the model were:

- first requirement will be the number of particles loaded between contacting wheel and specimen surface.
- it was assumed that only spherical particles abrade the surface and the material removed is often related to the volume included within a spherical segment. The geometrical relations of this segment are summarised in Fig. 7.9. [162]
- it was assumed that there is no friction between the face of the indentor(particles) and the specimen and the pressure is uniform across the indent and has a value of about 3Y i.e the hardness.

From the probability distributions in Fig.7.5, it can be assumed that there is a correlation between R and -a- and for a given -a- the depth 'h' of the wear groove can be calculated using equation $h=(2a)^2/8R$ given in Fig.7.9. The values of h calculated were consistent with experiments and scratch tests. Then the ratio Dp=h/a (Dp: depth of penatration) was calculated and is further indication of the wear mechanism. Typical values for Dp (0.006-0.03) clearly show that a ploughing mechanism of material removal exist.

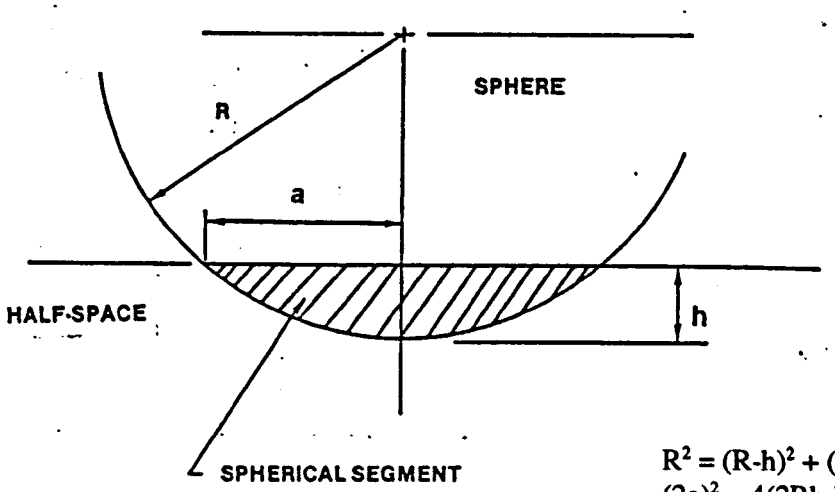

$R^2 = (R-h)^2 + (a)^2$
$(2a)^2 = 4(2Rh-h^2)$
which approximates to
$h = (2a)^2/8R$

Fig.7.9 : Geometrical relations for a rigid sphere indenting a compressible half-space.

The contribution to the wear process of each particle within a given particle size fraction is determined with the failure criterion defined by the Coffin-Manson LCF equation. 2N is the number of strain reversals i.e 2N is the number of abrasive particles required to generate 1 piece of wear debris. The thickness of each platelet(h') was estimated from Tabor's approximation as : $h' = 0.5a$. [158] At this depth below the surface the maximum shear stress occurs and as a rough assumption the onset of cracks will most probably occur there.

Finally, it was assumed that the contribution to the wear process from each particle size range is additive, which provides an estimate of the metal recession from the entire particle size distribution. An example of a complete calculation for the reference material M.St appears in Appendix C.

Table 4 presents tabulated results for all the materials under investigation, and Fig.7.10 shows a comparison of the theoretical and experimental results. The two dashed lines represent the scatter expected if the wear rate varied by a factor of 2. The model predicts the experimental results to better than a factor of 2 for the range of materials exhibiting different hardnesses from 200 to 800Hv and for loads varying from 44.5 to 197.5N.

Materials	Measured metal loss (μm)	Predicted metal loss (μm)	Nom.Load(N)
Mild Steel	220	120	44.5
	500	513	127.5
	840	968	197.5
440 C	130	106	44.5
	190	173	127.5
	240	308	197.5
N 18	280	288	44.5
	740	681	127.5
	890	904	197.5
N 18++	170	167	44.5
	250	250	127.5
	310	302	197.5

Table 4: Tabulated results for the measured and predicted values of metal recession rates(Rubber wheel).

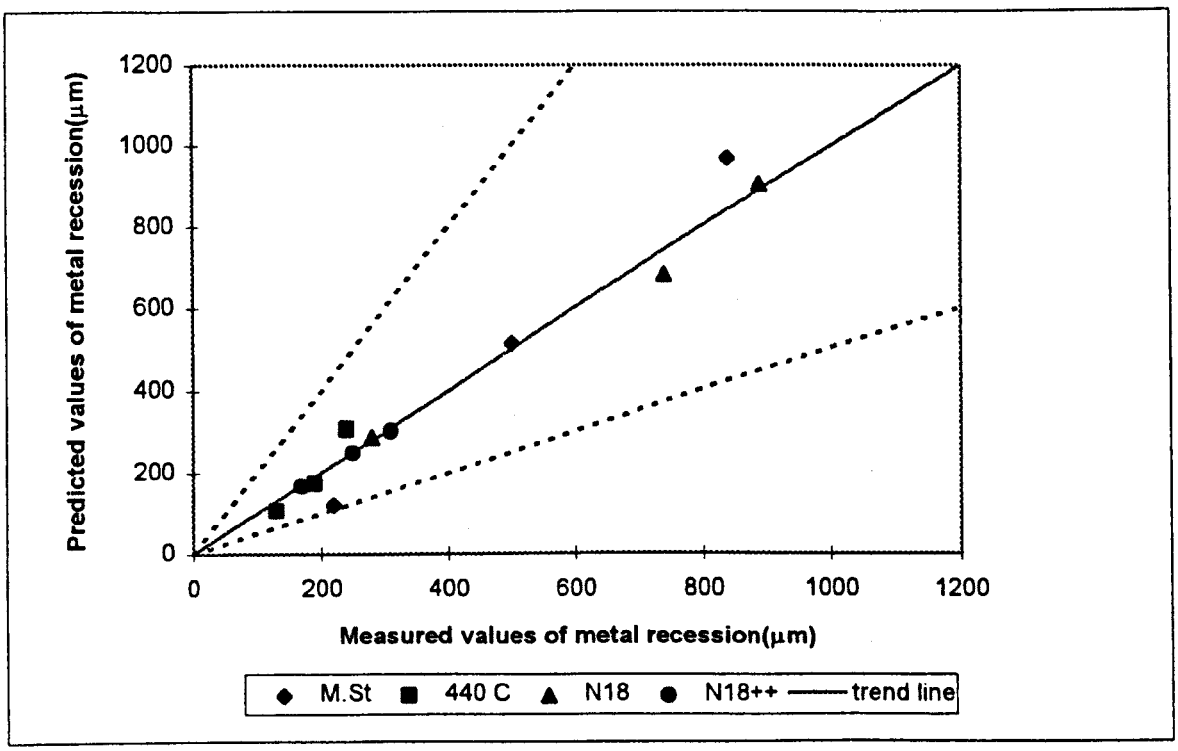

Fig.7.10 : Comparison of predicted and measured results for metal recession(Rubber wheel).

7.4.3 Modelling of 440C wheel abrasive wear tests

A similar procedure was followed for the modelling of the abrasive process when a 440C wheel was used and the same assumpions were made. These tests were carried out with loads of 60N and 240N. Tabulated values for the groove width(2a) for all the four materials are shown in Appendix C.

In contrast with the rubber wheel, the 440C wheel is less compliant. This had an effect on the number of particles which are loaded and the groove width(2a). The particle size distribution after the tests, Fig.6.22, showed that there is considerable break-up of the larger particles for the soft materials(M.St, N18) and even more break-up for the harder ones(440C, N18++). The distribution shifted to smaller particles and some of the larger particles disappeared. For the calculations of wear recession rates both sand particle distributions, before and after tests, were used as they should represent extreme conditions.

Table 5 presents the results using particle size distribution before tests. However, similar results were obtained for all the materials when the particle size distribution after tests was used. An example for M.St is also presented in this table.

Fig.7.11 shows a scatter diagram comparing the measured and predicted values of metal recession. The fit of the results on the graph is reasonable, although there is more scatter compared with the results of the rubber wheel tests. This scatter is more noticeable with M.St and N18. Even so, the results predict wear rate to better than a factor of 2.

Materials	Measured metal loss(μm)	Predicted metal loss(μm)	Nom.load(N)
Mild Steel	630	246 || 241(after)	60
	1190	2138 || 2096(after)	240
440 C	500	261	60
	800	645	240
N18	700	930	60
	1100	3107	240
N18++	550	420	60
	630	664	240

Table 5 : Tabulated results for the measured and predicted values of metal recession(440C wheel) using the sand distribution before the tests. For M.St there are also predicted values using the sand distribution after the tests.

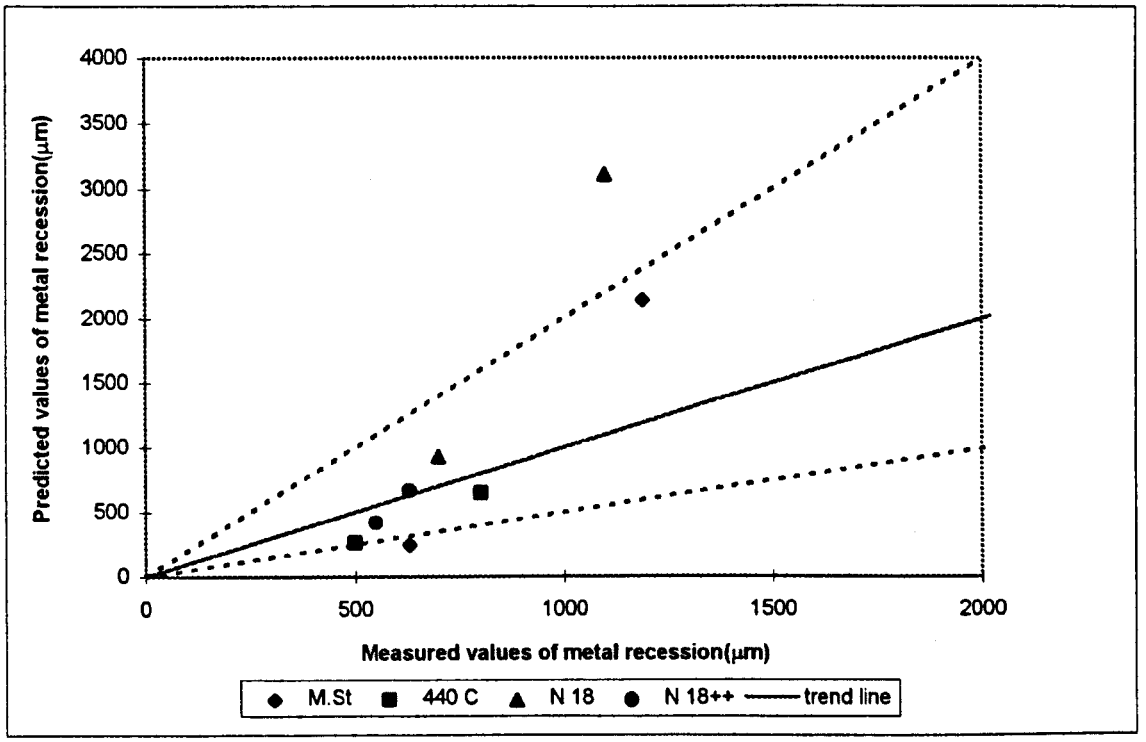

Fig.7.11 : Comparison of measured and predicted values for metal recession (440C wheel)- Particle size distribution before and after wear tests was used.

7.5 Influence of the environment

In many practical situations it is well recognised that corrosion can add to metal loss in the friction and wear of metals. However, by simply adding normal corrosion loss to mechanical wear loss does not necessarily add up to the total wear when the wear occurs under corrosive conditions. The total wear loss may be a great deal higher or lower than the sum of corrosive and mechanical wear. This can be due to two factors:[128]

- the mechanical and corrosive interactions are very sensitive to surfaces. The creation and removal of surface films determines which component prevails.
- the difference in the chemical state of the metal in the wear area from the surrounding area. The chemical difference sets up conditions for a galvanic corrosion cell between the worn area and the surrounding metal surface.

In terms of corrosion resistance, the alloys showed different behaviour depending on their composition and the solution. It was observed for the ferrous alloys(M.St, 440C) that immediately after sample immersion in the acid solution(3vol% H_2SO_4) a strong reaction, characterised by gas bubble formation(H_2), occurred, the gas evolution rate increasing with sulphuric acid concentration(results not presented for 30vol% H_2SO_4). The same alloys when tested at room temperature and in the same environment, showed different behaviour. The M.St corroded at a slower rate while 440C remained passive.

Following the above remarks some points of interest can be raised: a) the behaviour of M.St and 440C is related to the fact that the rate-determining step in the corrosion mechanism varies with sulphuric acid concentration and temperature.[163] b) At low acid concentration($\leq$5%) the corrosion potential is situated in the active region and the corrosion rate is controlled by the charge transfer at the metal-electrolyte interface. Increasing the acid concentration first increases the corrosion rate, but the formation of surface films leads to a change in the rate-determining step and a decrease in corrosion rate.[163]

The composition of the materials also seems to play a significant role. The absence of significant amounts of free chromium in M.St and 440C (in which chromium is mostly present in the form of carbides), results in corrosion rates which are orders of magnitude higher as experimental results with alloys with different Cr content show.[164]

XPS results(Appendix B), showed that Fe_2O_3 is formed on the surface of all specimens. Ferric oxide is abrasive. However, this film is extremely thin and easily removed by the abrasive action of the sand. Furthermore, there is no evidence of the existence of oxide debris and the wear debris in all cases was found to be metallic (Appendix B).

7.5.1 New approach for modelling of wear/corrosion process

A new approach was used to model the wear/corrosion process according to the way different materials behave during corrosion.

Figs.7.12 and 7.13 are plots of metal recession of M.St and 440C respectively against mass of abrasive sand taking part in the process. It shows predicted wear rates assuming a 440C wheel, experimental corrosion results, and the arithmetic addition of the above two compared with wear/corrosion results from the experiments. Because the experiments in the different environments were carried out with different amount of sand and for different duration, for comparison purposes they were normalised for both sand and time taking as a basis the wear/corrosion experiments.

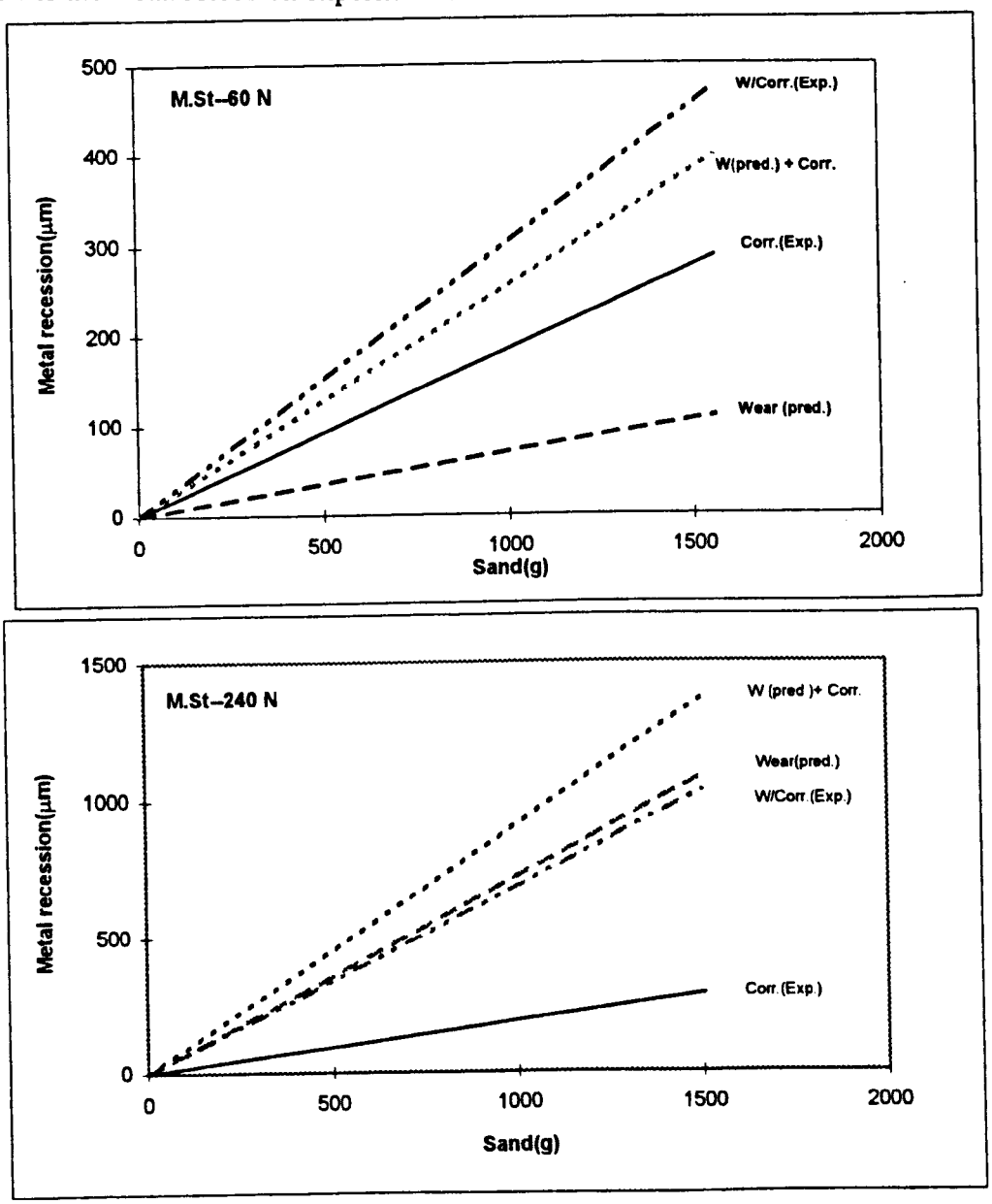

Fig.7.12 :Comparison of theoretical and experimental results for M.St, tested in different environments.

—— (corrosion results-experiments), ..- ..-(wear/corrosion results-experiments)

— — — (wear predicted), ...(arithmetic addition of wear(predicted+corrosion)

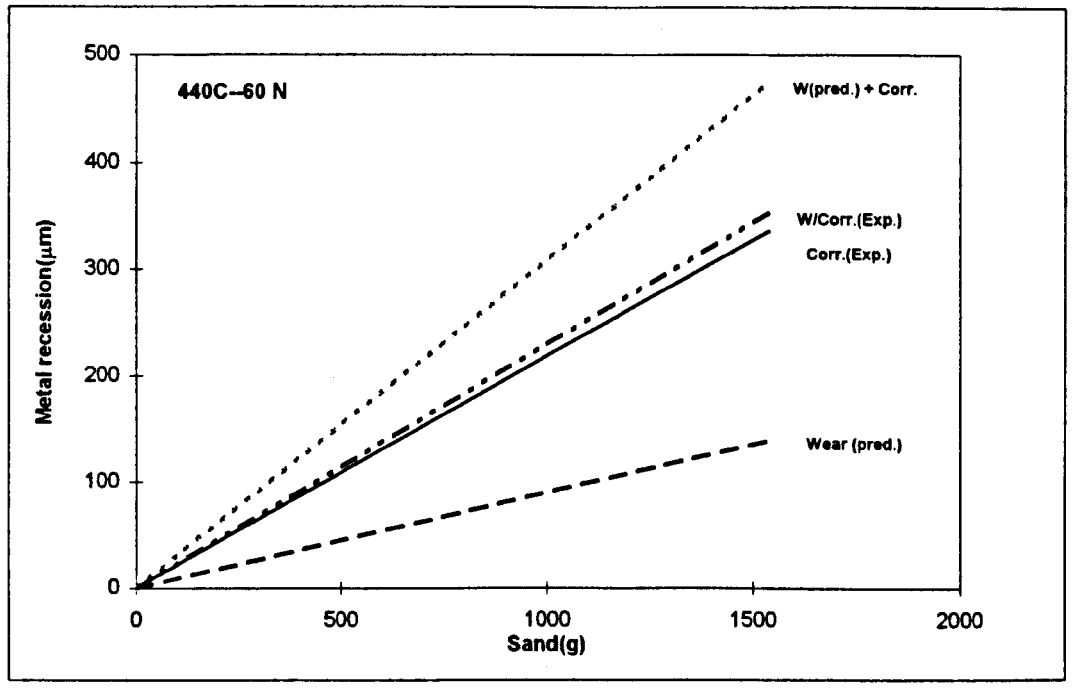

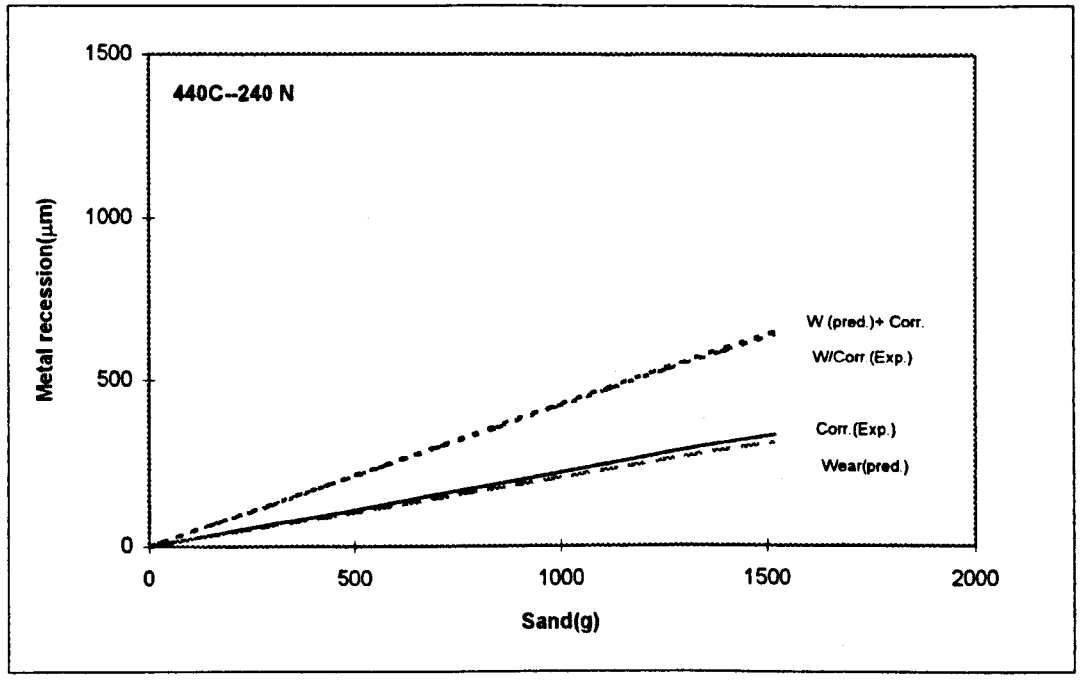

Fig.7.13 :Comparison of theoretical and experimental results for 440C, tested in different environments.

—— (corrosion results-experiments), ..- ..-(wear/corrosion results-experiments)

— — — (wear predicted), ...(arithmetic addition of wear(predicted+corrosion)

As can be seen for both ferrous materials(M.St and 440C) the arithmetic addition of wear/corrosion component does not add up to the experimental results, which is in agreement with data published, [128] although they are not far away. The difference in the results can be attributed to:

- chemical difference of the worn area and the surroundings- creation of a galvanic cell.
- formation of a very thin abrasive oxide(Fe_2O_3) which was detected by Auger, but there was little evidence of its existence in wear debris.
- moisture assisted fracture. Water assists the transition from ductile to brittle mode through surface charge and adsorption of various species.[165]

Moreover, at higher load(240N) it can be added that:

- large surface area exposed to corrosion(larger 2a)
- local temperature- probably higher than 90°C.

The behaviour of Ni-based alloys(N18 and N18++) was completely different. When tested at room temperature or in H_2O at 90±5°C they showed no corrosion at all. This is in agreement with data published which show that Ni possesses a high degree of resistance to corrosion by natural or distilled water and sulphuric acid at room temperature.[164] However, even at temperatures higher than ambient and for acid concentrations below 10%, the corrosion rate was very low. A combination of linear and parabolic oxidation is frequently encountered. Reaction may be interface-controlled(linear) during initial stages and diffusion limited(parabolic) after some time.[166]
The overall corrosion of the nickel is low without wear due to the creation of a passivating film which is removed very easily from inside the wear track.

The mechanism of passivation of nickel and the properties of the passive nickel have been studied extensively.[167,168] However, there is by no means agreement either on the mechanism of passivation of nickel or on the composition and thickness of the passive layer. The most prevailing view nowadays is that the passivity of nickel is due to the formation of a protective film of oxide or hydrated oxide, a few nanometers thick, although others[167] consider passivity to be due to a chemisorbed layer of O_2. Ellipsometric measurements in acidic solutions support the existence of surface oxide films on passive nickel several nanometers thick.[168]
Qualitative evidence for the presence of a compact solid film(not necessarily oxide) on passivated metal surface shows that such thin films reach a thickness of 3nm in dry air and the approximate thickness range of 1-10nm in the presence of aqueous phases.[169] This aqueous phase determines the initial interaction as the system passes from the active to the passive state. It has been postulated that an initial chemisorbed state on Ni, Cr, Fe exists which has features in common with metal/gaseous oxygen interaction.[170] With increase in anodic potential a distinct 'phase' oxide or other film substance emerges at a thickness of 1-4nm.

It is well established in the literature that there is an instantaneous formation of film on the surface of the passivating metals.[171,172] This film is usually very thin and not easy to measure. Abrasion will remove any passive film and expose newly deformed material to the

environment. The growth of new passive films occurs almost instantaniously but because of the high number of abrasive particles taking part in the process, the time between successive particles which remove this film is at the same order of magnitude. An abraded surface is in a higher state of disorder, which could change the kinetics of the surface reactions.

Fig.7.14 is a representation of the volume of material loss as a function of time. When there is no abrasion the curve (I) occurs, which represents the formation of a protective surface scale(parabolic kinetics) whilst abrasion+corrosion is covered by type(II) (paralinear kinetics). The corrosion is accelerated through oxide formation and removal, and the process involves direct metal removal through wear plus the formation and removal of a surface film.
An attempt will be made to model the process in terms of formation and removal of a 3-10nm thickness film.

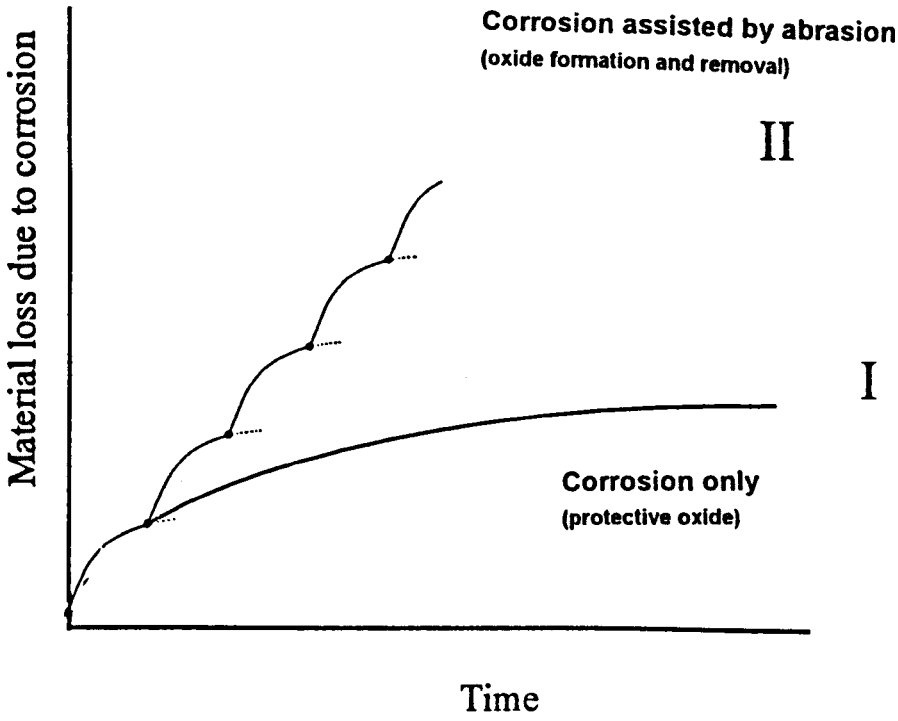

Fig.7.14: Schematic representation of the effect on metal recession rates I) only corrosion and b) abrasion+corrosion.

Figs.7.15 and 7.16 are plots of metal recession for N18 and N18++ respectively, against mass of abrasive sand taking part in the process. It shows predicted wear rates assuming a 440C wheel, experimental wear/corrosion results, wear assisted corrosion assuming a 3nm film and a 10nm film and the arithmetic addition of the latter plus the predicted wear rates. The corrosion of the Ni-based alloys is extremely low and difficult to resolve on the graph. All the results have been normalised with respect to the quantity of sand used in the wear/corrosion tests.

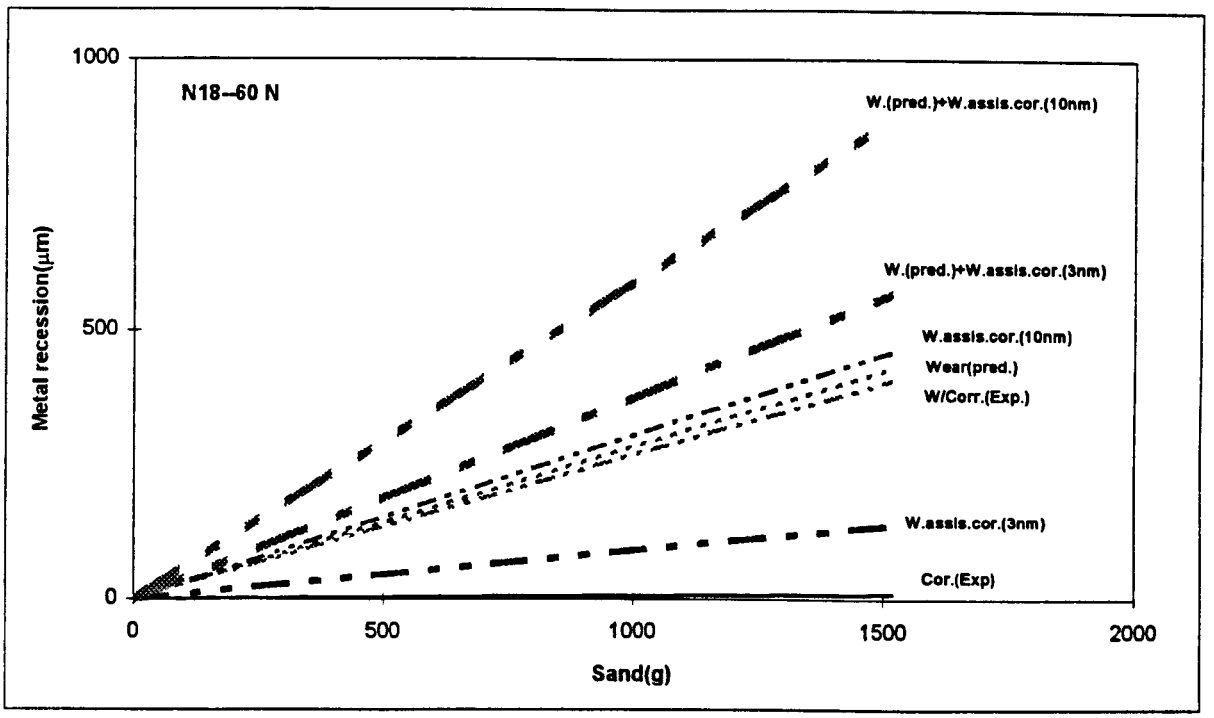

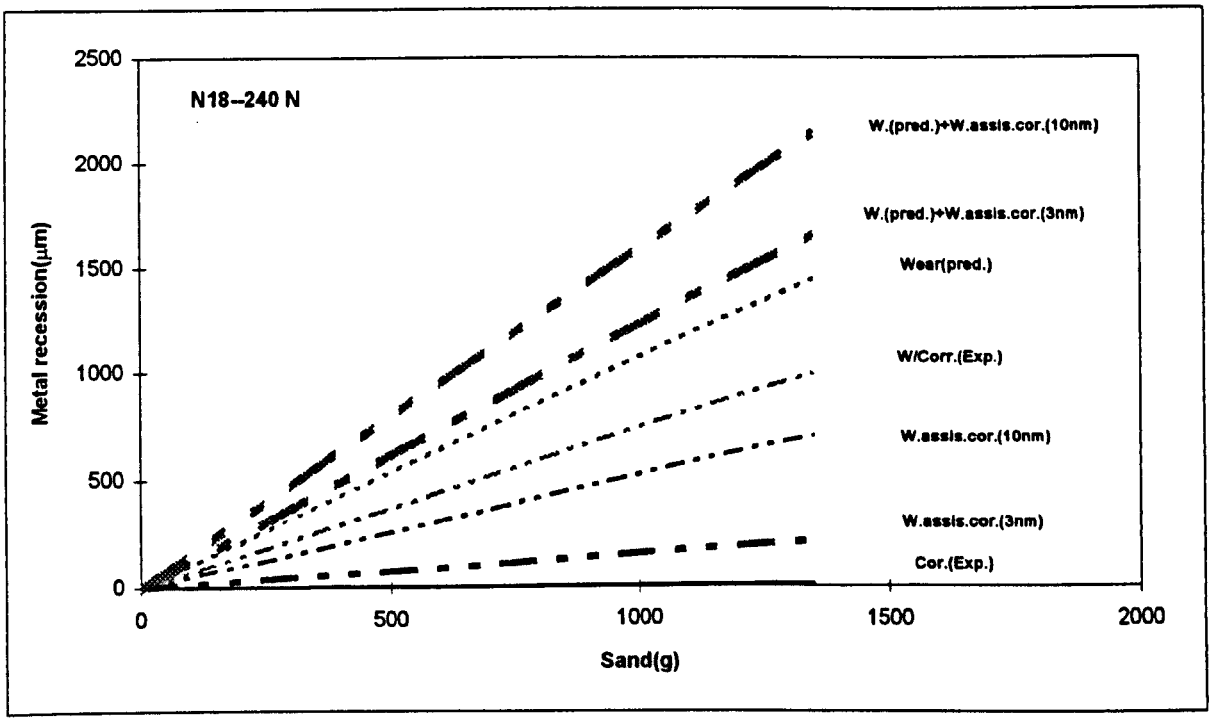

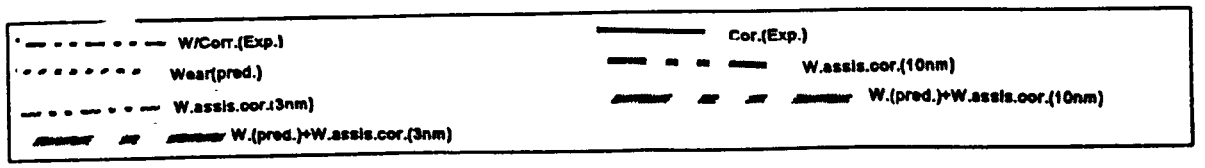

Fig.7.15 :Comparison of theoretical and experimental results for N18 tested in different environments.

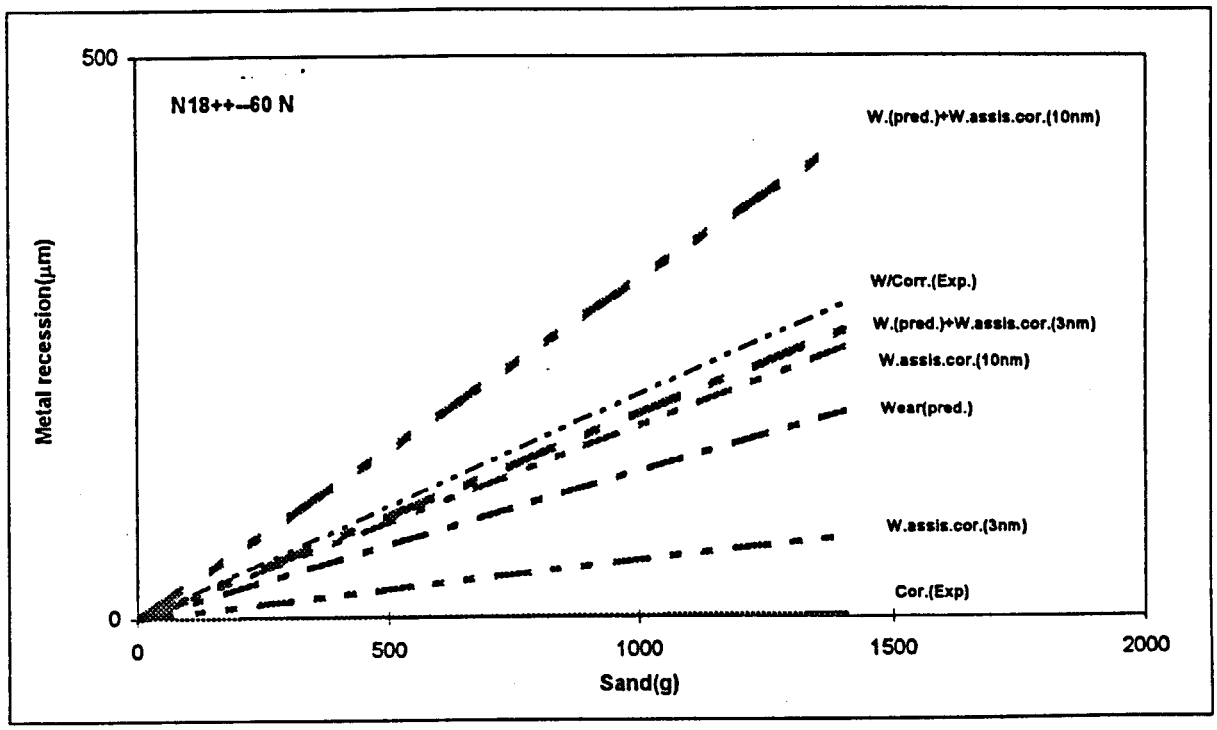

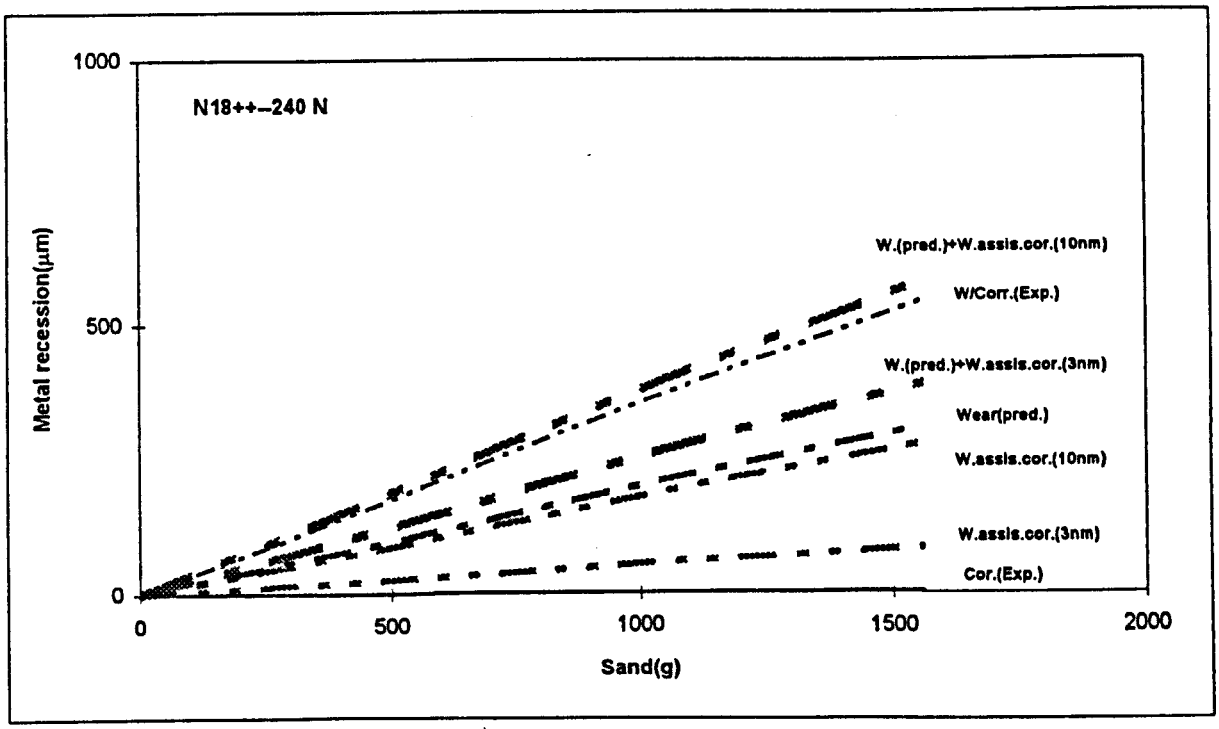

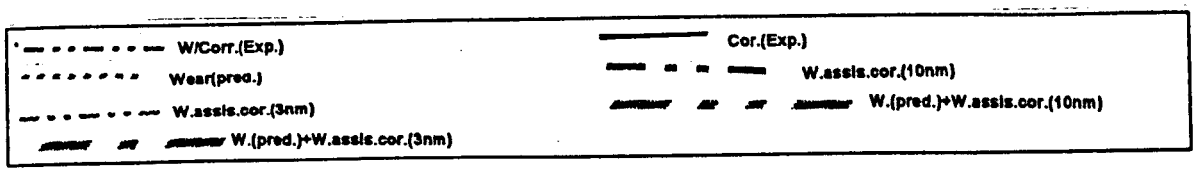

Fig.7.16 :Comparison of theoretical and experimental results for N18++ tested in different environments.

Table 6 presents the results(assuming a 5nm thick film) and Fig.7.17 is a scatter diagram showing the predicted values of metal recession against the experimental. The same values of groove size distribution(2a), as without corrosion-shown in Appendix C for the 440C wheel, were used although they were less clear on the specimens. The surface appeared very different when there was corrosion and very large grooves were formed, which is thought to be due to preferential channelling although on a microscale one can see individual particle grooves around the base of the large grooves. When localised grooves start to form it is likely that they will grow preferentially since the corrosion fluid will follow the route of least resistance and take the abrasive with it.
A similar process is observed in real systems e.g exhaust valve gutters. Hence the surface morphologies consist of large channels within which the abrasion/corrosion process occurs. Fig.6.26c illustrates the individual particle grooves within the base of the large channels shown in Fig.6.26a.

The predicted values of metal recession include wear + corrosion components. An average of 5nm film was used and the error bars used for the N18 and N18++ assume extreme cases of film thickness 3-10nm.

Materials	Measured mass loss(μm)	Predicted mass loss (μm)	Nom.load(N)
Mild Steel	473	398	60
	1027	1368	240
440 C	353	475	60
	640	648	240
N18	406	663	60
	914	1798	240
N18++	280	306	60
	547	447	240

Table 6 : Tabulated results for the measured and predicted values of metal recession-wear/corrosion(440C wheel).

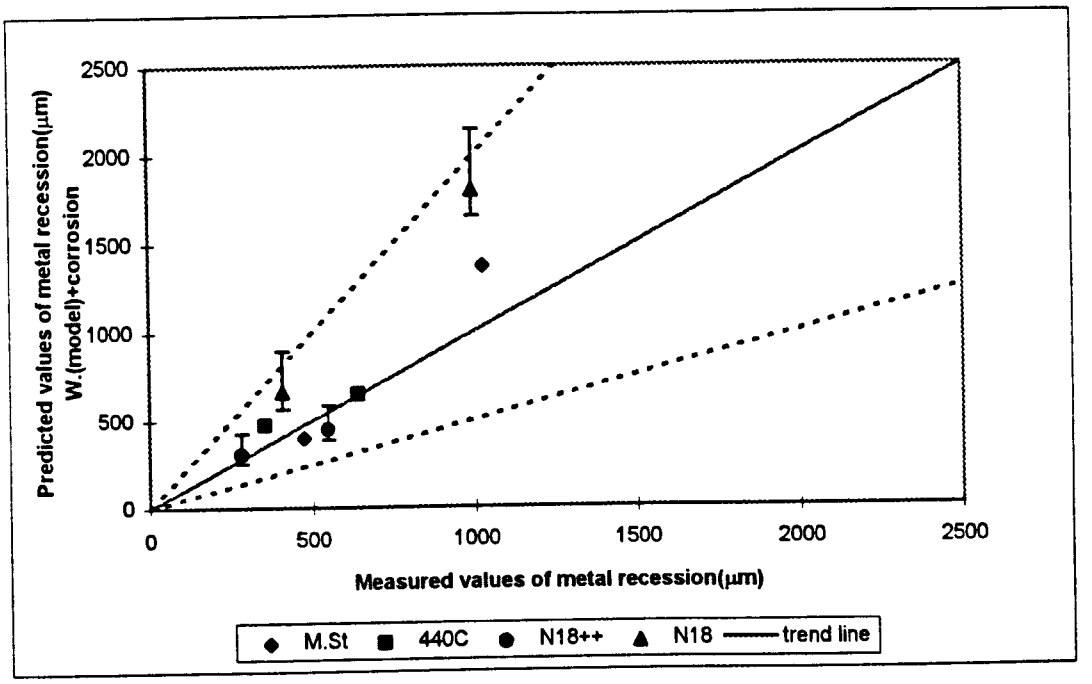

Fig.7.17 :Comparison of predicted and measured results for metal recession-wear/corrosion(440C wheel).

The fit of the results on the graph is good and although there is some scatter, more noticeable with N18, the model predicts wear rates to better than a factor of 2. The scatter of the results for the N18 alloy can be attributed to:

- the fact that the exact film thickness is not known nor the surface temperature which effects reaction rates.
- corrosion rates may be different for highly stressed material.
- preferential channelling of abrasive flow is modified by the presence of the liquid phase.
- as replicas of the wheel surface show, there is corrosion of the 440C wheel as well. The matrix is removed easier and the remaining carbides may act as in 2-body abrasion.
- considering all the above points and looking at the trends the softer materials M.St and N18 show, they tend to deviate from the line despite the higher load(197.5N) applied, and as higher rates are predicted than measured that points to the fact that preferential channelling, as mentioned before might play a very significant role.

7.5.2 Limitations of the modelling

The model presented here is a first attempt at the modelling of wear in a three-body situation. It is only realistic under certain conditions; the limitations are given in this section.

- it is assumed that material is removed by a ploughing type of mechanism which can be modelled by a low-cycle fatigue process.
- the model considers only spherical rigid particles which cause wear by sliding on a rigid-plastic surface. The wear debris generated which may act as abrasive and the

wear of the wheel are not considered.
- metal recession rates could be analysed statistically if a large number of section loss measurements were made.
- the model considers that all the particles contribute in the wear process although as the indentation tests showed, the very small particles may not take part in the wear process at all. However, the model does predict a very small contribution from the small particles in metal recession.
- the embedment of particles on the wheel surface is not considered. This is particularly relevant when the rubber wheel tests are considered.

7.5.3 General application of the modelling approach

The model which has been presented above accounts for and predicts the contribution of different variables to the wear process, for example;

- load. The effect of the applied load on metal recession rates by considering particle-surface interaction and groove size.

- metal properties. Hardness of material -i.e resistance to plastic deformation and hence groove size. N18 was expected to perform much better than M.St but it did not, because apart from the hardness there are other properties which should be taken into account e.g ductility and the model takes that into consideration.

- particle size distribution. The effect of different distributions on metal recession rates can be predicted.

- the influence of aqueous corrosion processes. Two alternatives were considered: a) direct dissolution of material with additive results and b) protective film formation which results in formation and removal of this film.

Modelling application allows one to look not only at external parameters such as load, particle size distribution, flux of particles but also the benefit of taking into account mechanical and physical properties like hardness and ductility. This allows the model to be used to explain the influence of external properties and helps in material selection and designing material with optimum properties.

Particle size effect on the mass of material removal is considered in depth in the literature as outlined in section 2.4.1.3. Fig.7.18 is a plot of particle size against metal recession of M.St for three different loads normalised for the same mass of abrasives. All the three curves as they appear on the graph look very similar to the initial particle size distribution. They show a bimodal distribution with peaks at about 120μm and 280μm. It seems that for metal recession what matters most is not only the individual particle sizes but the number of particles in each particle size.
Fig.7.18 also shows that for very small particle sizes the wear rates are small and there is a transition at about 100μm where the wear rates increase and then vary with particle size according to the precise particle size distribution.

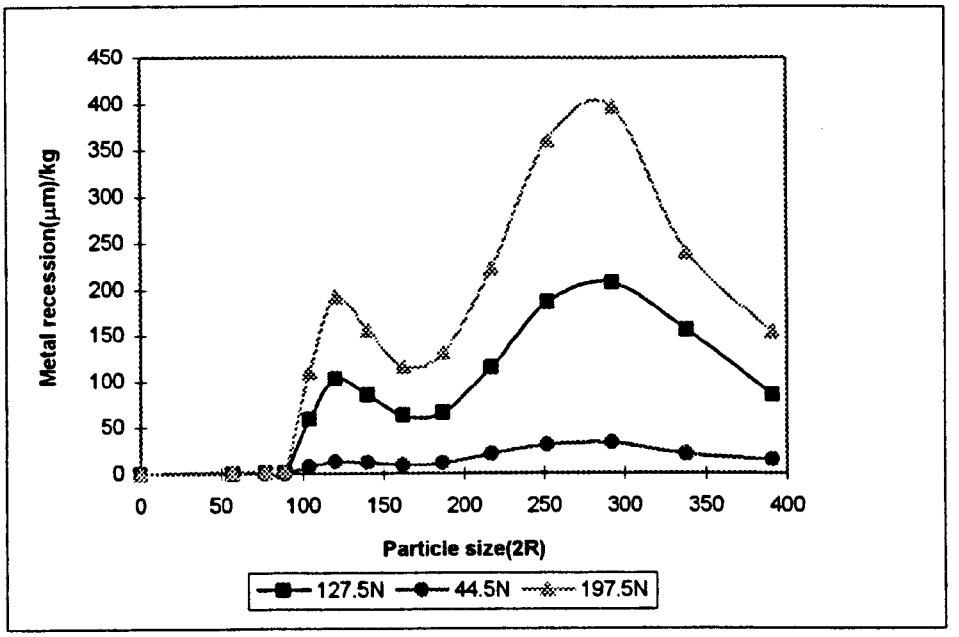

Fig.7.18: Particle size effect on material removal rates. Plot of particle size vs metal recession(M.St), normalised for 1 kg of abrasives.

Fig.7.19a is a plot of a log-normal particle size distribution. The predicted variation in metal recession with particle size when the distribution is divided-up into different particle size intervals such that each interval has a different mean and different width is shown in Fig.7.19b. The predicted contribution of each interval changes according to the width of each particular interval, although the differences are relatively small and the general trend suggests that metal recession increases as particle size increases.
The overall predicted metal loss is independent of the intervals because the same overall particle size distribution, having the same standard deviation, is considered. For this particular distribution the predicted metal loss was found to be 196±3μm.

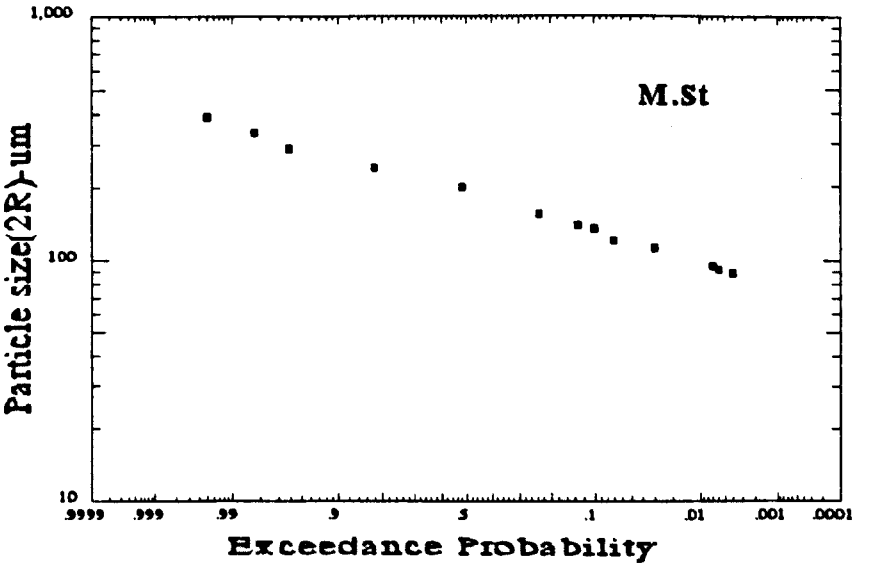

Fig.7.19: a) Log-normal plot of the particle size distribution shown in Fig.7.18 for 197.5N

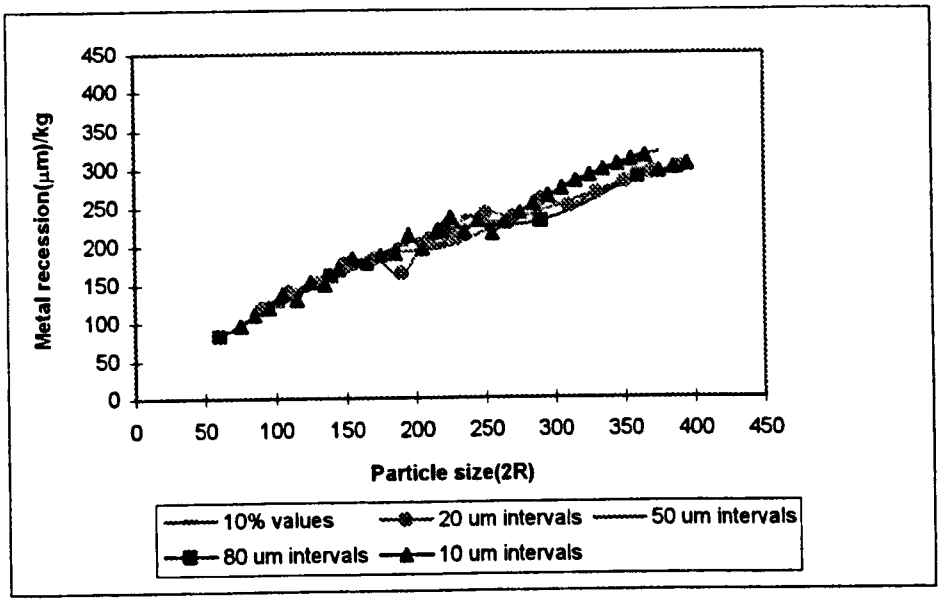

Fig.7.19 : continued - b) plot of metal recession vs particle size using the same particle size distribution as in Fig.7.19a but different particle size intervals

The effect of altering the particle size distribution e.g different standard deviation but same mean value or alternatively different mean values but same standard deviation, is presented in this section.

Fig.7.20 presents the results for a number of different particle size distributions having different mean but same standard deviation of ×/÷ 1.34. A nearly linear increase in metal recession can be seen and the higher the mean particle size of the distribution, the higher the metal recession rates.

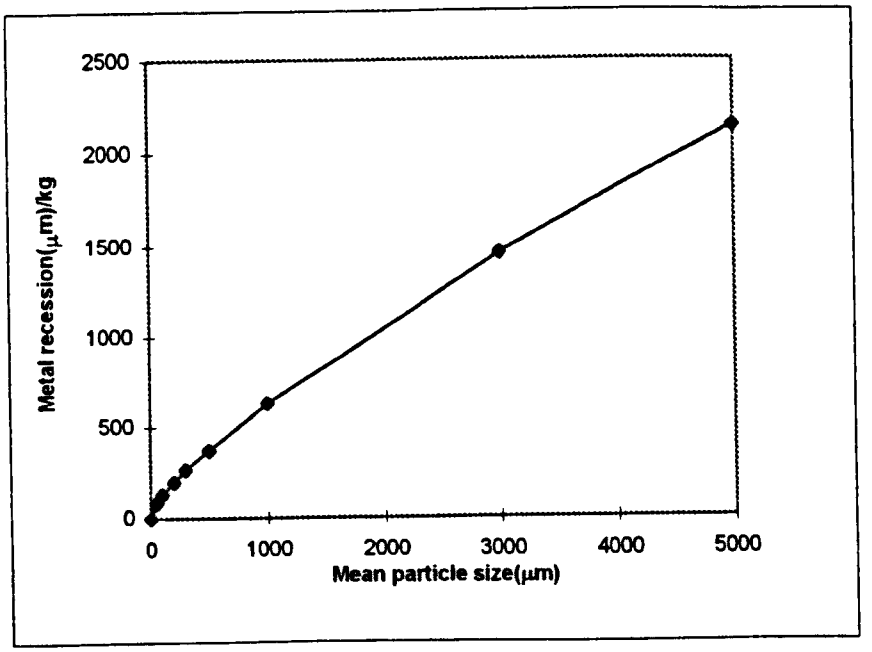

Fig.7.20: Metal recession vs mean particle size for a number of log-normal particle size distributions all having a standard deviation of ×/÷ 1.34.

In Fig.7.21 the results of a number of distributions(M.St at 197.5N) having the same mean but different standard deviation, are plotted. Three different means were used(100, 200 and 300μm) for comparison purposes. It can be seen from the graph that for small standard deviations there is no noticeable metal recession increase whilst as the deviation from the mean increases the metal recession increases, particularly for the larger particle sizes.

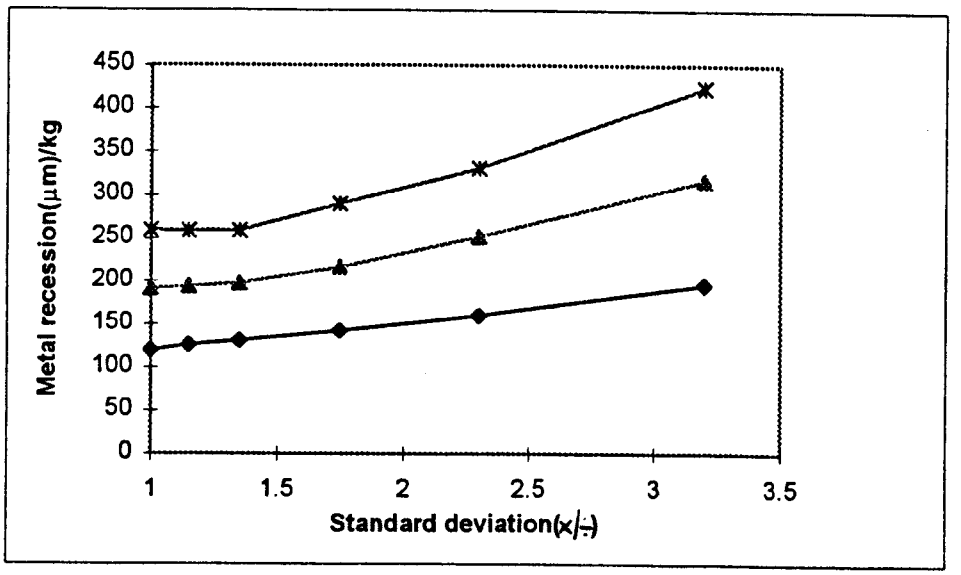

Fig.7.21 :Metal recession vs standard deviation for a number of particle size distributions having the same mean but different standard deviation. For M.St at 197.5N.

Fig.7.22 shows the effect of the load on the metal recession rates, assuming the same particle size distribution(200μm), for the three materials N18, 440C and N18++ under investigation. The wear rates for the harder materials, 440C and N18++ where the abrasives tend to break up, as mentioned in Fig.6.22, are less sensitive to loading whilst for the N18 as the load increases the increase of the wear rate is accerelated.

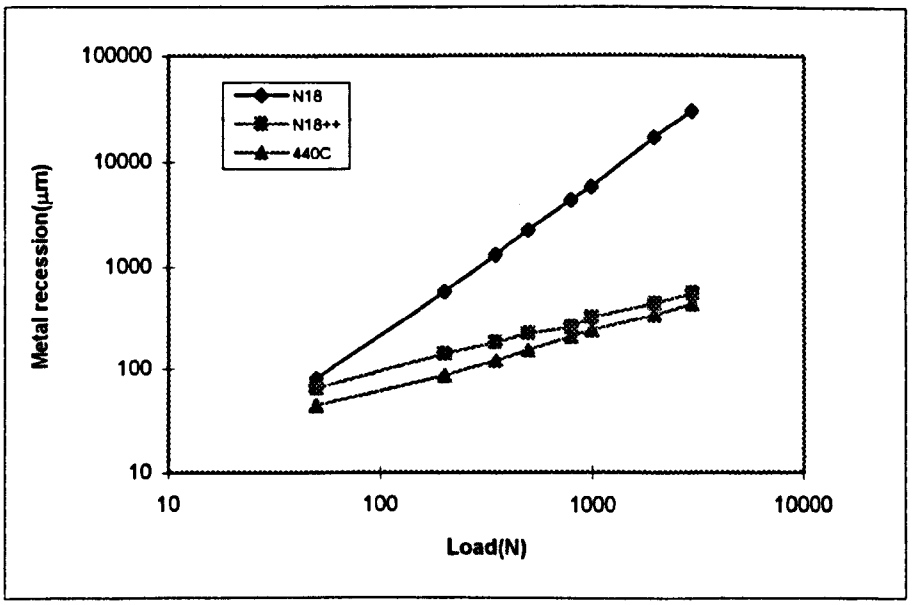

Fig.7.22 : Plot of the load(N) against metal recession(μm) for the materials under investigation.

This clearly illustrates the benefits of selecting materials such as 440C and N18++ when more severe abrasion conditions are expected. The relative hardness between the material and the abrasive is of particular importance as this provides a good indication as to whether the material will undergo a high level of plastic deformation or the abrasive will fracture and less damage will result. The two types of behaviour are well illustrated in Fig.7.22 for N18 and 440C / N18++.

Fig.7.23 is a plot of relative corrosion rate against wear rate used to determine the effect of corrosion on the materials under investigation in different environments(wear and wear/corrosion). The relative corrosion rates are defined on the x axis with the numbers 0-5. The number 0 defines wear only, number 1 defines wear + corrosion conditions used in the experiments, and numbers 2-5 an increase in corrosion rates only twice up to 5 times higher relative to 1. As can be seen from the plot when there is only wear the 440C and N18++ showed the same behaviour with low wear rates as compared to the N18. However, as the corrosion increases the behaviour of the two materials, 440C and N18++ deviates. N18++ provides much improved wear resistance as the severity of the corrosion increases. This will have a major impact on the lifetime of components that are used in highly corrosive environments but that are also exposed to abrasive wear conditions.

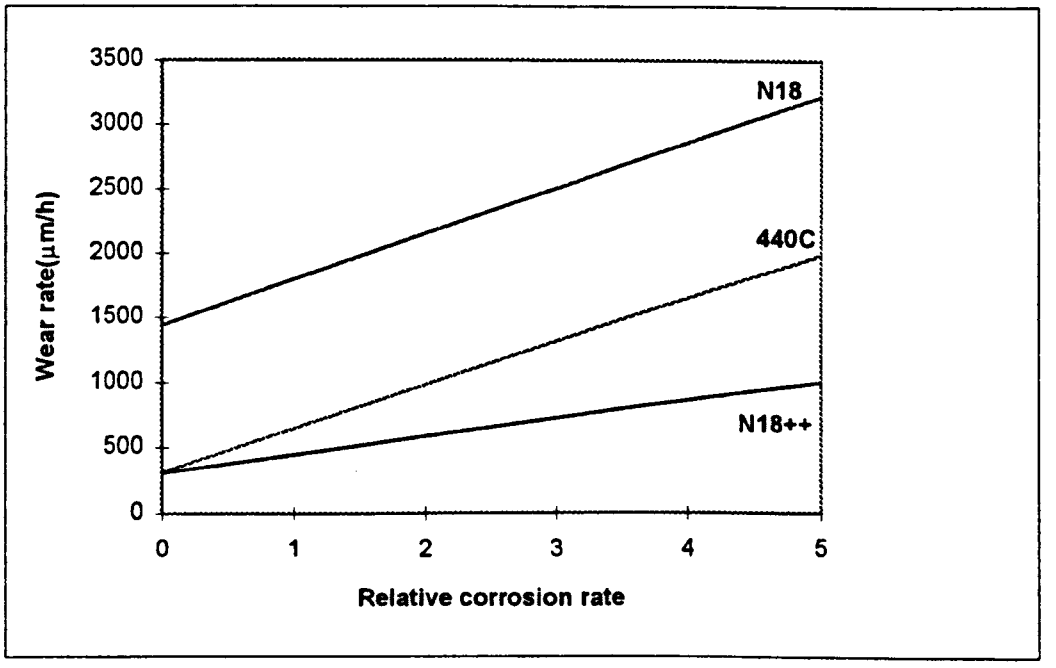

Fig.7.23 :Plot showing the behaviour of the materials under investigation in different environments(wear and wear/corrosion)

7.5.4 Further validation of the model

An important requirement of the model is that it should provide a satisfactory ranking of materials for a given set of wear/corrosion conditions. The model developed in this study was used to rank some of the materials presented in Appendix A according to their hardness and wear rates, considering an average particle size of 200μm.
These initial abrasive wear experiments were conducted by incrementing the load at 5 mins intervals, with the aim of measuring wear rate as a function of load. For this modelling exercise, the metal loss values for each load increment were predicted and then totalled to give the final metal loss.

Table 7 presents the ranking of the materials and Fig.7.24 is a scatter diagram showing the measured and predicted values of the same materials plus for the four main materials under investigation (M.St, N18, N18++, 440C).

Materials	Hardness(Hv)	Measured mass loss(Exp.)(μm)	Ranking	Predicted mass loss(mod)(μm)	Ranking
316 SS	210	310	4	281	4
Nim 105	370	660	6(worst)	787	6(worst)
R 95(HOT)	470	512	5	388	5
K 190	650	60	3	102	3
M 390	680	50	2	101	2
D2	740	40	1 (best)	74	1(best)

Table 7: Ranking of different materials according to their hardness and metal loss

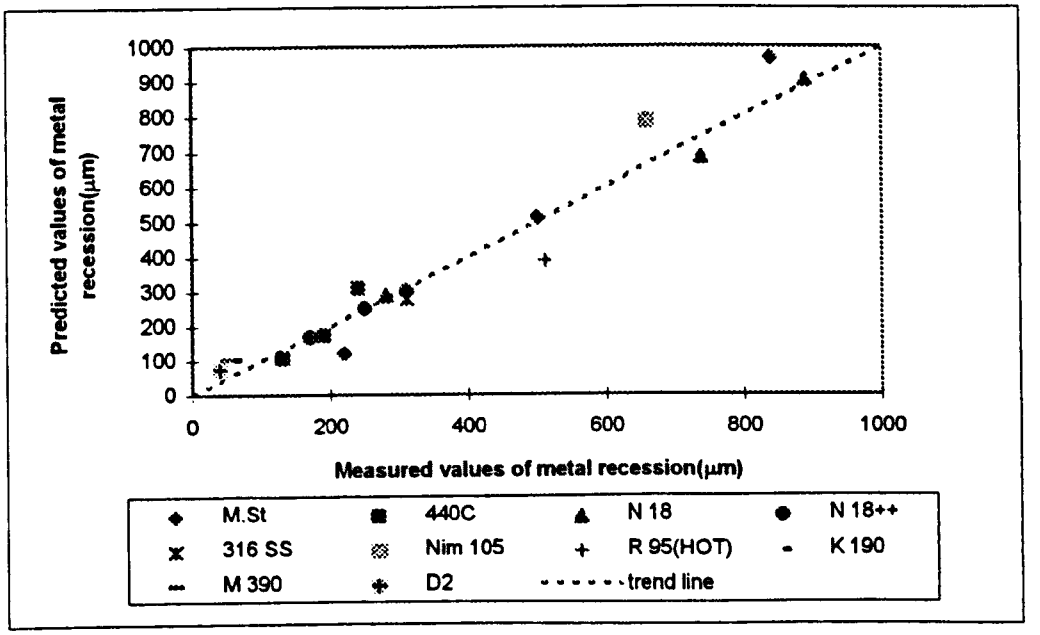

Fig.7.24: Scatter diagram of measured and predicted values of metal recession for all the materials in Table 7 plus the four main materials(M.St, N18, N18++, 440C)

The agreement between the predicted and measured abrasive wear rates is excellent. This is further confirmation that the modelling approach can be used to predict the wear behaviour of a wide range of materials under complex loading conditions, provided that the mechanism of material removal is appropriate, i.e corresponds to a LCF process.

The predicted ranking of the materials is also excellent. Although the results generally demonstrate that abrasive wear resistance increases as hardness increases, M.St and 316 SS exhibit far better wear resistance than expected from their hardness values, compared to other alloys such as N18 and Nim 105. However, the model predicts this response by taking into account material ductility and fracture behaviour.

CHAPTER EIGHT

8. Conclusions

8.1 Abrasive wear tests

1. ASTM G 65-93 dry sand abrasive wear test, has proved to be a satisfactory method for assessing the low stress abrasive wear of materials. From the materials tested, 440C and N18+5%TiC+5%TiN performed the best, with the N18 and Mild Steel exhibiting similar but inferior performance.

2. The wear rate increased with load and material loss was proportional to the amount of abrasive.

3. The mechanism of abrasive wear for all of the materials was attributed to a "ploughing" process resulting from the cyclic stressing of surface material.

4. The surface morphologies of the wear scar and wear debris analysis showed that ploughing was the predominant metal removal mechanism. This was also consistent with the very low Dp = h/a ratios(depth of penetration) that were measured.

5. The particle size distribution, groove width distribution and wear debris size distribution all followed a log-normal distribution indicating that all three parameters were interrelated.

6. Replacing the rubber wheel with a 440C wheel increases the wear rate due to the lower compliance of the metal wheel and the higher loads applied to each particle. This resulted in some fragmentation of the larger particles.

7. The wear rate increased with load and was typically between 2and 5 times higher compared to the rubber wheel. Also, the presence of abrasives gave wear rates higher by a factor of 100 when compared with similar test without abrasives(i.e sliding wear only).

8.2 Abrasive/corrosive tests

The effect of corrosion on metal removal rates under abrasive wear conditions was evaluated using the 440C wheel.

1. The ferrous alloys(M.St and 440C) were directly dissolved in the corrosive medium whilst the Ni-based alloys(N18 and N18++) formed a protective surface layer.

2. A linear increase of the corrosion induced wear was encountered for all the different environments and at higher load the wear rate was increased by a factor of 2-3.

3. The different concentrations of the corrosive medium, H_2SO_4 (0.3 to 30vol%) and the addition of the cysteine(up to 10wt%) had no significant effect on the wear rates.

4. The surface wear morphology was consistent with a 'ploughing' type of mechanism, but for the less wear resistant materials(Mild Steel and N18), large channels were formed. These channels tended to concentrate the abrasive which was carried in the corrosive fluid, resulting in more localised recession.

8.3 Modelling

1. Archard's wear equation was employed, using a mean value for $K=2.5x10^{-3}$, in order to predict wear rates and compare them with experimental results obtained from the dry sand abrasive wear tests with both the rubber wheel and 440C wheel. The agreement was better than one order of magnitude.

2. The ploughing mechanism was modelled in terms of a LCF process using the Coffin-Manson equation. The model predicts effects of load, material properties and abrasive particle distribution to better than a factor of 2.

3. A new approach was used to model the wear/corrosion process according to the way different materials behave during corrosion.
a) for the ferrous alloys(M.St and 440C), the arithmetic addition of the predicted wear rates assuming a 440C wheel plus experimental corrosion results, was compared with wear/corrosion results from the experiments and a reasonable agreement was found.
b) for the Ni-based alloys the formation and removal of a 5nm thick film was assumed and the model predicts wear rates to better than a factor of 2.

8.4 Recommendations to minimise metal recession due to wear and wear/corrosion

For good abrasive wear resistance and abrasion/corrosion resistance, the following requirements can be proposed.

- a small mean particle size for the abrasive.
- the least possible particle flux.
- a narrow particle size distribution(small standard deviation).
- the lowest possible loads.
- high material hardness(resistance to plastic deformation), material should be at least as hard as the abrasive.
- high material ductility.
- high material work hardening exponent.

- Under severe corrosion conditions, materials should form a very thin protective surface film - but the increase in metal loss is likely to be related to the flux of abrasives, as this determines the time between formation and removal of the film. Hence, even when very thin(nm) film is formed these may have a significant effect on metal loss under abrasive wear conditions.

CHAPTER NINE

9. Suggestions for further work

1. The ASTM G65-93 abrasive wear test is a simple reliable test for the assessment of the abrasive wear resistance of materials. However, the standard would benefit from being modified, particularly in terms of the quantity of abrasive applied during a test. At present the standard calls for a sand flow rate of 300-400 g/min.

2. Better hopper design in order to elliminate friction between the side walls and the abrasives and achieve a consistent delivery of the abrasives.

3. Relating 'a' (groove width) to Hv (hardness) by doing simple indentation tests in order to be able to predict metal recession rates from hardness values.

3. Study a wider range of conditions -e.g higher loads, larger particles etc. so that the h/a ratio becomes ≥ 0.4 which is the lower limit for the onset of cutting.

4. The influence of second phase particles e.g N18+TiC+TiN should be studied in greater detail. As mentioned in the literature review, different rules of mixture have been used to evaluate the performance of materials which include second phases. In this particular work this option was not examined but is clearly needed particularly considering the excellent performance of N18 with TiC, TiN additions. Of particular interest would be a study of the effect of different ceramic particle sizes and volume fractions on the metal recession rate.

REFERENCES

1. T.S. Eyre:'Wear characteristics of Metals'
Tribology International, vol.10, 1976, pp.203-212

2. G.F. Archer and D.J. Stephenson: 'Surface engineering of twin-screw extruder barrels'. Proc. Of the Int. Conf. On Hot-isostatic pressing-HIP '93. L.Delay and H.Tas(eds). Elsevier Science B.V, Holland, 1994, pp. 291-300

3. K. Stevens: 'Characterisation and Quality control of surface treatments and coatings'. Surface engineering S.A Meguid(ed.). Elsevier Applied Science, Holland, 1990, pp.125-131

4. G.F. Archer and D.J. Stephenson: 'Bimetallic coatings for twin-screw extruder barrels'. Mat.Res.Soc.Symp.Proc., Mat.Res.Soc.(Pub.), Pittsburgh-USA, Vol.251, 1992, pp. 87-92

5. M. Pierronet and G. Raisson(eds): 'Production of clad and bimetal components by the HIP-assisted diffusion bonding of steels and superalloys'. Proc. of the 4th Int. Conf. on Isostatic Pressing. Pub. MPR Publishing Services Ltd, Shrewsbury.
Stratford-upon-Avon, UK, Nov.1990, pp. 30.1-30.14

6. I.V. Kragelskii and E.A. Marchenko: 'Wear of machine components'
J. of Lubrication Technology, Vol.104, (9), Jan. 1982, pp. 1-7

7. J.T. Burwell and C.D. Strang: 'On the empirical law of adhesive wear'
J.Appl.Phys.,vol.23, 1952, p.18-28

8. F.P. Bowden and D.Tabor: 'Friction and Lubrication of solids'. Vol.I ,1950 & vol.II 1964. Calendon Press, Oxford, pp. 299-303

9. N.P. Suh: 'An overview of the delamination theory of wear'.
Wear, vol.44, 1977, pp.1-16

10. J.F. Archard and W. Hirst: The wear of metals under unlubricated conditions
Proc.Roy.Soc., A 236, 1956, pp. 397

11. D. Tabor: 'Wear : A critical Synoptic View'. Proc.Inter. Conference on wear of materials, St.Louis Missouri, Apr.1977, Pub. By ASME, N.Y, pp. 1-10

12. T.F.J. Quinn: 'The classification, laws, mechanisms and theories of wear'.
Part VII, Fundamentals of tribology, MIT Press 1980, pp. 477-492

13. E.R. Bowen and V.C. Westcott: 'Wear particle atlas' -Final report on contract No : N-156-74-C, 1682 for Naval Air Eng. Center, 12, N.J-USA, 1976

14. V. Ikranov: 'Abrasive wear mechanism'. Proc. Of the 4th European Tribology Congress Eurotrib '85, vol.4, (5), France Sep.1985, pp. 189-196

15. N. Masaiko: 'Trends in engine technology and Tribology'.
Tribology International, vol.27, (1), Jan.1994, pp.3-7

16. R.D. Arnell,P.B. Davies,J. Halling and T.L. Whomes: Tribology: Principles and design applications. Mc Millan Education Ltd, London 1991

17. D.J. Neadle: Lubricants recycling in "Ecological and economical Aspects of Tribology", Ind.Lubrication and Tribology, vol.46,(4), Jul-Aug 1994, pp.5-7

18. A.J.Mathews,J. Artlen,P. Holiday and P. Stevenson: 'UK Engineering coatings Industry in 2005'. Published by DTI, 1992

19. War on wear: 'Tribology action campaign'. IMechE, March 1992
Tribology International, Vol. 25, (3), 1992, pp. 214-215

20. J.T. Burwell: 'Survey of possible wear mechanisms'.
Wear, vol.1, 1958, pp. 119-141

21. E. Rabinowitz and A. Mutis: 'Effect of abrasive particle size on wear'.
Wear, vol.8, 1965, pp. 381-390

22. G.V. Toporov: 'The influence of structure on the abrasive wear of cast iron.
Friction and wear of machinery, (12), ASME, N.York 1960, pp. 39-59

23. H.S. Avery: 'Classification and precision of abrasion of materials'.
ASME, 1977, N.York, pp.148-157

24. A.R. Lansdown and A.L. Price: 'Materials to resist wear-Guide to their selection and use'. Pergamon press, Swansea, U.K , 1989, pp. 74-77

25. T.F. Norman: 'Abrasive wear of materials' -Handbook of Mech.wear
C.Lipson and L.Colwell (eds), Univ. of Mitchigan Press, 1961, pp. 277-314

26. M.J. Murray,P.J. Mutton and I.D. Watson: 'Abrasive wear mechanisms in steels'.
J. of Lubric. Techn, vol.104, Jan.1982, pp.9-15

27. J. Yu and S.D. Bhole: 'Wear tester for tillage tool materials'.
Tribology International, Vol.23, Oct.90, (5), pp. 309-316

28. K. Kato and A.K. Hokkirigawa: 'An experimental and theoretical investigation of ploughing, cutting and wedge formation during abrasive wear'.
Tribology International, Vol.21, (1), Feb.88, pp. 53-57

29. K.C. Ludema: 'A perspective on wear models'.
ASTM Standardisation News, vol.56, Sep.1978, pp. 13-17

30. N.P. Suh: 'The delamination theory of wear'.
Wear, vol.25, 1973, pp. 111-124

31. J.P. Hirth and J. Lothe: 'Theory of dislocations'.
McGraw-Hill, N.York 1968, pp. 14-26

32. J.M. Challen and P.L.B. Oxley: 'An explanation of the different regimes of friction and wear using asperity deformation models'. Wear, vol.53, 1979, pp. 229-243

33. A.G. Evans and D.B. Marshall: 'Wear mechanisms in Ceramics'. ASM Materials Science Seminar., Pittsburgh, Oct.1980, pp. 439-448

34. M.M. Kruschov: 'Principles of abrasive wear'.
Wear, vol.28, 1974, pp. 69-88

35. M.V. Swain: 'Fracture mechanics of Ceramics'.
J. Amer.Cer. Soc.,vol.3, 1978, p.257

36. B.R. Lawn and R. Wilshaw: 'Indentation fracture; principles and applications
J.of Materials Science,vol.10, 1975, pp. 1049-1081

37. A.G. Evans and T.R. Wilshaw: 'Quasi-static particle damage in brittle solids'.
I. Observations, analysis and implications. Acta Mettal.,vol.24, 1976, pp. 939-956

38. T.E. Fischer,M.P. Anderson,R. Salter and S. Jahanmir: 'Wear of Materials'.
K.Ludema(ed.), ASME 1987

39. A. Wang and I.M. Hutchings:Wear of alumina fibre-aluminium metal matrix composite by two-body abrasion. Mat.Sci.and Tech.,vol.5, 1989, pp. 71-76

40. J. Tong,Y.Y. Sun and H.Y. Zheng: 'Abrasive wear mechanisms of composite alloys'.
Tribology International Vol.18, (2), Apr. 1985, pp. 101-111

41. R.D. Haworth: 'The abrasive resistance of metals'.
Transactions Am.Soc.of Metals, vol.41, 1949, pp. 819-824

42. M.A. Moore: 'A review of two-body abrasive wear'. Wear, vol.27, 1974, pp. 1-17

43. M.A. Moore: 'The effect of particle shape on abrasive wear'. Inter.Conf. on the Fundamentals of Friction and Wear of Materials, Reston, VA, K.C. Ludema(Ed.), Apr.1983 ASME, NY 10017

44. M.M. Kruschov and M.A. Babichev : 'Research on wear of metals'. Chapter 8
NEL Transl. No 893-Nat.Eng.Lab, East Kilbride 1960

45. C.K. Nathan and W.J.D. Jones: 'The empirical relationship between abrasive wear and the applied conditions'. Wear, vol.9, 1966, pp. 300-309

46. T.O. Mulhearn and L.E. Samuels: 'The abrasion of metals: a model of the process'.

Wear, vol.5, 1962, pp. 478-498

47. J. Larsen-Basse : 'Influence of grit diameter and specimens size on wear during sliding abrasion'. Wear, vol.12, 1968, pp. 35-53

48. C. Allen,B.E. Protheroe and A. Ball: 'The abrasive-corrosive wear of stainless steel'. Wear, vol.74, 1981, pp. 287-305

49. A. Misra and I.Finnie:An experimental study of three-body abrasive wear
Proc. of the 3rd Int. Conf. on wear of materials., ASME, Japan Soc. Of Lubric. Eng. and ASTM, San Fransisco 1981, pp. 426-431

50. G.P Tilly: 'A two stage mechanism of ductile erosion'.
Wear, vol.23, 1973, pp. 87-96

51. J. Larsen-Basse: 'Influence of grit size on groove formation during sliding abrasion'. Wear,vol.11, 1968, pp. 213-222

52. I. Finnie: 'Erosion of surface by solid particles'.
Wear, vol.3, 1960, pp. 87-103

53. J. Goddard and H. Willman: 'A theory of friction and wear during the abrasion of metals'. Wear, vol.5, 1962, pp. 114-135

54. D.J. Stephenson and J.R Nicholls: 'Modelling of erosive wear'. Corrosion Science, vol.35, (5-8), 1993, pp. 1025-1026

55. B.W.E. Avient,J. Goddard and H. Wilman: 'An experimental study of friction and wear during abrasion'. Proc.Roy.Soc., A 258, London 1960, pp. 159-180

56. S.W. Date and S. Malkin: 'Effect of grit size on abrasive with coated abrasives'.
Wear, vol.40, 1976, pp. 223-235

57. S. Malkin,K.L. Wiggins,M. Osman and G.R.W. Swalling: 'Size effect in abrasive process'. Proc.of the 13th Matador Conf., S.A Tobias and F.Koenigsberger(Eds), Mc Millan-London (Pub.), Birmingham 1972, pp.291-296

58. A,B. Van Groenon: 'The high speed size effect in grinding: the role of heat generation'.
Wear, vol.44, 1977, pp. 203-211

59. N.P. Suh and N. Saka: 'Abrasive wear mechanisms and the grit size effect'.
Wear, vol.55, 1979, pp.163-190

60. J. Larsen-Basse and P.L.B. Oxley: 'Effect of strain rate sensitivity on scale phenomena in chip formation'. Proc. of the 13th Inter.Matador Conf., S.A Tobias and F.Koenigsberger(Eds), Mc Millan-London (Pub.), Birmingham 1972, pp. 209-216

61. M.A. Moore and R.M. Diuthwaite: 'Plastic deformation below worn surface'.
Met.Trans. 7A, 1976, pp. 1833-1839

62. G.P. Tilly and W. Sage: 'The interaction of particle and material behaviour in erosion processes'. Wear, vol.16, 1970, pp. 447-465

63. A. Misra and I. Finnie: 'On the size effect in abrasive and erosive wear'. Wear, vol.65, 1981, pp. 359-373

64. D. Graham and R.M. Baul: 'An investigation into the mode of metal removal in the grinding process'. Wear, vol.19, 1972, pp. 301-314

65. J. Larsen-Basse and I.A Tanouye: 'Strain-rate effect in low-speed two-body abrasion'. Inter. Conf. on wear of materials in St. Louis, K.C. Ludema(ed.), ASME NY 1977, p.194

66. N.P. Suh,N. Saka and M.C. Sin: 'Effect of abrasive grit size on abrasive wear'. Progress report, Lab. for Manuf. and Productivity. School of Engineering, M.I.T, June 1978, pp. 163-179

67. I.R. Kramer and L.J. Demer: 'The effect of surface removal on the plastic behaviour of aluminium single crystals'. Trans. AIME, vol.221, 1961, pp. 780-786

68. T. Fourie: 'The flow stress gradient between the surface and center of deformed copper single crystals'. Phil.Mag., Vol.17, 1968, pp. 735-756

69. D.M. Marsh: 'Fracture of solids'. Interscience, N.York 1963, p. 119

70. J.C Fischer: 'Discussion of creep behaviour of zinc modified by copper surface layer'. Trans.AIME, vol.194, 1952, pp. 52-53

71. M.M Kruschov and M.A Babichev: 'Research on wear of metals'.Chapter 2 NEL Transl. 889, Nat.Eng.Lab. East Kilbride, 1960

72. R.C.D. Richardson: 'The wear of metals by hard abrasives'. Wear, vol.10, 1967, pp. 219-230

73. E. Rabinowitz,L.A. Dunn and P.G Russell: 'A study of abrasive wear under three-body conditions'. Wear, vol.4, 1961, pp. 345-355

74. J. Larsen-Basse and S.S. Sokolski: 'Influence of atmospheric humidity on abrasive wear II, 2-body abrasion', Wear, vol.32, 1975, pp. 9-14

75. J. Larsen-Basse: 'Influence of atmospheric humidity on abrasive wear I; 3-body abrasion'. Wear, vol.31, 1975, pp. 373-379

76. K.H. Zum-Gahr: 'Formation of wear debris by the abrasion of ductile metals'. Wear, vol.74, 1981-1982, pp. 353-373

77. C.D Richardson: 'The maximum hardness of strained surfaces and the abrasive wear of metals and alloys'. Wear, vol.10, 1967, pp. 353-382

78. D.E. Diesburg and F. Borik: 'Optimising abrasion resistance and toughness in steels and

irons for the mining industry'. Symposium- Materials for the mining Industry, Barr, R.R(ed.). Climax Molybdenum Co., USA 1974, pp. 15-41

79. C. Rubinstein: 'A note on the relation between the abrasion resistance and the hardness of metals'. Wear, vol.8, 1965, pp. 70-72

80. W.M. Garrison and R.A Garriga: 'Ductility and the abrasive wear of an ultra high strength steel'. Wear, vol.85, 1984, pp. 347-360

81. M.A. Moore,R.C.D. Richardson and D.G. Atwood: 'The limiting strength of worn metal surfaces. Met.Trans.,vol.3, 1972, pp. 2485-2491

82. A. Ball: 'On the importance of work hardening in the design of wear-resistant materials'. Wear, vol.91, 1983, pp. 201-207

83. H.S. Avery: 'Work hardening in relation to abrasion resistance'. Symposium- Materials for the Mining Industry, Barr, R.R(ed.). Climax Molybdenum Company, 1981, pp.43-76

84. U. Bryggman: 'Abrasion resistance of some steels related to mechanisms of gouging wear'. Report UPTEC, 22R, PhD Thesis Upsala University, 1983

85. H.W. Gillett: 'Considerations involved in the wear testing of metals'.
ASTM Symposium on wear of Metals, J.Ind.Eng.Chemistry, vol.24, 1932, p.1200

86. Metals Handbook. Failure analysis and prevention. 'Wear failures', vol.10, 8th ed., Metals Park, Ohio 44073, ASME 1976, pp. 134-158

87. M.M. Kruschov and M.A. Babichev: 'Friction and Wear in machinery'. No 12, ASME, N.York 1960, p. 5

88. R.T. Spurr and T.P. Newcomb: 'Abrasive wear of metals'. Proc.Conf. Lubrication and wear, Inst. of Mech. Engineers, London 1957, p. 269

89. F. Borik: 'Using tests to determine the influence of metallurgical variables on abrasion'. Metals Eng.Quat., Vol.12, (2), 1972, pp. 33-39

90. G.V. Toporov: 'The influence of structure on the abrasive wear of cast iron'.
Friction and wear in Machinery, No 12, ASME, N.York 1960, pp. 39-59

91. A. Misra and I. Finnie: 'A review of abrasive wear of metals'.
Tran. of ASME, Vol.104, Apr.1982, pp. 94-101

92. R.C Tucker and A.E Miller: 'Low-stress abrasive and adhesive wear testing, selection,and use of wear tests for metals'. ASTM, STP 615, 1976, pp. 68-90

93. F. Borik and D.L. Sponseller: 'Gauging abrasion test for materials used in Ore and Rock crushing'. ASTM Jour. of Materials, Vol.6, 1971, pp. 576-605

94. S.L Narashimham and J.M Larson: 'Valve gear wear and materials'.

SAE Paper 851497. International off-highway and power plant exposition, Wisconsin 1985, pp. 1-30

95. H.C. Meng and K.C. Ludema: 'Wear models and predictive equations: their form and content'. Wear, vol.181-183, 1995, pp. 443-457

96. R.G. Bayer:" Comments on Engineering needs and wear models"
ASTM STP 1105, Philadelphia USA, 1991

97. Workshop on the use of surface deformation Models to predict Tribology behaviour. Proc. Published under the title "Approaches to modelling of Friction and Wear", ch.26
F.F Ling, C.H Pan (eds), Columbia University, New York 1986, pp. 147-151

98. F.A. Nichols,A.I. Michaels and L.A. Northcutt: International Workshop on wear modelling. Proc. of a workshop published under the title "Modelling of wear in energy conversion and utilisation technologies, Argone National Lab. USA, June 1988, pp.65-68

99. D.A. Tabor: 'Status and direction of Tribology as a science in the 80's. Understanding and Prediction'. Trib.International, vol. 12, (1), 1979, pp. 36-37

100. J. Larsen-Basse: 'Success and failure of simple models for abrasive wear'.
ASTM STP 1105, Philadelphia USA, 1991

101. M.M. Kruschov and M.A. Babichev: 'Research on wear of metals' in Issled. Iznashivanira Metallov, Izd.Akad. NAUK, Moscow, ch.8
NEL Translation 893, Nat.Eng.Laboratory East Kilbride, 1960

102. R.L. Aghan and L.E. Samuels: 'Mechanism of abrasive polishing'.
Wear, vol.16, 1970, pp. 293-301

103. T. Sakamoto and T. Tsikuzoe: 'Friction and prow formation in a scratch process of copper by a diamond cone'. Wear, vol.44, 1977, pp. 393-397

104. E. Rabinowitz: 'A study of abrasive wear under three-body condition'. Friction and wear of materials. John Wiley and Sons Inc., N.York 1965, pp. 137-142

105. J.F Archard:'Contact and rubbing of flat surfaces'. J. of applied Physics, vol.24, 1953 pp. 981-988

106. M.M. Kruschov and M.A. Babichev: 'Abrasive wear-Investigation of the wear of metals'. Akademiya NAUK SSSR, Moscow 1970, pp.108-110

107. T.O. Mulhearn and A.J. Sedrikis: 'Mechanics of cutting and rubbing in simulated abrasive processes'. Wear, vol.6, 1963, pp. 457-466

108. M.A. Moore: 'Abrasive wear; Fundamentals of friction and wear of materials'.
D.A Ringley(ed.), ASME Metals Park, Ohio, 1981 pp.73-118

109. K.H. Zum Gahr: 'Abrasive wear of ductile metals'.

Wear,vol.74, 1981-1982, pp.353-373

110. T.C. Buttery and J.F. Archard: 'Grinding and abrasive wear'. Proc. of the Institution of Mech. Engineers. Vol.185,(43), pp. 537-551

111. K. Kato,K. Hokkirigawa,T. Kayaba and Y. Endo: 'Three dimensional shape effect on abrasive wear'. Trans. Of the ASME, vol.108, July 1986, pp. 346-351

112. M.A. Moore and F.S. King: 'Abrasive wear of brittle solids'.
Wear, vol.60, 1980, pp.123-140

113. A.A Torrance: 'A new approach to the mechanics of abrasion'.
Wear, vol.67, 1981, pp. 233-257

114. T. Tsukizoe and T. Sakamoto: 'Friction and scratch deformation of metals'.
Proc.JSLE-ASLE Inter.Lubric.Conf.Tokyo, 1975. Elsevier Amsterdam, 1976, p. 49

115. S. Jacobson,S. Per Wallen and S. Hogmark: 'Fundamental aspects of abrasive wear studied by a new numerical simulation model. Wear, vol.123, 1988, pp. 207-223

116. J. Halling: 'Note on the form of wear laws'. Wear, vol.76, 1982, pp. 263-266

117. W.M. Garrison: 'Kruschov's rule and the abrasive wear resistance of multiphase solids'. Wear, vol.82, 1982, pp. 213-220

118. M.A. Zamzam: 'Abrasive wear of aluminium matrix composites'., Metall., vol.43, (3), 1991, pp. 250-254

119. L.H. Lee,W.H. Lu and S.L.I. Chan: 'Abrasive wear of powder metallurgy Al alloy 6061-SiC particle composites'. Wear, vol.159, 1992, pp. 223-231

120. D.A. Rigney: 'Fundamentals of friction and wear of materials'.
ASM, Metals Park, Ohio, 1981

121. W. Sinn and S. Fretti: 'Abrasive wear of multiphase materials'.
Wear, vol.129, 1989, pp. 105-121

122. K.H. Zum Gahr: 'How microstructure affects abrasive wear resistance'.
Metal Progress, vol. 116, Sep.1979, pp. 46-52

123. N. Axen and S. Jacobson: 'A model for the abrasive wear resistance of multiphase materials'. Wear, vol.174, 1994, pp. 187-199

124. N. Axen and B. Lundberg: 'Abrasive wear in intermediate mode of multiphase materials'. Tribology International, Vol.28,(8), Dec.1995, pp. 523-529

125. T.E. Fischer: 'Tribochemistry'.
Ann.Rev.of Materials Science, Vol.18, 1988, pp. 303-323

126. T.F.G Quinn: 'The origins of oxidational wear'.
Tribology International ,vol.16, (5), 1983, pp. 257-271

127. T.F.G. Quinn: 'An experimental study of the thermal aspects of sliding and their relation to the unlubricated wear of steel'.
Proc. Inst. Mech. Eng., vol.183, (39), 1968-69. p. 129

128. A.W. Bachelor and G.W. Stachowiako: 'Predicting synergism between corrosion and abrasive wear'. Wear, vol.123, 1988, pp.281-291

129. A.W. Lui and G.R. Hoey: 'Corrosive and erosive wear of metals in mineral slurries'. Can. Metall. Q., vol.12, (2), 1973, pp. 185-190

130. C. Allen,A. Ball and B.E. Protheroe: 'The abrasive-corrosive wear of stainless steels'. Wear, vol.74, 1982, pp. 287-305

131. W. Schumacher: 'Corrosion wear synergy of alloy and stainless steels'.
Proc. of Intern. Conf. on Wear of Materials, K.C.Ludema(Ed.), ASTM, N. York, 1985, pp. 558-566

132. A. Misra and I. Finnie: 'An experimental study of three-body abrasive wear'.
Wear, vol.85, 1983, pp. 57-68

133. A. Ball and J.J. Ward: 'An approach to material selection for corrosive-abrasive wear by systematic in-situ and laboratory testing'.
Tribology International,, vol.18, (6), Dec. 1985, pp. 347-351

134. J. Jia-lin and T. Jing-Lin: 'Wear-corrosion behaviour of cast-in composite materials reinforced by WC particles'. Wear, vol.138, 1990, pp. 23-32

135. F.H Stott and J.E. Breakell: 'The influence of corrosion on the wear of cast iron in sulphuric acid solutions'. Wear, vol.135, 1989, pp. 119-134

136. J.J. Broese : Motorship 19, 1947, p. 687

137. D. Kotlyar,C.H. Pitt and M.E. Wadsworth: 'Simultaneous corrosion and abrasion measurements under grinding conditions'. Corr.,vol.44, (4), Apr. 1988, pp. 221-228

138. R.E.J. Noel and A. Ball: 'On the synergistic effects of abrasion and corrosion during wear'. Wear, vol.87, 1983, pp. 351-361

139. S.W. Watson,B.W. Madsen and S.D. Cramer: 'Wear-corrosion study of white cast irons'. Wear, vol.181-183, 1995, pp. 469-475

140. B.W. Madsen: 'Standard guide for determining the synergism between wear and corrosion'. ASTM G119-93, 1994, pp. 507-512

141. D.J. Dunn: 'Metal removing mechanisms comprising wear in mineral processing'.
Proc.of Inter. Conference on wear of Materials. K.C Ludema (Ed.), ASME, N.York

1985, pp. 501-508

142. H. Van de Velde: 'Stainless steel in food and beverage industry'. Stainless steel Jan/Feb 1992, pp. 28-31

143. K.R. Kreisher: Modern Plastics Int., May 1992, p. 55

144. R.C. Bohinski: 'Modern concepts in Biochemistry'. Allyn and Bacon(Eds), Boston USA, 1973, p.60

145. A.A. Aksut and S. Bilgic: 'Effect of aminoacids on corrosion of cobalt and nickel in H_2SO4'. Corrosion science, vol.33, (3), 1992, pp. 379-387

146. R.C.D. Richardson: 'Unidirection wear tests on soft abrasives and the wear resistance of steel surfaces of nearly uniform hardness'. N.I.A.E Note 12(1), J.Agric.Eng.Res, Silsoe 1967, pp.22-29

147. J.M. Prado and S. Arques: 'Dry wear resistance of a carbonitrided steel'. Wear, vol.103, 1985, pp. 321-331

148. J. Yu and S.D. Bhole: 'Wear tester for tillage tool materials'. Tribology International, Vol.23, (5), Oct. 90, pp. 309-316

149. K. Kato and K. Hokkirigawa: 'The effect of hardness on the transition of the abrasive wear mechanism of steels'. Wear, vol.123, 1988, pp. 241-251

150. T. Kayaba and K. Kato: 'Wear of materials'. ASME N.York 1979, p. 45

151. J.M. Challen and P.L.B. Oxley: 'An explanation of the different regimes of friction and wear using asperity deformation models'. Wear, vol.53, 1979, pp. 229-243

152. N.C. Welsh: 'The dry wear of steel'. Phil.Trans.Roy.Soc.Series A, vol.257, 1965, pp. 31-50

153. R.S. Dwyer-Joyce,R.S. Sayles and E. Ioannides: 'An investigation into the mechanisms of closed three-body abrasive wear'. Wear, vol.175, 1994, pp. 133-142

154. W. Lortz: 'A model of the cutting mechanism in grinding'. Wear, vol.53, 1979, pp. 115-128

155. M.J. Murray,P.J. Mutton and J.D. Watson: 'Abrasive wear mechanisms in steels'. Proc. International Conference on wear of materials, K.C Ludema (ed.), W.A Glaeser, and S.K Rhee (eds), ASME, N.Y, 1979, pp. 257-265

156. N.P. Suh,H. Sin and N. Saka: 'Abrasive wear mechanisms and the grit size effect'. Wear, vol.55, 1979, pp. 163-190

157. I.V. Kragelskii: 'Friction and wear'. Butterworths, London 1965, pp. 98-102

158. D. Tabor: 'The hardness of metals'. Oxford University Press, 1951, pp. 67-76

159. E.G Dieter:'Mechanical Metallurgy'.SI Metric Ed.,McGraw-Hill,1988, pp.390-393

160. F.M. Ashby and D.R.H. Jones: 'Engineering materials. An introduction to their properties and applications'. International Series on materials science and technology, vol.34, 1989, pp. 38-49

161. J.D. Morrow: 'Internal friction, Damping and Cyclic Plasticity'. ASTM STP No 378,ASTM Philadelphia USA, 1965, p.72

162. W.F. Adler: 'Assessment of the state of knowledge pertaining to solid particle erosion'. Final Report CR79-680, Pub. by Effects technology, Inc., santa Barbara, CA 93111, 30 June 1989, pp. 138-139

163. W.P.G. Rengstoff,M. Kazuhisa and H.D. Buckley:'Friction and wear of iron in corrosive media'. NASA Technical Paper 1985, March 1982, pp. 1-16

164. W.P.G. Rengstoff,M. Kazuhisa and H.D. Buckley:'Friction and wear of Nickel in Sulphuric acid'. NASA Technical Paper 2290, April 1984, pp. 1-20

165. D. Golini and D.S. Jacobs:'Physics of loose abrasive microgrinding'. Applied Optics, vol.30, (19), July 1991, pp. 2761-2777

166. P. Kofstad: 'High temperature oxidation of metals'.
John Wiley & Sons Inc., 1966, pp. 21-46

167. E. Kunze and K. Scwabe: 'Anodic behaviour of Nickel and its alloys'. Corrosion science, vol.4, 1964, p. 108-111

168. J. Bockris,A.K.N. Reddy and B. Row: 'Mechanisms of Nickel passivation in acidic solutions'. J. Electrochemical Soc., vol.113, 1133, 1966, pp. 128-131

169. L. Shreir: 'Passivity, Passivation, Breakdown, Pitting'. Corrosion, Vol.1, 2nd edition, 1976, p.1:115

170. H.H. Uhlig:The structure and properties of thin oxide films. Proceedings of the 3rd Inter. Congress on Met. Corrosion, vol.1, Moscow 1969, pp. 39-46

171. G.P.T. Landberg: 'The applicability of rate laws'. J. Chem.Physics, vol.23, 1955, p. 80-83

172. H.H. Uhlig: 'Electron microscope studies of oxide layers'. Corr. Science, vol. 7, 1967, pp. 18-21

173. W.C. Young: 'Roark's formulas for stress and strain'. 6th ed., McGraw-Hill Co., 1989, p. 13-15

Appendix A

1. Chemical composition of potential materials for extruder barrels

2. Heat treatment of alloys

POTENTIAL MATERIALS FOR EXTRUDER BARRELS

MATERIALS	*PROC.ROUTE*	*COMPOSITION*														*HV(20)*
		Ni	Co	Cr	Fe	C	Si	Mo	Al	Ti	W	Nb	B	Mn	V	kg/mm2
MILD STEEL	W				bal.	0.25	0.35							1		230
K 190	PM(HOT)HT			12.5	bal.	2.3		1.1							4	650
M 390	PM(HOT)			20	bal	1.9		1							4	680
Ni 601	PM(HOT)	bal.		15	4.5	1	4				0.6		3.5			810
N18+30%NiTiC	PM(HOT)															630
Ni 401	PM(HOT)	bal.		9.5	3	0.4	2.8						1.8			440
D2	C			12	bal.	1.5	0.25	0.75						0.3	0.6	740
NIM 105	W	bal.	20	15		0.12		5	5.7	1.2						370
316 SS	W	14		18	bal.	0.08	1	3								210
440 C	C(HT)			18	bal.	1.2	1	0.75						1		720
R 95	PM(HOT)	bal.	8	14		0.06		3.5	3.5	2.5	3.5	3.5				470
R 95	PM(HIP)HT															480
N 18	PM(HOT)	bal.	15.7	11.5		0.015		6.5	4.35	4.35						380
N18	PM(HIP)															420
N18+5%TiC+5%TiN	PM(HOT)															520
Aluminised	HT															450

PM:Powder metallurgy HOT:Hot pressing HIP:Hot Isostatic Pressing HT:Heat treatment

C:Cast W:Wrought

HEAT TREATMENT OF ALLOYS

440 c	N 18	R 95	K 190	PACK ALUMINISED
Heat to 1020° C	Heat 1170° C	Heat 1150° C	Heat 950° C	Heat 900° C(1 H)
Gas Quench	Rapid Quench below 600° C	Air cool 1 H	Furnace cool 6 H	Air cool
Temper 720° C				
Heat to 950-980° C	Heat 700° C	Heat 870° C	Heat 600° C	Heat 1120° C(1/2H)
Gas Quench	Air cool 24 H	Air cool 1 H	Air cool 3 H	
Temper 3 times				
560° C	Heat 800° C	Heat 650° C	Heat 925° C	Heat 850° C
480° C	Air cool 4 H	Air cool 24 H	Air cool 3 H	Argon cool 24 H
480° C				

Appendix B

1. Abrasion wear tests - Cast and Wrought materials

2. Abrasion wear tests - HIPped materials

3. Abrasion wear tests - Hot pressed materials

4. EDX analysis of the worn surface of M.St

5. EDX analysis of the wear debris of M.St

6. EDX analysis of the wear debris of 440C

7. EDX analysis of the wear debris of N18

8. EDX analysis of the wear debris of N18++

9. Sliding wear test results - 440C wheel

10. EDX analysis of the corroded surface of M.St

11. Auger results for the corroded surface of N18

12. EDX analysis of the wear/corroded surface of M.St

13. Auger results for the standard

14. Auger results for the wear/corroded surface of M.St in different environments

15. EDX analysis of the wear/corroded surface of 440C

16. Sliding/corrosive wear test results for M.St

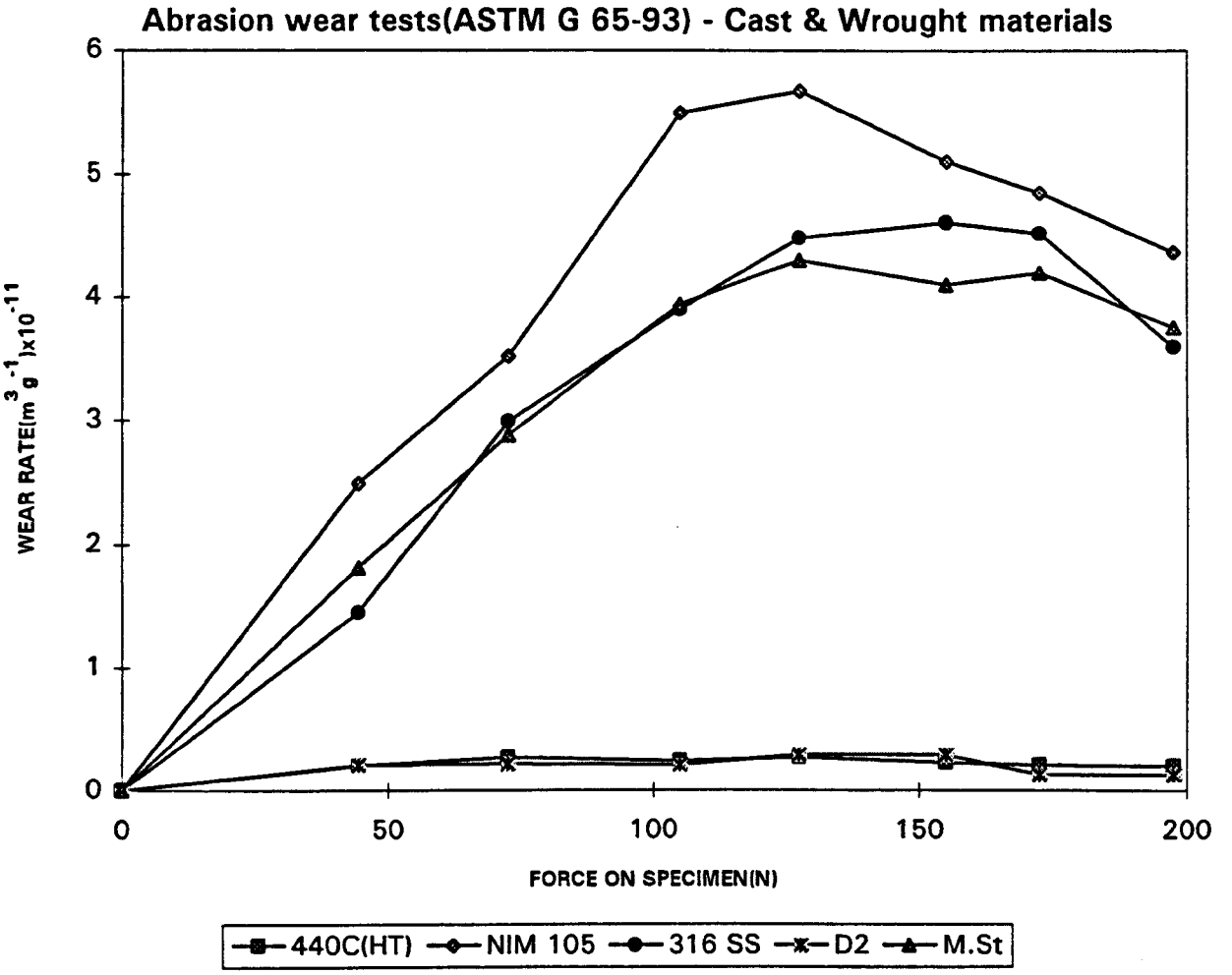
Abrasion wear tests(ASTM G 65-93) - Cast & Wrought materials
WEAR RATE(m 3 g -1)x10 -11
0
1
2
3
4
5
6
0
50
100
150
200
FORCE ON SPECIMEN(N)
440C(HT)
NIM 105
316 SS
D2
M.St

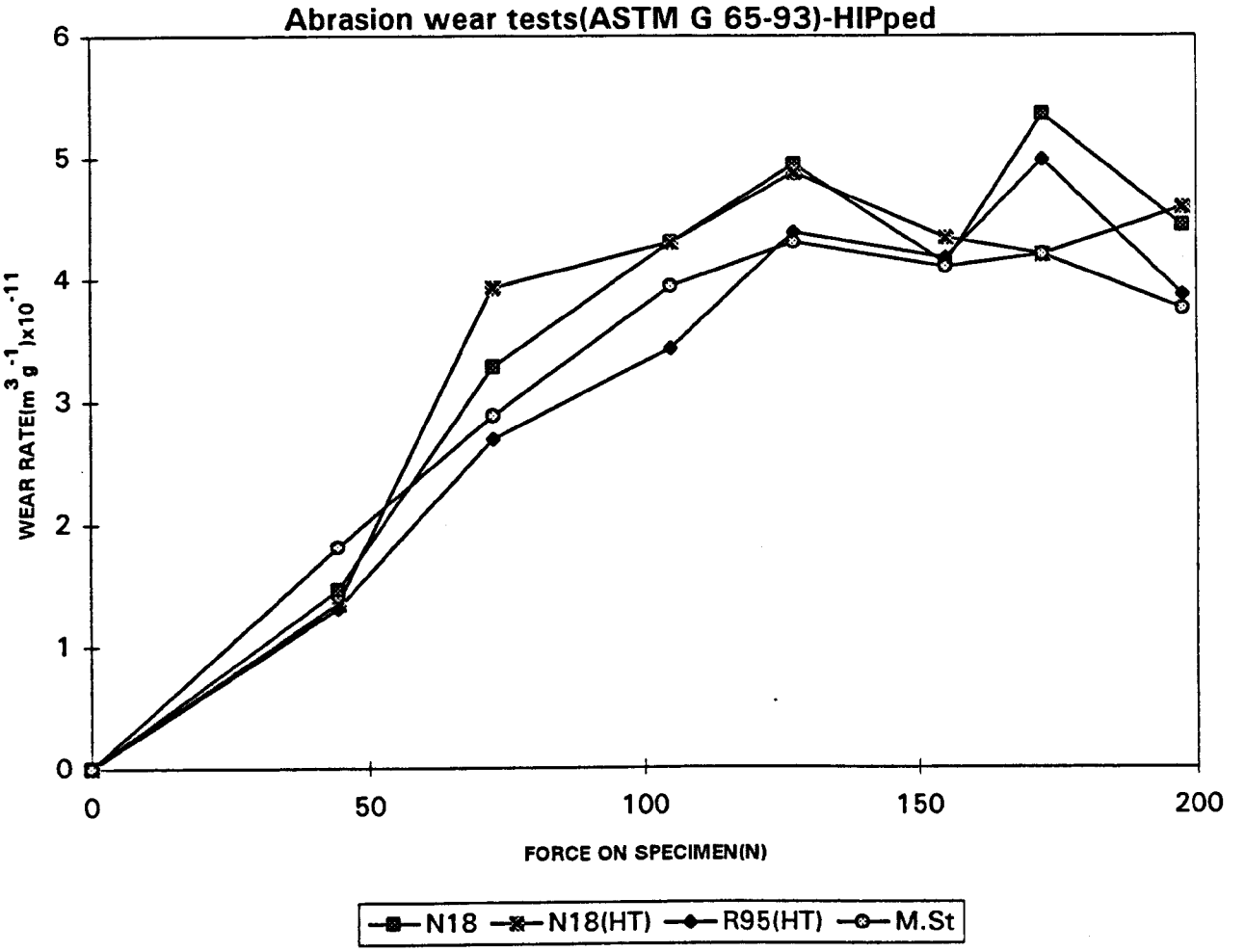
Abrasion wear tests(ASTM G 65-93)-HIPped
WEAR RATE(m3 g-1)x10-11
0
1
2
3
4
5
6
0
50
100
150
200
FORCE ON SPECIMEN(N)
N18
N18(HT)
R95(HT)
M.St

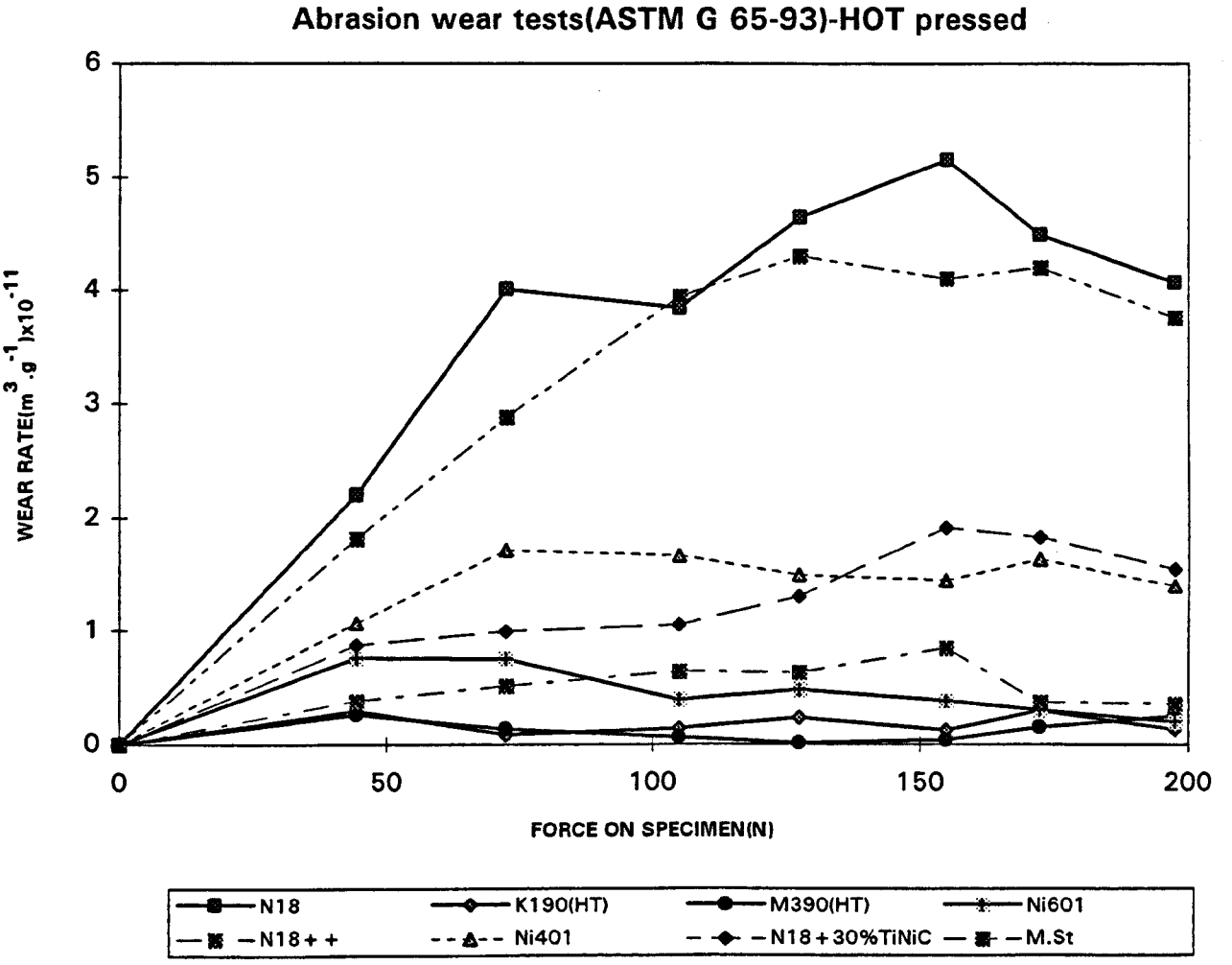
Abrasion wear tests(ASTM G 65-93)-HOT pressed
WEAR RATE(m3 .g-1)x10-11
0
1
2
3
4
5
6
0
50
100
150
200
FORCE ON SPECIMEN(N)
N18
K190(HT)
M390(HT)
Ni601
N18++
Ni401
N18+30%TiNiC
M.St

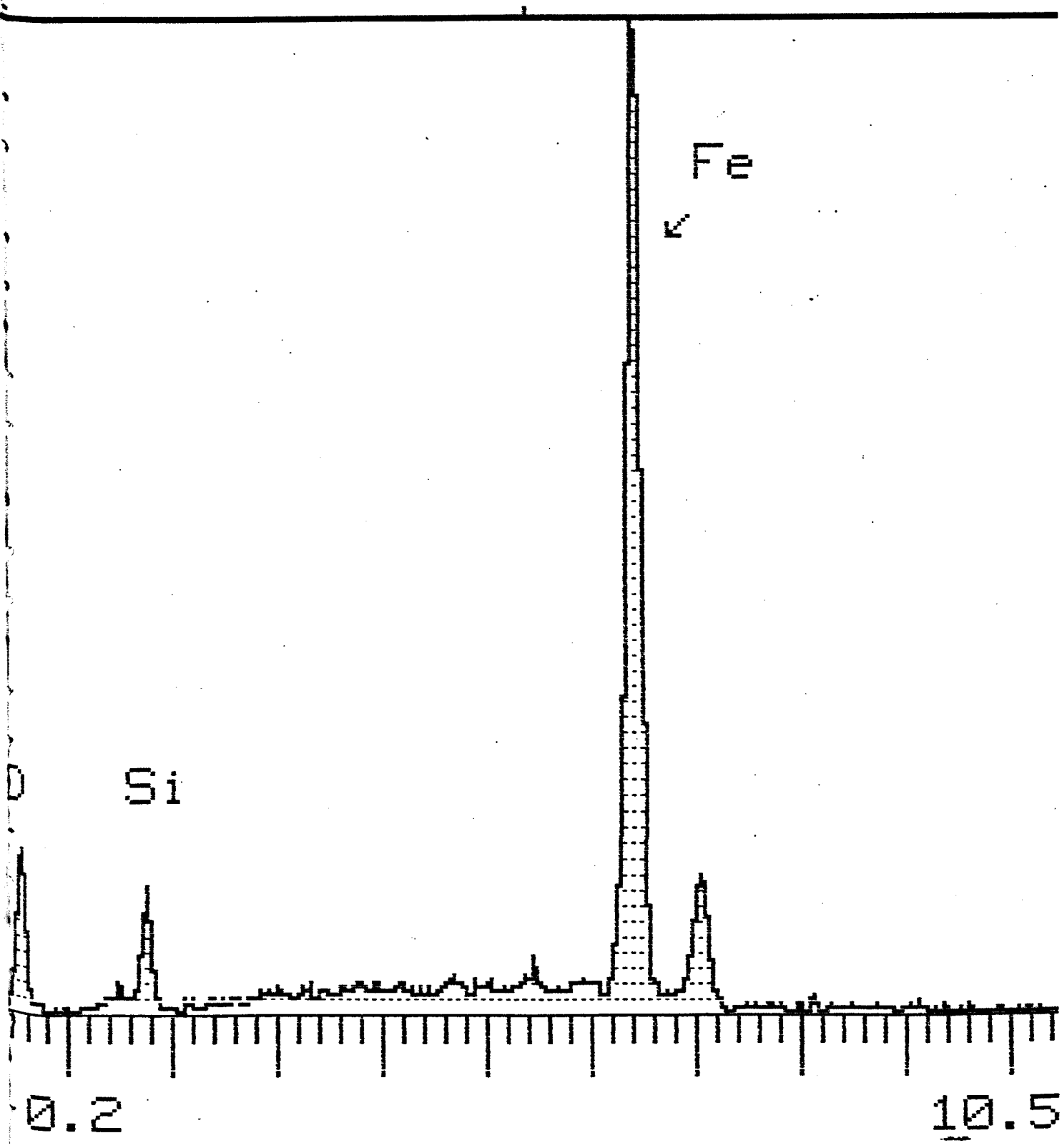

Dry sand abrasive wear test - Rubber wheel
Spot analysis on the worn surface of M.St

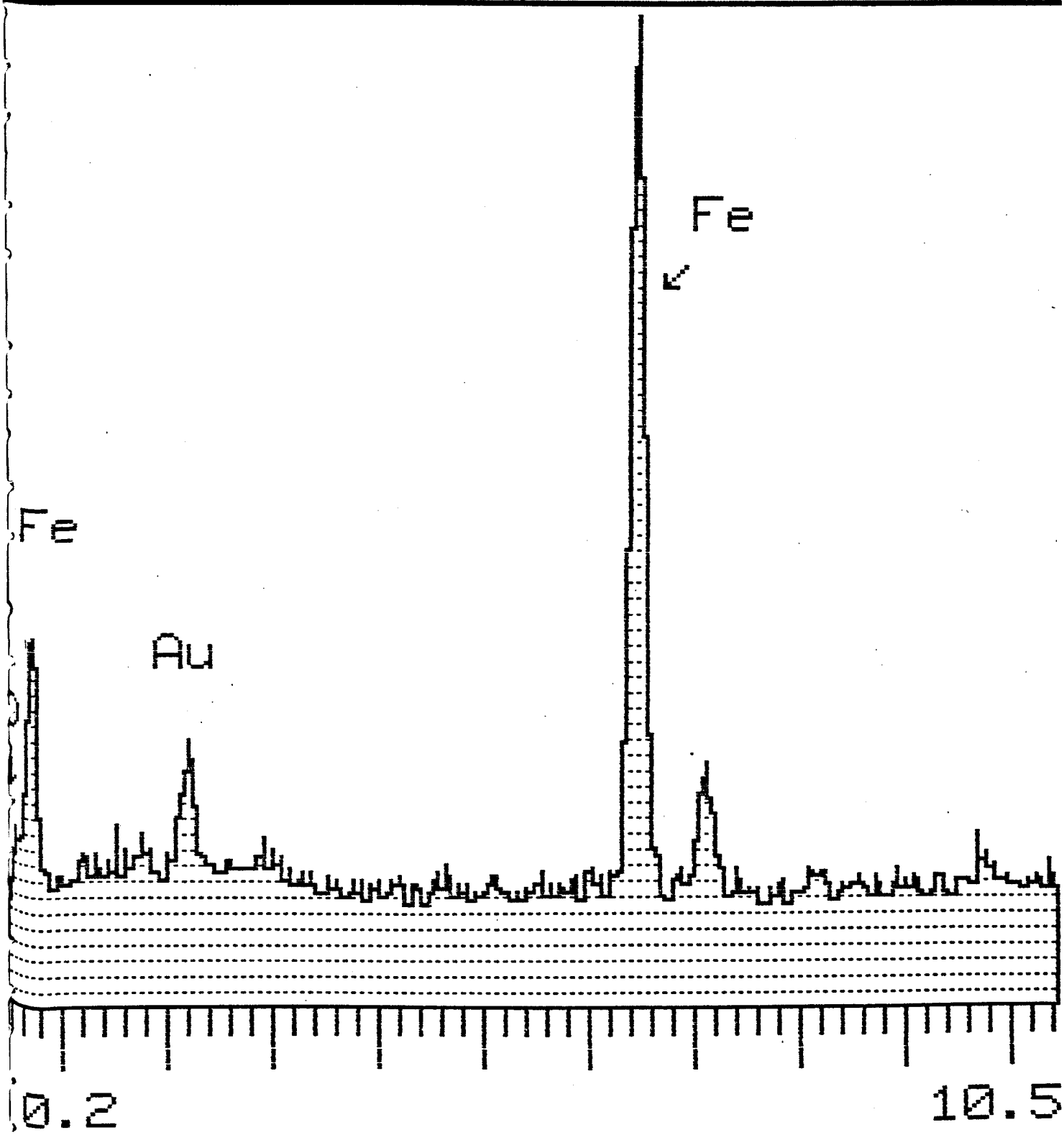

EM A: **EDX analysis of wear debris collected during dry sand abrasive wear tests on the rubber wheel (M.St)**
Test duration for 40 mins at 197.5 N

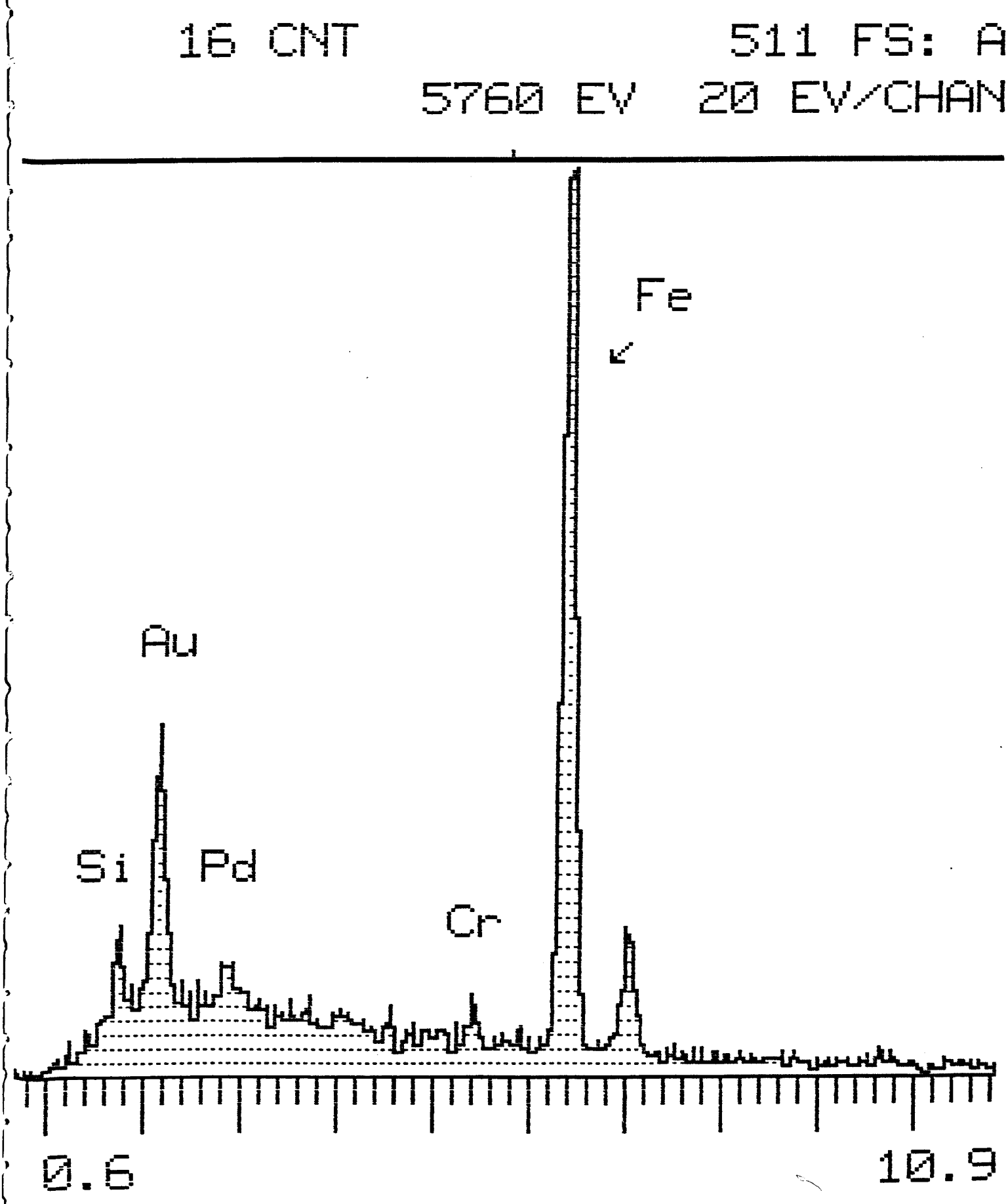

MEM A: **EDX analysis of wear debris collected during dry sand abrasive wear tests on the rubber wheel (440C)**
Test duration for 40 mins at 197.5 N

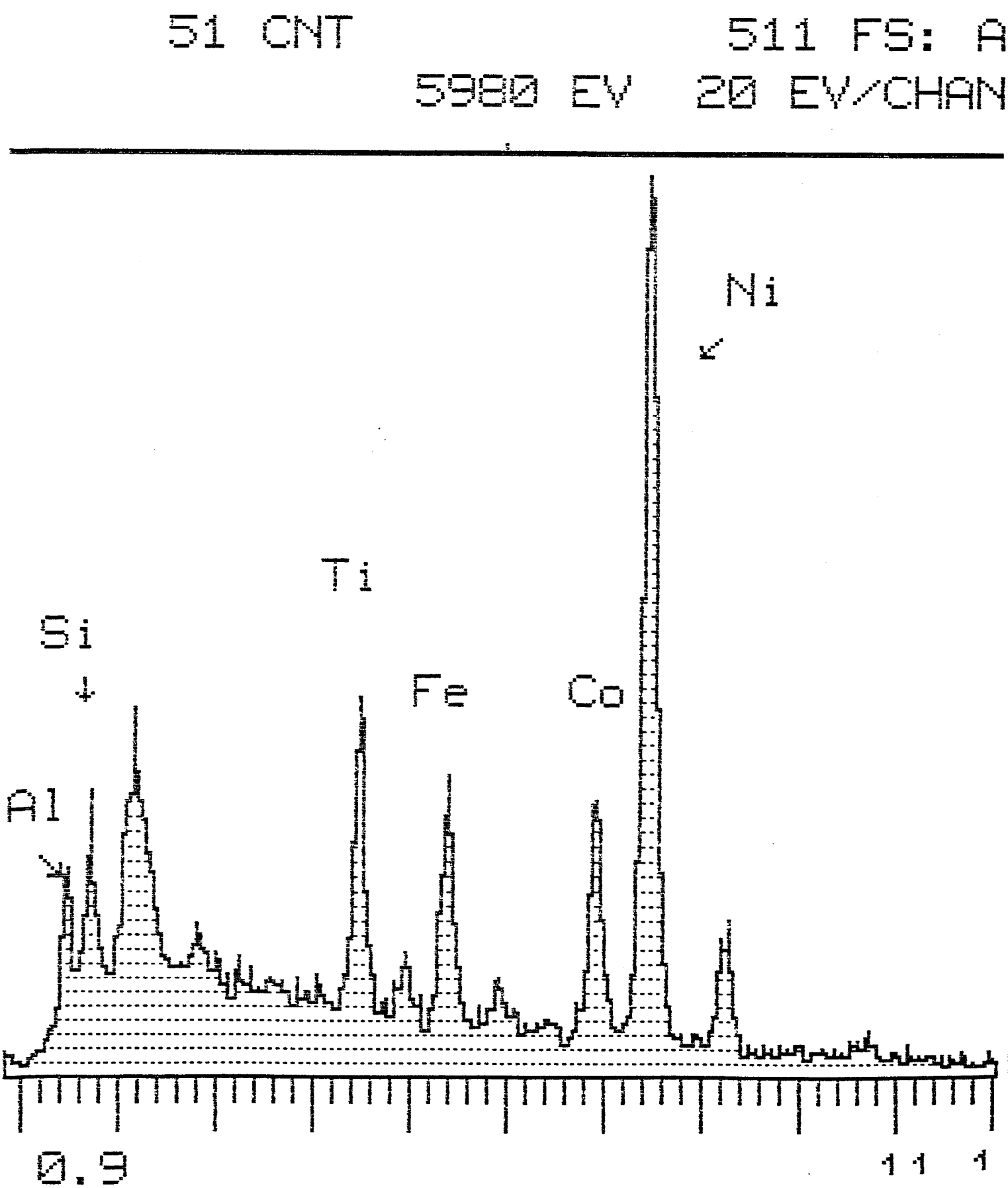

EDX analysis of wear debris collected during dry sand abrasive wear tests on the rubber wheel (N18)
Test duration for 40 mins at 197.5 N

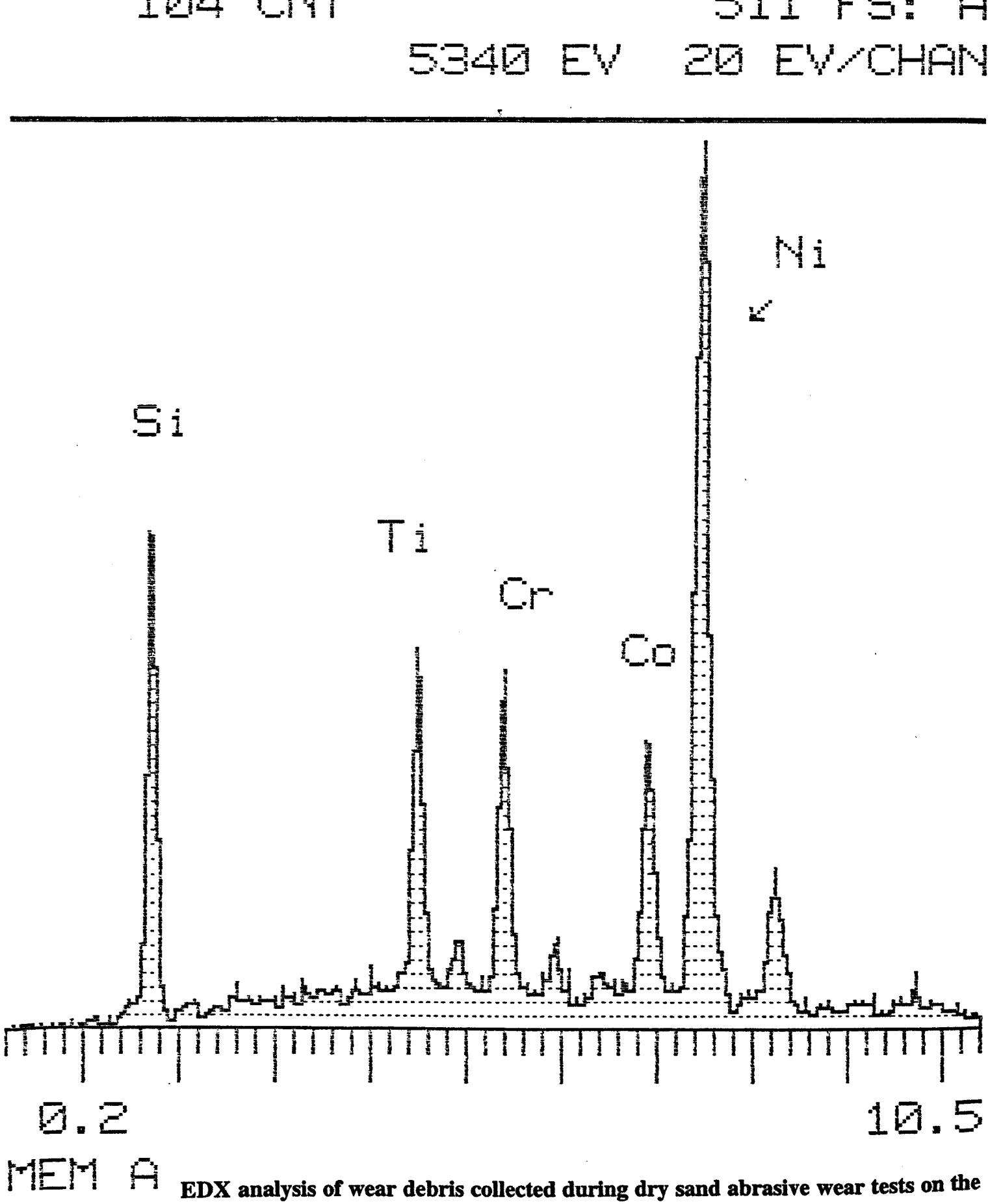

EDX analysis of wear debris collected during dry sand abrasive wear tests on the rubber wheel (N18++)
Test duration for 40 mins at 197.5 N

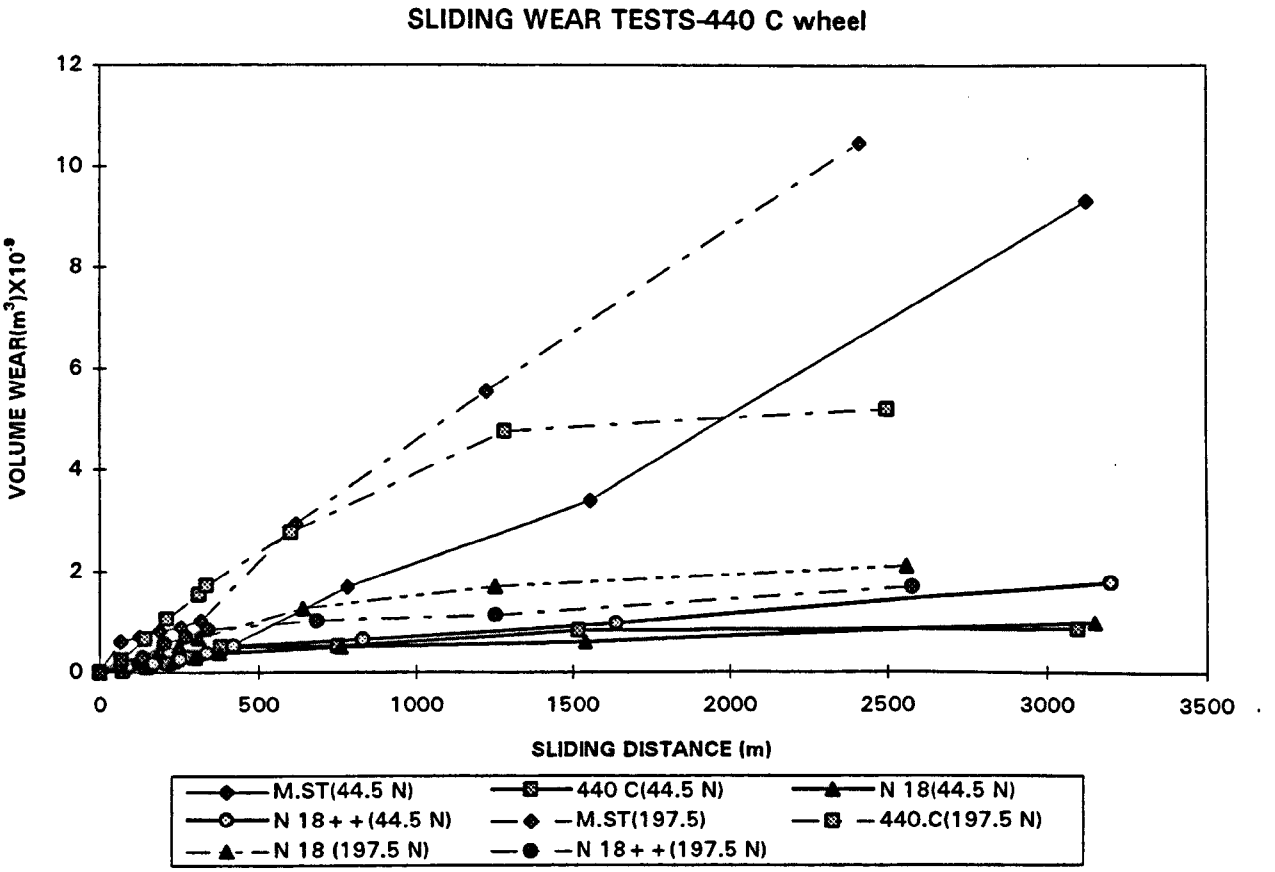
SLIDING WEAR TESTS-440 C wheel
VOLUME WEAR(m³)X10⁻⁹
12
10
8
6
4
2
0
0
500
1000
1500
2000
2500
3000
3500
SLIDING DISTANCE (m)
M.ST(44.5 N)
440 C(44.5 N)
N 18(44.5 N)
N 18+ +(44.5 N)
M.ST(197.5)
440.C(197.5 N)
N 18 (197.5 N)
N 18+ +(197.5 N)

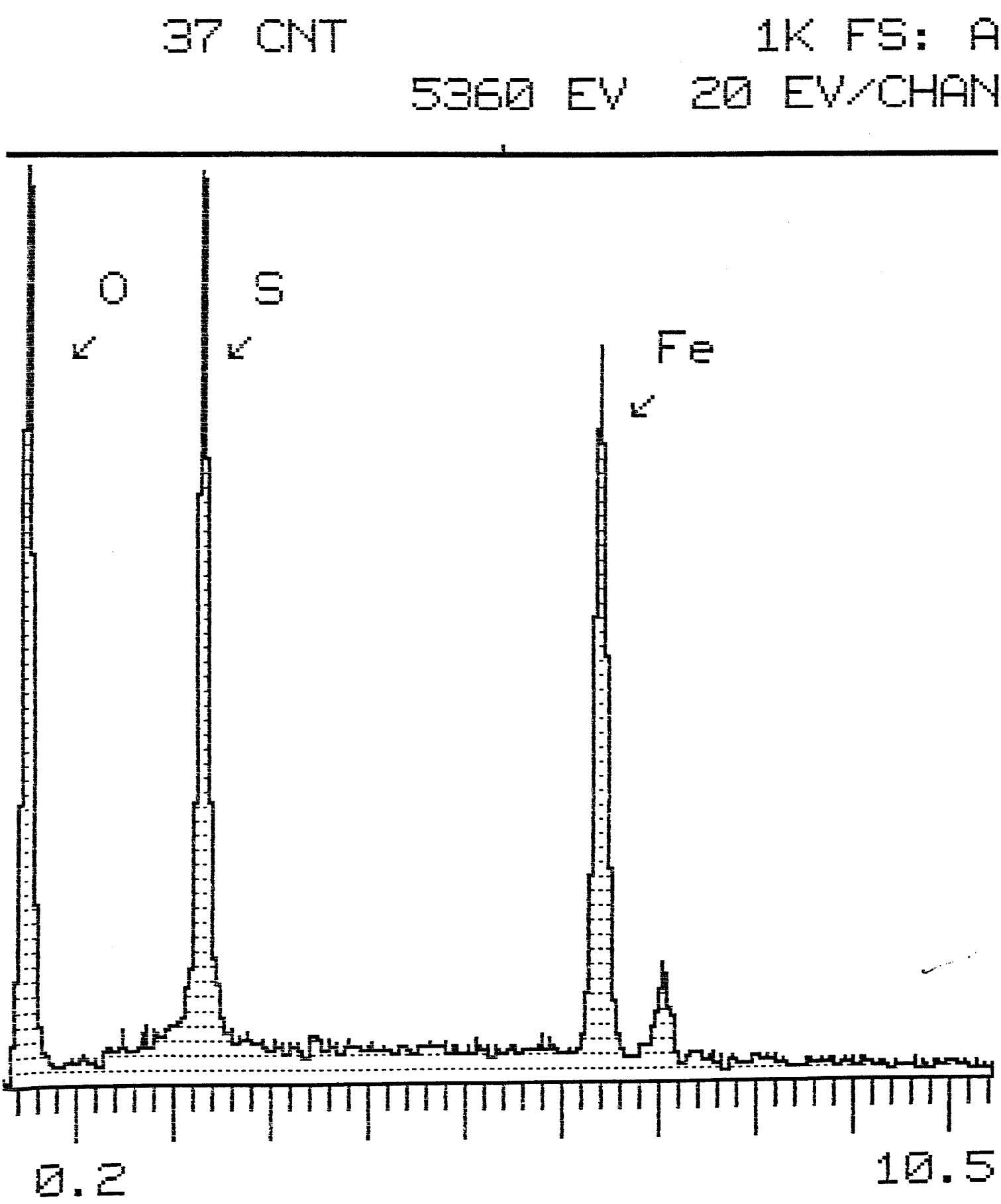

Corrosion of M.St specimen in 3wt% H_2SO_4 after 64 mins at 90±5°C

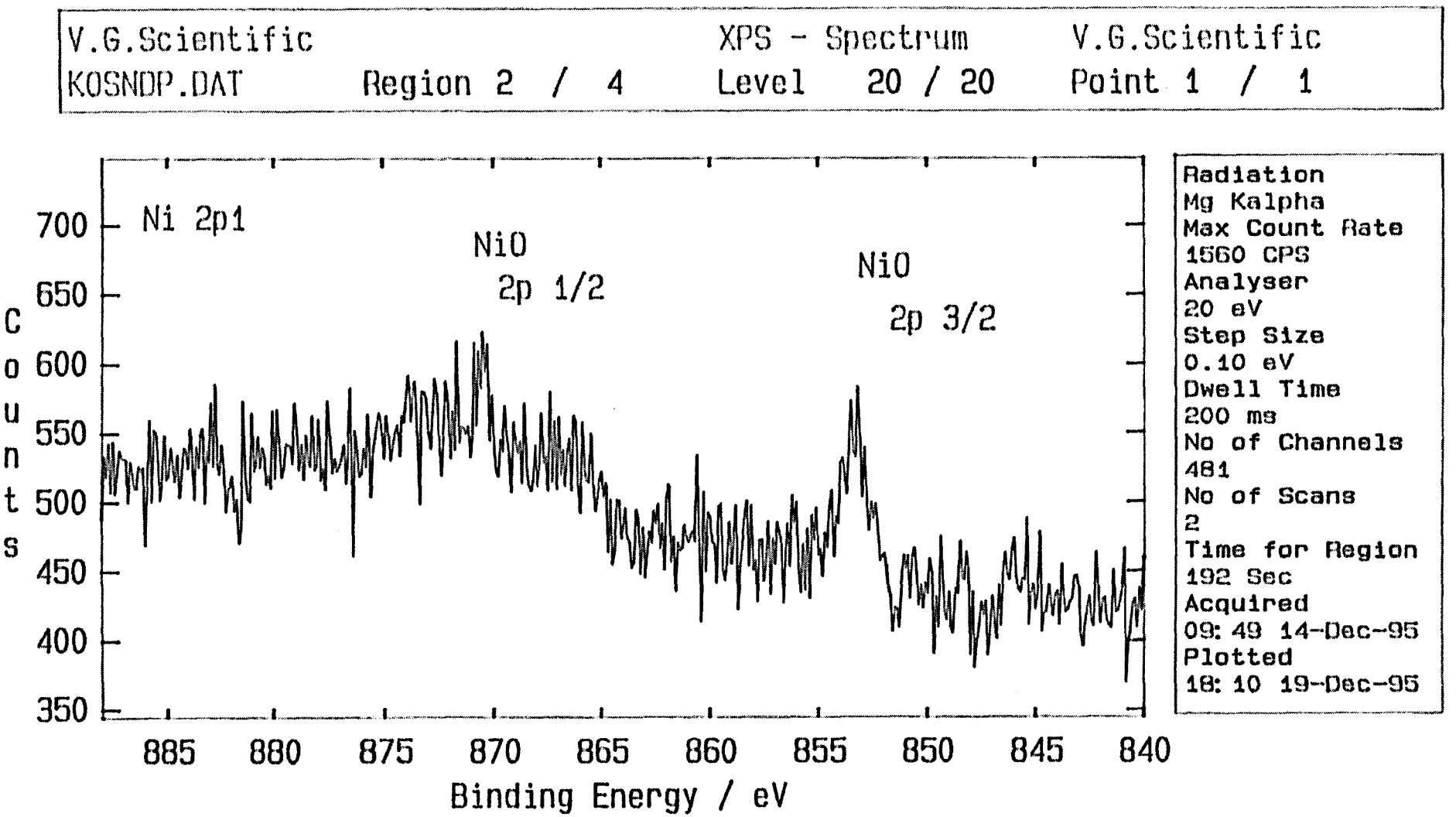
V.G.Scientific
XPS - Spectrum
V.G.Scientific
KOSNDP.DAT
Region 2 / 4
Level 20 / 20
Point 1 / 1
Ni 2p1
NiO
2p 1/2
NiO
2p 3/2
Counts
700
650
600
550
500
450
400
350
885
880
875
870
865
860
855
850
845
840
Binding Energy / eV
Radiation
Mg Kalpha
Max Count Rate
1560 CPS
Analyser
20 eV
Step Size
0.10 eV
Dwell Time
200 ms
No of Channels
481
No of Scans
2
Time for Region
192 Sec
Acquired
09:49 14-Dec-95
Plotted
18:10 19-Dec-95

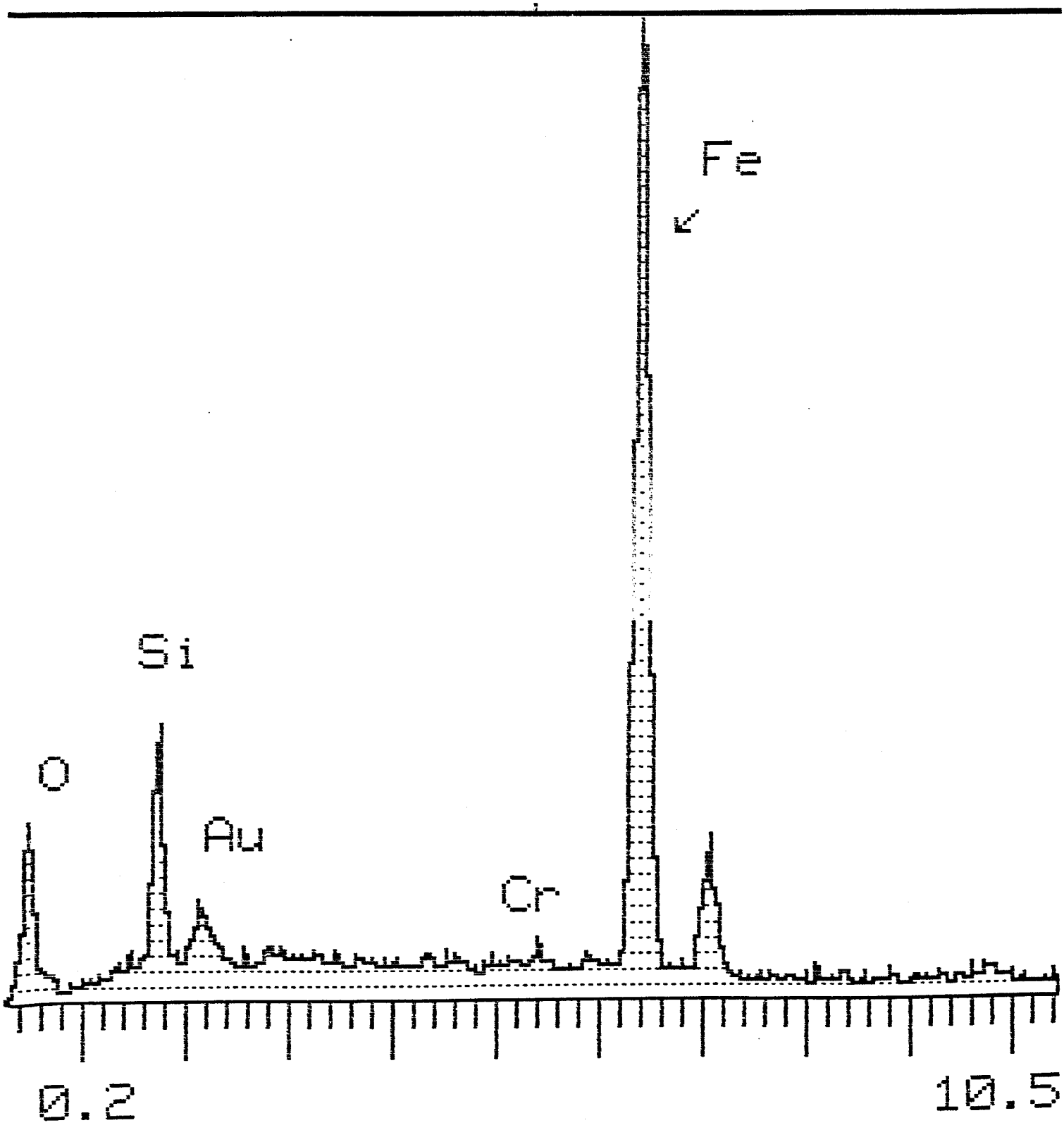

Spot analysis of M.St specimen
Abrasion-corrosion in a 3wt% H_2SO_4 solution for 1 h

V.G.Scientific		XPS - Spectrum	V.G.Scientific
KOSDP2.DAT	Region 2 / 3	Level 11 / 13	Point 1 / 1

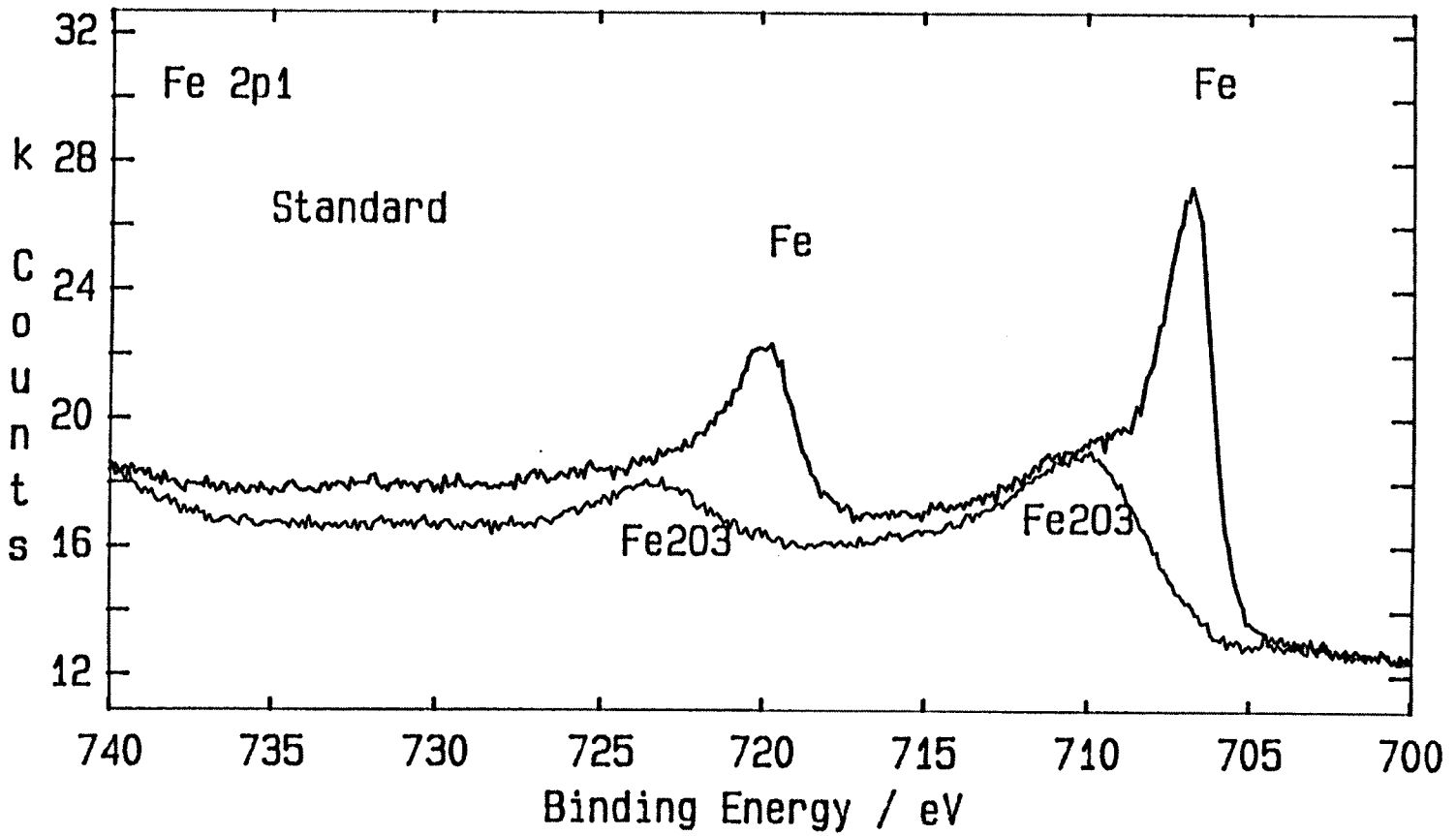

Spectrum 1

KOSDP2.DAT

Region 2

Level 2

Point 1

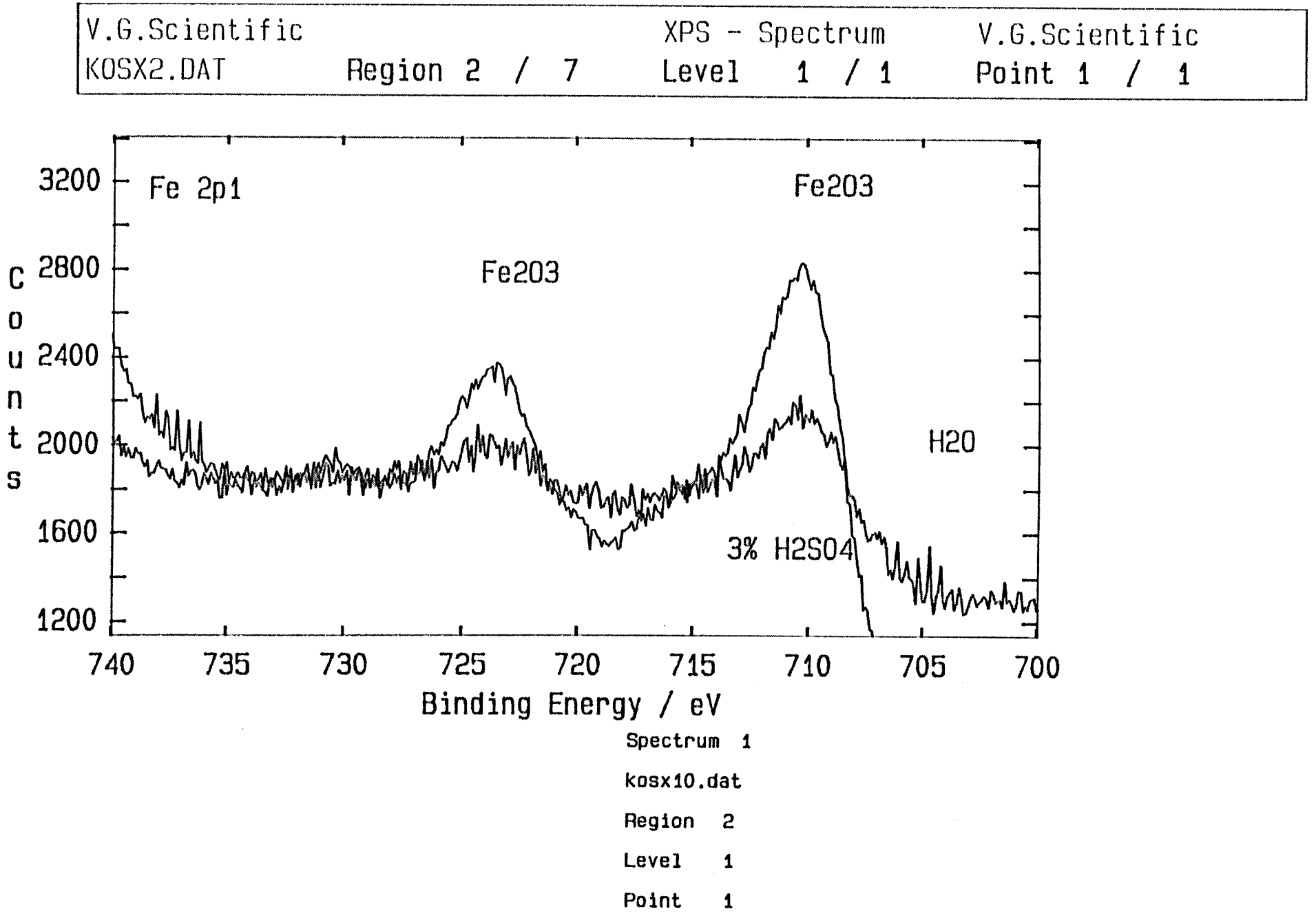
V.G.Scientific
KOSX2.DAT
Region 2 / 7
XPS - Spectrum
Level 1 / 1
V.G.Scientific
Point 1 / 1
Fe 2p1
Fe203
Fe203
H20
3% H2S04
Counts
3200
2800
2400
2000
1600
1200
740
735
730
725
720
715
710
705
700
Binding Energy / eV
Spectrum 1
kosx10.dat
Region 2
Level 1
Point 1

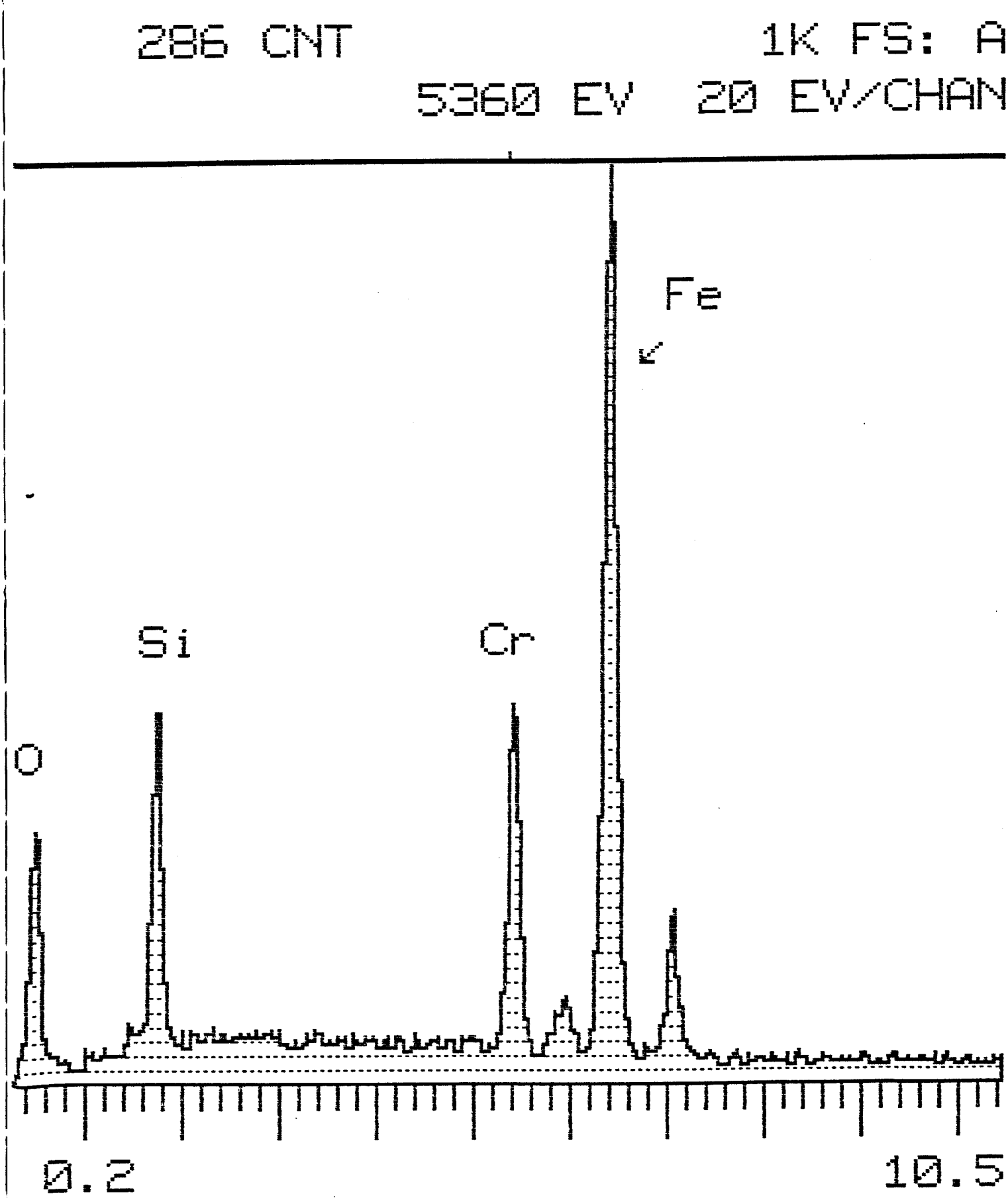

Spot analysis of 440C specimen
Abrasion-corrosion in a 3wt% H_2SO_4 +10wt% Amin. solution for 1 h

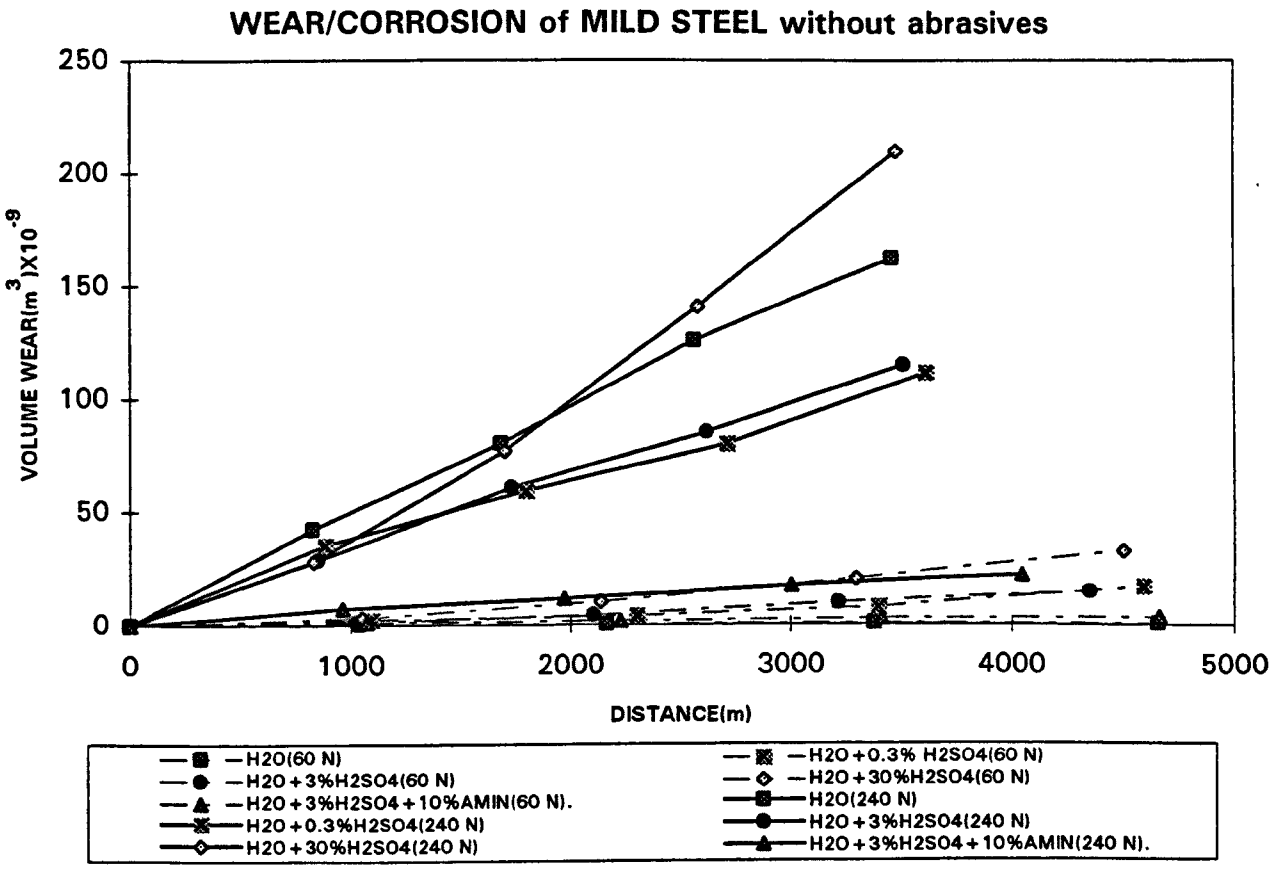
WEAR/CORROSION of MILD STEEL without abrasives
VOLUME WEAR(m3)X10-9
250
200
150
100
50
0
0
1000
2000
3000
4000
5000
DISTANCE(m)
H2O(60 N)
H2O+3%H2SO4(60 N)
H2O+3%H2SO4+10%AMIN(60 N).
H2O+0.3%H2SO4(240 N)
H2O+30%H2SO4(240 N)
H2O+0.3% H2SO4(60 N)
H2O+30%H2SO4(60 N)
H2O(240 N)
H2O+3%H2SO4(240 N)
H2O+3%H2SO4+10%AMIN(240 N).

Appendix C

1. Probability plots for the measured values of groove width(2a) fot the M.St
2. Probability plots for the measured values of groove width(2a) for the 440C
3. Probability plots for the measured values of groove width(2a) for the N18
4. Probability plots for the measured values of groove width(2a) for the N18++
5. Tabulated values for groove width(2a) for all the four materials - rubber wheel
6. An example of a complete calculation of metal recession for the M.St(197.5 N) using the developed model
7. Tabulated values for groove width(2a) for all the four materials - 440C wheel

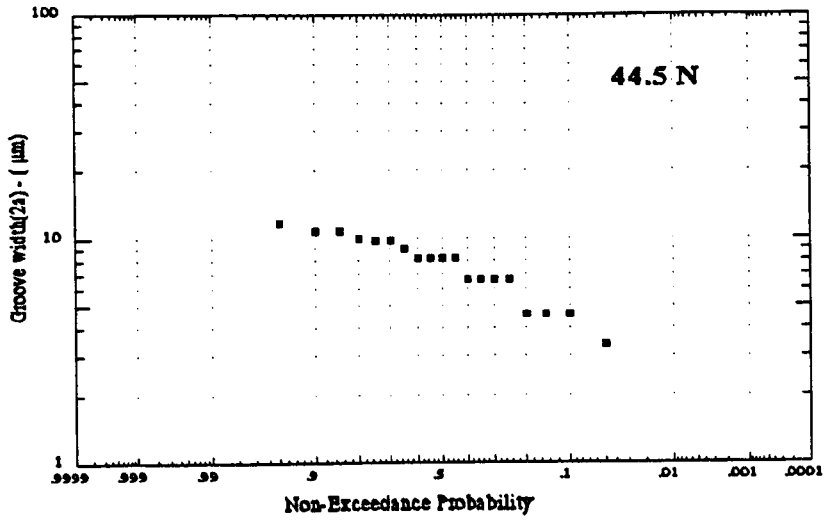

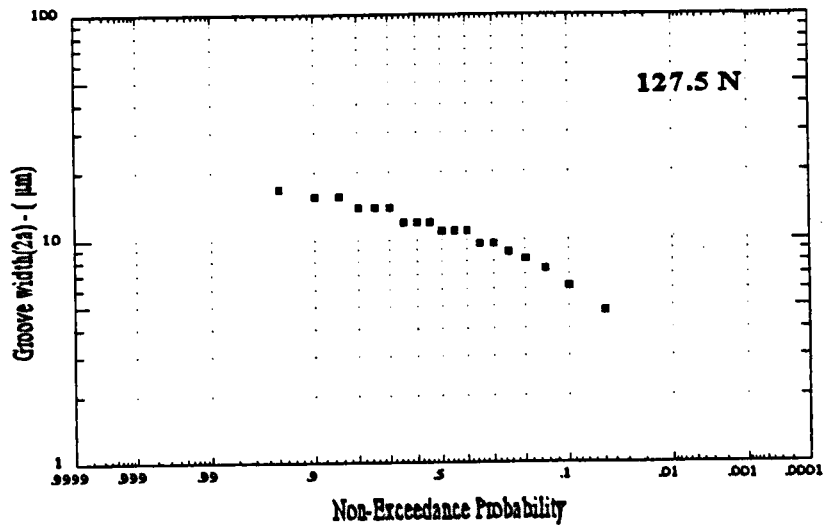

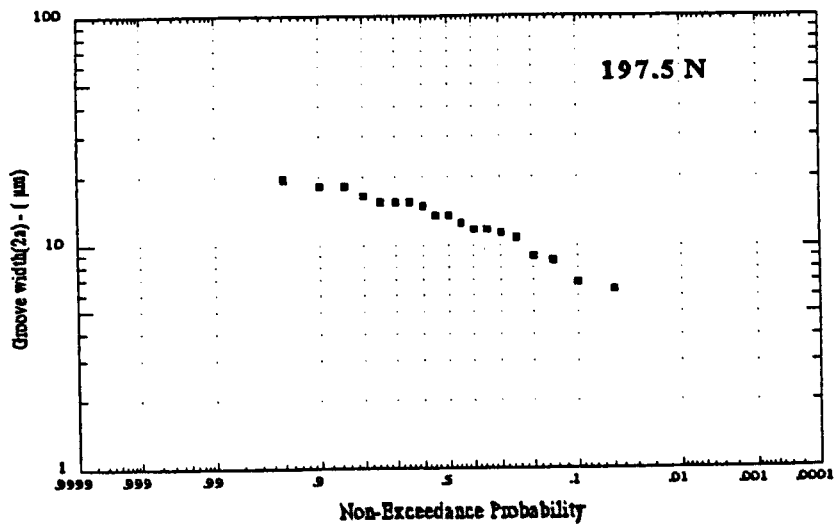

Probability plots for the measured values of groove width(2a) for the M.St

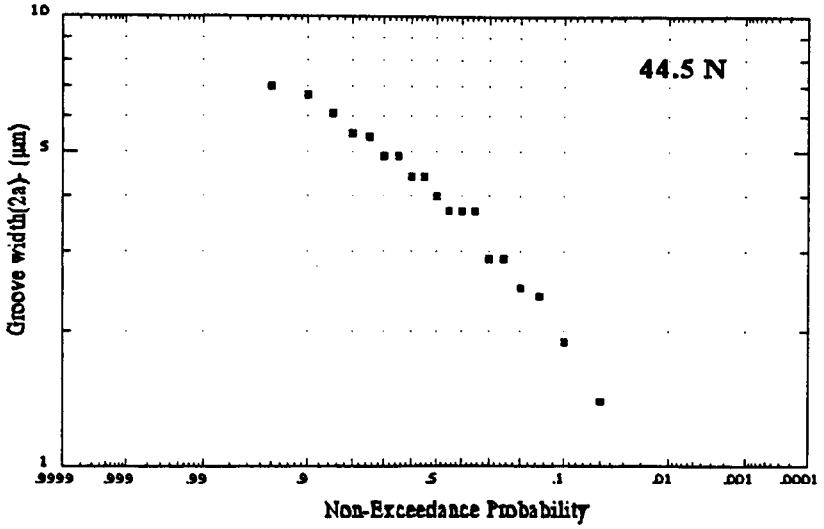

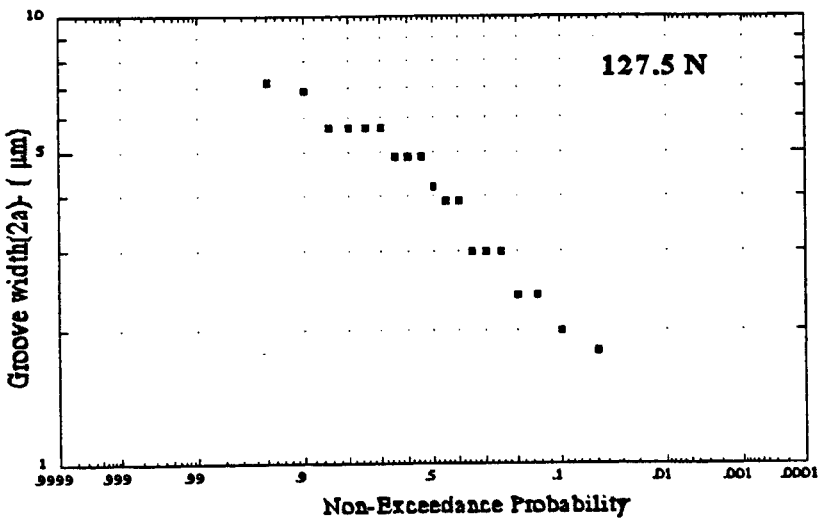

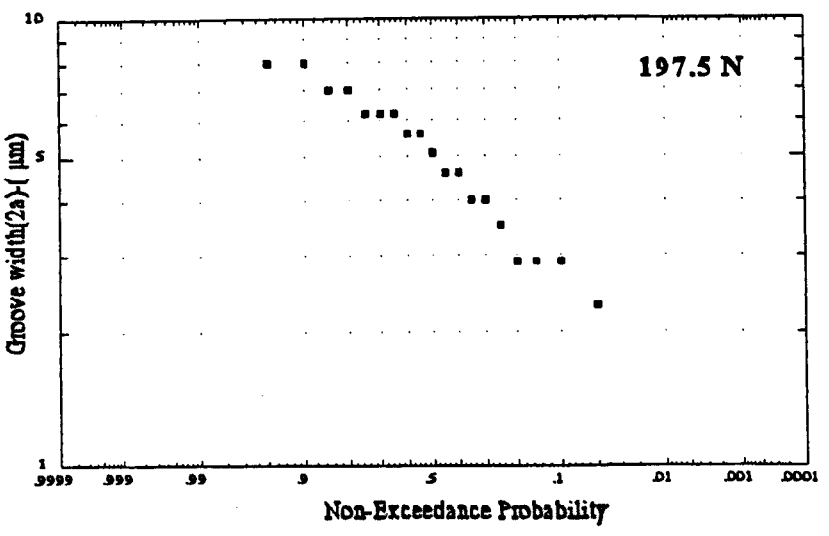

Probability plots for the measured values of groove width(2a) for the 440C

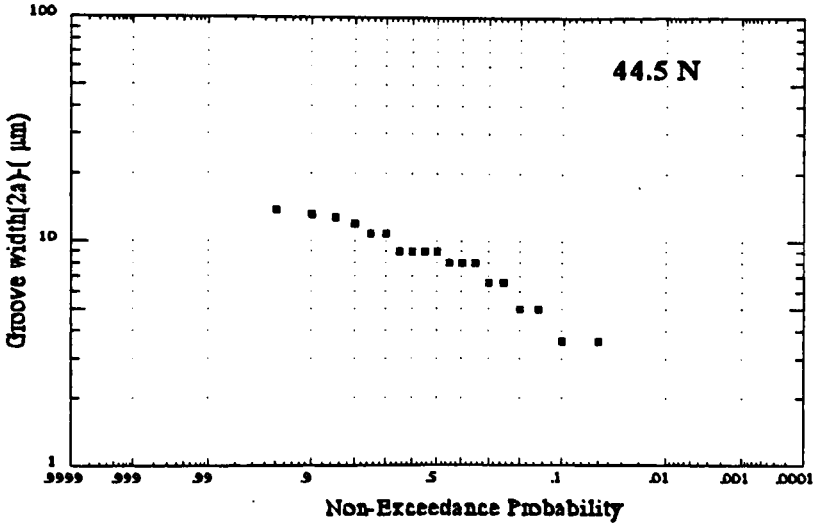

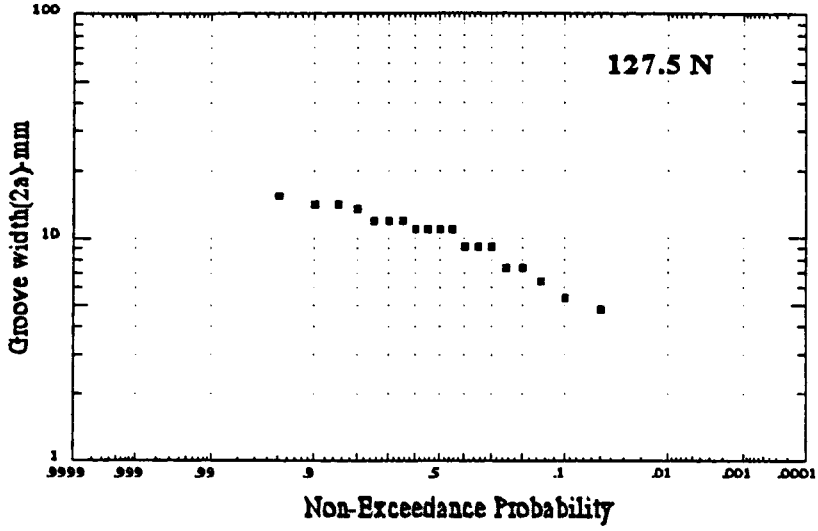

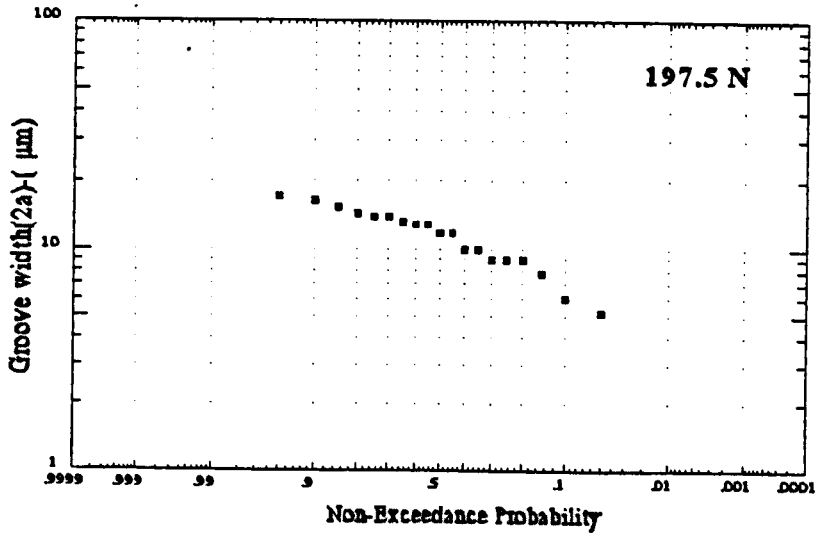

Probability plots for the measured values of groove width(2a) for the N18

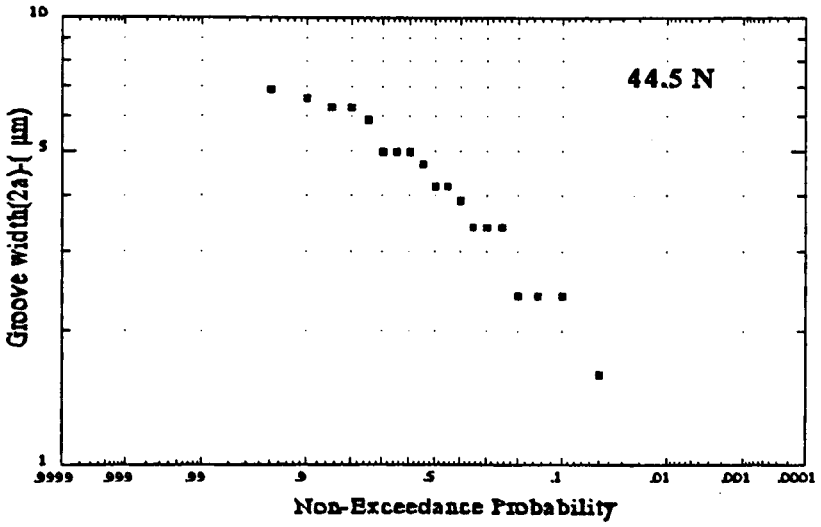

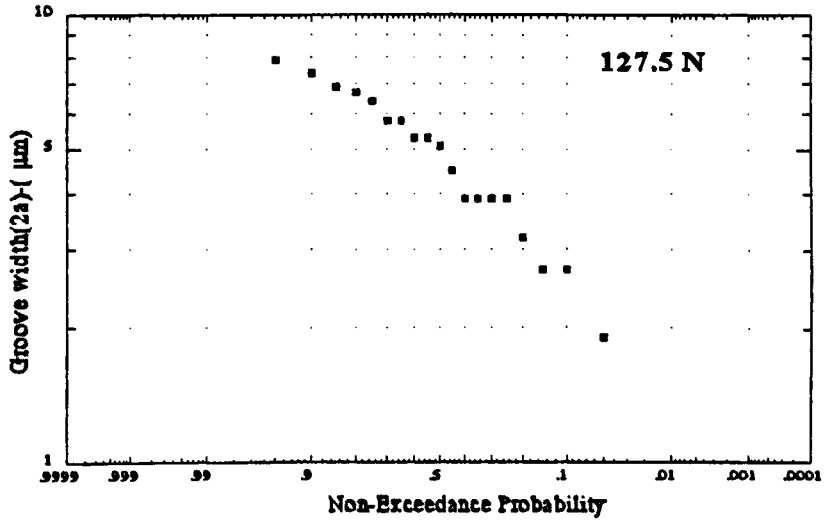

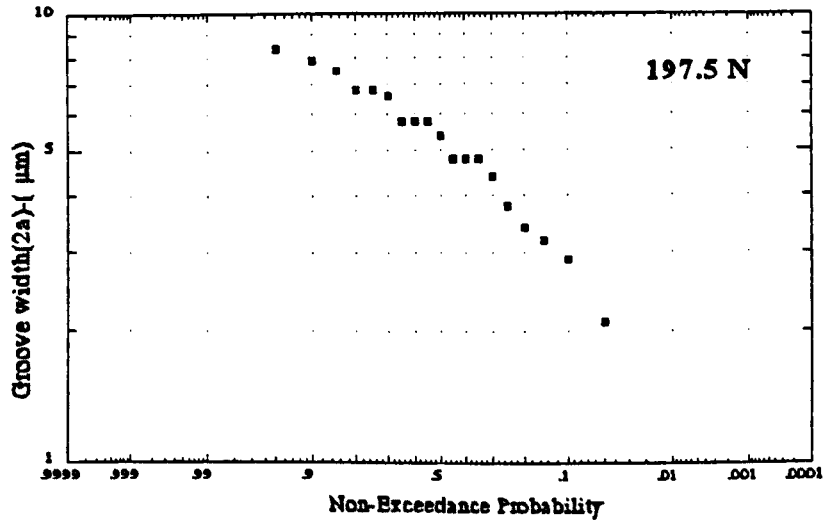

Probability plots for the measured values of groove width(2a) for the N18++

Rubber wheel

Values of 2a for different loads and materials taken from the probability plots

Particle size(2R) (μm)	M.St 44.5N (μm)	M.St 127.5N (μm)	M.St 197.5N (μm)	N18 44.5N (μm)	N18 127.5N (μm)	N18 197.5N (μm)	440C 44.5N (μm)	440C 127.5N (μm)	440C 197.5N (μm)	N18++ 44.5N (μm)	N18++ 127.5N (μm)	N18++ 197.5N (μm)
391	14.8	21.9	25	16.8	19.4	21.1	8.7	9.2	9.9	9.0	9.6	9.9
338	13.5	21	23.1	15.3	17.8	19.4	7.9	8.3	9.0	8.2	8.8	9.1
292	12.4	18.7	21.6	14.2	16.6	18.2	7.3	7.7	8.4	7.6	8.2	8.4
252	10.2	15.2	17.6	11.4	13.6	15.0	5.7	6.1	6.8	6.1	6.6	6.8
217	7.8	11.4	13.2	8.5	9.5	11.7	4.1	4.4	5.1	4.6	5.0	5.2
187	5.6	8.4	9.8	6.1	7.8	8.8	2.6	2.9	3.6	3.2	3.5	3.7
162	4.5	7	8	4.8	6.5	7.5	1.9	2.2	2.9	2.6	2.9	3.1
140	4	6.2	7.1	4.0	5.6	6.6	1.6	1.8	2.5	2.3	2.5	2.7
120	3.4	5.4	6.2	3.6	5.2	6.1	1.4	1.4	2.2	2.0	2.1	2.3
104	2.6	4	4.6	2.4	4.1	4.8	0.5	0.7	1.5	1.3	1.5	1.6
89	0.8	1.4	1.8	0.7	1.6	2.4	0.0	0.0	0.4	0.1	0.3	0.4
77	0.6	1.2	1.4	0.4	1.5	2.1	0.0	0.0	0.3	0.0	0.0	0.2
57	0.2	0.6	0.8	0.2	0.8	1.6	0.0	0.0	0.0	0.0	0.0	0.0

Calculation of metal recession for M.St **197.5 N** **Rubber wheel**

%	2R(um)	R(um)	Grains/g	Tot.No of pls/Kg	2a(μm)	a(μm)	h(μm)	h/a(μm)	Nt	Δερ	2N	h'	h"
0.5	391	195.5	12093	60465	25	12.50	0.39962	0.0320	508	0.0128	967	6.25	0.76900
1.2	338	169	18720	224640	23.1	11.55	0.39468	0.0342	550	0.0137	819	5.78	2.88128
2.1	292	146	29034	609714	21.6	10.80	0.39945	0.0370	588	0.0148	672	5.40	8.33388
13.7	252	126	45171	6288711	17.6	8.80	0.30730	0.0349	722	0.0140	776	4.40	49.43148
30.6	217	109	69773	21997116	13.2	6.60	0.19982	0.0303	962	0.0121	1108	3.30	68.06808
28.5	187	93.5	110545	31505325	9.8	4.90	0.12840	0.0262	1296	0.0105	1591	2.45	37.44843
10.2	162	81	170026	17342652	8	4.00	0.09877	0.0247	1588	0.0099	1845	2.00	11.84048
3.3	140	70	263438	8993454	7.1	3.55	0.09002	0.0254	1789	0.0101	1727	1.78	5.16899
2.9	120	60	418330	12131570	6.2	3.10	0.08008	0.0258	2048	0.0103	1648	1.55	5.57010
3.6	104	52	642637	23134788	4.6	2.30	0.05087	0.0221	2761	0.0088	2430	1.15	3.96487
2.7	89	44.5	1025399	27685773	1.8	0.90	0.00910	0.0101	7056	0.0040	17191	0.45	0.10272
0.1	77	38.5	1583400	1583400	1.4	0.70	0.00636	0.0091	9071	0.0036	22434	0.35	0.00272
0.2	57	28.5	3903357	7806714	0.8	0.40	0.00281	0.0070	15875	0.0028	42851	0.20	0.00230
99.6				159364322									194
												Sand(Kg)	5
												Metal recession (μm)	968

Wheel dia.= 219 mm **V=** 64 rpm

ε_f = 0.2 **c =** - 0.40

Sand feed rate 125 g/min **n =** 0.3

Explanation of the Table

% =percentage of particles in each particle size

R =particle radius

Grains/g =Nr of particles per g. assuming spherical particles

Tot.No of pls =Nr of particles per kg

a =half groove size

h/a =depth of penetration

Nt =Nr of grooves on the scar width)

$\Delta\varepsilon\rho$ =plastic strain amplitude

2N =strain reversals to failure

h'=chip thickness

h" =total amount of metal recession

Sand(Kg) =total amount of sand used in the experiments

440C wheel

Experimental values of 2a for different loads and materials

Particle size(2R) (μm)	M.St 60N (μm)	M.St 240N (μm)	N18 60N (μm)	N18 240N (μm)	440C 60N (μm)	440C 240N (μm)	N18++ 60N (μm)	N18++ 240N (μm)
391	18.6	30.5	21.2	25.7	11	12.1	11.3	12.1
338	17	28.2	19.3	23.7	10	11	10.3	11.1
292	15.6	26.4	17.9	22.2	9.2	10.2	9.6	10.2
252	12.9	21.5	14.4	18.3	7.2	8.3	7.7	8.3
217	9.8	16.1	10.7	14.3	5.2	6.2	5.8	6.3
187	7.1	12	7.7	10.7	3.3	4.4	4	4.5
162	5.7	9.8	6	9.2	2.4	3.5	3.3	3.8
140	5	8.7	5	8.1	2	3.1	2.9	3.3
120	4.3	7.6	4.5	7.4	1.8	2.7	2.5	2.8
104	3.3	5.6	3	5.9	0.6	1.8	1.6	2
89	1	2.2	0.9	2.9	0	0.5	0.1	0.5
77	0.8	1.7	0.5	2.6	0	0.4	0	0.2
57	0.3	1	0.3	2	0	0	0	0